Efficient Metal-Promoted Biomimetic Catalysis of Phosphoryl Transfer Reactions in Alcohols

By

C. Tony Liu

A thesis submitted to the Department of Chemistry, Queen's University

In conformity with the requirements for the

Degree of Doctor of Philosophy

Queen's University

Kingston, Ontario, Canada

July, 2011

Abstract

Understanding enzymatic reactions has many invaluable implications that could lead to useful pharmaceutical and commercial applications. Phosphoryl transfer reactions are perhaps the most prevalent chemical transformations in Nature. Phosphate esters are highly resistant to hydrolytic and nucleophilic degradation in the absence of catalysts, and enzymes that faciliate phosphoryl transfer reactions are among the most catalytically efficient enzymes in Nature.

A common strategy for understanding enzyme catalysis involves designing small molecule enzyme mimics. Our approach is to focus on the reaction medium inside the enzyme active sites, which is generally accepted to be non-aqueous and have an effective dielectric constant like organic solvents. We find that by switching from water to light alcohols (methanol and ethanol), a dinuclear **3.3**:$Zn(II)_2$ complex can accelerate the solvolytic cleavages of simple phosphate diesters (both DNA and RNA models) by $\geq 10^{12}$ times relative to the background reactions. A series of detailed mechanistic investigations revealed that the catalyzed cleavage of phosphate diesters proceeds via a multi-step process. Furthermore, comparison between the catalysis observed in methanol and ethanol is provided. In addition, the rate-limiting step of the three-step catalytic process changes depending on the leaving groups of the substrates for the transesterification of a series of 2-hydroxylpropyl aryl phosphates promoted by **3.3**:$Zn(II)_2$.

The same dinuclear $Zn(II)_2$ complex is also very efficient at catalyzing the methanolysis of a series of methyl aryl phosphates (DNA models). Additional catalysis through leaving group assistance was observed for methyl aryl phosphates that contain

ortho-nitro and *ortho*-carbomethoxy substituents. To better understand the effectiveness of leaving group assistance in phosphoryl transfer reactions, we studied the solvolytic cleavage of a homologous set of phosphate mono-, di-, and triesters in methanol, and found that the reactions can be greatly accelerated ($10^{14\text{-}15}$-fold rate acceleration for the phosphate mono- and diesters) solely through Cu(II)-promoted leaving group stabilization.

Finally, to highlight the importance of the reaction medium, in the last chapter we present an unprecedented result whereby, in ethanol containing trace amounts of water, the same dinuclear $Zn(II)_2$ catalyst can preferentially promote the hydrolysis of a DNA model substrate with catalytic efficacy that matches enzyme catalysis.

Acknowledgments

If I could go back in time, would I do it all over again? Without a doubt, this has been a wonderful and fulfilling journey and I could not think of a better alternative. More importantly, none of this would be possible without the help and support of many friends, colleagues, and family. First and formost, I want to thank my supervisor, Dr. R. Stan Brown for convincing me to change my mind and pursue my PhD degree in his lab. Thank you for your trust and for taking a chance on me. Since then, words cannot describe my deepest gratitude to Stan, who has profoundly impacted my life. Throughout the years, Stan provided constant guidance and support, while fostering a high standard of quality. He is a supervisor that constantly challenges you to improve while giving you the creative flexibility to think and develop the direction of your research. Combined with his unwavering passion for Chemistry, there is not a better teacher/mentor that I would ask for; it has been an unbelieveable learning experience working in his lab, and it is my great wish that he will be proud of my future endeavors.

Just as influential to my development is Dr. Alexei A. Neverov, whom I am greatly indebted to. His guidance and support has been instrumental to my development during my time here, and I am where I am because of him. His limitless knowledge of chemistry and his enthusasim for discovery has been both a great inspiration and an invaluable resource to learn from. Over the past few years, it has been a wonderful learning experience (beyond chemistry) working with him, and we shared many memorable discussions. I will always treasure his friendship, which I hope will continue to flourish in the future, and when 'I think about him, now and then,' I will always think: Thank you Alex.

During my time in the Brown group, I have had the pleasure of working with many wonderful people and outstanding researchers; many of whom I had the privilege of collaborating with. I want to especially thank Chris I. Maxwell and Mark F. Mohamed, who have accompanied me since day 1 as we all started our PhD in Brown's lab at the same time. Their friendships and support made it an unforgettable experience. I want to thank Dr. Josephine S.W. Tsang who introduced me to the addictive research life in Dr. Brown's lab, and Dr. Dave R. Edwards for many insightful discussions. I also want to thank Dr. Zhong-Lin Lu, who opened the door to a fruitful project for me.

Outside chemistry, I am truly grateful for the support provided by friends and family. I am blessed with the unconditional support and love from my partner, Suzanne L. Day, who has been by my side through tough times (multiple root canals) and amazing times (exploring the world). Outside of my supervisors, she is probably the only person that has read every piece of my work, and still snickers when she sees the word "cleavage", which I use a lot. Lastly, I owe more than words can describe to my father Hsiao-Chang Liu and my mother Chiu-Wen Lin. They sacrificed so much for their children and continue to provide unconditional support for both my sister and I. Every day it gives me reason to become better in order to show them that their sacrifices are worth it, and ultimately it is my greatest desire to make them proud of what I do and of who I have become. I also want to acknowledge my little sister, Pheobe Liu, whom I care about dearly and I wish her nothing but the best.

Without them, I am nothing.

Statement of Originality

To the best of the author's knowledge, the original work in this thesis includes the following:

1. Mechanistic study of the catalyzed cleavages of RNA and DNA model substrates by a simple dinuclear **2.2**:$Cu(II)_2$ complex in methanol, where the individual events in the multi-step catalytic process can be monitored via spectrophotometric means.

2. Kinetic study of the transesterification of a series of 2-hydroxylpropyl aryl phosphates (RNA model) by a simple dinuclear **3.3**:$Zn(II)_2$ catalyst in ethanol showing a change in the rate-limiting step depending on the substrate. Also a brief comparison of the solvent effect changes between different solvents is made.

3. Energetic analysis of catalyzed cleavages of DNA and RNA model substrates by dinuclear **3.3**:$Zn(II)_2$ and **2.2**:$Cu(II)_2$ in alcohol media to dissect the individual components responsible for the catalysis observed and to quantify the magnitude of catalysis in terms of the free energy of stabilization for the transition state.

4. Kinetic study of the catalyzed methanolysis of a series of methyl aryl phosphates (DNA model) by a simple dinuclear complex **4.1**:$Zn(II)_2$ in methanol.

5. The dinuclear **4.1**:$Zn(II)_2$ catalyst exhibits additional catalysis for the methanolysis of methyl aryl phosphates containing *ortho*-nitro and *ortho*-carbomethoxy substituents through leaving group assistance. It is the first time that such mode of catalysis between metal complexes and substrates with aryloxy leavinging groups containing *ortho*-nitro and *ortho*-carbomethoxy substituents has been reported.

6. Demonstration of efficient Cu(II)-promoted leaving group assistance for a homologous set of phosphate mono-, di-, and triesters in methanol where LGA alone can provide upto $10^{14\text{-}15}$-fold rate acceleration for the solvolytic cleavages of phosphate mono- and diesters. Also, in the presence of Cu(II)-promoted LGA, the cleavage of a phosphate mono- and diesters appear to be mechanistically different from the uncatalyzed processes.

7. A biomimetic system in ethanol containing trace amount of water where a simple man-made dinuclear Zn(II) complex (**6.3**) can selectively promote the hydrolysis of a DNA model substrate with enzyme-like efficiency.

Table of Contents

List of Figures

List of Tables

List of Schemes

List of Abbreviations

12N3	1,5,9-triazadodecane
Abs	absorbance
AP	alkaline phosphatase
ApG	adenylyl(3'→5')guanosine
BNPP	*bis*(*p*-nitrophenyl) phosphate
^{o}C	degrees celsius
cat	catalyst
d	doublet
dd	doublet of doublets
DMF	dimethylformamide
DNA	deoxyribonucleic acid
ESI-TOF	electrospray ionization – time of flight
Et	ethyl
Et_3N	triethylamine
HPNPP	2-hydroxypropyl-*p*-nitrophenyl phosphate
HRMS	high resolution mass spectrometry
Hz	hertz
Int	intermediate
K_{auto}	autoprotolysis constant
LGA	leaving group assistance
LRMS	Low resolution mass spectrometry
m	multiplet

M(II)	metal ion with +2 charge
Me	methyl
MHz	megahertz
MNPP	methyl-*p*-nitrophenyl phosphate
NLLSQ	non-linear least square
ms	millisecond
nm	nanometer
NMR	nuclear magnetic resonance
OAr	aryloxy group
Lg(or LG)	leaving group
OTf	triflate (trifluoromethanesulfonate)
P=O	phosphorus double bonded to oxygen
P=S	phosphorus double bonded to sulphur
P-OLg	bond between phosphorus and the leaving group
RNA	ribonucleic acid
s	singlet
sub	substrate
t	triplet
T	temperature
TBA	tetrabutylammonium
TMPP	2,2,6,6-tetramethylpiperidine
TS	transition state
UpA	uridylyl(3'→5')adenosine

UpU	uridylyl(3’→5’)uridine
UV/vis	ultraviolet-visible

Chapter 1 - General Introduction

1.1 – Phosphoryl Transfer Reactions

Phosphoryl transfer reactions represent, arguably, a set of the most prevalent and vital biological chemical transformations in Nature. Phosphorylation and hydrolysis reactions of phosphate monoesters play important roles in numerous biological processes, including energy regulation, modulating protein function, metabolism, and signal transduction.[1,2,3] As polymeric chains of phosphate diesters, DNA and RNA are extremely resistant to solvolytic degradation, making them suitable candidates for the storage of genetic blueprints of living organisms.[3] Numerous key intermediates in biochemical transformations are phosphate esters. In fact, it has been suggested that ~1/3 of all proteins in organisms undergo reversible phosphorylation in order to carry out basic biological functions.[4] Although phosphate triesters are not naturally occurring biological molecules, they are commercially important as pesticides[5] owing to their toxicity as acetylcholinesterase inhibitors.[6] Many enzymes have evolved the ability to hydrolyze these man-made toxic compounds.[2]

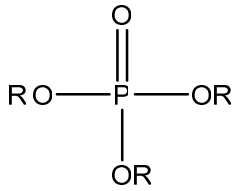

Figure 1-1. General structure of phosphate esters: monoester (R′ = R′′ = H, R ≠ H), diester (R′′ = H, R′and R ≠ H), and triester (R, R′, and R′′ ≠ H).

A major factor contributing to the prevalence of phosphate esters (Figure 1-1) in biological systems is that they are kinetically very stable. Under physiological conditions and in the absence of enzymes, the hydrolytic cleavages of phosphate mono- and diesters with unactivated leaving groups have estimated half-times of ~10^{12} years (monoesters), ~110 years (RNA), and ~$10^{8\text{-}10}$ years (DNA).[7] However, phosphoesterases are among the most efficient enzymes, capable of accelerating the cleavage of phosphate triesters by 10^{11} to 10^{12} times,[8] diesters by 10^{15} to 10^{21} times,[7] and phosphate monoesters by >10^{17} times[9] under physiological conditions. Therefore, due to the great acceleration afforded by enzymes to bring various phosphoryl transfer reactions into a viable timescale that is conducive for life, considerable effort has been devoted to understanding the origin of enzymatic efficiency.

1.2 – Enzyme Catalysis

Many enzymes that are responsible for cleaving phosphate esters contain two or more transition metal ions (Zn^{2+}, Ca^{2+}, Mg^{2+}, Fe^{3+}, and Mn^{2+}) in close proximity (~ 4 Å apart) in the active sites (Figure 1-2)[3], and their catalytic roles have been discussed at length.[2,3,10] Examples of these metallo-phosphoesterases include phospholipase C,[3] ribonuclease H from HIV reverse transcriptase,[11] 3,5-exonuclease from DNA polymerase I,[21b] P1 nucleases,[12] and alkaline phosphatase[3]. Furthermore, it has been found that several soil-dwelling bacteria, *Pseudomonas diminuta*,[13] *Flavobacterium sp.*,[14] and *Agrobacterium radiobacter P230*,[15] possess enzymes with di-Zn(II) catalytic cores that are capable of effectively decomposing phosphotriester-based insecticides. In some cases, the dinuclear catalytic core is accompanied by an ancillary M^{2+} ion close by that,

although not directly interacting with the phosphate substrate during the chemical transformation, does influence the overall activity.[3,16] Alkaline phosphatase is perhaps the most extensively studied metalloenzyme in the literature.[2,3,17] Its main function is to catalyze the hydrolysis of phosphate monoesters into inorganic phosphate. It is a homodimer with two Zn(II) ions and one Mg(II) ion inside the active sites (Figure 1-2) of each subunit. The di-Zn(II) core (metal ions are 3.9 Å apart)[18] is essential to the catalytic activity. While it has been suggested that the third Mg(II) binds a hydroxide that can act as a general base[19], there is also evidence that this ion induces conformational changes in the subunits of the homodimer and facilitates the release of the reaction product.[20]

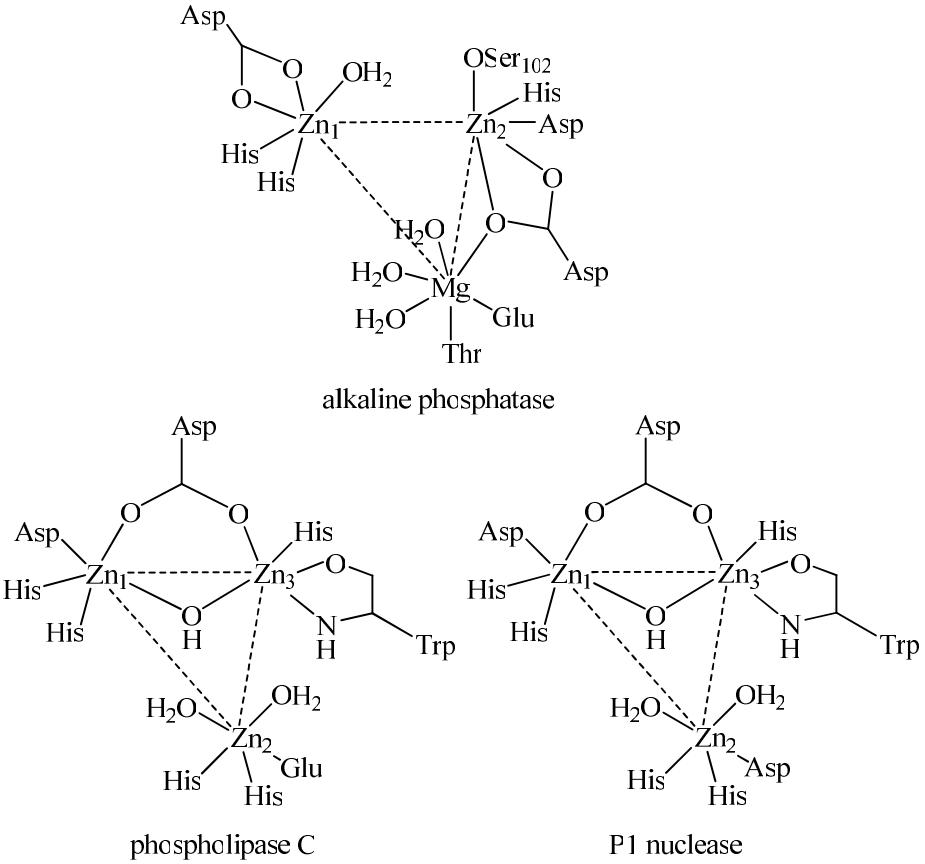

Figure 1-2. Representation of the multinuclear active sites of alkaline phosphatase phospholipase C, and P1 nuclease (re-sketched from Ref. [3b]).

It is generally accepted that these enzymatic processes proceed through a 'two metal ion phosphoryl transfer mechanism' (Figure 1-3), first proposed by Steitz.[21] In this mechanism, the metal ions are responsible for 1) Lewis acid activation of the substrate via M^{+x}---O=P binding; 2) lowering the pK_a of a metal-bound nucleophile (ROH or HOH) to increase the concentrations of the nucleophile anion at physiological pH; 3) delivery of a metal-bound hydroxide or alkoxide that serves as a nucleophile or a base; 4) electrostatic stabilization of the anionic substrate and nucleophile/base through binding to the (+)-charged active site and subsequent lowering of the transition state energy of the reaction[22]; and 5) stabilization of the leaving group through metal ion coordination. In order to gain better insights into enzymatic mechanisms, studies aimed at emulating and quantifying the enzymatic catalysis through small molecule metal complexes have attracted strong interest in the research community.[3b,10,23,24] Due to the obvious difference in the structural complexity between actual enzymes and small molecule model systems, model catalysts are designed to utilize several, but rarely all, of the main modes of enzymatic catalysis discussed above.

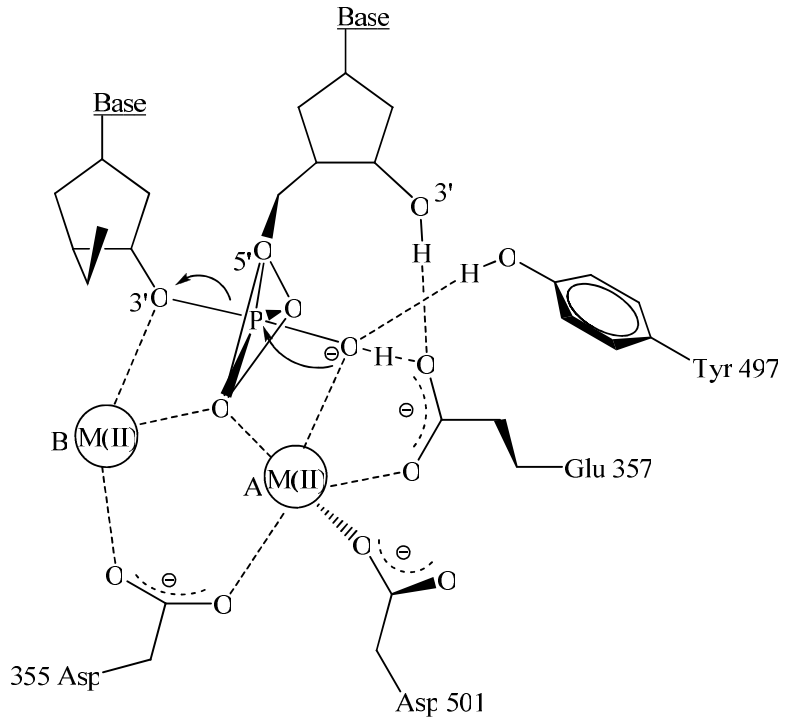

Figure 1-3. Proposed transition state structure for DNA hydrolysis inside the 3′-5′ exonuclease dinuclear active site of *E. coli* DNA polymerase I (re-sketched from Ref. [21b]). Metal ion A is proposed to facilitate the formation and delivery of a nucleophilic hydroxide while metal ion B assists in the departure of the 3′-hydroxyl group.

1.3 – Mechanisms for Phosphoryl Transfer Reactions

Phosphoryl transfer reactions proceed through three possible mechanistic regimes that can be considered as different positions along a continuum (Figure 1-4). In one extreme is the stepwise dissociative, S_N1-like pathway that involves the formation of a metaphosphate intermediate. The other extreme is the stepwise associative pathway that involves the formation of a pentacoordinated phosphorane intermediate. The third domain lies in the middle marked by a concerted mechanism with no intermediate. In the concerted pathway, the degree of nucleophile bond formation and leaving group bond

fission in the transition state could be different depending on the participating molecules and the conditions. In general, phosphoryl transfer from monoesters has been characterized as advancing through a loose transition state (TS) with bond fission ahead of bond formation. In comparison, reactions with phosphate diesters and triesters progress through tighter transition states (Figure 1-4).[2]

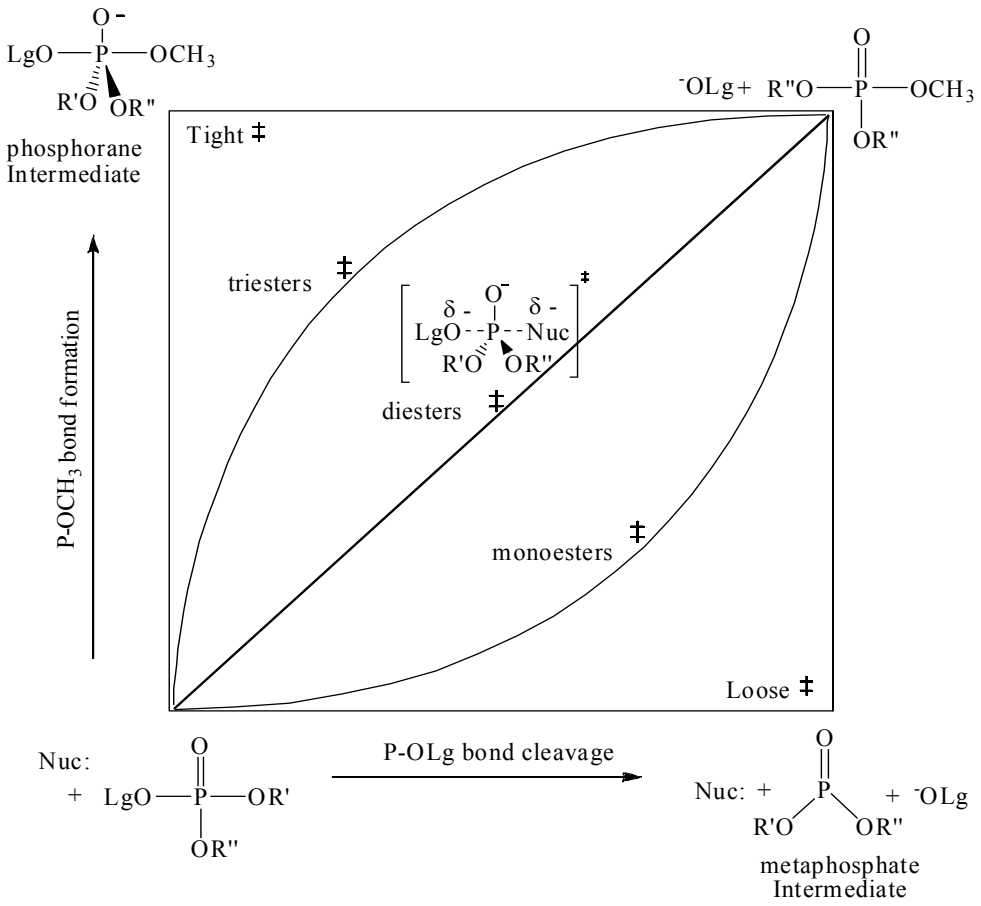

Figure 1-4. A simplified More O'Ferrall Jencks diagram depicting the 2D energy surface for three general phosphoryl transfer reactions where the decomposition of a phosphate monoester is believed to have a loose transition state which becomes increasingly "tighter" TS for phosphate diesters and triesters.

1.4 – Phosphate Monoesters

Phosphate monoesters have two ionizable protons with the first pK_a of an alkyl phosphate monoester being ~2 and the second pK_a being ~6.8. In the absence of catalysts, the hydrolytic cleavages of alkyl phosphate dianions have a half-life ~1.1 x 10^{12} years at 25 ^{o}C.[7] Although the hydrolysis reaction is thermodynamically favorable, a huge kinetic barrier is imposed by the unfavorable electrostatic repulsion between anionic phosphate substrates and anionic nucleophiles. Simple alkyl and aryl phosphate monoesters are commonly used as model substrates in research studies. In most cases, the monoanionic form is more susceptible to hydrolysis than the dianionic counterpart. A rare exception is 2,4-dinitrophenyl phosphate[25] where the dianionic form reacts faster than the monoanion form via a "dissociative-like" transition state where the P-OLg (Lg = leaving group) is almost completely broken. Studies have shown that hydrolysis of phosphate monoester dianions exhibit near zero entropies of activation, small dependence of reaction rates on the basicity of the nucleophile, high sensitivity of rates on the leaving group pK_a,[25,26] and substantial P-^{18}OLg bond cleavage through ^{18}O kinetic isotope study[27]. Despite demonstrating all the characteristics of a dissociative mechanism, complete inversion of stereochemistry for the solvolysis of a chiral phosphate monoester (^{16}O, ^{17}O, ^{18}O labeled) in 50% (v/v) aqueous methanol was observed,[28] suggesting a very loose transition state along a concerted pathway.

When the leaving group is not as activated as 2,4-dinitrophenoxy, the monoanion reacts faster through a rate enhancing protonation of the departing oxygen. This is achieved either through the formation of a zwitterionic ($^{-}$O)$_2$P-O(H^+)-Lg species prior to the rate-limiting chemical step or through an intramolecular proton transfer process with

an intervening water molecule (Figure 1-5).[25,29] Protonation of the bridging oxygen in the transition state results in reduced developing charge on the leaving group and the reaction rates also become less sensitive to the nature of the leaving group pK_a.[25] This is a common outcome of accelerating the rate of the reaction through leaving group stabilization, which will be discussed in more detail in a later chapter. Overall, literature data confirm that the hydrolysis of the monoanions also proceeds through a concerted pathway with a loose transition state.[25,28]

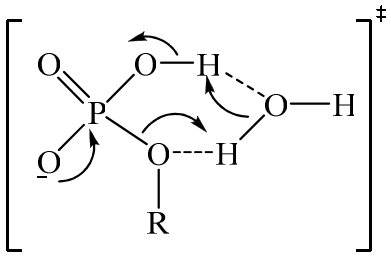

Figure 1-5. Proton transfer within a six-membered cyclic transition state involving a water molecule.

1.5 – Phosphate Diesters

The rate for the uncatalyzed hydrolysis of simple phosphate diesters is sensitive to both the nature of the nucleophiles and the leaving groups.[30] The neutral hydrolysis of *bis*-(2,4-dinitrophenyl) phosphate monoanion is associated with a highly negative entropy of activation ($\Delta S^{\ddagger}$ = -25.5 cal/mol•K)[31], which is roughly 30 entropy units lower than that for neutral hydrolysis of 2,4-dinitrophenyl phosphate dianion. Along with other experimental data,[31,32] reactions between acyclic phosphate diesters and oxyanion nucleophiles most likely involve a concerted pathway without the formation of a phosphorane intermediate.[33]

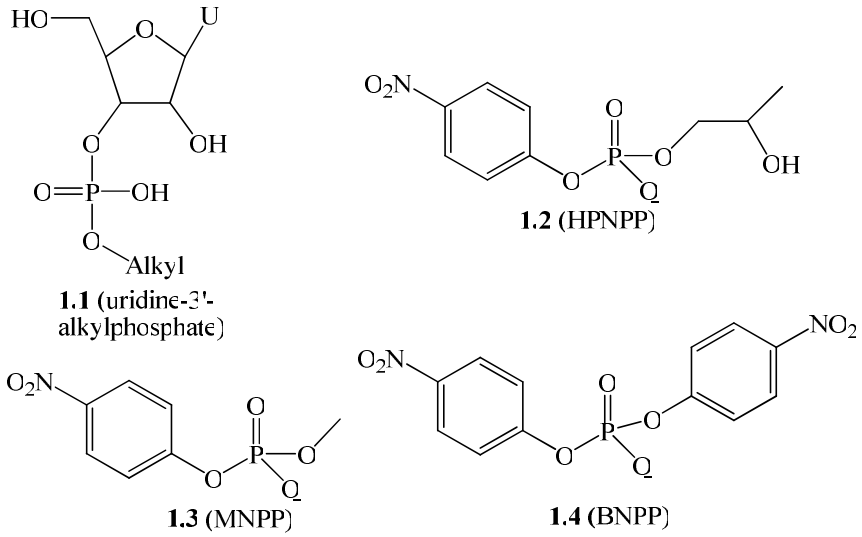

However there is good evidence that phosphate diesters having an internal nucleophilic β-hydroxy group, such as uridine 3′-phosphate diesters (eg. **1.1**) and probably 2-hydroxypropyl phosphates (eg. **1.2**),[34] do react through the formation of stable pentacoordinate phosphorane intermediates[35,36]. Williams *et al.* have demonstrated that base-promoted transesterification of uridine 3′-phosphate esters (Figure 1-6A) exhibits a break in the Brønsted plot of the log of the second order rate constant (k_2^{-OH}) vs. the pK_a of the conjugate acid of the leaving group $^-$OR. The break occurs at the quasi-symmetrical point where the pK_a of the conjugate acid (HOR) of the leaving group is close to the pK_a of the nucleophilic 2′-OH group (pK_a =12.85). This is consistent with a step-wise mechanism with rate-limiting cyclization for substrates with good leaving groups (HOR pK_a < 12.58) and rate-limiting P-OR bond fission from the phosphorane intermediate produced from substrates with poorer leaving groups (HOR pK_a > 12.58).[35] Under acidic conditions, the hydrolysis of neutral uridine-3′-alkylphosphate (**1.1**) produces both the cyclic 2′,3′-phosphate (**1.5**) and the uridine 2′-phosphate diesters (**1.6**; Figure 1-6B).[37] This again suggests the presence of a cyclic phosphorane intermediate

that is stable enough to isomerize, yielding uridine-2′-alkylphosphate.[38,39] In contrast, under basic conditions, no isomerization of uridine 3′-alkylphosphate was observed, suggesting that, if formed, the anionic phosphorane is too unstable to undergo pseudo-rotation and isomerization to yield the 2′-phosphate diester.

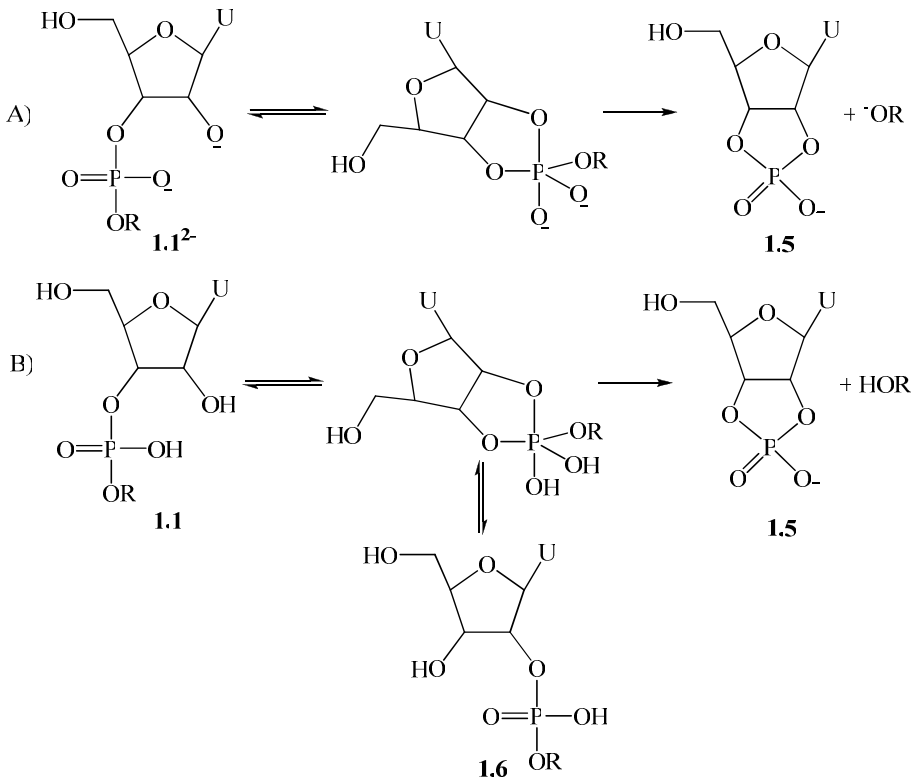

Figure 1-6. A) Base-promoted cyclization of uridine-3′-alkylphosphates and uridine-3′-arylphosphates; B) Acid-promoted cyclization and isomerization of uridine-3′-alkylphosphate.

Even with an intramolecular nucleophilic reaction, the half-life for the cleavage of RNA at 25 ^{o}C and pH 7 has been estimated to be around 110 years. Meanwhile the half-time for the P-O cleavage of DNA in water at 25 ^{o}C and pH 7 has been estimated to be around 10-1000 million years.[7] This makes it difficult to conduct mechanistic studies on

phosphate diesters, especially DNA. Often activated diesters such as diaryl phosphates and methyl aryl phosphates are used as model substrates.[10,23] A very popular model substrate for RNA is 2-hydroxylpropyl-4-nitrophenyl phosphate (HPNPP, **1.2**), which contains an internal nucleophilic hydroxyl group to mimic the 2′-OH group of RNA. Similarly, methyl *p*-nitrophenyl phosphate (MNPP, **1.3**) and *bis*(*p*-nitrophenyl) phosphate (BNPP, **1.4**) are commonly used as DNA models. In addition to their greater reactivity, these model substrates generate a *p*-nitrophenol or *p*-nitrophenoxide leaving group that can be easily monitored by UV-vis spectrophotometry. Substrates with a *p*-nitrophenyl leaving group have the advantage of simple visualization and fast reaction times, but they do not faithfully represent the natural substrates, which contain much poorer leaving groups.[23a,40] Therefore, any mechanistic conclusions based on a single substrate or substrates with similar leaving groups must be made with caution. An alternative strategy would be to conduct a structure-reactivity study with a series of substrates with varying leaving groups and performs long extrapolation. However, even reactions involving less activated aryloxyl leaving groups, such as phenyl or *p*-chlorophenyl, can be extremely slow and must be monitored under elevated temperature, followed by subsequent extrapolation of the reaction rate back to physiological temperature.

1.6 – Mono-Metallo Enzyme Mimics

Zinc is the second most abundant transition metal in biological systems following iron, and it has been found in many metalloenzymes responsible for phosphoryl transfer reactions.[3] Some of the properties that make zinc a desirable catalytic metal include rapid ligand exchange, flexible and diverse coordination geometry, intermediate polarizability,

Lewis acidity, high bioavailability, and lack of redox activity.[3e] Therefore, it is not surprising to find many phosphoesterases containing one or more zinc ions. [3b,10,23,24]

Since the early 1950s, various groups have shown that metal ions alone in water can promote the cleavage of phosphate diesters, but at pH values above the pK_a of the $M^{x+}(H_2O)_n \rightleftharpoons M^{x+}(^{-}OH)(H_2O)_{n-1} + H_3O^{+}$ ionization, the metal hydroxo species often exist as gels or insoluble polymeric species, which complicate mechanistic analysis. In many cases the use of various ligands to form active metal complexes circumvents the latter problem.[23,24] Complexation with anionic ligands often results in complexes with reduced catalytic activity due to a reduced Lewis acidity.[23,41]

One of the first synthetic metal complexes designed for catalyzing the transesterification of HPNPP (**1.2**) involved Zn(II) and imidazole.[42] The results from that study are consistent with Lewis acid catalysis by Zn(II) to increase the electrophilicity of the phosphorous center. The catalytically active species contains one Zn(II) ion, and the optimized Zn(II)/imidazole system exhibited an 850-fold rate acceleration over the background hydroxide catalyzed reaction at 37 ^{o}C and pH 7 in water. Since then, there has been a lot of interest in stable metal complexes with neutral macrocyclic ligands that do not compromise the Lewis acidity of the metal ions.23,[43,44] A survey of a wide range of ligands (Figure 1-7)[43] reveals a few interesting trends.

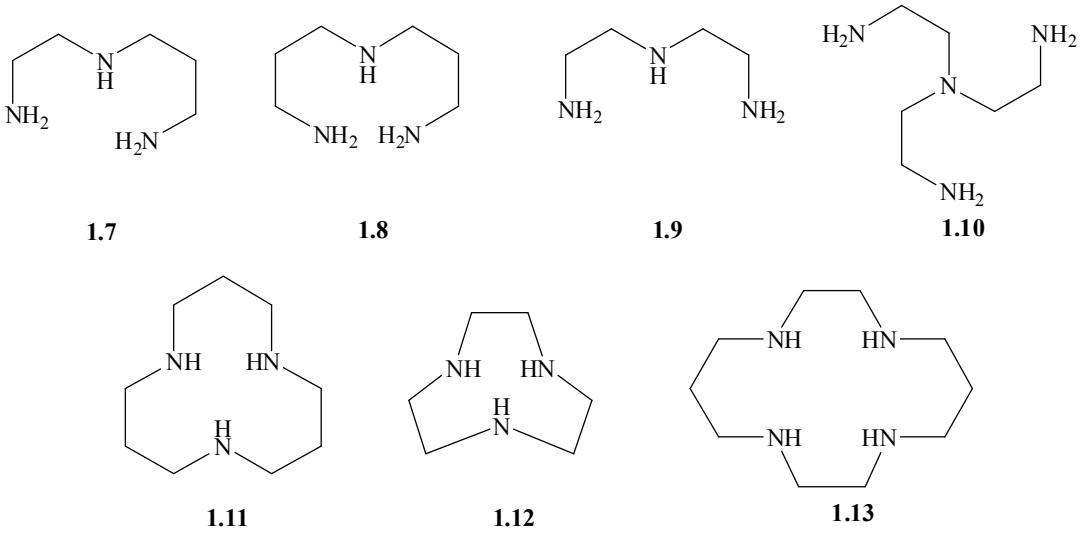

Figure 1-7. Various neutral tridentate and tetradentate ligands for binding metal ions.

First, the architecture of the ligand plays a significant role in the activity of the catalyst. Tetradentate ligands reduce the Lewis acidity of the metal ion to a greater extent than the tridentate ones. As a consequence, the metal bound water molecules in tetradentate ligand derived complexes are less acidic, which indicates that: a) it is more difficult to generate the active M^{2+}-$^{-}$OH nucleophile or base; and b) the metal-bound hydroxide will probably be more nucleophilic due to higher basicity. However, tetradentate-Zn(II) complexes (**1.10** and **1.13**) are less effective at catalyzing the transesterification of HPNPP despite having a more basic metal-bound water molecule. Similar findings were reported by Koike and Kimura[45], where the authors rationalized that when the four binding sites on Zn(II) are occupied by a tetradentate macrocycle, the increased steric crowding around the metal center disfavors metal-substrate interaction. In addition, even if Zn(II) were to expand its coordination number and adopt the trigonal bipyrimidal geometry that is often observed in biological systems,[3] it would still not be able to simultaneously bind both the phosphate substrate and a hydroxide/alkoxide. In

contrast, metal complexes with tridentate ligands allow sufficient room to recruit both the phosphate substrate and a lyoxide in a trigonal bipyrimidal geometry.

Another interesting feature is that the metal-bound water in Zn(II)-complexes containing linear ligands (**1.7** – **1.9**) have higher pK_a values than those with macrocycles (**1.11, 1.12**). Having a more acidic metal-bound water/alcohol is especially attractive, because it means that under physiological pH a higher concentration of the active metal-hydroxide/alkoxide species will be present.

Due to the intrinsic stability of DNA model compounds, it is a more challenging task to study metal catalyzed reactions unless the catalyst can substantially increase the rate of the reaction or if a highly activated substrate is used. One of the first reports of metal catalyzing the cleavage of BPNP (**1.4**) involved Zn(II)-complexes of TREN (**1.10**) and 2,2'-bipyridyl.[46] It was shown that the mono-Zn(II) complex with 2,2′-bipyridyl provides a 53-fold rate acceleration over the background hydroxide promoted hydrolysis of BPNP at pH 7 and 25 ^{o}C, whereas the mono-Zn(II):**1.10** only provides a two-fold rate acceleration for the same reaction.[46] One way to construct a more efficient catalyst is to attach an internal nucleophile to the metal complex (such as the use of ligands **1.14**-**1.17**).[47,23f] Although the presence of a pendant alcohol on the ligand can greatly accelerate the cleavage of BPNP, the phosphorylated complexes generated from the nucleophilic attack do not undergo further hydrolysis to regenerate the catalyst.

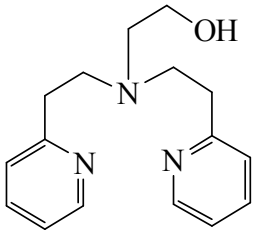

1.14

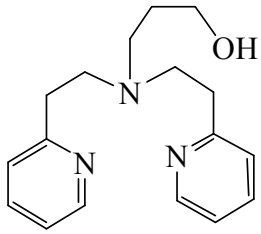

1.15

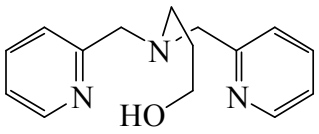

1.16

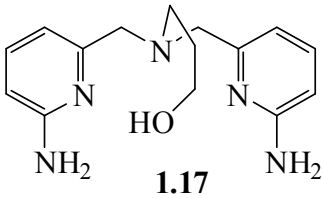

1.17

1.7 – Multinuclear Enzyme Mimics

Multinuclear complexes have attracted growing attention as enzyme mimics since the extraordinary catalytic efficiency exhibited by natural metallonucleases is often derived from the cooperativity in the dinuclear core.[2,3,23,24] One of the first attempts to incorporate two metal ions into a synthetic ligand was by Breslow and Chapman, who managed to accelerate the transesterification of the RNA model HPNPP by 1072-fold relative to the background hydroxide reaction using the di-Zn(II) complex of ligand **1.18**.[44b] $Zn(II)_2$:**1.18** catalyst is about five times more reactive than the analogous mononuclear Zn(II):**1.19** complex under similar experimental conditions. $Zn(II)_2$:**1.18** is also approximately five times more effective at catalyzing the hydrolysis of DNA model BPNP than the mononuclear Zn(II):**1.19** catalyst. This appears to be a common theme, since when comparison can be made, the dinuclear catalysts are often more efficient than the mononuclear counterpart. The dinuclear $Zn(II)_2$:**1.20** is roughly 200 times more potent at facilitating the cleavage of HPNPP than the mononuclear Zn(II):**1.21**.[48] There are other examples of using di-Zn(II) complexes (with ligands **1.22,**[49] **1.23,**[50], and **1.24** -

1.26[51]) to promote the hydrolysis of phosphate diesters, but none of these demonstrates significant rate acceleration over the background hydroxide reaction.

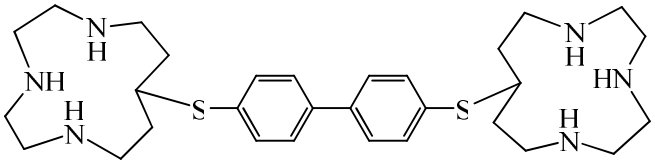

1.18

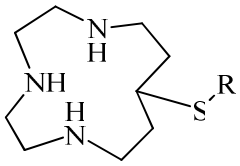

1.19

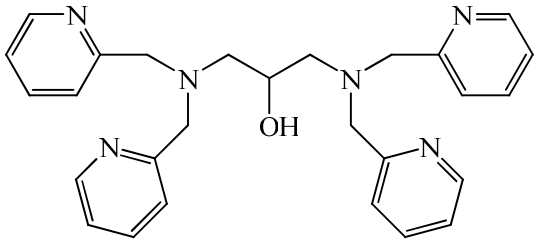

1.20

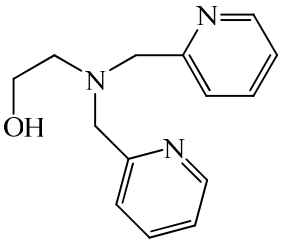

1.21

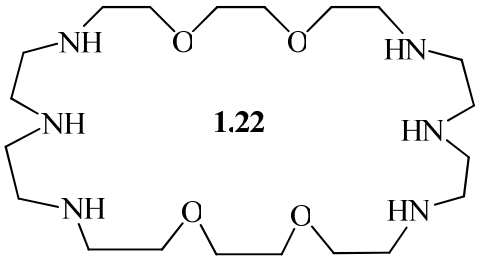

1.22

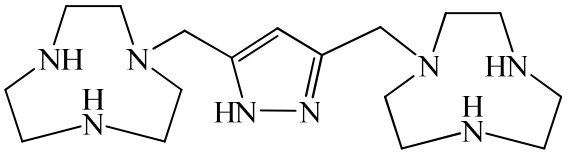

1.23

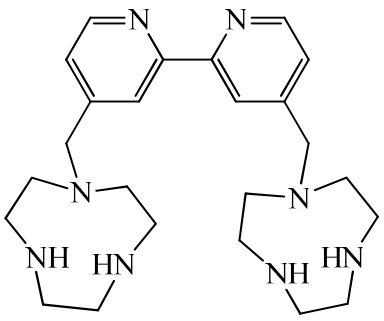

1.24

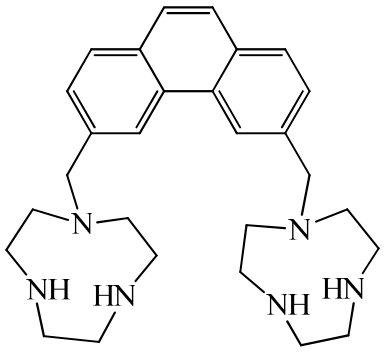

1.25

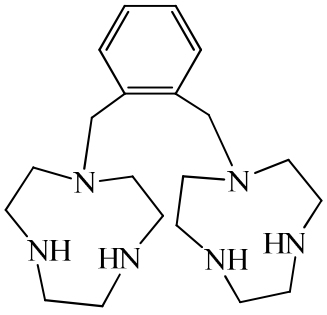

1.26

Reinhoudt and Engbertsen *et al*. briefly explored the effectiveness of trinuclear catalysts by attaching different numbers of metal binding 2,6-bis(aminomethyl)pyridine units onto the upper rim of a calyx[4]arene (**1.27**).[52] They found that between the mono-, di-, and tri - Zn(II) complexes of **1.27**, the trimetallic complex can provide approximately 32,000-fold rate acceleration over the hydroxide promoted transesterification of HPNPP at pH 7 and 25 ^{o}C. Although the tri-Zn(II) complex exhibited 35 times greater reactivity than the monometallic complex, the difference in reactivity between the trinuclear complex and the 1,3-dimetallic complex of **1.27** was minimal.

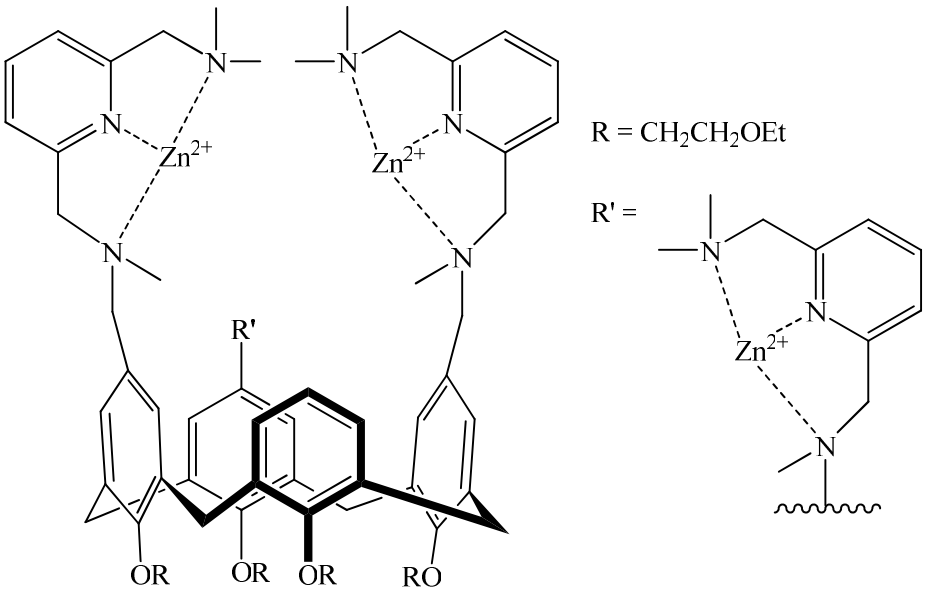

1.27

Comprehensive compendia of some notable metal complexes used as catalysts for the solvolytic cleavages of phosphate diesters in water are available.[23,24] In most cases, the dinuclear catalysts are not significantly better than the mononuclear counterpart to justify why many metallonucleases feature a dinuclear core in the active sites. Also, in many cases, the synthetic metallo-enzyme mimics do not facilitate the hydrolysis of

simple phosphate diesters any better than hydroxide alone. There are a few notable exceptions (eg. $Zn(II)_2$:**1.28**[24a] and di-Co(III) complexes **1.29**[53]) where significant rate acceleration over the hydroxide reaction was observed for the cleavage of phosphate diesters, but the magnitude of the acceleration still pales in comparison with those observed in enzymatic catalysis.

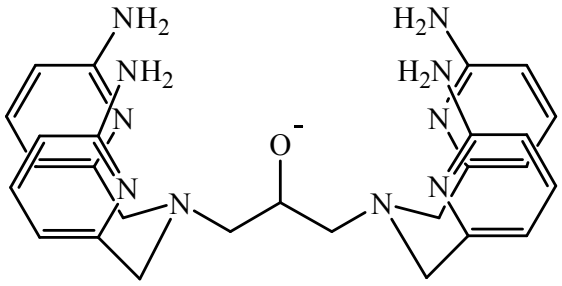

1.28

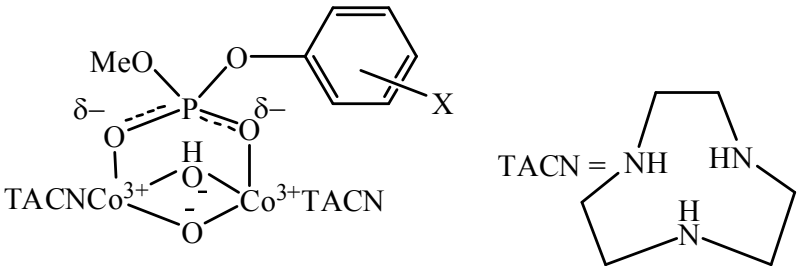

1.29

The di-Zn(II) complex of **1.28** is one of the exceptions, and it is one of the most efficient catalysts for the cleavage of phosphate diesters in water. In the presence of $Zn(II)_2$:**1.28**, the cyclization of HPNPP (**1.2**) exhibits saturation kinetics with a second order rate constant of 53 $M^{-1}s^{-1}$ at pH 7.4 and 25 ^{o}C in water. Compared to the background hydroxide-promoted reaction under the same conditions, catalyst $Zn(II)_2$:**1.28** provides approximately 10^6-fold rate acceleration for the cyclization of HPNPP (**1.2**).[24a] A component of the catalytic efficacy was attributed to double Lewis acid activation of the phosphate substrate by the dinuclear core of the catalyst. The reactivity of

$Zn(II)_2$:**1.28** was further compared with a similar complex, $Zn(II)_2$:**1.20**, showing that the presence of the 2-amino groups resulted in enhanced catalysis (second order rate constant for the cyclization of HPNPP by $Zn(II)_2$:**1.28** is about 100 times greater than that by $Zn(II)_2$:**1.20** in water). Part of the enhanced catalytic activity is due to stronger binding of the substrate to the metal complex, which was attributed to hydrogen bond interaction between the phosphate substrate and the 2-amino groups.

Interestingly, catalyst $Zn(II)_2$:**1.28** (1 mM) is also capable of providing 10^6-fold rate acceleration for the cleavage of uridyl(3′-5′)uridine at pH 7.3 and 25 ^oC in water. This demonstrates that $Zn(II)_2$:**1.28** is just as effective at catalyzing the cleavage of a phosphate diester that contains a much poorer leaving group than *p*-nitrophenoxy (as in HPNPP). This is another rare exception since many catalysts that are capable of catalyzing the cleavage of activated phosphates, such as HPNPP (**1.2**) and BNPP (**1.4**), are unable to catalyze the cleavage of substrates with much poorer leaving groups (less activated aryloxyl or alkyl leaving groups).

1.8 – Modelling Enzymatic Reactions

One strategy by which an enzyme can accelerate a specific reaction is to alter the mechanism of the reaction so that the same chemical transformation in the presence of the catalyst would progress through a different and more energetically favorable pathway. This has prompted much debate as to whether enzyme and synthetic catalysts alter the transition states of the uncatalyzed phosphoryl transfer reactions in order to realize substantial catalysis.[54] There is evidence both supporting similar transition states[54,61a,b] or

different transition states[54c-f] between catalyzed and background lyoxide facilitated reactions. It is very interesting that Herschlag and Zalatan found that the extent of substrate bond cleavage in the transition states of the alkaline phosphatase (AP)-catalyzed and the uncatalyzed cleavage of phosphate diesters are similar.[54b] This is also true for the cleavage of monophosphates. Although this is just one example and it certainly cannot be used for generalization, it does raise an interesting issue. For a multi-step process such as phosphoryl transfer reaction where intermediate formation is possible,[2] if a catalyst can greatly stabilize the various transition states and intermediates along the reaction pathway, it might funnel the reaction through a different, but lower energy, pathway. This has provided researchers with new directions for designing catalytic systems. This will be discussed in more detail in chapter 5 where efficient metal-promoted leaving group stabilization appears to influence the transition state for the solvolysis of phosphate esters.

1.9 – Modelling Reaction Environment

As mentioned above, the bulk of enzyme models are studied in aqueous solution.[23,24] At first glance, this seems like a reasonable approach since the typical water content of a cell is approximately 70% by weight. However, the catalytic activities observed by the synthetic catalysts are nowhere close to enzymatic efficiency. More recently, there is emerging consideration of the idea that the "active sites of enzymes are nonaqueous, and the effective dielectric constants resemble those in organic solvents rather than that in water".[55] This is due to the presence of many hydrophobic residues and

functional groups that decorate the enzyme active site. Considering that the electrostatic forces between charged species will be greater in low polarity/dielectric medium where the degree of solvation is reduced compared to water, changing the reaction medium could have considerable impact on the interaction between charged and dipolar substrates and the catalyst. For example, through an inhibition study it was found that alkaline phosphatase exhibits stronger binding for phosphonic acids that contain bulky aromatic/hydrophobic groups.[56] Earlier work from Dr. R. S. Brown's research group has demonstrated that significant catalysis can be achieved for the transesterification of phosphates and carboxylate esters in alcohol medium in the presence of lanthanide and some transition metal catalysts.[10a,d].

There are several advantages in studying these types of reactions in alcohol instead of water. First, where most M^{2+} and M^{3+} systems have the tendency to form insoluble oligomeric chains between the metal ions and hydroxide in water at high pH, the analogous systems are completely soluble in alcohol throughout the ${}^{s}_{s}\mathrm{pH}$[57] region where the formation of the metal ion alkoxides occurs. This makes it easier to study reactions in alcohol, and sometimes it can eliminate the necessity of complexing ligands to stabilize metal ions. Secondly, alcohols have lower dielectric constants and polarity relative to water (D_r or ε = 78 (water), 31.5 (methanol), 24.3 (ethanol))[58], which should enhance electrostatic attraction between cationic metal ion and any anionic or dipolar substrates. For example, for metal-catalyzed transesterification of phosphates or carboxylate esters, often there is a pre-equilibrium binding process (K_b) between the catalyst and the substrate prior to the chemical event (k_{cat}). This means that the overall rate of the reaction would be proportional to $k_{cat}K_b$. According to the Coulomb expression

in eq. 1, the electrostatic potential energy (P.E.) for the association of spherical ions in solution is inversely proportional to the dielectric constant of the medium:

$$P.E. = (z_+ e)(z\_e)/(4\pi D_0 D_r r) \quad (1)$$

where z_+ and z_- are the absolute values for the charges on the cation and the anion, e is the elementary charge (1.602 x 10^{-19} Coulombs), r is the distance between the centers of the two ions, D_0 is the permittivity of a vacuum (8.854 x 10^{-12} C^2 N^{-1} m^{-2}) and D_r is the relative permittivity or the dielectric constant of the medium. Everything else being constant, shifting from water (D_r = 78) to methanol (D_r = 31.5) increases the electrostatic potential energy for the association of two oppositely charged species by a factor of 2.5. For a hypothetical binding process with a binding energy of 3.0 kcal/mol in water, the binding constant between the two oppositely charged species increases by ~2000-fold in passing from water to methanol at 25 ^oC (ignoring specific changes in solvent effects and changes in entropy upon binding for simplicity).[59] In theory, a larger binding constant could potentially increase the reaction rate by increasing the $k_{cat}K_b$ value. In principle, catalysis would only be possible if the enhanced interaction between the catalyst and the substrate leads to greater energy stabilization for the rate-limiting transition state of the catalyzed reaction relative to binding of the ground state.

The third major advantage of catalytic systems in alcohol is that the products generated from the reaction do not exhibit significant product inhibition. A phosphate diester is generated from the alcoholysis of a phosphate diester, whereas a dianionic phosphate monoester is generated from the hydrolysis of a phosphate diester (Figure 1-8).

Being doubly negatively charged at ≥ neutral pH (where most synthetic catalysts are active with the formation of metal-bound alkoxide/hydroxide), the dianionic monophosphate product will bind stronger to the cationic metal catalyst than the monoanionic diester substrate. Therefore, alcoholysis reactions in alcohol do not have the issue of product inhibition that is commonly observed in water.[10,23,24] Other important advantages include improved catalyst and substrate solubility, and higher complexation constant between metal ions and various chelating ligands in alcohols. These two factors can easily render studying certain catalytic systems impossible in water.

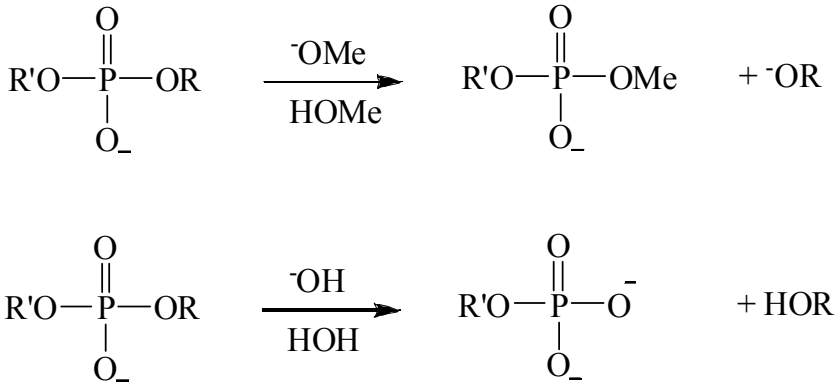

Figure 1-8. Methanolysis (top) and hydrolysis (bottom) of phosphate diester.

1.10 – Cooperativity in Zn(II)-Catalyzed Transesterification of an RNA Model in Alcohols

Earlier reports have demonstrated that the medium effect exerted by alcohols can bring together two Zn(II):1,5,9-triazacyclododecane complexes ([Zn(II):**1.11**]$_2$) to cooperatively catalyze the cleavage of an RNA model HPNPP (**1.2**). In water, the complex HO$^-$:Zn(II):**1.11** binds phosphate diesters very weakly (binding constant K_B <

0.5 M^{-1}) and the catalyzed cleavage of HPNPP in water is linear in [HO^-:Zn(II):**1.11**] and does not show any evidence for higher order terms in complex concentration.[43,45] However, when the same catalytic system is moved into methanol, an upward curvature in the plot of k_{obs} vs. [Zn(II):**1.11**] is observed,[60] consistent with the onset of a catalytic process that is bimolecular in catalyst. Interestingly, by shifting the reaction medium into an even less polar solvent in ethanol, not only can the third-order process involving one molecule of HPNPP and two molecules of Zn(II):**1.11** be observed at lower [catalyst], saturation kinetics are also observed (Figure 1-9),[61] indicating significant buildup of the dinuclear complex [Zn(II):**1.11**]$_2$:HPNPP, which has higher reactivity than the mononuclear species [Zn(II):**1.11**]:HPNPP. In fact, at approximately one ^s_spH unit lower than neutrality in ethanol[62,63] and 25 ^oC, the rate constant for the catalyzed transesterification of HPNPP in the dinuclear complex [Zn(II):**1.11**]$_2$:HPNPP is about 1.7 trillion times larger than the background ethoxide reaction.

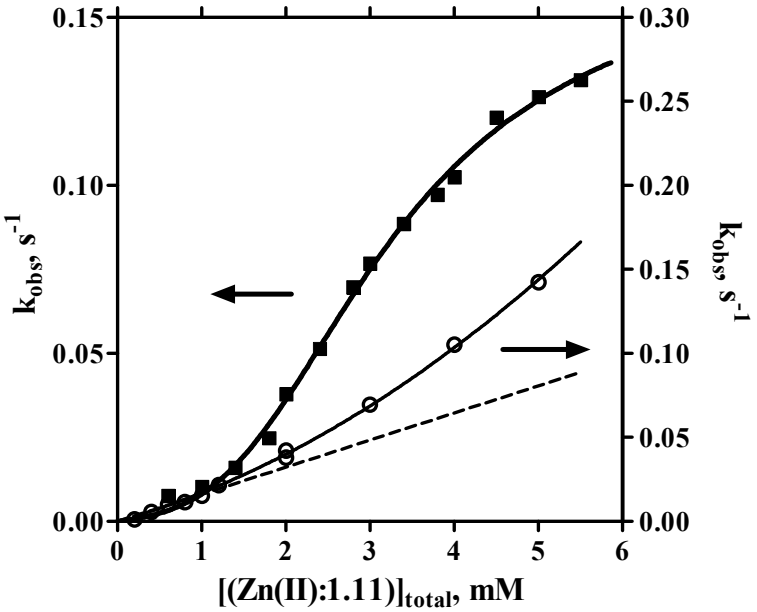

Figure 1-9. Plot of k_{obs} vs. total $[(Zn(II):\mathbf{1.11}]_{total}$ for the cyclization of HPNPP (**1.2;** 8 x 10^{-5} M) in ethanol (■, left y-axis) and methanol (○, right y-axis). The dotted line corresponds to a process first order in [Zn(II):**1.11**], while solid lines are nonlinear least square fits to kinetic expressions for the reactions of both the mononuclear [Zn(II):**1.11**] and the dinuclear $[Zn(II)_2$:**1.11**] complexes as described in ref. [61].

Furthermore, Zn(II) ion alone readily forms highly reactive dimeric complex of $[Zn(II):HPNPP]_2$ in ethanol in the absence of any complexing ligands. This is described by the process illustrated in Figure 1-10, where the maximum rate constant for the cleavage of HPNPP inside this dinuclear complex is 2.92 ± 0.06 s^{-1} at $^{s}_{s}$pH 7.1 and 25 ^{o}C, which is about 4 x 10^{14} times greater than the background ethoxide reaction at this $^{s}_{s}$pH .[61] The second molecule of the phosphate diester appears to play an important structural role to stabilize the dinuclear core. Consistent with this idea, a highly catalytically active complex can be generated *in situ* by mixing Zn(II) ion with nonreactive phosphate,

diphenyl phosphate, in ethanol. The above examples clearly demonstrate that highly efficient catalytic systems for phosphoryl transfer reactions can be achieved with dinuclear complexes. Also, in alcohols the solvent effect can enhance the cooperative benefit of a dinuclear reactive core by encouraging its formation.

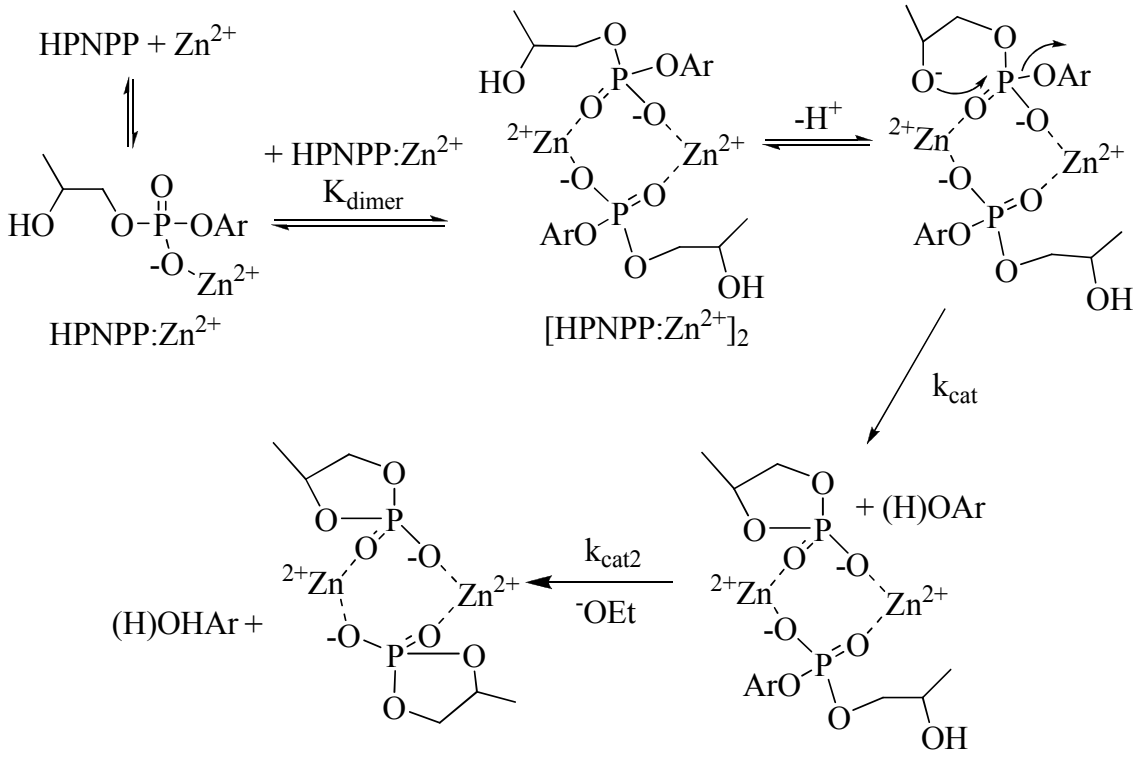

Figure 1-10. Zn(II)-promoted cyclization of HPNPP (**1.2**) in ethanol; modified from ref. [61].

1.11 – A Dinuclear Zn(II) RNase and DNase Enzyme Mimic in Methanol

The obvious approach to fully realize the catalytic benefits a dinuclear catalytic core is to physically link two metal complexes together as has been done in many small molecule enzyme mimics water. This should lower the entropic penalty by transforming a

trimolecular process to a bimolecular one. A common structural motif among dinuclear enzyme mimics in water is the presence of a fixed bridging alkoxide group such as in ligands **1.28** and **1.30**,[23,24] where the alkoxide group reduces the electrostatic repulsion between the two cationic metal centers.[10c,64] This shielding effect seems to be critical in water to form stable dinuclear complexes that hold two metal centers in close proximity. However, the presence of the fixed bridging alkoxide group should reduce the available coordination number around the metal ions, as well as the overall Lewis acidity of the catalyst, thus affecting the acidity of the metal-bound solvent molecule. Subsequently, Mohamed *et al.* have shown that the incorporation of the bridging alkoxide group into the catalyst architecture is detrimental to catalytic efficiency relative to an analogous complex without it, as one would expect.[65]

Stable dinuclear complexes can be easily formed in alcohols with ligands lacking a fixed bridging alkoxide group. These include $Zn(II)_2$:**1.31**,[60] $Cu(II)_2$:**1.31**,[66] $Zn(II)_2$:**1.32,**[67] and various different di-Zn(II) complexes reported by our group.[65,68] Often, the two metal ions are transiently bridged by a solvent alkoxide or a phosphate substrate. Besides facilitating more favorable formation of a dinuclear complex, the medium effect exerted by the less polar alcohol solvents has a profound impact on the catalytic efficiency by stabilizing interaction between the catalyst and the transition state of the reaction as described in an earlier section.

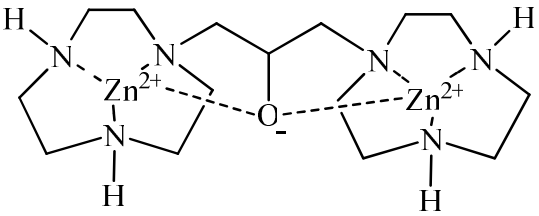

$Zn(II)_2$:**1.30**

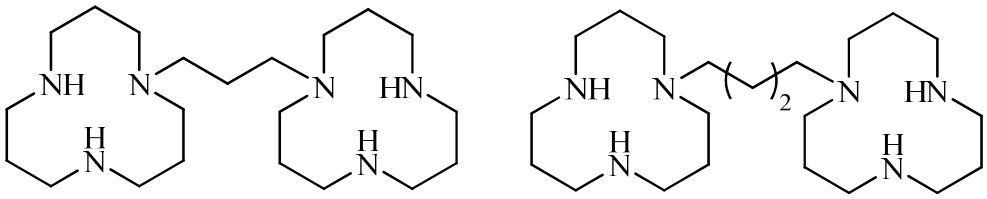

1.31 **1.32**

In an early account, R. S. Brown's lab reported highly efficient catalysis for the cleavage of an RNA model (HPNPP; **1.2**) and a DNA model (MNPP; **1.3**) by a dinuclear complex $Zn(II)_2$:**1.31** in methanol.[60] The same complex has been reported to be relatively unreactive (~1.2 – 4.4 times better than mononuclear Zn(II):**1.11**) for the same type of reaction in water.[69] The X-ray crystal structure of $Zn(II)_2$:**1.31** grown in methanol (Figure 1-11) shows the two metal ions are bridged by a hydroxide with Zn-Zn distance being 3.67 Å,[70] which is similar to the metal-metal distance (~4 Å)[3] that is commonly observed for the dinuclear core inside enzyme active sites. In terms of catalysis, $Zn(II)_2$:**1.31** provides ~10^{12}-fold rate acceleration for the cleavage of HPNPP and MNPP over the background methoxide reactions at $^{s}_{s}$pH = 9.8 (neutrality in methanol = $^{s}_{s}$pH 8.38)[57] and 25 ^{o}C in methanol. Over the last few years, my research (described in the following section) involved several mechanistic investigations stemming from the impressive metal ion catalysis observed in methanol.

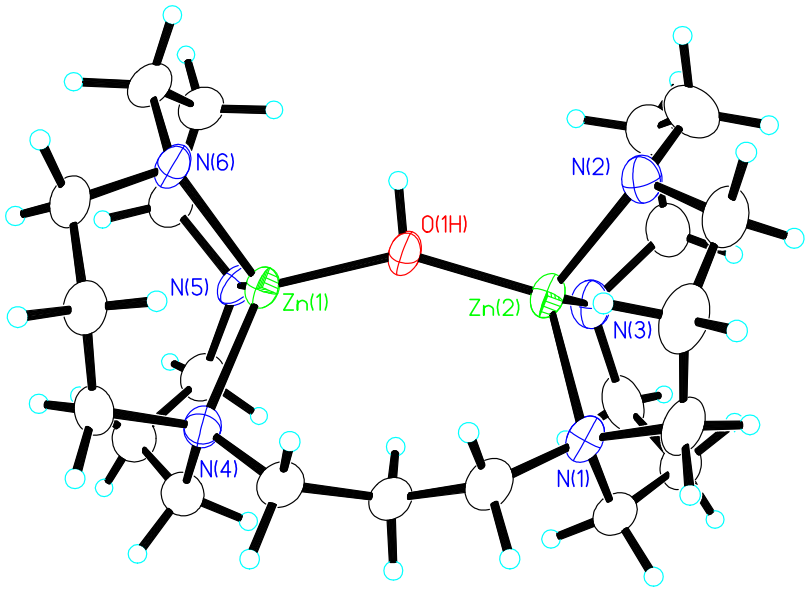

Figure 1-11. X-ray crystal structure of **1.31**:Zn_2:($^-$OH)($CF_3SO_3^-$)$_3$($HOCH_3$) with counterions and solvating methanol omitted for clarity. Reproduced from ref. [70].

1.12 – Research Outline

The dinuclear catalyst Zn(II)$_2$:**1.31** in alcohols was, and still is, the most efficient small molecule enzyme mimic reported in the literature for the cleavage of phosphate diesters. It provides rate accelerations for the cleavage of simple phosphate diesters that are close to those observed in natural enzymes (~10^{17}-fold rate acceleration).[7] These observations posed a few important questions that needed to be addressed. First, what role does the catalyst, Zn(II)$_2$:**1.31,** play in the phosphoryl transfer reactions? Second, what is the mechanism for the catalyzed reaction, and does the catalyzed process proceed through a different reaction pathway than the simple alkoxide promoted reactions? Also,

what comparisons can be made between the mechanisms for the phosphoryl transfer reactions in alcohols, both catalyzed and uncatalyzed, and the wealth of available hydrolysis data? Furthermore, what is the origin of the highly efficient catalysis? Finally, the most fundamental query would be what we can learn from these simple enzyme mimics that can be applied to actual enzymatic catalysis in Nature, and can we create an artificial system that can rival enzyme catalysis in terms of reaction rate.

To answer those questions, I decided to first focus on the highly efficient dinuclear $Zn(II)_2$:**1.31** catalytic systems in alcohols. It offered the opportunity to probe many mechanistic details that would eitherwise be impossible to accomplish with less effective catalytic systems. For example, catalyst $Zn(II)_2$:**1.31** allowed us to study the cleavage of less activated phosphate substrates (with poorer leaving groups) in alcohols because the catalysis is efficient enough to bring those reactions into a manageable experimental timescale. Furthermore, catalyst $Zn(II)_2$:**1.31** binds phosphate substrates strongly in alcohols, while substrate-catalyst complex is rarely kinetically observed in most catalytic systems in water. This allowed us to probe the initial binding event between the catalyst and the substrate prior to the transesterification step. Using $Zn(II)_2$:**1.31** as a model for the dinuclear core in the phosphoesterases active sites, we investigated the catalyzed cleavage of series of DNA and RNA analogues in alcohols. We wanted to know for our minimalist enzyme model (just the dinuclear core), what are the roles of the metal ions and how does the catalyst facilitate the cleavage of phosphate diesters. In addition, we wanted to know whether just the dinuclear core and an alcohol reaction medium are sufficient in achieving the type of catalysis observed in enzymes.

Since such a simple modification, switching the reaction medium from water to methanol, drastically alters the complex's ability to catalyze the transesterification of phosphate diesters, comparisons were made between our catalytic systems in alcohols with existing examples in aqueous medium. We also examined the effect of moving the dinuclear $Zn(II)_2$:**1.31** catalytic system into ethanol, an even less polar solvent than methanol, since we were interested in how this shift influences the catalytic efficacy of $Zn(II)_2$:**1.31**, in promoting the phosphoryl transfer reactions.

Another one of our goals was to promote phosphoryl transfer reactions by utilizing three of the proposed major modes of enzyme catalysis: substrate activation, nucleophile activation, and leaving group assistance. We wanted to know if it is possible to generate a catalytic system that has all three modes acting together. At the same time, we were also interested in quantifying the individual components of catalysis.

1.12.1 – Mechanistic Understanding of Efficient Catalysis by a Dinuclear RNase and DNase Mimic in Alcohols

Based on the kinetic difference between the catalyzed cleavage of an RNA model HPNPP (**1.2**) and a DNA model MNPP (**1.3**), a three-step mechanism for the catalytic reaction was proposed.[60] It involves an initial binding step between the dinuclear catalyst $Zn(II)_2$:**1.31** and a phosphate diester followed by a rearrangement step that generates the catalytically active complex that will undergo subsequent chemical cleavage to generate the products. To confirm our proposed mechanism, we decided to take advantage of the highly colored nature of Cu(II) ions and study the catalyzed phosphoryl transfer reaction with the analogous di-Cu(II) complex, $Cu(II)_2$:**1.31**. In Chapter 2, we report

investigations probing the immediate coordination environment surrounding the Cu(II) ions to gain information on the otherwise spectrophotometrically silent binding and rearrangement events of the dinuclear Zn(II) complexes. We provide detailed kinetic data for all three events in the catalytic process in the presence of the $Cu(II)_2$:**1.31** complex.

Furthermore, we were also interested in expanding the substrate scope of the phosphate diesters. We were very interested in how the catalyzed reaction is influenced by the intrinsic reactivity of the phosphate substrate, which can be tuned by altering the substituents on the leaving group. For a multi-step process such as this, it is very possible that moving through a continuum of substrates with different reactivity, the rate-limiting step will change. Unlike the majority of studies in the literature where often only substrates of the *p*-nitrophenyl derivatives (eg. **1.2** and **1.3**) are used, we decided to synthesize a series of RNA (**1.33**) and DNA (**1.34**) model compounds with a wide range of leaving groups (from very activated nitro-substituted phenols to a phenol with an electron donating *para*-methoxy substituent). As will become clear, it would be otherwise impossible to arrive at the same mechanistic conclusion (or the same depth of understanding) without conducting a detailed kinetic study on a series of substrates with different electronic properties. This will be discussed in more detail in Chapter 3 and Chapter 4. In Chapter 3, we also investigate the differences between methanol and ethanol as reaction media.

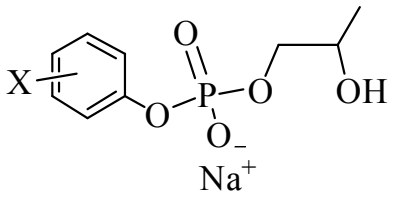

1.33

a. X = 4-NO_2
b. X = 4-NO_2, 3-CH_3
c. X = 3-NO_2
d. X = 4-Cl
e. X = 3-OCH_3
f. X = H
g. X = 4-OCH_3

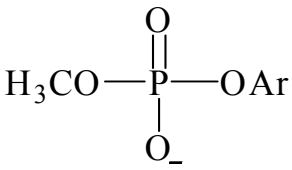

1.34

a. 2, 4-dinitrophenyl
b. 2-chloro-4-nitrophenyl
c. 4-chloro-2-nitrophenyl
d. 2-(methoxycarbonyl)-4-nitrophenyl
e. 2, 4, 5-trichlorophenyl
f. 4-nitrophenyl
g. 2-nitrophenyl
h. 2-nitro-4-methoxyphenyl
i. 3-nitrophenyl
j. 4-chlorophenyl
k. 3-methoxyphenyl
l. 2-(methoxycarbonyl)phenyl
m. phenyl
n. 4-methoxyphenyl

1.12.2 – Catalyzing Phosphoryl Transfer through Metal-Faciliated Leaving Group Stabilization

As mentioned previously, the three proposed major functions of metal ions in metalloenzyme catalysis are Lewis acid activation of substrate, activation and delievery of nucleophile to the reaction center, and stabilization of the leaving group as it departs. Most reported metal-containing enzyme mimics,[23,24] including $Zn(II)_2$:**1.31** (except a small set of special substrates that will be discussed in Chapter 4), catalyze phosphoryl transfer reactions through activating the substrate and the nucleophile.

While difficult to incorporate into catalyst design, leaving group assistance is extremely vital in Nature, since phosphoesterases do not cleave substrates that are activated by having aryloxy leaving groups with strong electron withdrawing

substituents. Especially with the solvolysis of phosphate monoesters which has substantial P-OLg bond fission in the transition state, stabilizing the leaving group as it departs should significantly enhance the reaction rate. Although metal-promoted leaving group stabilization is believed to be a crucial component of many enzymatic reactions, such as the cleavage of phosphate monoesters by alkaline phosphatase,[3] it has rarely been demonstrated to be effective in small molecule enzyme mimics. The major obstacle resides in the design of the metal complexes. When given the choice, metal ions prefer to bind to the non-bridging oxygens, where the majority of the negative charge resides. Therefore, efficient metal-promoted leaving group assistance has rarely been demonstrated in the literature due to the synthetic challenges of positioning the metal ion at the appropriate location to better stabilize the transition state relative to the ground state. We were interested in a catalytic system that provides additional catalysis via leaving group assistance (Chapter 4), and one where we could isolate and quantify the efficacy of metal-promoted leaving group stabilization for the solvolyses of phosphate esters (Chapter 5).

1.12.3 – An Artificial Enzyme with Efficiency Rivalling Natural Enzyme

The ultimate goals of modeling enzymatic reactions are not only to be able to understand how they function, but being able to construct a synthetic catalytic system that can perform the same type of chemical transformation with equal or better efficiency than enzymes. Since enzymes perform hydrolytic cleavage of phosphate esters, concerns regarding our dinuclear systems in alcohol were raised despite demonstrating the undisputable large catalysis that has not been seen to date in water. First, the transesterification of an RNA model involves an intramolecular cyclization, which will

be the same regardless of the solvent system. For DNA model substrates, the catalytic systems are referenced to the appropriate background alkoxide promoted reactions, and we have shown that the phosphoryl transfer reactions in alcohols are generally mechanistically similar to those in water. Therefore, mechanistic conclusions derived from studies in alcohol are expected to be relevant to the situation in water. Finally, the alcohol medium provides a much closer model for the lower effective polarity of the reaction environment inside enzyme active sites than bulk water.

The importance of an appropriate reaction medium as well as the catalytically beneficial solvent effect of low dielectric medium cannot be ignored. To bring this journey full circle, we demonstrated a very simple biomimetic system that can faciliate phosphoryl transfer reactions to water (hydrolysis) with similar efficiency as phosphoesterases. As shown in Chapter 6, a small modification to our dinuclear catalytic system allows us to take advantage of the solvent effect while selectively carrying out the *hydrolysis* of a simple DNA model compound with enzyme-like catalysis (>10^{17}-fold rate acceleration for our catalyzed system) in ethanol containing trace amount of water.

1.13 - References

[1] Westheimer, F. H. *Chem. Rev.* **1981**, *64*, 317.

[2] (a) Hengge, A.C. *Adv. Phys. Org. Chem.* **2005**, *40*, 49 and references therein; (b) Hengge, A. C.; Onyido, I. *Curr. Org. Chem.* **2005**, *9*, 61; (c) Cleland, W. W.; Hengge, A. C. *Chem. Rev.* **2006**, *106*, 3252.

[3] (a) Cowan, J. A. *Chem. Rev.* **1998**, *98*, 1067; (b) Weston, J. *Chem. Rev.* **2005**, *105*, 2151; (c) Wilcox D. E. *Chem. Rev.* **1996,** *96*, 2435; (d) Sträter, N.; Lipscomb, W. N.; Klabunde, T.; Krebs, B. *Angew. Chem. Int. Ed. Engl.* **1996**, *35*, 2024; (e) Lipscomb, W. N.; Sträter, N. *Chem. Rev*. **1996**, *96*, 2375.

[4] Cohen, P. *Eur. J. Biochem.* **2001**, *268*, 5001.

[5] (a) Toy, A.; Walsh, E. N. In *Phosphorus Chemistry in Everyday Living*. 2nd ed.; American Chemical Society: Washington, DC. 1987: Chapters 18-20. (b) Quin, L. D. In *A Guide to Organophosphorus Chemistry. Wiley*: New York, 2000. (c) Gallo, M. A.; Lawryk, N. J. In *Organic Phosphorus Pesticides. The Handbook of Pesticide Toxicology*. Academic Press: San Diego, CA. 1991.

[6] (a) Main, R. A.; Iverson, F. *Biochem. J.* **1966**, *100*, 525; (b) Emsley, J.; Hall, D. in The Chemistry of Phosphorus. Wiley, New York. 1976, p 494.

[7] (a) Wolfenden, R. *Chem. Rev.* **2006**, *106*, 3379; (b) Wolfenden, R.; Snider, M. J. *Acc. Chem. Res.* **2001**, *34*, 938; (c) Schroeder, G. K.; Lad, C.; Wyman, P.; Williams, N. H.; Wolfenden, R. *Proc. Natl. Acad. Sci. USA* **2006**, *103*, 4052; (d) Wolfenden, R.; Ridgeway, C.; Young, G. *J. Am. Chem. Soc.* **1998**, *120*, 833; (e) Warshel, A.; Sharma, P. K.; Kato, M.; Xiang, Y.; Liu, H.; Olsson, M. H. *Chem. Rev.* **2006**, *106*, 3210.

[8] Donarski, W. J.; Dumas, D. P.; Heitmeyer, D. P.; Lewis, V. E.; Raushel, F. M. *Biochemistry*, **1989**, *28*, 4650.

[9] Zalatan, J. G.; Herschlag, D. *J. Am. Chem. Soc.* **2006**, *128*, 1293.

[10] (a) Brown, R. S.; Lu, Z.-L.; Liu, C. T.; Tsang, W. Y.; Edwards, D. R.; Neverov, A. A. *J. Phys. Org. Chem.* **2009**, *22*, 1; (b) Williams, N. H.; Takasaki, B.; Wall, M.; Chin, J. *Acct. Chem. Res.* **1999**, *32*, 485; (c) Morrow, J. *Comm. Inorg. Chem.* **2008**, *29*, 169; (d) Brown, R. S.; Neverov, A. A. *Adv. Phys. Org. Chem.* **2008**, *42*, 271.

[11] Davies, J. F.; Hostomska, Z.; Hostomsky, Z.; Jordan, S. R.; Mahews, D. A. *Science* **1991**, *252*, 88.

[12] Lahm, A.; Volbeda, S.; Suck, D. *J. Mol. Biol.* **1990**, *215*, 207.

[13] Dumas, D. P.; Caldwell, S. R.; Wild, J. R.; Raushel, F. M. *J. Biol. Chem.* **1989**, *264*, 19659.

[14] Mulbry, W. W.; Karns, J. S.; Kearney, P. C.; Nelson, J. O.; McDaniel, C. S.; Wild, J. R. *Appl. Environ. Microbiol*. **1986**, *51*, 926.

[15] Horne, I.; Sutherland, T. D.; Harcourt, R. L.; Russell, R. J.; Oakeshott, J. G. *Appl. Environ. Microbiol.* **2002**, *68*, 3371.

[16] (a) Jedrzejas, M. J.; Setlow, P. *Chem. Rev*. **2001**, *101*, 607; (b) Bosron, W. F.; Anderson, R. A.; Falk, M. C.; Kennedy, F. S.; Vallee, B. L. *Biochemistry* **1977**, *16*, 610.

[17] Parkin, G. *Chem. Rev.* **2004**, *104*, 699.

[18] Sowadski, J. M.; Handschumacher, M. D.; Murthy, H. M. K.; Foster, B. A.; Wykoff, H. W. *J. Mol. Biol*. **1985**, *186*, 417.

[19] Stec, B.; Holtz, K. M.; Kantrowitz, E. R. *J. Mol. Biol.* **2000**, *299*, 1303.

[20] Orhanovic, S.; Pavela-Vrancic, M.; Flogel-Mrsic, M. *Acta. Pharm.* **1994**, *44*, 87.

[21] (a) Freemont, P. S.; Friedman, J. M.; Beese, L. S.; Sanderson, M. R.; Steitz, T. A. *Proc. Natl. Acad. Sci. USA* **1988**, *85*, 8924; (b) Beese, L. S.; Steitz, T. A. *EMBO J.* **1991**, *10*, 25.

[22] Fothergill, M.; Goodman, M. F.; Petruska, J.; Warshel, A. *J. Am. Chem. Soc.* **1995**, *117*, 11619

[23] (a) Mancin, F.; Tecillia, P. *New J. Chem*. **2007**, *31*, 800; (b) Mancin, F.; Scrimin, P.; Tecilla, P.; Tonellato, U. *Chem. Commun.* **2006**, 2540; (c) Morrow, J. R.; Iranzo, O. *Curr. Opin. Chem. Biol*. **2004**, *8*, 192; (d) Williams, N. H. *Biochim. Biophys. Acta*, **2004**, *1697*, 279; (e) Williams, N. H.; Takasaki, B.; Wall, M.; Chin, J. *Acc. Chem. Res*. **1999**, *32*, 485; (f) Livieri, M.; Mancin, F.; Saielli, G.; Chin, J.; Tonellato, U. *Chem. Eur. J.* **2007**, *13*, 2246; (g) Webb, S. J. *Annu. Rep. Prog. Chem., Sect. B,* **2007**, *103*, 392; (h) Lönnberg, H. *Org. Biomol. Chem*., **2011**, *9*, 1687.

[24] (a) Feng, G.; Natale, D.; Prabaharan, R.; Mareque-Rivas, J. C.; Williams, N. H. *Angew. Chem. Int. Ed.* **2006**, *45*, 7056; (b) Iranzo, O.; Kovalevsky, A. Y.; Morrow, J. R.; Richard, J. P. *J. Am. Chem. Soc*. **2003**, *125*, 1988; (c) O'Donoghue, A.; Pyun, S. Y.; Yang. M.-Y.; Morrow, J. R.; Richard, J. P. *J. Am. Chem. Soc.* **2006**, *128*, 1615; (d) Williams, N. H.; Cheung, W.; Chin, J. *J. Am. Chem. Soc.* **1998**, *120*, 8079; (e) Yatsimirsky, A. K. *Coord. Chem. Rev.* **2005**, *249*, 1997.

[25] Kirby, A. J.; Varvoglis, A. G. *J. Am. Chem. Soc.* **1967**, *89*, 415.

[26] Kirby, A. J.; Jencks, W. P. *J. Am. Chem. Soc*. **1965**, *87*, 3209.

[27] (a) Hengge, A. C., Edens, W. A.; Elsing, H. *J. Am. Chem. Soc*. **1994**, *116*, 5045; (b) Gorenstein, D. G.; Lee, Y.-G.; Kar, D. J. *J. Am. Chem. Soc.* **1977**, *99*, 2264.

[28] Buchwald, S. L.; Friedman, J. M.; Knowles, J. R. *J. Am. Chem. Soc.* **1984**, *106*, 4911.

[29] Hoff, R. H.; Hengge, A. C. *J. Org. Chem.* **1998**, *63*, 6680.

[30] (a) Khan, S. A.; Kirby, A. J. *J. Chem. Soc. B.* **1970**, 1172; (b) Kirby, A. J.; Younas, M. *J. Chem. Soc. B*. **1970**, 1165.

[31] Kirby, A. J.; Younas, M. *J. Chem. Soc. B*. **1970**, 510.

[32] Hengge, A. C. *Acc. Chem. Res.* **2002**, *35*, 105.

[33] (a) Williams, A., *Concerted Organic and Bio-Organic Mechanisms,* CRC Press, Boca Raton, USA, 2000, pp 161-181; (b) Bourne, N.; Williams, A. *J. Am. Chem. Soc.* **1984**, *106*, 7591; (c) Bourne, N.; Chrystiuk, E. Davis, A. M.; Williams, A. *J. Am. Chem. Soc.* **1988**, *110*, 1890; Ba-Saif, S. A.; Davis, A. M.; Williams, A. *J. Org. Chem.* **1989**, *54*, 5483.

[34] Brown, D. M.; Usher, D. A. *J. Chem. Soc.* **1966**, 6558.

[35] Lönnberg, H.; Strömberg, R.; Williams, A. *Org. Biomol. Chem.* **2004**, *2*, 2165.

[36] (a) Haake, P. C. *J. Am. Chem. Soc.* **1961**, *83*, 1102; (b) Davis, A. M.; Hall, A. D.; Williams, A. *J. Am Chem. Soc.* **1988**, *110*, 5105; (c) Segal, Y.; Granoth, I. *J. Am. Chem. Soc*. **1978**, *100*, 5130.

[37] a) Oivanen, M.; Schnell, R.; Pfleiderer, W.; Lönnberg, H. *J. Org. Chem*. **1991**, *56*, 3623; b) Jarvinen, P.; Oivanen, M.; Lonnberg, H. *J. Org. Chem*. **1991**, *56*, 5396.

[38] F. H. Westheimer, *Acc. Chem. Res.* **1968**, *1*, 70.

[39] (a) Ovianen, M.; Mikhailov, S. N.; Padyukova, N. S.; Lönnberg, H. *Acta. Chem. Scand.* **1995**, *49*, 307; (b) Thatcher, G. R. J. Kluger, R. *Adv. Phys. Org. Chem.* **1989**, *25*, 99.

[40] Menger, F. M.; Ladika, M. *J. Am. Chem. Soc.* **1987**, *109*, 3145.

[41] Mikkola, S.; Kaukinen, U.; Lönnberg, H. *Cell Biochem. Biophys.*, **2001**, *34*, 95.

[42] Breslow, R.; Huang, D.-L.; Anslyn, E. *Proc. Natl. Acad. Sci. USA* **1989**, *86*, 1746.

[43] Bonfá, L.; Gatos, M.; Mancin, F.; Tecilla, P.; Tonellato, U. *Inorg. Chem.* **2003**, *42*, 3943.

[44] (a) Breslow, R.; Berger, D.; Huang, D.-L. *J. Am. Chem. Soc.* **1990**, *112*, 3686; (b) Chapman, W. H.; Breslow, R. *J. Am. Chem. Soc.* **1995**, *117*, 5462.

[45] Koike, T.; Kimura, E. *J. Am. Chem. Soc.* **1991**, *113*, 8935.

[46] De Rosch, M. A. Trogler, W. C. *Inorg. Chem.* **1990**, *29*, 2409.

[47] (a) Liang, H.-C.; Zhang, Y.; Hetu, M. M. *Inorg. Chem. Commun.* **2007**, *10*, 204; (b) Zhang, Y.; Liang, H.-C. *Inorg. Chem. Commun.* **2006**, *9*, 460.

[48] Feng, G.; Mareque-Rivas, J. C.; Williams, N. H. *Chem. Commun*., **2006**, 1845.

[49] Bazzicalupi, C.; Bencini, A.; Bianchi, A.; Fusi, V.; Giorgi, C.; Paoletti, P.; Valtancoli, B.; Zanchi, D. *Inorg. Chem.* **1997**, *36*, 2784.

[50] Vichard, C.; Kaden, T. A. *Inorg. Chim. Acta,* **2002**, *337*, 173.

[51] Arca, M.; Bencini, A.; Berni, E.; Caltagirone, C.; Devillanova, F. A.; Isaia, F.; Garau, A.; Giorgi, C.; Lippolis, V.; Perra, A.; Tei, L.; Valtancoli, B. *Inorg. Chem.* **2003**, *42*, 6929.

[52] (a) Molenveld, P.; Engbersen, J. F. J.; Reinhoudt, D. N. *Chem. Soc. Rev.* **2000**, *29*, 75; (b) Molenveld, P.; Stikvoort, W. M. G.; Kooijman, H.; Spek, A. L.; Engbersen, J. F. J.; Reinhoudt, D. N. *J. Org. Chem.* **1999**, *64*, 3896; (c) Molenveld, P.; Engbersen, J. F. J.; Reinhoudt, D. N. *Angew. Chem. Int. Ed.* **1999**, *38*, 3189.

[53] Williams, N. H.; Cheung, W.; Chin, J. *J. Am. Chem. Soc.* **1998**, *120*, 8079.

[54] (a) O'Brien, P. J.; Herschlag, D. *Biochemistry* **2002,** *41,* 3207; (b) Zalatan, J. G.; Herschlag, D. *J. Am. Chem. Soc.* **2006**, 128, 1293; (c) McWhirter, C.; Lund, E. A.; Tanifum, E.; Feng, G.; Sheikh, Q. I.; Hengge, A. C.; Williams, N. H. *J. Am. Chem. Soc.* **2008**, *130*, 13673; (d) Humphry, T.; Forconi, M.; Williams, N. H.; Hengge, A. C. *J. Am. Chem. Soc.* **2004**, *126*, 11864; (e) Humphry, T.; Iyer, S.; Iranzo, O.; Morrow, J. R.; Richard, J.; P.; Paneth, P.; Hengge, A. C. *J. Am. Chem. Soc.* **2008**, *130*, 17858; (f) Feng, G.; Tanifum, E. A.; Adams, H.; Hengge, A. C.; Williams, N. H. *J. Am. Chem. Soc.* **2009**, 131, 12771.

[55] Cleland, W. W.; Frey, P. A.; Gerlt, J. A. *J. Biol. Chem.* **1998**, *273*, 25529; (b) Simonson, T.; Carlsson, F.; Case, D. A. *J. Am. Chem. Soc*. **2004**, *126*, 4167.

[56] Landt, M.; Boltz, S. C.; Butler, L. G. *Biochemistry.* **1978**, *17*, 915.

[57] For the designation of pH in non-aqueous solvents we use the forms recommended by the IUPAC, *Compendium of Analytical Nomenclature. Definitive Rules 1997* 3rd ed., Blackwell, Oxford, U. K. 1998. Since the autoprotolysis constant of methanol is $10^{-16.77}$, neutral ${}^{s}_{s}\mathrm{pH}$ is 8.4.

[58] Harned, H. S.; Owen, B. B., *The Physical Chemistry of Electrolytic Solution*; ACS Monograph Series 137, 3rd ed.; Reinhold Publishing: New York, 1957, p 161.

[59] according to $\log (K_b^{MeOH}/K_b^{H2O}) = (\Delta G_{MeOH} - \Delta G_{H2O})/2.303RT$

[60] Neverov, A. A.; Lu, Z.L.; Maxwell, C. I.; Mohamed, M. F.; White, C. J.; Tsang. J. S. W.; Brown, R. S. *J. Am. Chem. Soc.* **2006**, *128*, 16398.

[61] Liu, C. T.; Neverov, A. A.; Brown, R. S. *Inorg. Chem*. **2007**, *46*, 1778.

[62] Autoprotolysis constants of methanol and ethanol are $10^{-16.77}$ and $10^{-19.1}$ M^2 at 25 ^{o}C, respectively (Ref [63]). Therefore, neutral ${}^{s}_{s}\mathrm{pH}$ in methanol and ethanol are 8.39 and 9.55.

[63] For details regarding standardization of electrodes and measurement of ${}^{s}_{s}\mathrm{pH}$ in methanol and ethanol see: a) Gibson, G. T. T.; Neverov, A. A.; Brown, R. S. *Can. J. Chem*. **2003**, *81*, 495; b) Gibson, G. T. T.; Mohamed, M. F.; Neverov, A. A.; Brown, R. S. *Inorg. Chem.* **2006**, *45*, 7891.

[64] Iranzo, O.; Elmer, T.; Richard, J. P.; Morrow, J. R. *Inorg. Chem.* **2003**, *42*, 7737.

[65] Mohamed, M. F.; Neverov, A. A.; Brown, R. S. *Inorg. Chem*. **2009**, *48*, 11425.

[66] Lu, Z.-L; Liu, C. T.; Neverov, A. A.; Brown, R. S. *J. Am. Chem. Soc.* **2007**, *129*, 11642.

[67] Liu, C. T.; Melnychuk, S. A.; Liu, C.; Neverov, A. A.; Brown, R. S. *Can. J. Chem.* **2009**, *87*, 640.

[68] Mohamed, M. F.; Brown, R. S. *J. Org. Chem*. **2010**, *75*, 8471.

[69] Kim, J.; Lim, H. *Bull. Korean Chem. Soc.* **1999**, *30*, 491.

[70] Bunn, S. E.; Liu, C. T.; Lu, Z.-L.; Neverov, A. A.; Brown, R. S., *J. Am. Chem. Soc.* **2007**, *129*, 16239.

Chapter 2 – A Simple Dinuclear DNase and RNase Model System in Methanol

2.1 – Preface

With minor changes, this chapter is largely as it was published in Journal of American Chemical Society (Lu, Z.-L; Liu, C. T.; Neverov, A. A.; Brown, R. S. *J. Am. Chem. Soc.* **2007**, *129*, 11642). Except for obtaining suitable crystals and the subsequent determination of the X-ray structures of the di-Cu(II) complexes, all experiments (synthesis, kinetics, MS experiment, and analytical data collection) were performed by C. Tony Liu. The table of crystal data and refinement details (Table 1 in the published article) has been removed here. The original kinetic data and the complete characterization of the new compounds synthesized for the study can be found in the Supporting Information section for the original paper. The first draft of the manuscript was prepared by me and the final version was prepared in collaboration with Dr. R. Stan. Brown and Dr. Alex A. Neverov. Eq. (3) given below has been corrected from the original expression of $(\Delta\Delta G^{\neq}_{stab} = (\Delta G_{Bind} + \Delta G_{M} + \Delta G^{\neq}_{cat}) - \Delta G^{\neq}_{Non})$, which places a (+)-sign in front of the ΔG_M term. Since K_M refers to the dissociation constant for the Michaelis complex, and we are interested in the binding energy of catalyst and substrate, the correct form of the equation should be $-\Delta G_M$.

2.2 – Introduction

Due to its great stability, the phosphodiester linkage is important for holding together the RNA and DNA biomolecules that are responsible for the storage of genetic information[1,2,3,4,5,6,7]. The half-times for hydrolysis of RNA[8] and DNA[9] at pH 7 and 25 ^{o}C

have been reported to be 110, and up to 100 billion years, respectively. Certain phosphodiesterase enzymes promote the cleavage by up to a factor of 10^{15-16}, giving some of the most spectacular rate enhancements known. Many of these contain active sites with two or more metal ions (usually Zn^{2+} and in some cases Mg^{2+}, Ca^{2+} and Fe^{2+}) as exemplified by ribonuclease H from HIV reverse transcriptase[5], 3′,5′-exonuclease from DNA polymerase I[6], the P1 nucleases[7], and phospholipase C[1,2,3,4]. Not surprisingly, intense research is directed at understanding the origins of catalysis of phosphate diester cleavage provided by metal ion containing systems[10,11,12,13]. The earlier work[10-13] and more recent reports[14,15,16,17,18,19,20] indicate that dinuclear complexes are typically more reactive than their mononuclear counterparts, although in some cases they are slower or only weakly accelerating[18,21,22]. Very recently we reported on the exalted catalysis of the cleavage of an RNA model, 2-hydroxypropyl *p*-nitrophenyl phosphate (HPNPP; **2.1**), promoted by a dinuclear Zn^{2+}-complex ($Zn(II)_2$:**2.2**) in methanol[23]. The plot of k_{obs} for the process vs. [$Zn(II)_2$:**2.2**] in the presence of 1 eq. of added methoxide (which attaches to the metal ions to form $Zn(II)_2$:**2.2**:($^{-}OCH_3$) and maintains the $^{s}_{s}pH$ [24] at 9.5-9.8) was linear with a slope of k_2^{obs} = 275,000 $M^{-1}s^{-1}$. This catalytic k_2^{obs} value is 10^8 larger than the methoxide promoted cyclization of **2.1** (2.56 x 10^{-3} $M^{-1}s^{-1}$)[23], and far exceeds anything previously seen in water. A similar plot for the methanolysis of a DNA model (methyl *p*-nitrophenyl phosphate (MNPP; **2.3**) exhibits Michaelis-Menten behavior with K_M and k_{max} values of 0.37 ± 0.07 mM and (4.1 ± 0.3) x 10^{-2} s^{-1}. That two closely related substrates exhibit such different kinetic behavior seemed unusual and was rationalized by invoking the mechanism given in Scheme 2-1 where the rate-limiting step with **2.1** was

its binding (k_1 or k_2) while that with the slower reacting **2.3** was the chemical step of methanolysis of the bound substrate (k_3).

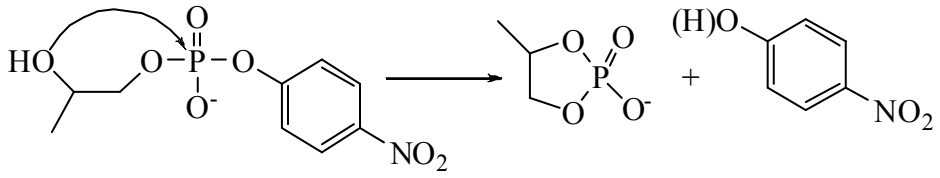

HPNPP, 2.1 **cyclic phosphate**

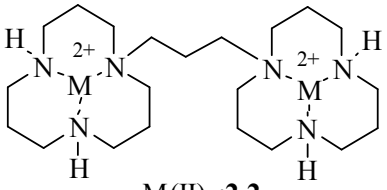

M(II)$_2$:**2.2**

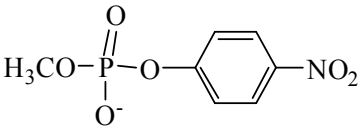

2.3 (MNPP)

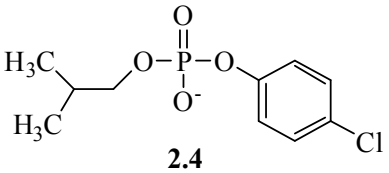

2.4

Scheme 2-1. Stepwise catalytic cycle for the M(II)$_2$:**2.2**-promoted cleavage of phosphate diesters (M = Zn(II) or Cu(II), S = phosphodiester substrate, charges omitted for simplicity).

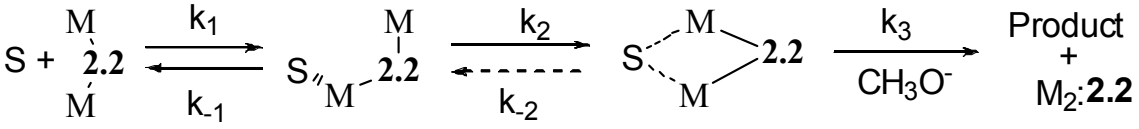

Herein we present results with the Cu(II)$_2$ complex of **2.2** that supports the above mechanism. While it is true that Cu(II) complexes prefer five- and six-coordinate environments which are different from Zn(II) complexes, several of the former are known to catalyze phosphoryl transfer reactions of phosphate diesters and interesting

information of relevance to the mechanism of action has been obtained from their study.[16,22,25,26,27,28,29] Unlike Zn(II) complexes, those with Cu(II) are also highly colored which can give information about changes in the immediate coordination environment around the metal ion. As will be shown, the $Cu(II)_2$:**2.2** complex greatly catalyzes the cleavages of both **2.1** and **2.3**, and it also exhibits two clearly defined steps confirmed with **2.3** and diester **2.4** which appear to be associated with the binding of these substrates to $Cu(II)_2$:**2.2**.

2.3 – Experimental

2.3.1 - Materials

Methanol (99.8% anhydrous), sodium methoxide (0.5 M solution in methanol, dibenzyl phosphate and $Cu(CF_3SO_3)_2$ were purchased and used without further purification. Methyl-*p*-nitrophenyl phosphate (MNPP, **2.3**) and 2-methylpropyl *p*-chlorophenyl phosphate (MPClPP, **2.4**) were prepared according to a general published method.[30] 1,3-*Bis*-N_1,N_1-(1,5,9-triazacyclododecyl)propane (**2.2**) was synthesized for a previous study[23] using a literature recipe[31]. The sodium salt of 2-hydroxypropyl *p*-nitrophenyl phosphate (**2.1**) was prepared according to a slight modification[33] of the literature procedure[32]. The dinuclear complex (**2.2**:$Cu(II)_2$:($^-OCH_3$)) was prepared as a 2.5 mM solution in methanol by sequential addition of aliquots of stock solutions of sodium methoxide, 1,3-*bis*-N_1-(1,5,9-triazacyclododecyl)propane (**2.2**)[31] and $Cu(CF_3SO_3)_2$ in relative amounts of 1:1:2. *It has been found that this order of addition is essential for the formation of the complex and even then its complete formation is achieved only after 10-15 minutes (as monitored by the increase in catalytic activity as a function of time).*

2.3.2 - Methods

^{1}H NMR and ^{31}P NMR spectra were determined at 400 and 162.04 MHz. The $CH_3OH_2^+$ concentration was determined using a combination glass electrode (Radiometer model # XC100-111-120-161) calibrated with standard aqueous buffers (pH = 4.00 and 10.00) as described in previous papers[23,33]. The ${}^{s}_{s}pH$ values in methanol[34] were determined by subtracting a correction constant of -2.24 from the readings obtained from the electrode, while the autoprotolysis constant was taken to be $10^{-16.77}$. The ${}^{s}_{s}pH$ values for the kinetic experiments were simply measured from solutions of the complexes which were made *in situ* by the addition of 1 eq. of ligand **2.2**, one eq. of $NaOCH_3$ and 2 eq. of $Cu(OTf)_2$: the values determined in this way lie in the region of 7.0-7.6, but mostly at 7.2-7.4 for the concentrations where the catalysis was investigated. While the methodology gives some variance in the measured ${}^{s}_{s}pH$ values, particularly at low concentrations of metal ion, we have found that the addition of buffers to control the ${}^{s}_{s}pH$ retards the reaction probably due to inhibition by the associated counterions binding to the catalyst. The first and second ${}^{s}_{s}pK_a$ values for **2.2**:$Cu(II)_2$:($HOCH_3$) (0.4 mM) were determined from duplicate measurements to be 6.77 ± 0.01 and 7.82 ± 0.03 by measuring the ${}^{s}_{s}pH$ at half neutralization whereby the [**2.2**:$Cu(II)_2$:($^-OCH_3$)]/[**2.2**:$Cu(II)_2$:($HOCH_3$)] or [**2.2**:$Cu(II)_2$:($^-OCH_3$)$_2$]/[**2.2**:$Cu(II)_2$:($^-OCH_3$)] ratios were 1.0. This involved treating **2.2**:$Cu(II)_2$:($^-OCH_3$), prepared as described above at 0.4 mM, with ½ eq. of 70% $HClO_4$ or $NaOCH_3$ diluted to an 0.05 M stock solution in anhydrous methanol, and measuring the ${}^{s}_{s}pH$.

2.3.3 - Kinetics

The rates of cleavage of MNPP (**2.3**) (0.04 mM) catalyzed by **2.2:**$Cu(II)_2$:($^-OCH_3$) (5 x 10^{-5} to 6 x 10^{-4} M) were followed by monitoring the appearance of *p*-nitrophenol at 320 nm at 25.0±0.1 °C. The fast rates of binding steps of substrates **2.1**, **2.3** and **2.4** (0.03 mM) to **2.2**:$Cu(II)_2$:($^-OCH_3$) in anhydrous methanol were followed by observing the changes in the $Cu(II)_2$ band at 340 nm at 25 ^oC using a stopped-flow reaction analyzer with a 10 mm light path. In the case of **2.1**, the second binding step is superimposed on that for the production of *p*-nitrophenol which leads to a rise in absorbance as shown in Figure 2-1. For the sets of experiments with **2.1** and **2.3** the [**2.2**:$Cu(II)_2$:($^-OCH_3$)] was varied from 0.25 to 1.0 mM. The two fast steps (termed herein as the first and second binding events) for **2.4** (0.03 mM) were followed at 340 nm and 380 nm while using stopped-flow spectrophotometry at 25 ^oC with the [**2.2**:$Cu(II)_2$:($^-OCH_3$)] being varied from 0.4 to 1.0 mM. The first order rate constants (k_{obs}) for first and second events with all substrates were obtained by fitting the UV/vis absorbance vs. time traces to a standard bi-exponential model. The second order rate constants for the first binding event (k_1) for each substrate were determined from the slopes of k_{obs} vs. [**2.2**:$Cu(II)_2$:($^-OCH_3$)] plots, while the second binding event for each was found to be independent of the [**2.2**:$Cu(II)_2$:($^-OCH_3$)] and is simply referred to as k_2.

2.3.4. - Mass Spectra

The methanolysis of 0.5 mM of MNPP (**1.3**) by 0.5 mM of catalyst was also monitored by ESI mass spectroscopy with the following conditions: ESI+ mode, declustering potential = 80.0 V, N_2 carrier gas, ion spray voltage = 5500 V, resolution = 10,000, and direct syringe injection. The reaction progress was followed by comparing

the relative ratio of the sums of the integrated intensities of all product species, or all the substrate species in solution vs. the sums of the integrated intensities of all product and substrate species in solution (respectively **2.2**:$Cu(II)_2$:$(X^-)(Y^-)((CH_3O)_2PO_2^-)$ or **2.2**:$Cu(II)_2$:$(X^-)(Y^-)((NO_2C_6H_4O)(CH_3O)PO_2^-)$, where X^- and Y^- = $CF_3SO_3^-$, **2.3** or $(CH_3O)_2PO_2^-$. MS spectra were taken at time = 0.7, 3.7, 13.7, 22.7, 42.7, and 116.7 minutes, and samples were removed from the reaction mixture by syringe and manually injected.

2.3.5 - X-ray Diffraction

The crystal structures of **2.2**:$Cu(II)_2$:$(^-OH)(H_2O)(CF_3SO_3^-)_3$ and **2.2**:$Cu(II)_2$:$(^-OH)((C_6H_5CH_2O)_2PO_2^-)(CF_3SO_3^-)_2$ were determined using a Bruker SMART APEX II X-ray diffractometer with graphite-monochromated Mo K_α radiation (λ = 0.71073 Å), operating at 50 kV and 30 mA over 2θ ranges of 3.86 ~ 50.00º. No significant decay was observed during the data collection at -93 ^oC. Crystals of **2.2**:$Cu(II)_2$:$(^-OH)(H_2O)(CF_3SO_3^-)_3$:0.5 $CH_3CH_2OCH_2CH_3$ suitable for study were grown from a methanol solution containing 1 eq. each of **2.2** and $NaOCH_3$ along with 2 eq. of $Cu(OTf)_2$ placed in the lower chamber of a necked-down sealed tube, which was gently overlaid with an ether layer which was allowed to diffuse into the methanolic solution over four days. Crystals of **2.2**:$Cu(II)_2$:$(^-OH)((C_6H_5CH_2O)_2PO_2^-)(CF_3SO_3^-)_2$ were grown from a methanol solution containing 1 eq. each of **2.2** and dibenzyl phosphate along with 2 eq. each of $Cu(^-OTf)_2$ and $NaOCH_3$. The methanol solution was allowed to evaporate slowly over four days without protection from the atmosphere at ambient temperature. The crystal data and structural refinement details can be found in the published manuscript. The ORTEP

diagrams at the 50% probability level for each of the two complexes are given in Figure 2-6 and Figure 2-7.

2.4. – Results

Given in Figure 2-1 is the Abs. vs. time profile for the methanolysis of 0.03 mM **2.1** promoted by 0.5 mM **2.2**:$Cu(II)_2$:($^-OCH_3$) (^s_spH = 7.4) determined at 340 nm. The trace is clearly bi-phasic indicating at least two events. The absorbance vs. time data were fit by NLLSQ to a standard bi-exponential model for an A→B→C process under the assumption that the absorbance change for the second step was constant and controlled by the appearance of *p*-nitrophenol with a fixed ΔA_2 of 0.05 abs. units. The pseudo-first order rate constants for the first and second events are 10.4 s^{-1} and 0.72 s^{-1}.

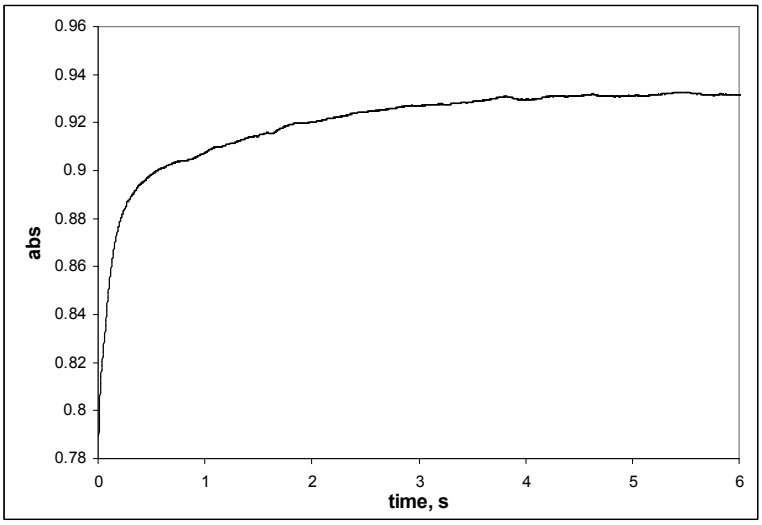

Figure 2-1. Absorbance vs. time profile for the reaction of 0.5 mM **2.2**:$Cu(II)_2$:($^-OCH_3$) and 0.03 mM **2.1** in methanol, ^s_spH = 7.4, followed at 340 nm.

Shown in Figure 2-2 are the plots of the pseudo-first order rate constants for the first and second events observed for the methanolysis of 0.03 M HPNPP obtained under pseudo-first order conditions of excess catalyst concentration, 0.25 mM < [**2.2**:$Cu(II)_2$:($^-OCH_3$)] < 1.0 mM, ^s_spH = 7.4 ± 0.2. The second order rate constant for the first event (k_1), calculated as the linear regression of the line, is 18,000 ± 700 $M^{-1}s^{-1}$, and at the 95% confidence level, the rate constant (k_2) for the second event is not dependent on the [**2.2**:$Cu(II)_2$:($^-OCH_3$)], the average value being 0.7 s^{-1}.

To probe further the origins of the first and second event, we switched to the DNA model, **2.3**, which does not possess the intramolecular 2-hydroxypropyl group and for which the release of *p*-nitrophenol is slower than that from **2.1** by a factor of at least 3200-fold[33,35]. Shown in Figure 2-3 is a plot of the k_{obs} vs. varying [**2.2**:$Cu(II)_2$:($^-OCH_3$)] where the rate of formation of the *p*-nitrophenol product was followed at 320 nm by conventional UV/vis kinetics. The plot shows Michaelis-Mentin behavior with strong binding. The data for this can be fit to a universal binding equation, eq. (1)[36] that is applicable to both strong and weak binding situations:

$$k_{obs} = k_{cat}(1 - ((1 + K_d * [Lim] + [Ex] * K_d - X))/(2K_d)/[Lim]) \quad (1)$$

where [Lim] and [Ex] refer to total concentrations of limiting and excess reagents and X is given in eq. (2).

$$X = \{(1 + 2K_d * [Lim] + 2 * [Ex] * K_d + K_d^2 * [Lim]^2 - 2 * K_d^2 * [Ex][Lim] + [Ex]^2 * K_d^2\}^{0.5} \quad (2)$$

NLLSQ fitting of the data to eq. (1,2) gives a K_M of 0.079 ± 0.018 mM, and a k_{cat} for the fully bound substrate of (2.40 ± 0.04) x 10^{-3} s^{-1}.

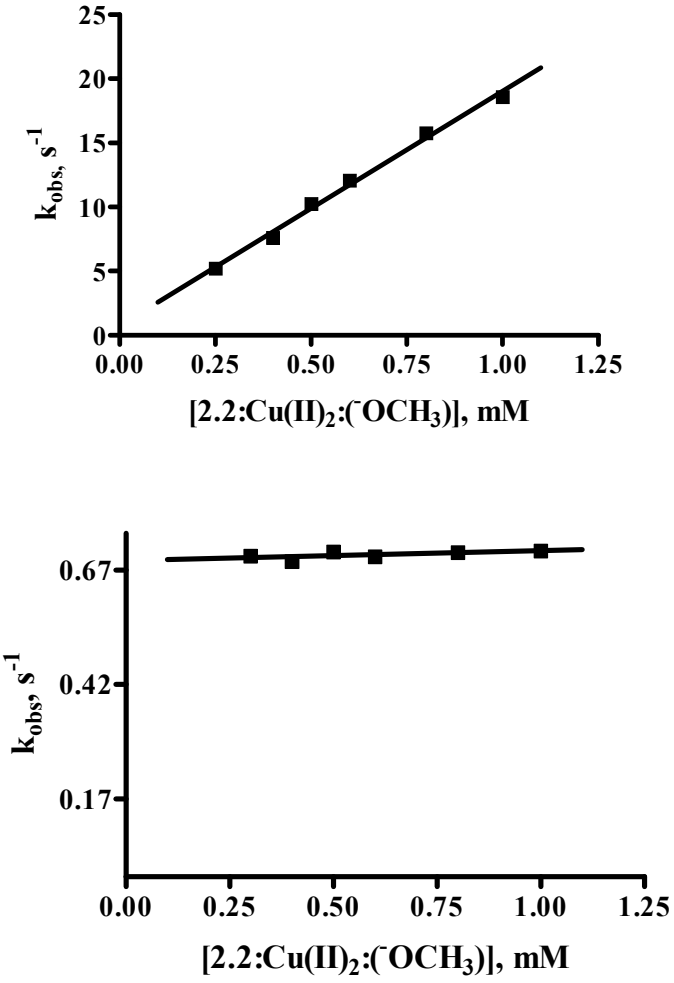

Figure 2-2. (Top) A plot of k_{obs} vs. [**2.2**:Cu(II)$_2$:($^-$OCH$_3$)] for the first event with NaHPNPP (**2.1**; 3 x 10^{-5} M) at 340 nm in anhydrous methanol. The gradient of the line is 18,000 ± 700 $M^{-1}s^{-1}$, ^s_spH = 7.4 ± 0.2. (Bottom) A plot of k_{obs} vs. [**2.2**:Cu(II)$_2$:($^-$OCH$_3$)] for the second event with NaHPNPP (**2.1**; 3 x 10^{-5} M) at 340 nm in anhydrous methanol. The gradient is 0.022 ± 0.013 $M^{-1}s^{-1}$, intercept = 0.690 ± 0.008 s^{-1}, ^s_spH = 7.4 ± 0.2

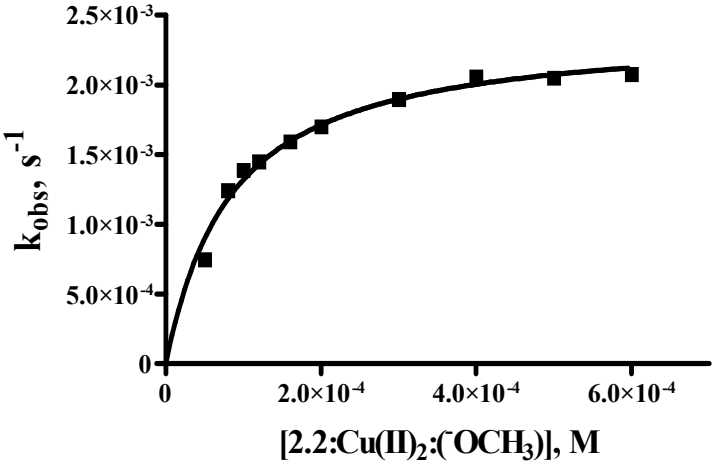

Figure 2-3. A plot of the first order rate constants for methanolysis of 0.01 mM **2.3** vs. [**2.2**:$Cu(II)_2$:($^-OCH_3$)]. The line through the data is a fit to the expression in eq. (1,2) giving a K_M of 0.079 ± 0.018 mM and a k_{cat} of (2.40 ± 0.07) x 10^{-3} s^{-1}; ^s_spH = 7.2 ± 0.2.

When the absorbance vs. time profile for the methanolysis of **2.3** promoted by **2.2**:$Cu(II)_2$:($^-OCH_3$) is monitored at 320-340 nm on the stopped-flow timescale there is evidence for three events, with two rapid events coming before the one relating to the release of *p*-nitrophenol from the bound substrate. Shown in Figure 2-4 are traces for the methanolysis of 0.05 mM **2.3** promoted by 0.5 mM **2.2**:$Cu(II)_2$:($^-OCH_3$) observed at λ=340 (for the first two steps) and 320 nm (for the final step) and ^s_spH = 7.1 emphasizing the three temporally well-separated events with rate constants of 2.4 s^{-1}, 0.57 s^{-1} and 2.10 x 10^{-3} s^{-1}.

The absorbance vs. time traces for the first two steps of the reaction of **2.3** were monitored at 340 nm as a function of varying [catalyst], 0.25 mM < [**2.2**:$Cu(II)_2$:($^-OCH_3$)] < 1.0 mM, ^s_spH = 7.2 ± 0.2. The first step is linear in [catalyst] (k_1 = 20,200 ± 600 $M^{-1}s^-$

[1]), but the second step is independent of [**2.2**:Cu(II)$_2$:($^-$OCH$_3$)], the average value for k_2 being 0.53 ± 0.06 s^{-1} (Table 2-1).

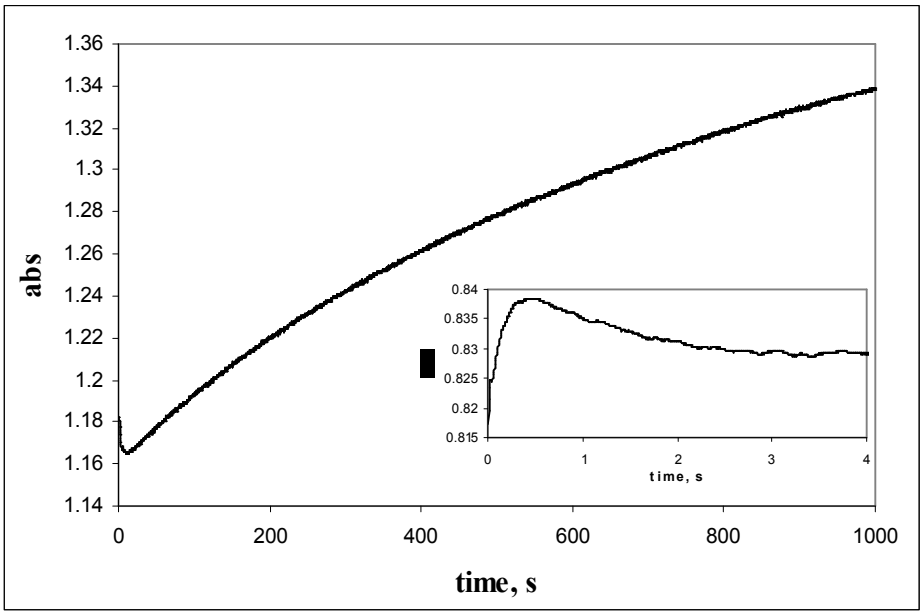

Figure 2-4. An absorbance vs. time profile for the reaction of 0.05 mM **2.3** in the presence of 0.5 mM **2.2**:Cu(II)$_2$:($^-$OCH$_3$) showing the three temporally well defined events; large graph, slow event of product formation followed at 320 nm; inset, the two fast preliminary events followed at 340 nm; T = 25 ^{o}C, ^s_spH = 7.1.

The methanolysis reaction of 5 x 10^{-4} M each of **2.3** and **2.2**:Cu(II)$_2$:($^-$OCH$_3$), in anhydrous methanol was monitored by electrospray mass spectrometry at various times after mixing of the two components. The integrated intensities of all major peaks containing the methanolysis product (dimethyl phosphate) or substrate (**2.3**) bound to **2.2**:Cu(II)$_2$ along with any counterions present, eg. (respectively **2.2**:Cu(II)$_2$:(X$^-$)(Y$^-$)((CH$_3$O)$_2$PO$_2^-$) or **2.2**:Cu(II)$_2$:(X$^-$)(Y$^-$)((NO$_2$C$_6$H$_4$O)(CH$_3$O)PO$_2^-$), X$^-$, Y$^-$ = triflate anion, **2.3** or product) were summed to obtain (I_{prod} + $I_{\mathbf{2.3}}$). The reaction progress was monitored by observing the I_{prod}/((I_{prod} + $I_{\mathbf{2.3}}$), and $I_{\mathbf{2.3}}$/(I_{prod} + $I_{\mathbf{2.3}}$) ratios as a function of time (0.7,

3.7, 13.7, 22.7, 42.7, and 116.7 minutes). Figure 2-5 displays the results from which one can calculate the first order rate constants of k_{prod} = 0.031±0.007 min^{-1} and $k_{\mathbf{2.3}}$ = 0.022±0.003 min^{-1}.

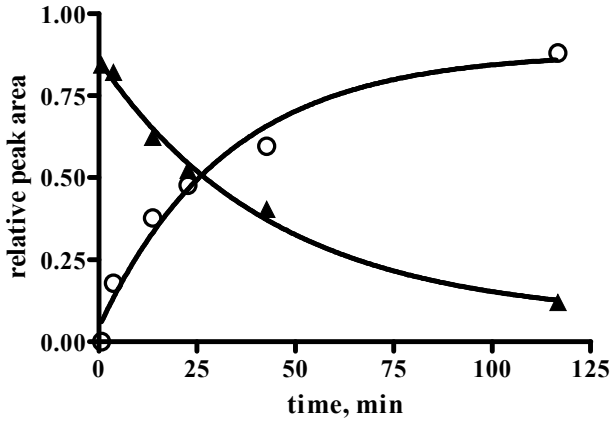

Figure 2-5. A plot of the relative sums of the integrated intensities of the product (I_{prod}) or substrate ($I_{\mathbf{2.3}}$) ESI peak ratios ((I_{prod}/(I_{prod} + $I_{\mathbf{2.3}}$), ○, and $I_{\mathbf{2.3}}$/((I_{prod} + $I_{\mathbf{2.3}}$), ▲) as a function of time for the methanolysis reaction of 0.5 mM each of **2.3** and **2.2**:$Cu(II)_2$:($^-OCH_3$). Lines through the data are NLLSQ fits to a standard exponential model giving k_{prod} = 0.031 ± 0.007 min^{-1} and $k_{\mathbf{2.3}}$ = 0.022±0.003 min^{-1}.

In order to investigate the behavior of a DNA derivative which sterically more closely resembles **2.1** but is far less reactive, we investigated the Abs. vs. time profiles at 340 nm for the reaction of $5x10^{-5}$ M **2.4** with varying [**2.2**:$Cu(II)_2$:($^-OCH_3$)] (not shown). This substrate also exhibits the up/down behavior in the UV/vis spectrum as a function of time with a linear dependence on [catalyst] for the first step (k_1 = 8,700 ± 300 $M^{-1}s^{-1}$) and a second step that is independent of [catalyst], k_2 = 0.49 ± 0.03 s^{-1} at an average ^s_spH of 7.1 ± 0.1 (Table 2-1).

Table 2-1. Various rate constant for binding and chemical steps for substrates **2.1**, **2.3** and **2.4** reacting with **2.2**:$Cu(II)_2$:($^-OCH_3$), T = 25 ^oC.

Substrate ↓/rate constant→	k_1 ($M^{-1}s^{-1}$)	k_2 (s^{-1})	k_3 (s^{-1})
2.1[a]	18,000 ± 700	0.7	7.0[b]
2.3[c]	20,200 ± 600	0.53 ± 0.06	(2.40 ± 0.07)x10^{-3} [d]
2.4[e]	8,700 ± 300	0.49 ± 0.03	N.O.

a. ^s_spH = 7.4 ± 0.2

b. assumed to be at least 10-fold faster than k_2, see text

c. ^s_spH = 7.1 ± 0.2

d. based on saturation data in Figure 2-3 with K_M = 0.079 ± 0.018 mM, ^s_spH = 7.2 ± 0.2

e. ^s_spH = 7.1 ± 0.1

X-ray Diffraction Structures

Single crystal X-ray diffraction studies were done on crystals of **2.2**:$Cu(II)_2$ grown under conditions where: a) the components, **2.2**, $Cu(OTf)_2$ and $NaOCH_3$, were added to dry methanol in a 1:2:1 ratio, followed by diffusion of an ether layer into the methanol solution over a period of about 4 days; and b) the components **2.2**, $Cu(OTf)_2$, $NaOCH_3$ and the sodium salt of dibenzyl phosphate,[37] were added to dry methanol in a 1:2:1:1 ratio, and the solution slowly evaporated in the ambient atmosphere over a period of about 4 days. Shown in Figure 2-6 and Figure 2-7 are the structures of **2.2**:$Cu(II)_2(^-OH)(H_2O)(CF_3SO_3^-)_3$:0.5 $CH_3CH_2OCH_2CH_3$ and **2.2**:$Cu(II)_2(^-OH)(C_6H_5CH_2O)_2PO_2^-$

)($CF_3SO_3^-$)$_2$ without the associated triflate counterions (or $CH_3CH_2OCH_2CH_3$) while selected bond distances and angles are given in Table 2-2.

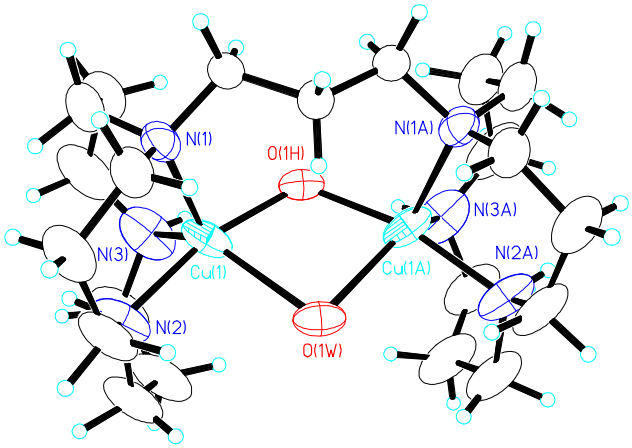

Figure 2-6. Molecular structure of **2.2**:Cu(II)$_2$($^-$OH)(H_2O)($CF_3SO_3^-$)$_3$:0.5 $CH_3CH_2OCH_2CH_3$ shown as an ORTEP diagram at the 50% probability level, counterions omitted for clarity.

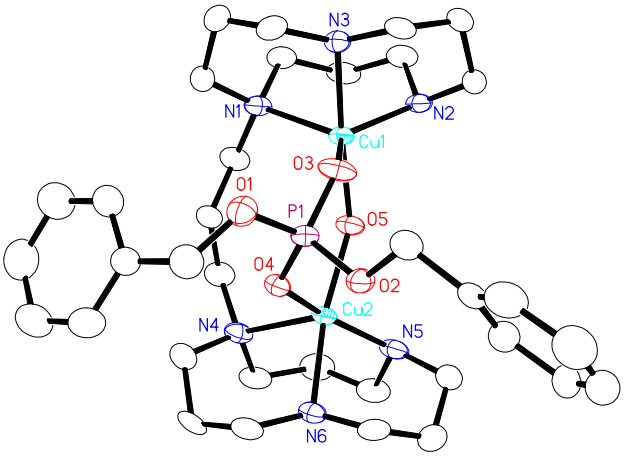

Figure 2-7. Structure of **2.2**:Cu(II)$_2$($^-$OH)($C_6H_5CH_2O)_2PO_2^-$)($CF_3SO_3^-$)$_2$ at 50% probability level; counterions omitted for clarity.

Table 2-2. Selected bond distances and angles for **2.2**:$Cu(II)_2(^{-}OH)(H_2O)(CF_3SO_3^{-})_3$:0.5 $CH_3CH_2OCH_2CH_3$ and **2.2**:$Cu(II)_2(^{-}OH)(C_6H_5CH_2O)_2PO_2^{-})(CF_3SO_3^{-})_2$ as determined from X-ray diffraction.

Parameter	**2.2:$Cu(II)_2$ (^{-}OH)(H_2O)**	**2.2:$Cu(II)_2(^{-}OH)$ ($C_6H_5CH_2O)_2PO_2^{-}$)**
Cu-Cu (Å)	3.260	3.680
Cu1-OH (Å)	1.897	1.944
Cu2-OH (Å)	1.987	1.945
Cu1-O(H_2); Cu2-O(H_2) (Å)	2.342, 2.342	
Cu1-OP; Cu2-OP (Å)		2.022; 1.986
O5---P (Å)		3.189
< Cu1-OH-Cu2 (^{o})	118.46	140.44
< Cu1-OH_2-Cu2 (^{o})	88.22	
< OH-Cu1-OH_2; OH-Cu2-OH_2 (^{o})	76.66; 76.66	
< OH-Cu1-OP; OH-Cu2-OP (^{o})		89.39; 89.00
<O_3-P-O_4 (^{o})		118.83

2.5 – Discussion

2.5.1 - X-ray Diffraction Structures

The partial structures shown in Figure 2-6 and Figure 2-7, devoid of associated triflate counterions, reveal that the two metal ions in each are five-coordinate and buried rather deeply in the ligand which resembles two tri-coordinating ‘ear-muffs’. These impede access to the metal ions from all orientations except those perpendicular to the

Cu-Cu axis and distal to the C_3 linking spacer. Apparently there is some flexibility within the ligand that accommodates a variable Cu-Cu distance which ranges from 3.26 to 3.68 Å in passing from **2.2**:Cu(II)$_2$($^-$OH)(H_2O)($CF_3SO_3^-$)$_3$:0.5 $CH_3CH_2OCH_2CH_3$ to **2.2**:Cu(II)$_2$($^-$OH)($C_6H_5CH_2O$)$_2PO_2^-$)($CF_3SO_3^-$)$_2$. In the former the two Cu(II) ions and coordinated HO^- and OH_2 are nearly planar, the intersection angle between the Cu1-($^-$OH)-Cu2 and Cu1-(OH_2)-Cu2 planes being only 1.1^o. The doubly coordinated phosphate diester in **2.2**:Cu(II)$_2$($^-$OH)(($C_6H_5CH_2O$)$_2PO_2^-$)($CF_3SO_3^-$)$_2$ has its O3-P1-O4 plane twisted by 68.4^o relative to the Cu1---Cu2 axis. The bridging of the diester between the two Cu(II) ions typifies the sort of motif seen in dinuclear complexes where phosphate di and monoesters are coordinated to the complex[11,27,21,1,38]. It is perhaps important for the catalysis that the O_3-P-O_4 bond angle in **2.2**:Cu(II)($^-$OH)(($C_6H_5CH_2O$)$_2PO_2^-$)($CF_3SO_3^-$)$_2$ is expanded to 118.8 degrees which is similar to that seen with other bridging phosphates in dinuclear Cu(II) complexes[11,38c,d] and may be one reason for the exalted reactivity of the coordinated phosphate diesters in this system; the remaining four O-P-O bond angles are only mildly distorted from tetrahedral, being 105, 105, 106 and 110 degrees. Of note is the fact that the coordinated lyoxide Cu1-O5H-Cu2 is 3.189 Å away from the electrophilic P-centre and, when *bis*-coordinated, the O5H electron pairs are not oriented correctly to assume a nucleophilic role. Thus, it seems likely that if the metal coordinated lyoxide is the nucleophile, it must shed one of the coordinating Cu(II) ions and rotate to allow it to approach the phosphorus.

Given the fact that both crystals were grown from anhydrous methanol solutions (reported by the seller to contain 0.002% water or 1.0 mM and used as supplied), it is somewhat surprising to see that neither structure contains methoxide or methanol

coordinated to the metal ions, but rather contains only bridging hydroxide or water. The preference for HO^- or OH_2 bridging between the metal ions is not due to the difference in size as molecular modeling suggests that a methanol or methoxide can occupy the bridging positions without any severe steric interactions. Thus, it appears that the water and hydroxide are preferred possibly due to hydrogen bonded interactions with closely associated $CF_3SO_3^-$ counter ions in the crystal. We assume that when in methanol solution where the triflate ions can be reasonably well solvated, the bridging positions can be occupied by methoxide and methanol so that for the reaction of **2.3**, the product will be a di-methoxy ester as observed for the MS experiments.

2.5.2 – Kinetics:HPNPP (2.1) and 2.2:Cu(II)$_2$:($^-$OCH$_3$)

The Abs_{340nm} vs. time profile for the reaction of **2.1** with **2.2**:Cu(II)$_2$:($^-$OCH$_3$) shown in Figure 2-1 is biphasic with at least two discernable events. The data in Figure 2-2, where the kinetics of these two steps are determined by stopped-flow spectrophotometry under pseudo-first order conditions of excess [**2.2**:Cu(II)$_2$:($^-$OCH$_3$)] between 0.25-1.0 mM, indicate that the rate of the first rapid rise in absorbance is linearly dependent on [**2.2**:Cu(II)$_2$:($^-$OCH$_3$)], which is consistent with the formation of a **2.1**:(**2.2**:Cu(II)$_2$:($^-$OCH$_3$)) complex. At the concentrations of **2.2**:Cu(II)$_2$:($^-$OCH$_3$) investigated which are at least 5-fold larger than the [**2.1**], the absorbance change for the first event is constant signifying that essentially all the substrate is bound within the first event. This is consistent with the K_M of 0.079 mM found with **2.3** which indicates that these phosphate diester substrates have a high affinity for the catalyst. The second event, which also gives rise to the formation of *p*-nitrophenol product, is independent of [**2.2**:Cu(II)$_2$:($^-$OCH$_3$)] within experimental uncertainty and so must be a unimolecular

process that we suggest arises from a rearrangement of the first-formed **2.1**:(**2.2**:$Cu(II)_2$:($^-OCH_3$)) complex which places it into a configuration from which an even faster production of *p*-nitrophenol product occurs. Stopped-flow control experiments in the absence of the diesters indicate that neither of these events is attributable to simple dilution of the **2.2**:$Cu(II)_2$:($^-OCH_3$) catalyst. The overall process can be rationalized according to the simplified process presented in Scheme 2-2 where the first step, having a k_1 = 18,000 $M^{-1}s^{-1}$, leads to essentially complete formation of the **2.1**:(**2.2**:$Cu(II)_2$:($^-OCH_3$)) complex, while the second rearrangement step has an average pseudo-first order rate constant of $k_2 = 0.70\ s^{-1}$ at ^s_spH = 7.4 ± 0.2. The subsequent product forming step, k_3 in Scheme 2-1, must be faster than the second step (we have assumed by at least 10-fold) which accounts for the apparent rise in absorbance for the k_2 step relative to the cases with the slower reacting phosphates described below.

Scheme 2-2. Proposed reaction sequence for HPNPP (**2.1**) and **2.2**:$Cu(II)_2$:($^-OCH_3$), charges omitted for clarity.

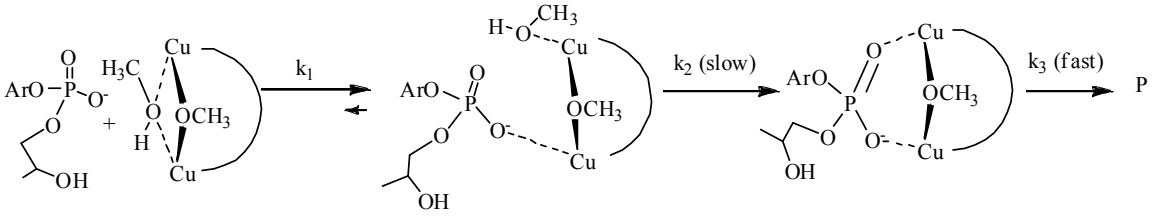

2.5.3 – Kinetics: Methyl *p*-Nitrophenyl Phosphate (2.3) and 2.2:$Cu(II)_2$:($^-OCH_3$)

Since the second event with **2.1** and **2.2**:$Cu(II)_2$:($^-OCH_3$), that we attribute to an intramolecular rearrangement, appears to be superimposed on a subsequent fast chemical process that forms the observable *p*-nitrophenol product, we switched to the DNA model **2.3** where the release of *p*-nitrophenol is far slower than with **2.1**[23,35]. When the kinetics of production of *p*-nitrophenol are monitored by normal UV/vis spectrophotometry at 320 nm under pseudo-first order conditions as a function of [**2.2**:$Cu(II)_2$:($^-OCH_3$)] at ^s_spH = 7.2 ± 0.2, one observes the saturation kinetic plot shown in Figure 2-3 which can be analyzed with eq. (1,2) to yield a K_M of 0.079 ± 0.018 mM and a k_{cat} of (2.40 ± 0.07) x 10^{-3} s^{-1}. The numerical value of K_M indicates that the binding of **2.3**, and presumably closely related phosphate diesters such as **2.1** and **2.4**, is strong. Based on the above analysis with **2.1** we expect three observed events for **2.3**, with the first two being attributed to binding and rearrangement, and the third to a slower chemical event that liberates the *p*-nitrophenol. Indeed, these expectations for the first two fast events are borne out by the data shown in Figure 2-4 in which the insert reveals a rapid rise/fall behavior followed at 340 nm. When these two events are followed at ^s_spH = 7.2 ± 0.2 by stopped-flow spectrophotometry at 0.25 mM < [**2.2**:$Cu(II)_2$:($^-OCH_3$)] < 1.0 mM (all values being above the K_M value so that the binding should be essentially saturated), one determines that k_1 = 20,200 ± 600 $M^{-1}s^{-1}$ and k_2 = 0.53 ± 0.06 s^{-1}.

The observed kinetic behavior for substrate **2.4**, which is far less reactive than **2.1** or **2.3** but sterically similar to the structure of **2.1**, closely parallels that of **2.3** for the first two binding steps where the first event was determined to be first order in [catalyst] with

k_1 = 8,700 ± 300 $M^{-1}s^{-1}$ while the second step was independent of [catalyst], k_2 being 0.49 ± 0.03 s^{-1} at an average $^{s}_{s}$pH of 7.1 ± 0.1. The k_3 step, which would pertain to the release of *p*-chlorophenol, is observed to be far slower than in the case of **2.3** and was not followed for this substrate.

2.5.4 - Electrospray MS Measurements

In order to probe the nature of the products of the reaction, the ESI mass spectra of aliquots removed from a methanol solution that was 0.5 mM in each of **2.3** and **2.2**:$Cu(II)_2$:($^{-}OCH_3$) were determined as a function of time. These are conditions where all the phosphate material should be bound 1:1 to the **2.2**:$Cu(II)_2$-complex. The ratios of the sums of the total integrated intensity of all the major peaks containing product $(CH_3O)_2PO_2^-$, (I_{prod}) and all those containing the starting material **2.3**, ($I_{\mathbf{2.3}}$) vs. (I_{prod} + $I_{\mathbf{2.3}}$) were plotted as a function of time as shown in Figure 2-5. At the end of the reaction, all the **2.3** was consumed and the only peaks that were observed were those attributable to **2.2**:$Cu(II)_2$:($^{-}OTf)_2$($(CH_3O)_2PO_2^-$) and **2.2**:$Cu(II)_2$:(^{-}OTf)($(CH_3O)_2PO_2^-)_2$.

2.5.5 - General Mechanistic and Energetic Considerations of the Catalysis.

The observed events for all three substrates are consistent with the simplified process shown in Scheme 2-1 and Scheme 2-2. The major difference is the relative rate of the k_3 process which varies from >> 0.7 s^{-1} for HPNPP, to (2.40 ± 0.07) x 10^{-3} s^{-1} for **2.3** and is too slow to measure within a reasonable time with **2.4**. The clearest case for three temporally well-separated events is that of the catalyzed methanolysis of **2.3** where there is evidence consistent with separate bimolecular catalyst:substrate binding and intramolecular rearrangement events, followed by the slower chemical step for

production of *p*-nitrophenol. The data in Scheme 2-1 indicate that the two events that precede the chemical step have very similar rate constants for all substrates which seem most consistent with more-or-less common binding processes. The value for the k_1 step seems small for ligand exchange on Cu(II) complexes, which in some cases can be very high (2-20 x 10^8 $M^{-1}s^{-1}$).[39] However the rates of binding to M(II) complexes in general are known[40] to be highly sensitive to crowding effects such as is the case here. The compactness of the **2.2**:$Cu(II)_2(^-OH)(H_2O)(CF_3SO_3^-)_3$ structure shown in Figure 2-7 suggests that substrate coordination to the Cu(II) ion(s) cannot occur by an associative process, but rather requires that the complex should open up, probably by an equilibrium dissociation of one of the Cu-O(H_2)-Cu bonds, to reveal a 4-coordinate Cu(II) with an open site to which the phosphate can then bind. If the equilibrium concentration of the open form is small, as expected, then the overall rate constant for the association of phosphate will be reduced accounting for the 9,000-20,000 $M^{-1}s^{-1}$ values for k_1 seen here. The second step is consistent with an intramolecular rearrangement, probably to form a doubly coordinated phosphate with a structure similar to what is shown in Figure 2-7 with a coordinated dibenzyl phosphate. The slowness of this step can also be attributed to the tight steric requirements that may impede the required dissociation of the bound solvent from the second Cu(II) prior to double coordination of the phosphate.

The effectiveness of the catalysis of the chemical steps with **2.1** and **2.3** can be measured in several ways. First, one could compare the effective second order rate constant for the catalytic reaction with **2.3** (given as k_{cat}/K_M = 2.4 x 10^{-3} s^{-1}/7.9 x 10^{-5} M = 30 $M^{-1}s^{-1}$) with that for the methoxide reaction (7.9 x 10^{-7} $M^{-1}s^{-1}$); by this measure, the acceleration imbued by **2.2:**$Cu(II)_2$:($^-OCH_3$) is 3.8 x 10^7-fold. This is similar to the

catalysis afforded for methanolysis of **2.3** by **2.2**:$Zn(II)_2$:($^-OCH_3$)[23], where the k_{cat}/K_M = (4.1 ± 0.3) x 10^{-2} s^{-1}/(0.37 ± 0.07) mM = 110 $M^{-1}s^{-1}$, the acceleration relative to the methoxide reaction being 1.4 x 10^8. In the case of the reactions with the RNA model **2.1**, the chemical step of production of *p*-nitrophenol is far faster than the limiting rearrangement process, so the calculation leads only to a lower limit for the acceleration. With **2.2**:$Cu(II)_2$:($^-OCH_3$), assuming that the K_M constant can be approximated by that found for **2.3** and that the chemical step is at least 10-fold faster than the rearrangement step (~7 s^{-1}), the acceleration is 3.5 x 10^7-fold (calculated as 7 s^{-1}/7.9 x 10^{-5} M/2.56 x 10^{-3} $M^{-1}s^{-1}$). Even if one uses the rate constant determined by the rate-limiting second rearrangement step (0.7 s^{-1}), the acceleration is 3.5 x 10^6. Alternatively, if the first binding step of the substrate to the complex is rate limiting at 18,000 $M^{-1}s^{-1}$, the acceleration relative to the methoxide reaction is computed as 7.0 x 10^6-fold. Comparison with the **2.2**:$Zn(II)_2$:($^-OCH_3$) catalyst is also complicated by the fact that the latter does not show Michaelis-Menten kinetics, but rather second order kinetics with a rate constant of 275,000 $M^{-1}s^{-1}$ where the rate-limiting step was proposed[23] to be substrate binding[41]. Using this number, the overall catalytic acceleration by the $Zn(II)_2$-complex is 1.1 x 10^8-fold.

A second way to compare the catalyst efficacy measures the rate acceleration relative to the methoxide reaction at the $^{s}_{s}$pH where the catalyst is operative (7.2 in the case of **2.2**:$Cu(II)_2$:($^-OCH_3$), 9.5 in the case of **2.2**:$Zn(II)_2$:($^-OCH_3$))[42]. This artificially enhances the computed catalysis for systems that operate at lower 'pH' values, but is a generally accepted method for enzymatic reactions where the efficacy of the catalyzed process is analyzed at neutral pH's where the enzymes operate. In this case, at $^{s}_{s}$pH 7.2

(or 9.5) the methoxide reactions of **2.1** and **2.3** would have first order rate constants of 6.9 x 10^{-13} (1.4 x 10^{-10}) s^{-1} and 2.1 x 10^{-16} (4.3 x 10^{-14}) s^{-1} respectively. For the **2.2**:$Cu(II)_2$ catalyst, where the rate-limiting step is the intramolecular rearrangement with **2.1** or **2.3** having a rate constant of ~0.7 s^{-1}, the respective accelerations are about 10^{12} and 10^{13}-fold. For a solution containing 1 mM of the **2.2**:$Zn(II)_2$ catalyst operating at $^{s}_{s}$pH 9.5, the acceleration of cleavage of **2.1** is 2 x 10^{12}-fold, while the acceleration exhibited by **2.2**:$Zn(II)_2$:($^{-}OCH_3$)-bound **2.3** (which decomposes with a pseudo-first order rate constant of 4.1 x $10^{-2}s^{-1}$)[23] is also about 10^{12}.

A recent analysis of the reaction of a dinuclear Zn(II) complex (**2.5**) reacting with HPNPP[43] presents a third, and more thermodynamically correct way of comparing the lyoxide and complex-catalyzed reactions by analyzing the transition state energetics and the stabilization of the lyoxide:substrate transition state through its binding to the catalyst[44]. Scheme 2-3 gives a thermodynamic cycle outlining the various reacting components to be considered from which is derived eq. (3) for the free energy of binding of the transition state for the catalyst promoted reaction relative to the methoxide reaction. In eq. (4) is the free energy calculation specific for the reaction with HPNPP and **2.2**:$Zn(II)_2$:($^{-}OCH_3$) which does not show saturation kinetics but does show an overall second order reaction with a first order dependence on [catalyst]. The terms in eq.s (3,4) are calculated from: a) k_{cat}/K_M from the saturation curve depicted in Figure 2-3 or that given in ref. 23 for the reaction of **2.3** with the Zn(II) complex; b) K_a/K_w can be readily interpreted as the binding constant of methoxide to the dinuclear complex, where K_a refers to the first acid dissociation constant for formation of **2.2**:$Cu(II)_2$:($^{-}OCH_3$) or **2.2**:$Zn(II)_2$:($^{-}OCH_3$) and K_w is the autoprotolysis constant for methanol ($10^{-16.77}$); and c)

k_{OCH3} is the second order rate constant for the methoxide reactions in the absence of complex. Listed in Table 2-3 are the various constants for the relevant terms in eq. (3) for the reaction with **2.3** and **2.1** with the **2.2**:$Cu(II)_2$ catalyst and **2.3** with the **2.2**:$Zn(II)_2$ catalyst, and those in eq. (4) for the reaction of HPNPP with the **2.2**:$Zn(II)_2$ catalyst.

Scheme 2-3. Thermodyamic cycle for the catalyzed and uncatalyzed cleavages of phosphate diesters.

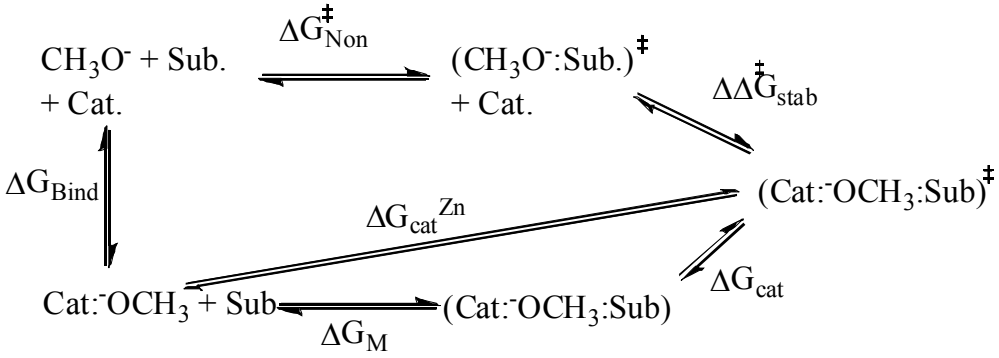

$$\Delta\Delta G^{\neq}_{stab} = (\Delta G_{Bind} - \Delta G_M + \Delta G_{cat}) - \Delta G^{\neq}_{Non} = -RT\ln\left[\frac{(k_{cat}/K_M)(K_a/K_w)}{k_{OCH3}}\right] \quad (3)$$

In Scheme 2-3, $\Delta G_{bind,}$ ΔG_{cat} and $\Delta G^{\neq}_{non}$ are the respective free energies for: 1) binding of methoxide to the catalyst; 2) the activation energy for unimolecular reaction of the Cat:$^-OCH_3$:Sub complex; and, 3) the activation energy for the reaction of methoxide alone with substrate. ΔG_M is the free energy for association of the substrate and Cat:$^-$

OCH_3 complex. In eq. (4), ΔG_{cat}^{Zn} is the free energy for the second order reaction of the Cat:$^{-}OCH_3$ complex with substrate, the associated rate constant being defined as k_1^{obs}.

$$\Delta\Delta G^{\neq}_{stab} = (\Delta G_{Bind} + \Delta G_{cat}^{\ Zn}) - \Delta G^{\neq}_{Non} = -RT \ln\left[\frac{(k_1^{obs})(K_a / K_w)}{k_{OCH3}}\right] \quad (4)$$

For **2.2**:$Cu(II)_2$:($^{-}OCH_3$)-promoted methanolysis of HPNPP, we can estimate a lower limit for the k_{cat} term as 0.7 s^{-1} from the rate limiting intramolecular rearrangement and estimate the K_M term as 7.9 x 10^{-5} M based on the one found for **2.3** (*vide supra*). In reality the k_{cat} term for the chemical step must be much greater which will actually give a larger stabilization of ΔG (an extra -1.4 kcal for each factor of 10 in rate constant at 25 ^{o}C). For **2.2**:$Zn(II)_2$:($^{-}OCH_3$) we see only second order kinetics for the reaction of catalyst and HPNPP substrate to produce *p*-nitrophenol, the limiting rate constant (k_1^{obs}) being 275,000 $M^{-1}s^{-1}$ which we have interpreted as being due to the productive binding of HPNPP and catalyst. Using these values, the lower limit for computed stabilization of the TS for the intramolecular transesterification of HPNPP with CH_3O^- bound by the $Cu(II)_2$ and $Zn(II)_2$ catalysts are -22.6 and -21.0 kcal/mol while those for the reaction of **2.3** promoted by the same two catalysts are -24.0 and -21.1 kcal/mol. These are very large energy reductions for two dinuclear catalysts promoting two different reactions where one involves a methoxide (either metal-coordinated or free) acting as a base followed by an intramolecular cyclization and subsequent formation of product, while the other reaction involves methoxide acting as a nucleophile on P.

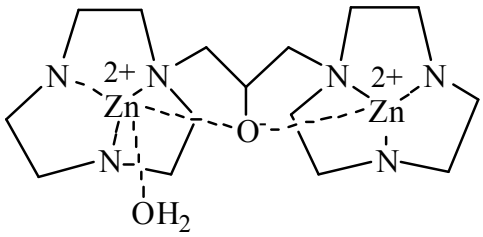

2.5

Table 2-3. Kinetic Parameters for **2.2**:$M(II)_2$:($^-OCH_3$) and methoxide ion promoted cleavages of **2.3** and HPNPP (**2.1**) at 25 ^oC in methanol.

Parameter	2.3 (Cu(II))	2.3 (Zn(II))	HPNPP (Cu(II))	HPNPP (Zn(II))
k_{OCH3} ($M^{-1}s^{-1}$)	$7.9x10^{-7}$ [a]	$7.9x10^{-7}$ [a]	$2.56x10^{-3}$ [b]	$2.56x10^{-3}$ [b]
K_M (M)	$7.9x10^{-5}$ [c]	$3.7x10^{-4}$ [a]	$7.9x10^{-5}$ [d]	-
k_{cat}/K_M ($M^{-1}s^{-1}$)	30	110 [a]	$9x10^3$	275,000[e]
K_a/K_w (M^{-1})	10^{10} [f]	$2.3x10^7$ [f]	10^{10} [f]	$2.3x10^7$ [f]
$(k_{cat}/K_M)(K_a/K_w)$ ($M^{-2}s^{-1}$)	$30x10^{10}$	$2.5x10^9$	$9x10^{13}$	$6.3x10^{12}$
$\Delta\Delta G_{stab}^{\neq}$ (kcal/mol)	-24.0	-21.1	$\geq$ 22.6	$\geq$ 21.0

a. From ref. 23.

b. From ref. 33.

c. From data in Figure 2-3.

d. K_M for **2.1** assumed to have the same binding constant as does **2.3**.

e. Given as second order rate constant observed in ref. 23 for the reaction of Zn(II) catalyst with HPNPP (k_1^{obs})

f. K_a from half neutralization of **2.2**:$Cu(II)_2$:($^-OCH_3$) and **2.2**:$Zn(II)_2$:($^-OCH_3$) by adding ½ eq. of acid, to the **2.2**:$M(II)_2$:($^-OCH_3$) complex, $^s_spK_a$ = 6.77 and 9.41 respectively.

The large TS binding energies of the **2.2**:$M(II)_2$ catalysts for **2.1** and **2.3** in methanol, while approximate given the assumptions, invite comparison with the value of -9.6 kcal/mol afforded for the cleavage of HPNPP by dinuclear Zn(II) complex **2.5** in water.[43] To our knowledge there are no such free energy comparisons possible from literature examples for the catalyzed cleavage of DNA models, presumably probably because these reactions are extremely slow in water unless catalyzed efficiently as is the case here in methanol. The combination of these two specific dinuclear complexes (whether Zn(II) or Cu(II) containing) and a medium effect engendered by the methanol, provides rate enhancements exceeding anything reported in water so far. Previously[23] we attributed this medium effect in the light alcohol solvents to a reduced dielectric constant that increases the potential energy of attraction between oppositely charged ions of the sort involved in metal catalyzed reactions of anionic substrates. In addition, a lower polarity medium is well known to promote reactions where charge is dispersed in the TS. The application of eq.s (3,4) allows one to assess the energetic consequences of the medium effect on the various rate and equilibrium steps shown in Scheme 2-3 for different catalytic systems as in eq. (5):

$$\Delta\Delta G^{\neq}_{stab} = -RT \ln\left\{\left(\frac{(k_{cat}/K_M)^{MeOH}}{(k_{cat}/K_M)^{HOH}}\right)\left(\frac{[K_a/K_w]^{MeOH}}{[K_a/K_w]^{HOH}}\right)\left(\frac{(k_{OH})^{HOH}}{(k_{OMe})^{MeOH}}\right)\right\} \qquad (5)$$

where the k_{cat}/K_M term can be replaced by the apparent second order rate constant for the catalyst reacting with HPNPP or **2.3**. Ideally one would like to compare the same catalyst in water and methanol, but this is not possible at present. Nevertheless, the energy differences ($\Delta\Delta G^{\neq}_{stab}$) shown in Table 2-4 shed light on which of the components contributes most to the observed increase in catalysis in moving between the two

systems. For example, the K_a/K_w term has a value of 1.43 x 10^6 M^{-1} in water with the Zn(II) catalyst **2.5**[43], 2.3 x 10^7 M^{-1} in methanol with **2.2**:$Zn(II)_2$, and 1 x 10^{10} M^{-1} in methanol with **2.2**:$Cu(II)_2$. Although the autoprotolysis constant for methanol ($K_w = 10^{-16.77}$) is lower than that of water, this only leads to an increase in the K_a/K_w term if the ${}^{s}_{s}pK_a^{methanol} < (pK_a^{water} + 2.77)$. The ${}^{s}_{s}pK_a$ for ionization of **2.2**:$Zn(II)_2$:($HOCH_3$) is 9.41 while the pK_a for **2.5** in water is 7.8-8.0[43] such that the respective K_a/K_w ratios for **2.5** and **2.2**:$Zn(II)_2$ differ by a factor of 16. This term contributes -1.64 kcal/mol to the stabilization of the TS ($\Delta\Delta G^{\neq}_{stab}$) for the reaction of **2.2**:$Zn(II)_2$ in methanol vs. **2.5** in water, but a more substantial -5.24 kcal/mol for the **2.2**:$Cu(II)_2$ complex in methanol because its ${}^{s}_{s}pK_a$ of 6.77 is nearly three units lower than that of the Zn(II) complex.

Table 2-4. Computed $\Delta\Delta G^{\neq}_{stab}$ afforded from each of the ratios of constants given in eq. (5) for the reactions of various systems in promoting the cyclization of HPNPP (**2.1**) at 25 °C.

Catalyst comparison↓	$-RT\ln\left(\frac{(k_{cat}/K_M)^{Me}}{(k_{cat}/K_M)^{H}}\right)$ **(kcal/mol)** [a]	$-RT\ln\left(\frac{[K_a/K_w]^{MeOH}}{[K_a/K_w]^{HOH}}\right)$ **(kcal/mol)**	$-RT\ln\left(\frac{(k_{OH})^{HOH}}{(k_{OMe})^{MeOH}}\right)$ **(kcal/mol)**	**Total $\Delta\Delta G^{\neq}_{stab}$ MeOH vs. H_2O (kcal/mol)**
2.2:$Zn(II)_2$ in MeOH vs. **2.5** in water	-7.6	-1.6	-2.2	-11.4
2.2:$Cu(II)_2$ in MeOH vs. **2.5** in water	-5.6	-5.2	-2.2	-13

a. The k_{cat}/K_M term is given as the second order rate constant for **2.2**:$Zn(II)_2$ promoted cylcization of **2.1** (2.75 x 10^5 $M^{-1}s^{-1}$), while that for **2.2**:$Cu(II)_2$ is given as 0.7 s^{-1}/7.9 x 10^{-5} M: the reported rate constant for the reaction of **2.5** with HPNPP in water is 0.71 $M^{-1}s^{-1}$ (ref.43).

The difference between the k_{OR} values for reaction of **2.1** with hydroxide in water (9.9×10^{-2} $M^{-1}s^{-1}$)[43] and methoxide in methanol (2.56×10^{-3} $M^{-1}s^{-1}$) contributes -2.2 kcal/mol to the overall $\Delta\Delta G^{\neq}_{stab}$. However, the analysis shows that the major part of the $\Delta\Delta G^{\neq}$ stabilization in the case of the **2.2**:$Zn(II)_2$ complex results from the apparent second order rate constant (k_{cat}/K_M) for the reaction which is 3.9×10^5 times larger than that seen in the case of **2.5** in water. The analogous value for **2.2**:$Cu(II)_2$ is 1.3×10^4 times larger, and thus contributes roughly as much as its K_a/K_w term to the overall $\Delta\Delta G^{\neq}_{stab}$ for the reaction.

2.6 – Conclusions

In the above we have provided structural data for two **2.2**:$Cu(II)_2$ complexes where the two central Cu ions are bridged by HO^-, H_2O, and HO^-, $(PhCH_2O)_2PO_2^-$ (Figure 2-6, Figure 2-7 respectively). These are germane to the solution forms of the resting catalyst in methanol where methoxide seems to be the active base or nucleophile, and to the state in which the reactive phosphate diesters **2.1** and **2.3** studied here might be bound prior to their cleavage. The kinetic studies of **2.2**:$Cu(II)_2$:$^-OCH_3$ with substrates **2.1**, **2.3**, **2.4** demonstrate that all have two fast steps that are interpreted as substrate binding to one of the Cu(II) centres, followed by an intramolecular rearrangement to form a putative double Cu(II) coordinated phosphate diester analogous to what is shown in Figure 2-7. For two of these systems, **2.1** and **2.3**, there is a chemical event that leads to the production of *p*-nitrophenol which is markedly accelerated relative to the background reaction promoted by methoxide. In fact the acceleration of the chemical step in the

reaction of **2.1** is so effective that the rate limiting steps become those of substrate binding and positioning.

The accelerations afforded to the decomposition of **2.1** and transesterification of **2.3** by **2.2**:$Cu(II)_2$:($^-OCH_3$) catalyst are among the fastest reported to date, the only faster ones being with our previously reported[23] **2.2**:$Zn(II)_2$:($^-OCH_3$) catalyst (also in methanol). An analysis of the free energy of binding of the **2.2**:$Cu(II)_2$ and **2.2**:$Zn(II)_2$ catalysts to the TS for the intramolecular cyclization of **2.1** and the phosphoryl transfer process of **2.3** indicates that these two dinuclear systems exhibit similar values of -21 to -24 kcal/mol which is significantly greater than what has reported for a dinuclear system catalyzing three analogous phosphoryl cyclizations in water (-7.2 to -9.6 kcal/mol)[43]. A detailed analysis partitions the origins of the differences in the free energies of stabilization of the methanol/**2.2** system vs. a water/**2.5** system into three main terms that are responsible for the $\Delta\Delta G^{\neq}_{stab}$, where the main contributions arise from the increased catalytic constants (k_{cat}/K_M).

These studies reinforce our previous contentions[23] that the combination of the dinuclear catalysts and an important medium effect contribute greatly to the acceleration of the cleavage of phosphate diesters and that such a combination may fulfill a key role in related enzymatic processes.

2.7 – References and Notes

[1] Weston, J. *Chem. Rev.* **2005***, 105*, 2151.

[2] Cowan, J. A. *Chem. Rev.* **1998,** *98*, 1067.

[3] Wilcox D. E. *Chem. Rev.* **1996**, *96*, 2435.

[4] Sträter, N.; Lipscomb, W. N.; Klabunde, T.; Krebs, B. *Angew. Chem. Int. Ed. Engl.* **1996**, *35*, 2024.

[5] Davies, J. F.; Hostomska, Z.; Hostomsky, Z.; Jordan, S. R.; Mathews, D. A. *Science*, **1991,** *252*, 88.

[6] Beese, L. S.; Steitz, T. A *EMBO*, **1991**, *10*, 25.

[7] Lahm, A.; Volbeda, S.; Suck, D. *J. Mol. Biol.* **1990**, *215*, 207.

[8] Schroeder, G. K.; Lad, C.; Wyman, P.; Williams, N. H.; Wolfenden, R. *Proc. Nat. Acad. Sci. USA.* **2006**, *103*, 4052.

[9] Williams, N. H.; Wyman, P. *Chem. Commun.* **2001**, 1268.

[10] Molenveld, P.; Engbertsen, J. F. J.; Reinhoudt, D. N. *Chem. Soc. Rev.* **2000**, *29*, 75.

[11] Williams, N. H.; Takasaki, B.; Wall, M.; Chin, J. *Acc. Chem. Res.* **1999**, *32*, 485.

[12] Mancin, F.; Scrimin, P.; Tecilla, P.; Tonellato, U. *Chem. Commun.* **2005**, 2540.

[13] Morrow, J. R.; Iranzo, O. *Curr. Opin. Chem. Biol.* **2004**, *8*, 192.

[14] Yamada, K.; Takahashi, Y.-i.; Yamamura, H.; Araki, A.; Saito, K.; Kawai, M. *Chem. Commun.* **2000,**1315.

[15] Feng, G.; Mareque-Rivas, J. C.; Williams, N. H. *Chem. Commun.* **2006**, 1845.

[16] Mancin, F., Rampazzo, E.; Tecilla, P.; Tonellato, U. *Eur. J. Chem.* **2004,** 281.

[17] Yang, M.-Y.; Iranzo, O.; Richard, J. P.; Morrow, J. R. *J. Am. Chem. Soc.* **2005,** *127*, 1064.

[18] Iranzo, O.; Elmer, T.; Richard, J. P.; Morrow, J. R. *Inorg. Chem.* **2003**, **42**, 7737.

[19] Iranzo, O.; Richard, J. P.; Morrow, J. R. *Inorg. Chem.* **2004**, **43,** 1743.

[20] Iranzo, O.; Kovalevsky, A. Y.; Morrow, J. R.; Richard, J. P. *J. Am. Chem. Soc.* **2003**, *125*, 1988.

[21] Bauer-Sienbenlist, B.; Meyer, F.; Farkas, E.; Vidovic, D.; Cuesta-Seijo, J. A.; Herbst-Irmer, R.; Pritzkow, H. *Inorg. Chem.* **2004**, *43*, 4189.

[22] Arca, M.; Bencini, A.; Berni, E.; Caltagiirone, C.; Devillanova, F. A.; Isaia, F.; Garau, A.; Giorgi, C.; Lippolis, V.; Perra, A.; Tei, L.; Valtancoli, B. *Inorg. Chem.* **2003**, *42,* 6929.

[23] Neverov, A. A.; Lu, Z.L.; Maxwell, C. I.; Mohamed, M. F.; White, C. J.; Tsang. J. S. W.; Brown, R. S. *J. Am. Chem. Soc.* **2006**, *128*, 16398.

[24] For the designation of pH in non-aqueous solvents we use the forms recommended by the IUPAC, *Compendium of Analytical Nomenclature. Definitive Rules 1997* 3rd ed., Blackwell, Oxford, U. K. 1998. Since the autoprotolysis constant of methanol is $10^{-16.77}$, neutral $^{s}_{s}$pH is 8.4.

[25] Rossi, L. M.; Neves, A.; Hörner, R.; Terenzi, H.; Szpoganicz, B.; Sugai, J. *Inorg. Chim. Acta* **2002**, *337*, 366.

[26] Deal, K. A.; Hengge, A. C.; Burstyn, J. N. *J. Am. Chem. Soc.* **1996,** *118*, 1713.

[27] Jagoda, M.; Warzeska, S.; Pritzkow, H.; Wadepohl, H.; Imhof, P.; Smith, J. C.; Krämer, R. *J. Amer. Chem. Soc.* **2005**, *127*, 15061.

[28] Fry, F. H.; Fischmann, A. J. ; Belousoff, M. J.; Spiccia, L.; Brügger, J. *Inorg. Chem.* **2005**, *44*, 941, and references therein.

[29] Deal, K. A.; Park, G.; Shao, J.; Chasteen, N. D.; Brechbiel, M. W.; Planalp, R. P. *Inorg. Chem.* **2001**, *40*, 4176.

[30] Kirby, A. J.; Younas, M. *J. Chem. Soc. B* **1970**, 1165.

[31] Kim, J.; Lim, H. *Bull. Korean. Chem. Soc.* **1999**, *20*, 491.

[32] Brown, D. M.; Usher, D. A. *J. Chem. Soc.* **1965**, 6558.

[33] Tsang, J. S.; Neverov, A. A.; Brown, R. S. *J. Am. Chem. Soc*. **2003**, *125*, 1559.

[34] Gibson, G.; Neverov, A. A.; Brown, R. S. *Can. J. Chem.* **2003**, *81*, 495.

[35] The second order rate constant for methoxide-catalyzed cleavage of **2.3** is k_2^{OMe-} = (7.9 ± 0.6) x 10^{-7} $M^{-1}s^{-1}$, see ref. (23), while that for reaction with **2.1** is 2.6 x 10^{-3} $M^{-1}s^{-1}$.

[36] Eq. (1) was obtained from the equations for equilibrium binding and for conservation of mass by using the commercially available MAPLE software, Maple V Release 5, Waterloo Maple Inc., Waterloo, Ontario, Canada.

[37] Since **2.1** and **2.3** react too quickly with methanol in the presence of the catalyst, dibenzyl phosphate was chosen as a non-reactive phosphate for crystal studies.

[38] (a) Feng, G.; Natale, D.; Prabaharan, R.; Mareque-Rivas, J. C.; Williams, N. H. *Angew. Chem. Int. Ed.* **2006**, *45*, 7056; (b) Wall, M.; Hynes, R. C.; Chin, J. *Angew. Chem. Int. Ed.* **1993**, *32*, 1633; (c) Young, M. J.; Chin, J. *J. Am. Chem. Soc.* **1995**, *117*, 10577.

[39] Tobe, M. L.; Burgess, J. In *Inorganic Reaction Mechanisms*, Addison Wesley Longman Ltd.: New York, 1999, pp.271-333.

[40] (a) Dukes, G. R.; Margerum, D. W. *Inorg. Chem.,* **1972**, *11*, 2952; (b) Pitteri, B.; Marangoni, G.; Viseutin, F. V.; Cattalini, L.; Bobbo, T. *Polyhedron*, **1998**, *17*, 475.

[41] It has been suggested that there is good evidence from other studies (see ref. 17) with a dinuclear Zn(II) complex (**2.5**) in aqueous solution that the binding involves the non-ionized form of the catalyst ($Zn(II)_2$:H_2O) and the 2-hydroxy deprotonated dianionic form of HPNPP rather than the $Zn(II)_2$:^-OH form of the catalyst and the protonated 2-OH form of HPNPP which we favour on the basis of our studies. While it is true that these two possibilities are kinetically equivalent, and cannot be distinguished on the basis of any of the existing catalytic studies with **2.5** in water, the available results we have with **2.2**:$Cu(II)_2$:($^-OCH_3$) or **2.2**:$Zn(II)_2$:($^-OCH_3$) reacting with HPNPP in methanol quickly rule out the former possibility. The pK_a for deprotonation of the 2-HO group of HPNPP in methanol should be at least as large or greater than that of methanol (K_w/[MeOH] = $10^{-16.77}$/30) or pK_a = 18.2. At a ^s_spH of 7.2 or 9.5 where the **2.2**:$Cu(II)_2$ and **2.2**:$Zn(II)_2$ are operative, the [$HPNPP^{2-}$] would be one part in 10^{11} and one part in $10^{8.7}$ respectively. Since the second order rate constants for binding of the HPNPP substrate, in whatever form, by the **2.2**:$Cu(II)_2$ and **2.2**:$Zn(II)_2$ catalysts are observed to be 18,000 and 275,000

$M^{-1}s^{-1}$ respectively, the reactions would have to exceed the diffusion limit of 10^{10} $M^{-1}s^{-1}$ by at least 10^4 if the dianionic form of the substrate were the active one.

[42] Since the autoprotolysis constant of methanol is $10^{-16.77}$ M^2, at $^{s}_{s}$pH 7.2 or 9.5 the $[CH_3O^-]$ is 2.69 x 10^{-10} or 5.4 x 10^{-8} M.

[43] O'Donoghue, A. M.; Pyun, S. Y; Yang, M.-Y.; Morrow, J. R.; Richard, J. P. *J. Am. Chem. Soc.* **2006**, *128*, 1615.

[44] Wolfenden, R. *Nature*, **1969**, *223*, 704.

Chapter 3 – Biomimetic Cleavage of RNA Models Promoted by a Dinuclear Zn(II) Complex in Ethanol

3.1 – Preface

With minor formatting changes and slight modification of the text for clarification, this chapter is largely as it was published in Journal of American Chemical Society (Liu, C. T.; Neverov, A. A.; Brown, R. S. *J. Am. Chem. Soc*. **2008**, *130*, 16711). Two new equations were added as ref. [13] and [17], which were originally in the Supporting Information section of the published account. All experiments (synthesis, kinetics, and analytical data collection) were performed by C. Tony Liu. The original kinetic data and the complete characterization of the new compounds synthesized for the study can be found in the Supporting Information section for the original paper. The first draft of the manuscript was composed by me and the final version was prepared in collaboration with Dr. R. Stan. Brown and Dr. Alex A. Neverov.

3.2 – Introduction

As an extension of studies of the highly efficient biomimetic DNase and RNase[1,2,3] complexes in methanol, where we have shown that the catalytic cleavage of a series of aryl 2-hydroxylpropyl phosphates (**3.1a-g**; simplified models of RNA) and aryl methyl phosphates (**3.2a-n**; models of DNA) promoted by the dinuclear Zn(II) and Cu(II) complexes of 1,3-bis-N_1,N_1'-(1,5,9-triazacyclododecyl)propane (**3.3**) in methanol can be greatly accelerated[4,5], we decided to explore other solvent systems. As discussed in Chapter 2, detailed mechanistic investigation led to the proposal that the catalyzed

cleavage follows a multi-step pathway consistent with a minimal process given in Scheme 3-1 consisting of a bimolecular binding step of the catalyst to the phosphate followed by a rearrangement to form the catalytically active species. This is followed by one or more chemical steps that result in the production of the aryloxy leaving group and a corresponding methoxylated phosphate diester product.[4,5]

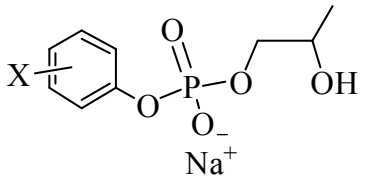

3.1

a. X = 4-NO_2
b. X = 4-NO_2, 3-CH_3
c. X = 3-NO_2
d. X = 4-Cl
e. X = 3-OCH_3
f. X = H
g. X = 4-OCH_3

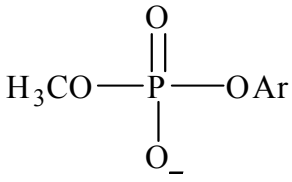

3.2

a. 2, 4-dinitrophenyl
b. 2-chloro-4-nitrophenyl
c. 4-chloro-2-nitrophenyl
d. 2-(methoxycarbonyl)-4-nitrophenyl
e. 2, 4, 5-trichlorophenyl
f. 4-nitrophenyl
g. 2-nitrophenyl
h. 2-nitro-4-methoxyphenyl
i. 3-nitrophenyl
j. 4-chlorophenyl
k. 3-methoxyphenyl
l. 2-(methoxycarbonyl)phenyl
m. phenyl
n. 4-methoxyphenyl

Scheme 3-1. Proposed Catalytic Mechanism [a]

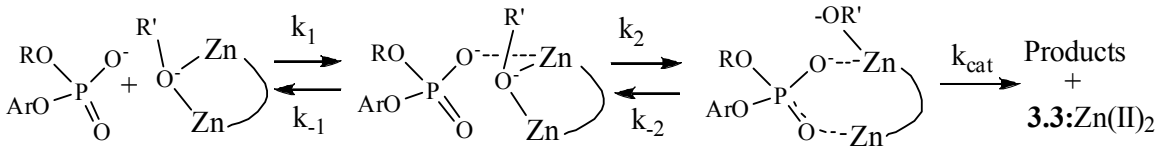

[a] R = CH_3 or 2-hydroxypropyl; $^{-}OR'$ = alkoxide

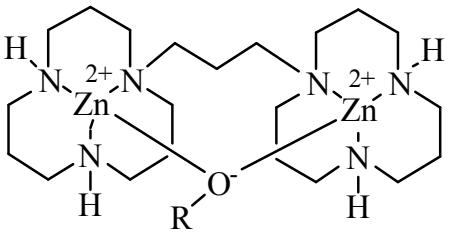

3.3:$Zn(II)_2$:^{-}OR

For both of these systems the synergy created between a highly active dinuclear **3.3**:$Zn(II)_2$:($^{-}OCH_3$) catalyst and the methanol solvent accelerates the cleavage of phosphate diesters by $10^{11\text{-}13}$ times relative to the methoxide promoted background reactions at $^{s}_{s}$pH 9.8 and 25 ^{o}C. That the rate enhancement far exceeds anything reported for this[6] or related catalytic RNase or DNase models in water[2,3,7] seems to be intimately tied to the reduced dielectric constant/polarity of the medium. Very recent work has shown that a different sort of medium effect provided by 80% DMSO/water confers very large rate accelerations of 2.7 x 10^9 to 4.4 x 10^{10} for the Eu(III) and La(III) catalyzed hydrolysis of **3.1a** at essentially neutral pH in that medium.[8]

It seems possible that a further reduction of polarity/dielectric constant, while still retaining significant hydrogen bonding such as would be the case with ethanol, (dielectric constant ϵ = 31.5 and 24.3 for methanol and ethanol respectively)[9] might lead to even higher catalytic rate enhancements for the cleavage of phosphate diesters by **3.3**:$Zn(II)_2$:($^{-}$OR).[10] Herein we report a comprehensive study of the catalytic cleavage of diesters **3.1a-g** promoted by **3.3**:$Zn(II)_2$ in anhydrous ethanol (99.9%). As will be seen, the kinetic pathways for all substrates proceed with a very strong substrate/catalyst saturation binding followed by a rate-limiting k_{cat}^{max} process which is shown to change from a chemical one for substrates with poor leaving groups, to a conformational change for those with good leaving groups. These are very fast reactions having k_{cat}^{max}/K_m terms

10^{12} to 10^{14} times larger than the corresponding second order rate constants for the ethoxide catalyzed reactions. Finally, in order to provide a deeper understanding of the catalytic process, we provide energetics calculations to determine the contributions of each of the kinetic and thermodynamic terms toward the acceleration achieved.

3.3 - Experimental

3.3.1 - Materials

Sodium ethoxide (21 wt. % solution in denatured ethanol, titrated against N/50 Fisher Certified standard aqueous HCl solution and found to be 2.68 M), and $Zn(CF_3SO_3)_2$, were purchased from Aldrich and used without further purification. Tetrabutylammonium ethoxide in ethanol (~ 40% , titrated against 1N Fisher certified standard aqueous HCl solution and found to be 1.08 ± 0.01 M) was obtained from Fluka. $HClO_4$ (70% aqueous solution, titrated to be 11.40 M) was purchased from Acros Organics and used as supplied. Anhydrous ethanol was purchased from Commercial Alcohols Inc. and was de-gassed by bubbling Ar through it for 1h before storing it under Ar. The de-gassed ethanol was freshly dispensed prior to each set of kinetic experiments, and kept for a maximum duration of 1h in an oven-dried, capped Erlenmeyer flask sealed with Parafilm® between uses. The [H_2O] in the freshly dispensed de-gassed ethanol was found to be 0.028 ± 0.007 M using a Mettler Toledo DL32 Karl Fischer Coulometer, while the [H_2O] for the ethanol that has been kept in an Erlenmeyer flask for 1h as described above (and used for experiments) was been determined to be 0.029 ± 0.007 M. The sodium salts of aryl 2-hydroxylpropyl phosphates (**3.1a-g**) were prepared and characterized as described earlier.[4] 1,3-Bis-N_1,N_1'-(1,5,9-triazacyclododecyl)propane

(**3.3**) was prepared as described.[5b] The dinuclear **3.3**:$Zn(II)_2$:($^{-}OCH_2CH_3$) complex was prepared as 2.5 mM stock solutions in de-gassed absolute ethanol by sequential addition of aliquots of stock solutions of sodium ethoxide, 1,3-bis-N_1,N_1'-(1,5,9-triazacyclododecyl)propane, and $Zn(CF_3SO_3)_2$ in stoichiometric ratios of 1:1:2. *The complete formation of the active di-zinc complex is achieved only after 50 min in ethanol as monitored by the change in catalytic activity over time. This same phenomenon was observed for creation of the active forms of the di-Zn(II) and di-Cu(II) forms of the catalysts in methanol.*[4,5]

3.3.2 - Methods

^{1}H NMR and ^{31}P NMR spectra were determined at 400 and 162.04 MHz. The $CH_3OH_2^+$ and $CH_3CH_2OH_2^+$ concentrations were determined using a combination glass electrode (Radiometer model # XC100-111-120-161) calibrated with Fisher Certified standard aqueous buffers (pH = 4.00 and 10.00) as described in a previous paper.[11] ${}^{s}_{s}pH$ values in ethanol were determined by subtracting a correction constant -2.54 from the readings obtained from the electrode, and the autoprotolysis constant of ethanol (K_{auto}) is taken to be $10^{-19.1}$.[11]

Literature ${}^{s}_{s}pK_a$ values[12] of a series of different substituted phenols in ethanol and the measured half-neutralization ${}^{s}_{s}pK_a$ values of *p*-nitrophenol and 2,4-dinitrophenol (0.5 mM of the phenols and 0.25 mM of $NaOCH_2CH_3$ in degassed absolute ethanol), were plotted against the aqueous pK_a values and found to fit a linear relationship, ${}^{s}_{s}pK_a^{EtOH}$ = (1.24±0.01)${}^{s}_{s}pK_a^{HOH}$ + (3.2±0.1) (11 phenols; r^2= 0.9990). This relationship was used to interpolate the ${}^{s}_{s}pK_a^{EtOH}$ values for the corresponding phenols of **3.1b**,**c**,**g** in ethanol.

3.3.3 - Kinetics of Transesterification of 3.1a-g in Ethanol.

The transesterification of phosphates **3.1a-g** in degassed absolute ethanol were followed by following the rates of the appearance of the corresponding phenolic products by regular and stopped-flow UV/visible spectrophotometry at 25.0 ± 0.1 ^{o}C at the wavelengths listed in Table 3-1.

Table 3-1. Table of the wavelengths used to monitor the **3.3**:$Zn(II)_2$:($^{-}OCH_3CH_3$)-catalyzed reactions (λ_{cat}) the base promoted reactions (λ_{base}) of phosphates **3.1** in ethanol at 25 ^{o}C.

Phosphate 3.1 -	**a**	**b**	**c**	**d**	**e**	**f**	**g**
λ_{cat} (nm)	320	323	340	284	282	280	292
λ_{base} (nm)	401	399	407	305			

For the complex-catalyzed reactions, a 2.5 mM stock solution of **3.3**:$Zn(II)_2$:($^{-}OCH_3CH_3$) in de-gassed absolute ethanol was prepared in a capped and sealed (with Parafilm®) oven-dried vial under N_2 at ambient temperature 1h prior to the kinetic experiments to ensure the complete formation of the catalyst complex. This solution was used to prepare solutions of the catalyst with concentrations ranging from 0.02 mM ≤ [**3.3**:$Zn(II)_2$:($^{-}OCH_2CH_3$)] ≤ 0.2 mM, which were then loaded into one syringe of the stopped-flow reaction analyzer. Solutions of (8 - 16) x 10^{-5} M of substrates **3.1a-g** in ethanol were loaded into the second syringe. The final concentration of the phosphates was (4 – 8) x 10^{-5} M. At each [**3.3**:$Zn(II)_2$:($^{-}OCH_2CH_3$)] the pseudo-first order rate constants (k_{obs}) were evaluated by fitting the UV/vis absorbance vs. time traces to a

standard exponential model. All reactions were followed to at least three half-times and found to exhibit good first order rate behavior. At least five kinetic runs were conducted at each [**3.3**:$Zn(II)_2$:($^-OCH_2CH_3$)], and only the average k_{obs} values are reported and used for analysis.

In order to determine the stability of the catalyst in the reaction medium, 8 x 10^{-5} M of **3.1a** in ethanol was loaded into one of the syringes in the stopped-flow reaction analyzer. An ethanol solution containing 0.8 mM of **3.3**:$Zn(II)_2$:($^-OCH_2CH_3$) was loaded into the other syringe. Judging from the rate of appearance of the phenol product at 320 nm at different times over 200 min. there was no decomposition of the catalyst during this time.

During the above kinetic experiments, the ionic strength was not controlled nor was the ${}^{s}_{s}pH$ controlled by buffers as we have found that the associated anions of these heavily inhibit the reactions. Thus, the ${}^{s}_{s}pH$ values were set by the catalytic system itself and were generally found to be 9.0 ± 0.2 in the plateau region of the k_{obs} vs [**3.3**:$Zn(II)_2$:($^-OCH_2CH_3$)] plots. However, a ${}^{s}_{s}pH$/log rate constant profile for the cleavage of **3.1e** catalyzed by **3.3**:$Zn(II)_2$ in ethanol was conducted in the following manner. First, varying amounts of $NaOCH_2CH_3$ or $HClO_4$ stock solutions (5 mM) in ethanol were added to solutions containing 2 x 10^{-4} M of a preformed **3.3**:$Zn(II)_2$:($^-OCH_2CH_3$) complex in ethanol which had been prepared an hour in advance to allow for complete formation of the catalyst complex. After the introduction of the additional acid or base the mixture was allowed to stand for 30 min to equilibrate (independent experiments showed that this time was optimum to attain the maximum kinetic activity) and then loaded into one of the two syringes of the stopped-flow analyzer while a 1.6 x 10^{-4} M solution of **3.1e** in ethanol was

loaded into the other. The final concentrations after mixing in the reaction chamber were 1 x 10^{-4} M of **3.3**:$Zn(II)_2$ and 8 x 10^{-5} M of **3.1e** in ethanol. The $^{s}_{s}pH$ values were measured at the end of the reactions. The $^{s}_{s}pH$/log rate constant profile plot given in Figure 3-5 shows a broad plateau from $^{s}_{s}pH$ 7.9-10, with the line through the data being derived from a fit of the solid squares data to a process that depended on two ionizable groups having $^{s}_{s}pK_a$ values of 7.2 and 10.8.

To determine the magnitude and type of $CF_3SO_3^-$ inhibition, a 4 x 10^{-5} M solution of **3.1a** was pre-mixed with varying concentrations of tetrabutylammonium triflate so that the final [triflate ion] ranged from 8 x 10^{-4} – 4.8 x 10^{-3} M, and the rate of the reaction in the presence of 0.2 mM of **3.3**:$Zn(II)_2$:($^-OCH_2CH_3$) at each [triflate anion] was monitored in duplicate in ethanol, ($^{s}_{s}pH$ = 8.54-8.85).

The rates of the ethoxide-catalyzed reactions of **3.1a-d** ((1-2) x 10^{-4} M) were determined by UV/vis spectrophotometry at 25.0 ± 0.1 ^{o}C in the presence of tetrabutylammonium ethoxide at various concentrations between 0.004 and 0.4 M in degassed absolute ethanol. The kinetic data were analyzed by the initial rate method in which the first 2 - 10% of the Abs. vs time traces for appearance of phenolate products were fitted to a linear regression and the so-obtained rates converted to first order rate constants (k_{obs}) by dividing them by the expected absorbance change if the reaction were to reach 100% completion. The reactions were carried out in duplicate and the plots of the average first order rate constants (k_{obs}) vs. [tetrabutylammonium hydroxide] were fitted to a standard linear regression model to find the second order rate constants (k_2^{-OEt}).

3.4 – Results

3.4.1 - Ethoxide-Catalyzed Transesterification of 3.1a-d in Ethanol

The ethoxide-promoted cleavages of **3.1a-d** in ethanol at 25.0 ± 0.1 ^{o}C were studied under pseudo-first order conditions of excess [$CH_3CH_2O^-$] and the kinetics of formation of the phenolate products were monitored by initial rate methods due to the slowness of the reactions. Phosphates **3.1e-g** react too slowly in base to determine the rate constants accurately in a reasonable time. In Figure 3-1 is a plot of the second order rate constants (k_2^{-OEt}) for substrates **3.1a-d** vs the $^{s}_{s}pK_a$ of the corresponding phenols in ethanol. These data were fit by linear regression as k_2^{-OEt} = (-0.90 ± 0.04) $^{s}_{s}pK_a$ + (7.2 ± 0.6), r^2 = 0.9955; n = 4, which was used to estimate the rate constants for **3.1e-g** given in Table 3-2.

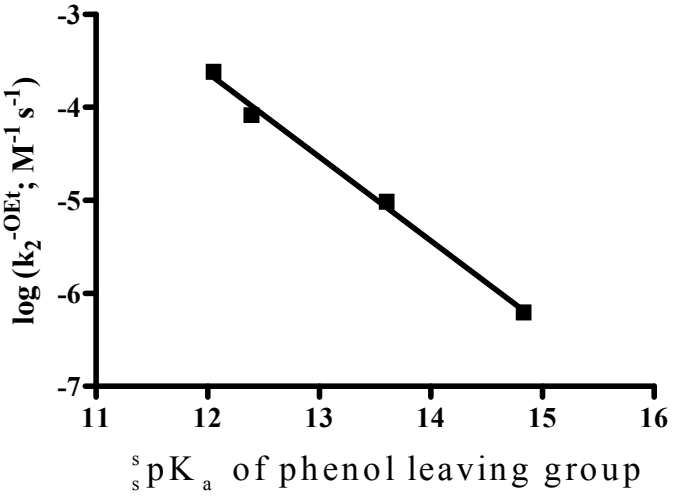

Figure 3-1. Brønsted plot of log (k_2^{-OEt}) vs. the $^{s}_{s}pK_a$ values for the ethoxide-promoted cleavage of **3.1a-d** in de-gassed absolute ethanol at 25.0 ± 0.1 ^{o}C. The data fit a standard linear regression of k_2^{-OEt} = (-0.90 ± 0.04) $^{s}_{s}pK_a$ + (7.2 ± 0.6); r^2 = 0.9955.

Table 3-2. Kinetic data (maximum rate constant for the **3.3**:$Zn(II)_2$:($^-OCH_2CH_3$)-catalyzed reactions corrected for triflate inhibition ($k_{cat}^{max\ corr.}$), second order rate constants for the ethoxide-promoted reactions (k_2^{-OEt}), and the catalytic rate accelerations, given as ($k_{cat}^{max\ corr.}/K_M$)/k_2^{-OEt}) for the cleavages of **3.1a-g** in ethanol at 25 ± 0.1 ^oC.

Phosphate diester	$^s_s pK_a$ of phenol	$k_{cat}^{max\ corr.}$ (s^{-1}) [a]	k_2^{-OEt} ($M^{-1}s^{-1}$)	($k_{cat}^{max\ corr.}/K_M$)/k_2^{-OEt} [c]
3.1a	12.05	168±6	(2.43±0.09) x 10^{-4}	2.2 x 10^{12}
3.1b	12.39	133±5	(8.3±0.4) x 10^{-5}	5.1 x 10^{12}
3.1c	13.60	139±3	(9.7±0.7) x 10^{-6}	4.5 x 10^{13}
3.1d	14.83	36±1	(6.3±0.3) x 10^{-7}	1.8 x 10^{14}
3.1e	15.15	14.5±0.3	3.7 x 10^{-7} [b]	1.2 x 10^{14}
3.1f	15.60	4.5±0.1	1.4 x 10^{-7} [b]	1.0 x 10^{14}
3.1g	15.92	2.67±0.06	7.4 x 10^{-8} [b]	1.1 x 10^{14}

a. $k_{cat}^{max\ corr.}$ values are determined as described in text by fitting the k_{obs} vs. [Cat] data to eq. (1) after correction for triflate inhibition

b. k_2^{-OEt} values for the base-promoted reactions of the less reactive substrates **3.1e-g** were estimated from the linear regression equation for the Brønsted plot in Figure 3-1.

c. Ratio of the apparent second order rate constant for the **3.3**:$Zn(II)_2$:($^-OCH_2CH_3$)-promoted reaction of **3.1** (given as $k_{cat}^{max\ corr.}/K_m$) and second order rate constant for the ethoxide reaction. K_m value represents the dissociation constant of **3.3:**$Zn(II)_2$:($^-OCH_2CH_3$):**3.1** Michaelis complex which has an upper limit of $10^{-6.5}$ M. See text.

3.4.2 – 3.3:Zn(II)$_2$:($^-$OCH$_2$CH$_3$)-Promoted Transesterification of 3.1 in Ethanol

Shown in Figure 3-2 is a representative plot of the uncorrected k_{obs} for reaction of **3.1a-g** vs total [**3.3**:Zn(II)$_2$:($^-$OCH$_2$CH$_3$)]$_t$ put into the solution. The plots for all the substrates follow the same general appearance, in passing from sub-stoichiometric amounts of catalyst to a roughly 2-fold excess of catalyst/substrate. All the plots show an apparent x-intercept and very strong 1:1 saturation binding superimposed on an inhibition curve that depends upon the increasing [$^-$OTf] (each equivalent of catalyst brings with it four eq. of triflate).

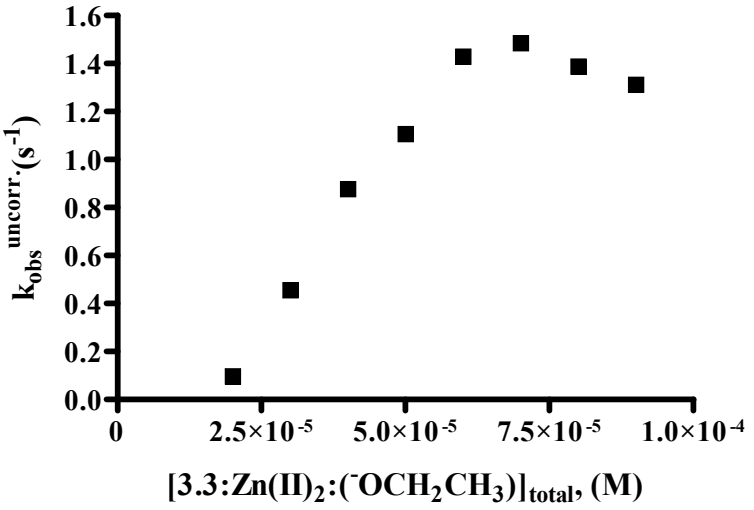

Figure 3-2. A plot of $k_{obs}^{(uncorr)}$ vs [**3.3**:Zn(II)$_2$:($^-$OCH$_2$CH$_3$)]$_t$ for the catalyzed transesterification of **3.1g** (5 x 10^{-5} M) at 292nm and 25 ^{o}C in absolute ethanol.

We have previously demonstrated that triflate anion is a competitive inhibitor of the catalysis of phosphate diesters exhibited by **3.3**:Zn(II)$_2$:($^-$OCH$_3$) with a K_i = 14.9 mM in anhydrous methanol.[5b] In ethanol, the affinity of triflate for the positively charged

catalyst is enhanced and analysis of the k_{obs} vs [$^{-}$OTf] data shown in Figure 3 for the **3.3**:Zn(II)$_2$:($^{-}$OCH$_2$CH$_3$) promoted reaction of **3.1a** in ethanol gives an inhibition constant of K_i = (0.36 ± 0.02) mM. The analysis of the data is somewhat complicated and requires explanation to account for the appearance of the primary data plot in Figure 3-2 and the considerable inhibition provided by triflate anion.

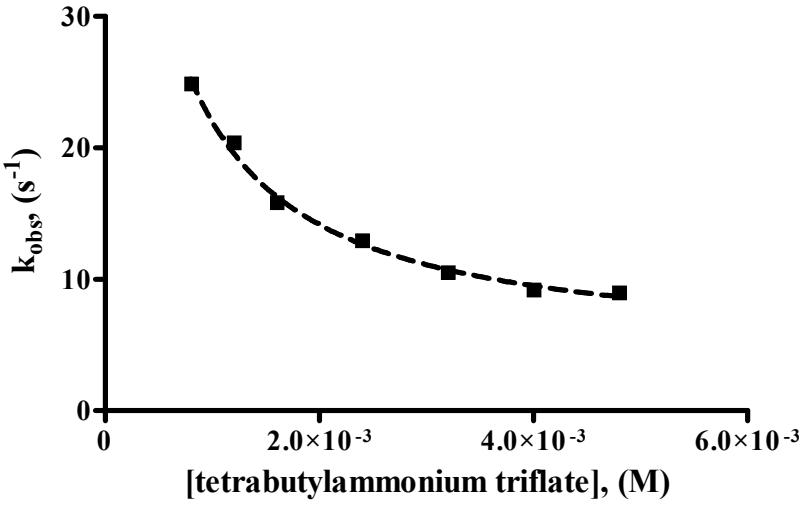

Figure 3-3. A plot of k_{obs} vs. [tetrabutylammonium triflate] for the catalyzed transesterification of **3.1a** (4 x 10^{-5} M) with [**3.3**:Zn(II)$_2$:($^{-}$OCH$_2$CH$_3$)]$_t$ = 0.2 mM at 320 nm and 25 ^{o}C in de-gassed absolute ethanol. The inhibition constant (K_i) for triflate anion was determined by fitting the data into an inhibition model[13] and was found to be (0.36 ± 0.02) mM (dashed line represents the fit).

Scheme 3-2. Uncompetitive triflate anion ($^{-}$OTf) inhibition of the **3.3**:Zn(II)$_2$:($^{-}$OCH$_2$CH$_3$)-catalyzed transesterification of **3.1** in ethanol.

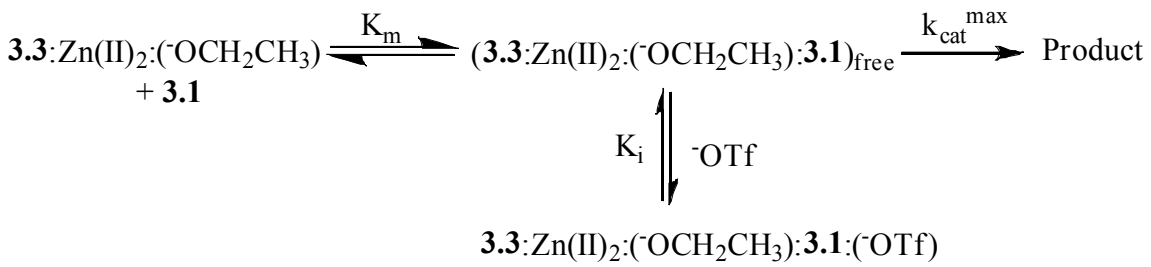

The appearance of the triflate inhibition plot in Figure 3-3 suggests that this anion is an uncompetitive[14] inhibitor following the simplified process given in Scheme 3-2 where K_i refers to the dissociation constant for the triflate inhibited complex, (**3.3**:Zn(II)$_2$:($^{-}$OCH$_2$CH$_3$):**3.1**:($^{-}$OTf)) in units of mM. The scheme is based on the assumption that the binding of the phosphate is far larger than that of triflate, and that there are two substrate-bound forms of the catalyst, namely (**3.3**:Zn(II)$_2$:($^{-}$OCH$_2$CH$_3$):**3.1**)$_{free}$, which leads to the product, and a triflate bound form, (**3.3**:Zn(II)$_2$:($^{-}$OCH$_2$CH$_3$):**3.1**:$^{-}$OTf), which has an insignificant reactivity relative to the latter. The first assumption seems justified by the fact that the K_m dissociation constants of all the (**3.3:**Zn(II)$_2$:($^{-}$OCH$_2$CH$_3$):**3.1a-g**) complexes are very small and estimated to be at most $10^{-6.5}$ M *vide infra*. The second assumption is reasonable since the fit of the experimental data gives the line in Figure 3-3 that asymptotically approaches a limiting value of zero for the observed rate constant (within experimental uncertainty) for a fully triflate bound complex. The amount of free catalytically active species (**3.3**:Zn(II)$_2$:($^{-}$OCH$_2$CH$_3$):**3.1**)$_{free}$ is calculated from eq. (1) while eq. (2) is used to provide a rate constant for catalyzed

cleavage of **3.1**[15] ($k_{obs}^{corr.}$) from the raw kinetic data ($k_{obs}^{uncorr.}$) after correction for the triflate inhibition.

$$[(\mathbf{3.3} : \mathrm{Zn(II)} : (^{-}\mathrm{OCH_2CH_3}) : \mathbf{3.1})]_{free} = \frac{(K_i)[(\mathbf{3.3} : \mathrm{Zn(II)} : (^{-}\mathrm{OCH_2CH_3}) : \mathbf{3.1})]_{total}}{K_i + [^{-}\mathrm{OTf}]} \qquad (1)$$

$$k_{obs}^{corr.} = \frac{k_{obs}^{uncorr.}(K_i + [^{-}\mathrm{OTf}])}{K_i} \qquad (2)$$

Eq. (3) is a universal expression[16] applicable to both strong and weak binding situations that has been used to analyze kinetic data for similar systems in methanol.[4,5] In eq. (3), [sub] refers to the initial concentration of **3.1**, [cat] refers to the concentration of *viable* catalyst, which is derived from the expression [cat] = $[cat]_{total}$ – A, where A is an independently fitted parameter that corresponds to the x-intercept value observed in the kinetic plots of k_{obs} vs [**3.3**:$Zn(II)_2$:($^{-}OCH_2CH_3$)]$_t$ for all substrates **3.1**. This intercept was previously observed in analogous plots obtained in methanol, and was explained by a dissociation of metal ion away from the catalyst at low concentrations which led to an inactive form.[4,5] K_B is defined as the binding constant (units of M^{-1}) between the catalyst and **3.1**. We define K_m (the reciprocal of K_B) as the dissociation constant of the non-triflate associated substrate:catalyst complex {(**3.3**:$Zn(II)_2$:($^{-}OCH_2CH_3$):**3.1**)$_{free}$} in units of M, with k_{cat}^{max} being the maximum rate constant going from the catalytically active species (**3.3**:$Zn(II)_2$:($^{-}OCH_2CH_3$):**3.1**)$_{free}$ forward to the product.

$$k_{obs} = k_{cat}(1 + K_B * [sub] + [cat] * K_B - X)/([sub] * (2K_B)) \qquad (3)$$

where:

$$X = \{(1 + 2K_B * [sub] + 2 * [\mathrm{cat}] * K_B + K_B^{\,2} * [sub]^2 - 2 * K_B^{\,2} * [\mathrm{cat}][sub] + [\mathrm{cat}]^2 * K_B^{\,2}\}^{0.5}$$

In Figure 3-4 is a plot of the $k_{obs}^{corr.}$ values vs $[(\mathbf{3.3}{:}Zn(II)_2{:}(^{-}OCH_2CH_3)]_{total}$ for the catalyzed cleavage of **3.1g** in ethanol where, due to the strong binding, the plot breaks sharply at the point where there is a 1:1 ratio of catalyst (over the amount at the x-axis intercept, A) and phosphate. Similar strong binding plots are observed for the **3.3**:$Zn(II)_2$:($^{-}OCH_2CH_3$)-catalyzed cleavage of each of **3.1a-g** in ethanol and the kinetic data are also fitted to eq. (3) in order to determine the $k_{cat}^{max\ corr.}$ values (after correcting for triflate inhibition): these are presented in Table 3-2.

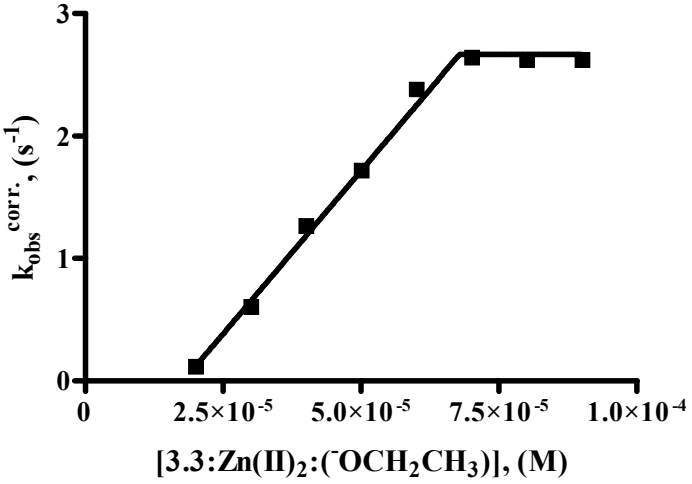

Figure 3-4. A plot of $k_{obs}^{(corr)}$ vs. [**3.3**:$Zn(II)_2$:($^{-}OCH_2CH_3$)] for the catalyzed cleavage of **3.1g** (5×10^{-5} M) at 292 nm and 25 ^{o}C in absolute ethanol. The raw data (Figure 3-2) was corrected for triflate inhibition using eq. (1,2). By fitting the corrected data to eq. (3) one obtains the line through the data with the maximum rate constant ($k_{obs}^{max\ corr.}$) of $2.67 \pm 0.06\ s^{-1}$ and $A = (1.78 \pm 0.01) \times 10^{-5}$ M.

Since the binding of the phosphate to the complex is so strong, accurate values for K_B cannot be obtained from the data at hand. However an upper limit can be estimated through an iterative procedure where the K_B value is increased until the goodness of fit

maximized. For all substrates, the goodness of the fits did not change when the K_B value exceeded $10^{6.5}$ M^{-1}, so we have assumed an upper limit for the binding constant for all substrates of $K_B = 3.2 \times 10^6$ M^{-1} (correspondingly $K_m = 3.2 \times 10^{-7}$M).

A ${}^{s}_{s}pH$ vs log $k_{obs}^{max\ corr.}$ profile (Figure 3-5) was constructed for the reaction of **3.1e** promoted by **3.3**:$Zn(II)_2$ as follows. A 2×10^{-4} M solution of the catalyst (**3.3**:$Zn(II)_2$:($^{-}OCH_2CH_3$)) was prepared in ethanol, as described in the experimental section, and then treated with varying amounts of $HClO_4$ or NaOEt to vary the ${}^{s}_{s}pH$. The mixtures were allowed to equilibrate for 30 minutes and then mixed by stopped-flow with 1.6×10^{-4} M of phosphate **3.1e**, and the kinetics of the reaction were monitored (final concentrations were half those in the syringes). At these concentrations all the substrate is bound to catalyst so the observed rate constant corresponds to k_{obs}^{max} which is then numerically corrected for triflate inhibition. Following the reaction, the ${}^{s}_{s}pH$ of the mixtures were measured and assumed to be representative of those during the reaction. The ${}^{s}_{s}pH$ /log $k_{obs}^{max\ corr.}$ plot of Figure 3-5 shows a hint of bell-shape with a broad plateau between $\sim {}^{s}_{s}pH$ 7.9 and 10, and when the solid squares data are fit to a two ${}^{s}_{s}pK_a$ model (Scheme 3-3, ref. (17)), this gives a computed $k_{cat}^{max\ corr.}$ of 13.7 s^{-1} (compare with the value of 14.5 ± 0.3 s^{-1} in Table 3-2 determined in a different way) and ${}^{s}_{s}pK_a^{1}$ and ${}^{s}_{s}pK_a^{2}$ values of 7.2 and 10.8.[18] Notable is the observation that below pH 7.7, the catalytic activity drops more precipitously than theory predicts, suggesting that the catalyst is not stable once the removal of the ethoxide (or its kinetic equivalent) commences. Therefore, none of the data in the shaded area was used for any fits.

Scheme 3-3. A proposed process depending on two $^{s}_{s}pK_a$ values for the catalyzed cleavage of **3.1** promoted by complex **3.3**:$Zn(II)_2$:($^{-}OCH_2CH_3$).

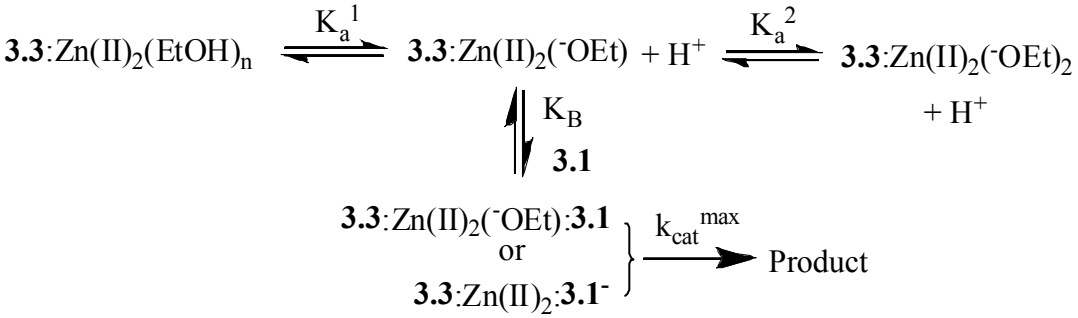

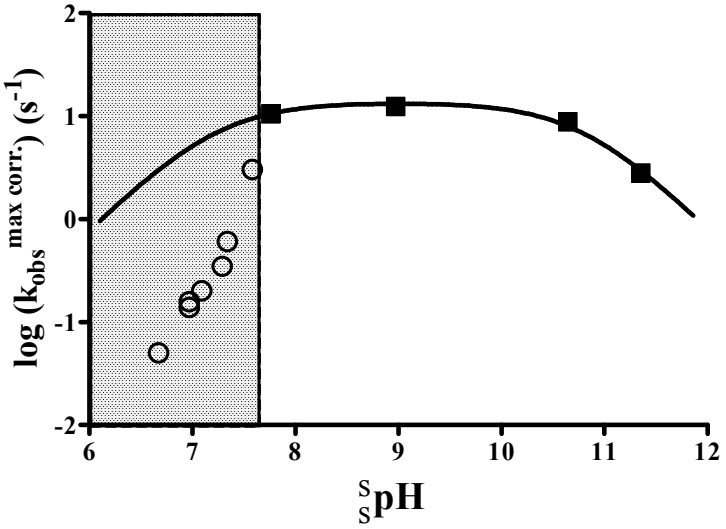

Figure 3-5. A $^{s}_{s}pH$ /log $k_{obs}^{max\ corr.}$ profile for the reaction of **3.3**:$Zn(II)_2$:($^{-}OCH_2CH_3$) and **3.1e** conducted at 25 ^{O}C at respective concentrations of 1 x 10^{-4} M and 8 x 10^{-5} M. The line through the square data points is computed on the basis of the process given in Scheme 3-3[17] having a bell-shaped $^{s}_{s}pH$ /rate profile giving two fitted $^{s}_{s}pK_a$ values of 7.2 ± 0.4[18] and 10.8 ± 0.1. The shaded data below $^{s}_{s}pH$ 7.7 were not used for fitting.

3.5 - Discussion

3.5.1 - Ethoxide-Promoted Reactions of Phosphates 3.1

The Figure 3-1 Brønsted plot for the ethoxide-promoted reactions of **3.1a-e** in ethanol has a β_{lg} value of -0.90 ± 0.04 which is slightly larger than the -0.72 ± 0.08[4] observed for the methoxide-promoted cyclization of **3.1a-g** in methanol and the hydroxide-promoted cyclization of 2-hydroxypropyl aryl phosphates in water (β_{lg} value of -0.62)[19]. There is considerable debate about whether the cleavage of phosphate diesters of type **3.1** is concerted or stepwise.[20,21] However, a recent study of the $^{-}$OH-promoted cleavage of uridine 3′-phosphate esters in water suggested a stepwise cleavage mechanism with the rate-limiting step for substrates with good leaving groups being the cyclization step (β_{lg} = -0.52) while that for substrates with poor leaving groups being the breakdown of the phosphorane (β_{lg} = -1.34).[22] In the latter report it was suggested that the original data for the base promoted cyclization of 2-hydroxypropyl aryl and alkyl phosphates[23] could be reinterpreted as being consistent with a stepwise process involving a five-membered cyclic phosphorane intermediate. The change in the rate-limiting step observed for such stepwise reactions occurs at the quasi-symmetrical point where the pK_a of the leaving group (HOR) is approximately the same as the pK_a of the nucleophilic 2-hydroxypropyl group. Since the ${}^{s}_{s}pK_a$ of the corresponding phenol leaving groups of phosphates **3.1a-d** are all lower than the ${}^{s}_{s}pK_a$ of the 2-hydroxylpropyl group (estimated to be about 21.7 in ethanol)[24] the k_2^{-OEt} constant for cyclization of all of **3.1a-g** should all fall on a Brønsted line corresponding to rate-limiting formation of a phosphorane intermediate. Assuming that the β_{eq} of -1.74 for the transfer of the phosphoryl group

between oxyanions in water[25] can be extrapolated to ethanol, the Leffler parameter, $\alpha = \beta_{lg}/\beta_{eq} = 0.52$ for the ethoxide reactions of phosphates **3.1a-g** in ethanol, suggests that in the transition state for cyclization the P-OAr bonding character progress some 52% of the way from the starting material to phenolate product with the aryloxy oxygen now having a net charge of ~ -0.16 = (+0.74-0.90) in the TS. Should the process really be concerted and proceed via a single TS, the analysis would be essentially the same suggesting that the TS is central, about halfway between starting material and product.

It is an expected consequence of reduced dielectric constant/polarity that the rates of reactions between species of the same charge type are retarded, while those between oppositely charged species are accelerated. For the lyoxide-promoted reaction of **3.1a** shown in eq. (4), k_2^{-OEt} is 2.4 x 10^{-4} $M^{-1}s^{-1}$, k_2^{-OMe} is 2.6 x 10^{-3} $M^{-1}s^{-1}$ [26] and that for the hydroxide promoted cyclization is reported to be 9.9 x 10^{-2} $M^{-1}s^{-1}$ [27] or 6.5 x 10^{-2} $M^{-1}s^{-1}$.[28] The 10-fold rate reduction in ethanol relative to methanol is a consequence of the reduced polarity/dielectric constant which opposes the pre-equilibrium formation of the dianionic form (**3.1a**$^-$).

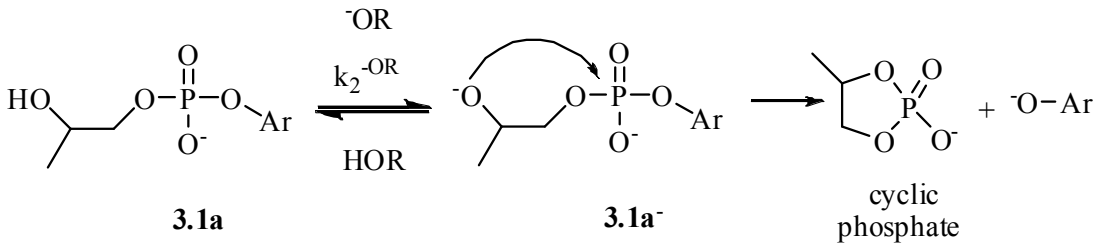

3.1a **3.1a**$^-$

(4)

As will be shown later, this same reduced dielectric constant/polarity effect considerably enhances the reactions of substrates **3.1** when they are bound to the

positively charged **3.3**:Zn(II)$_2$:($^-$OCH$_2$CH$_3$) catalyst as **3.3**:Zn(II)$_2$:($^-$OCH$_2$CH$_3$):**3.1** or the kinetic equivalent **3.3**:Zn(II)$_2$:**3.1**$^-$ in ethanol relative to methanol.

3.5.2 – 3.3:Zn(II)$_2$:($^-$OCH$_2$CH$_3$)-Catalyzed Transesterification of 3.1

The catalytically active form of the complex in this study is almost certainly stoichiometrically analogous to that found in methanol[4,5], comprising a 1:2:1 ratio of ligand:Zn(II)$_2$:($^-$OR). While **3.3**:Zn(II)$_2$:($^-$OCH$_3$) and **3.3**:Zn(II)$_2$:($^-$OCH$_2$CH$_3$) are stable when prepared as described in the Experimental Section, they form only slowly and so are not amenable to titrimetric studies to provide the thermodynamic ${}^{s}_{s}pK_a$ values. In past work we have estimated the first ${}^{s}_{s}pK_a$ by determining the ${}^{s}_{s}pH$ at half neutralization immediately following the addition of half an equivalent of $HClO_4$ to a methanol solution of **3.3**:Zn(II)$_2$:($^-$OCH$_3$). Here, it was found that the partial ${}^{s}_{s}pH$/rate profile shown in Figure 3-5 could be obtained by adding small amounts of $HClO_4$ or NaOEt to a preformed catalyst, allowing this mixture to equilibrate for some time, and then determining the $k_{obs}^{max\ corr.}$ for the kinetics of cleavage of substrate **3.1e** which is fully bound to the complex as **3.3**:Zn(II)$_2$:($^-$OCH$_2$CH$_3$):**3.1e** or a possible kinetic equivalent, **3.3**:Zn(II)$_2$:**3.1e**$^-$, where the 2-hydroxy group is deprotonated. The ${}^{s}_{s}pH$ values of the mixtures were measured following determination of the kinetics for generation of product and were assumed to be representative of those in the reacting solution. The log $k_{obs}^{max\ corr.}$/${}^{s}_{s}pH$ data in Figure 3-5 follow an apparent bell-shaped profile with the catalytic activity plateauing between ${}^{s}_{s}pH$ 7.9 and 10, suggesting that it is follows the process given in Scheme 3-3 with two ionizations having ${}^{s}_{s}pK_a$ values of ~7.2 and 10.8

determined from fitting the solid square data of the figure to an appropriate equation.[17] The kinetic data (○) obtained in the low ${}^{s}_{s}\mathrm{pH}$ domain do not fit the theoretical model and indicate that once the ethoxide begins to be removed from the complex, the system is unstable, probably dissociating one of the Zn(II) ions with concomitant loss of activity. This is consistent with our experience that indicates one cannot form these complexes in methanol/ethanol without having one equivalent of alkoxide present along with the ligand prior to the addition of the metal ions.

3.5.3 - Change in Rate-Limiting Step for the $k_{cat}^{max\ corr.}$ Term

The Brønsted plot given in Figure 3-6 exhibits a sharp downward break in log $k_{cat}^{max\ corr.}$ commencing at ${}^{s}_{s}\mathrm{pK_a} \sim 14.3$ suggesting a change in rate limiting step for the unimolecular term dealing with product formation from some form of catalyst:substrate complex. Unlike the case in methanol[4], all the kinetic data for the catalyzed cleavages of **3.1a-g** in ethanol exhibit saturation behaviour with very strong binding.

The fact that the $k_{cat}^{max\ corr.}$ terms for substrates **3.1a-c** containing good leaving groups are essentially independent of the ${}^{s}_{s}\mathrm{pK_a}$ ($\beta_{lg} = \sim 0$) indicates that the process that limits the rate for those substrates cannot be dependent on any chemical step where changes in the bonding of the P-OAr linkage are prominent. This is consistent with a non-chemical step such as a rearrangement process (k_2 in Scheme 3-1) becoming rate-limiting for substrates with good leaving groups (**3.1a-c**) while the rates of the reactions for substrates with poorer leaving groups (**3.1d-g**) are limited by some chemical step where there is a large dependence on the leaving group ($\beta_{lg} = -1.12$).

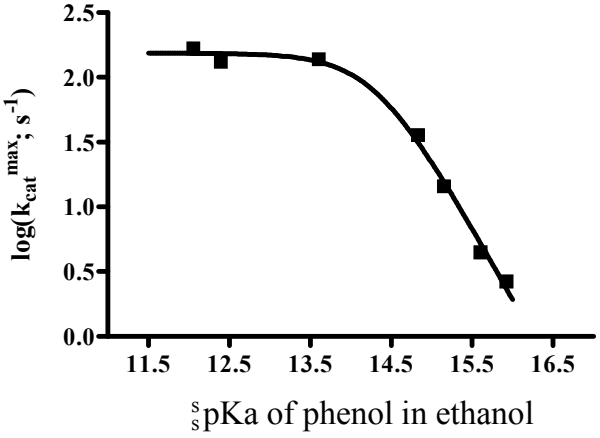

Figure 3-6. Brønsted plot of log ($k_{cat}^{max\ corr.}$) vs. the ${}^{s}_{s}pK_a$ values of the corresponding aryl leaving groups for the **3.3**:$Zn(II)_2$:($^{-}OCH_2CH_3$)-catalyzed cleavage of **3.1a-g** in absolute ethanol at 25 ^{o}C. The two lines cross at approximately ${}^{s}_{s}pK_a$ = 14.3. The line was constructed by NLLSQ fitting all the data to an expression $k_{cat}^{max\,corr.} = k_1k_2/(k_{-1}+k_2) = C_1C_2 10^{(\beta 1+\beta 2)pKa}/(C_{-1}10^{\beta -1pKa} + C_2 10^{\beta 2pKa})$.[29] The two fitted β values are -1.12 ± 0.12 and 0.0 ± 0.1.

These data and those previously in methanol[4] can be accommodated within the simplified model for the catalyzed reaction given in Scheme 3-1 with consideration of the effect of the reduced dielectric constant medium on the first equilibrium constant (K_{-1} = k_{-1}/k_1 in units of M). For the Debye-Hückel model for association of spherical ions in a medium of dielectric constant ε_r, the electrostatic potential energy of interaction between oppositely charged ions is:

$$P.E. = (z_+e)(z_-e)/(4\pi\varepsilon_0\varepsilon_r r) \qquad (5)$$

where r is the distance between the centers of the ions, z_+e and z_-e are their charges in coulombs (e is the proton charge), and ε_o is the permittivity of vacuum.[30] In passing from

water, to methanol and then ethanol, each 1 kcal/mol of potential energy of attraction increases by a factor of 2.5 and then 3.2, so there is a dramatic effect of reduced dielectric solvent on the binding of ions of opposite charge. That effect will increase the k_1 association rate constant and decrease the k_{-1} dissociation rate constant, consistent with the observed larger catalyst:substrate binding constant in ethanol relative to methanol. While the dielectric constant has an obvious role in increasing the binding, once the complex is formed the ensuing chemical transformation should be less sensitive to changes in ε since the reactants are intimate contact with solvent being excluded.

The solvent effect on the binding steps can be numerically evaluated using an approach similar to what we used before to analyze the change in rate limiting step in the **3.3**:$Zn(II)_2$:($^-OCH_3$)-catalyzed cleavage of **3.1a-g** in methanol.[4] In that case, analysis of the kinetic data suggested that the change in rate limiting step resulted from the substrate dependent partitioning of the doubly activated phosphate complex (k_{cat}^{max} vs. k_{-2}). Although the $k_{cat}^{max\ corr.}$ values we determined here for catalyzed cleavage of substrates **3.1c-g** with poorer leaving groups are very close to the analogous values determined in methanol, the observation that all substrates adhere to saturation kinetics in ethanol suggests there are important differences in the two solvents. The application of Michaelis-Menten kinetics to the process of Scheme 3-1 where the first step is treated as an equilibrium gives:

$$\text{rate} = \frac{dP}{dt} = \frac{k_{cat}^{max}[\mathbf{3}:Zn(II)_2:(^-OCH_2CH_3)]_{free}[\mathbf{3.1}]}{K_m + [\mathbf{3}.:Zn(II)_2:(^-OCH_2CH_3)]_{free}} \quad (6)$$

$$K_m = \frac{k_{-1}}{k_1} \bullet \frac{k_{-2} + k_{cat}^{max}}{k_2} = K_{-1}\frac{k_{-2}}{k_2} + K_{-1}\frac{k_{cat}^{max}}{k_2} \quad (7)$$

The K_m term can be broken down into two components as defined in eq. (7). With substrates **3.1d-g** having poor leaving groups where k_{cat}^{max} is less than k_{-2}, K_m is approximated as $K_{-1}(k_{-2}/k_2)$ and has an average value of ~ (9 ± 1) x 10^{-5} M in methanol and, since it is dominated by binding effects, is insensitive to the nature of the leaving group. In ethanol, the analogous data for all the substrates gives an upper limit of K_m of 3 x 10^{-7} M, which is a likely consequence of a reduction in the K_{-1} term pertaining to dissociation of phosphate away from **3.3**:$Zn(II)_2$:($^-OCH_2CH_3$). The fact that the break in the plot of Figure 3-6 is at $k_{cat}^{max\ corr.}$ ~150 s^{-1} suggests that this is the value for the proposed rearrangement step (k_2) to form the proposed doubly-activated phosphate by binding to both Zn(II) ions. Using this value it can be calculated that $K_{-1}k_{-2}$ is ~4.5 x 10^{-5} M•s^{-1}: assuming this same k_2 value obtains for the rearrangement step in methanol one calculates that $K_{-1}k_{-2}$ there would be 1.4 x 10^{-2} M•s^{-1}.

3.5.4 - The ${}^{s}_{s}pK_a$ Dependent $k_{cat}^{max\ corr.}$ Terms

The $k_{cat}^{max\ corr.}$ terms for the catalyzed cleavages of the bound substrates **3.1d-g** adhere to a Brønsted relationship having a β_{lg} of -1.12 ± 0.12 which is experimentally the same as was found for the catalyzed cleavage of **3.1c-g** in methanol (-0.97 ± 0.05)[4] and perhaps slightly larger than for the ethoxide promoted cleavage of **3.1a-d** in ethanol (-0.90 ± 0.04). While the rate limiting step is either a concerted displacement or formation of a phosphorane intermediate, a tentative conclusion can be drawn that there is a slightly more extensive change in the P-OAr bond in the **3.3**:$Zn(II)_2$:($^-OCH_2CH_3$)-catalyzed cleavage relative to the ethoxide promoted cleavage.

Shown in Scheme 3-4 is a proposed mechanism slightly expanded from that presented in Scheme 3-1 for the catalyzed cleavage based on the information gained in

ethanol. As a starting point we formulate the essential ethoxide in the **3.3**:$Zn(II)_2$ complex as bridging between the two metal ions based on the structural evidence gained with the diZn(II)[4] and diCu(II)[5c] complexes in methanol. Due to the high binding constant between **3.1** and **3.3**:$Zn(II)_2$:($^{-}OCH_2CH_3$), we propose formation of a large equilibrium amount of Comp 1 where there is binding of the phosphate to one of the metal ions with a loosening of the bridging ethoxide. This is followed by rearrangement step(s) where the phosphate becomes doubly activated by binding to both Zn ions. The k_2 step involves simultaneous removal of the coordinated ethoxide and deprotonation of the 2-hydroxypropyl group to yield Comp 2 which can undergo intramolecular cyclization (stepwise or concerted) to give the five-membered cyclic phosphate product.[31] An alternative rearrangement process via k_2' involves formation of Comp 2' having a coordinated ethoxide (bridging or singly coordinated), which subsequently acts as a general base to assist in the cyclization. A general base process is excluded in the case of a di Zn(II) complex promoting cyclization of **3.1a** in water[32] but is proposed as the viable mechanism for the Ln(III) promoted cleavages of **3.1a** in 80% DMSO/water,[8] so it is possible that there is a shift in mechanism from specific catalysis to general catalysis brought about by the medium effects that give the fast reactions observed here and previously.[4,5,8] Indeed the available evidence now allows us to rule out a specific base catalyzed process in ethanol where external ethoxide acts as the base to remove the proton from the 2-hydroxy group prior to cyclization. For the **3.3:**$Zn(II)_2$:($^{-}OCH_2CH_3$)-catalyzed cleavage of **3.1e** at $^{s}_{s}$pH 7.76, the observed $k_{cat}^{max\ corr.}$ is 10.6 s^{-1}. At that $^{s}_{s}$pH, the free [$^{-}$OEt] is 4.6 x 10^{-12} M (K_{auto} of ethanol is $10^{-19.1}$ M^2)[11], so the rate constant for

cleavage promoted by external $^{-}$OEt would need to be 2.65 x 10^{12} $M^{-1}s^{-1}$, exceeding the diffusion limit in ethanol[33] by a factor of 265.

Scheme 3-4. Proposed mechanism for the catalyzed reaction in ethanol. (Zn charges omitted for simplicity).

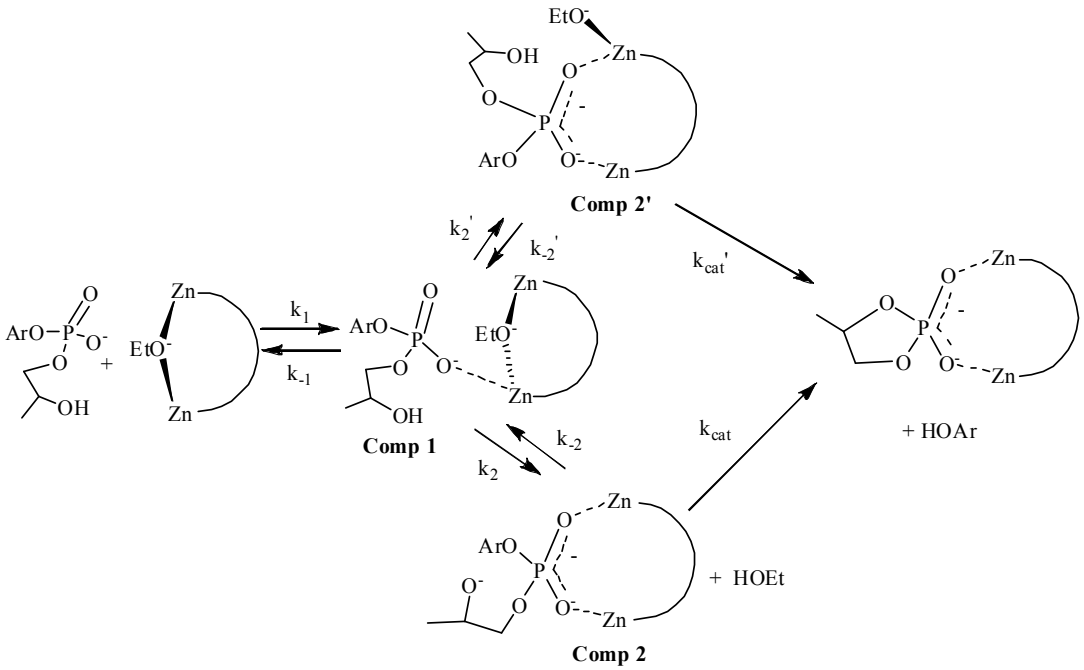

3.5.5 - Energetic Considerations for the Catalysis

In Table 3-2 are presented $(k_{cat}^{max\ corr.}/K_m)/k_2^{-OEt}$ values indicating the catalytic second order rate constants in ethanol are 10^{12} to 10^{14} larger than the corresponding ethoxide promoted reactions. Although the experimental k_{cat}^{max} values in ethanol and methanol for substrates **3.1c-g** are close to each other, the $(k_{cat}^{max}/K_m)/k_2^{-OMe}$ ratios for these substrates in methanol vary from about 4 x 10^8 to 4 x $10^{9.4}$ The kinetic data clearly indicate the apparent 10^4 larger activity in ethanol stems from respective 10 to 100-fold and at least 100-fold reductions in both the k_2^{-OR} terms and K_m terms relative to their

values in methanol. An alternative comparison that gives apparently spectacular accelerations relates the $k_{cat}^{max\ corr.}$ values to the presumed ethoxide reaction at the $^{s}_{s}pH$ where the catalyzed reactions were conducted. The [$^{-}$OEt] at $^{s}_{s}pH$ 9.0 is ~10^{-10} M, so that for **3.1c-g**, the catalytic acceleration would be 10^{17}-fold![34] By this measure, the catalytic acceleration in ethanol is 10^{5} larger than in methanol, but this stems from three main factors, including the 10 to 100-times less reactivity of the alkoxide reaction in ethanol, the decreased autoprotolysis constant of ethanol relative to methanol ($10^{-16.77}$ M^2) and the lower working $^{s}_{s}pH$ (9.0 vs 9.8).

The more thermodynamically correct method to evaluate the catalytic efficacy of enzyme- or synthetic catalyst-promoted reactions compares the free energy of binding of the catalyst to the transition state of the presumed lyoxide promoted reaction.[35,36,3] Following the procedures we used to analyze the **3.3**:$Zn(II)_2$:($^{-}OCH_3$) promoted cleavages of **3.1a-g** and **3.2a-n** in methanol[4,5], we consider in Scheme 3-5 a cycle encompassing the **3.3**:$Zn(II)_2$:($^{-}OCH_2CH_3$) and ethoxide reactions for **3.1a-g** in ethanol: the definitions of the terms are given in reference [4]. Eq. (8) provides the calculated free energy of binding of the catalyst to the ethoxide:substrate complex ($\Delta\Delta G^{\ddagger}_{stab}$); i.e. [**3.3:**$Zn(II)_2$:($^{-}OCH_2CH_3$):**3.1**]‡ and [$CH_3CH_2O^{-}$:**3.1**]‡.[4,5]

Scheme 3-5. Thermodyamic cycle for the catalyzed and uncatalyzed cleavages of phosphate diesters in ethanol

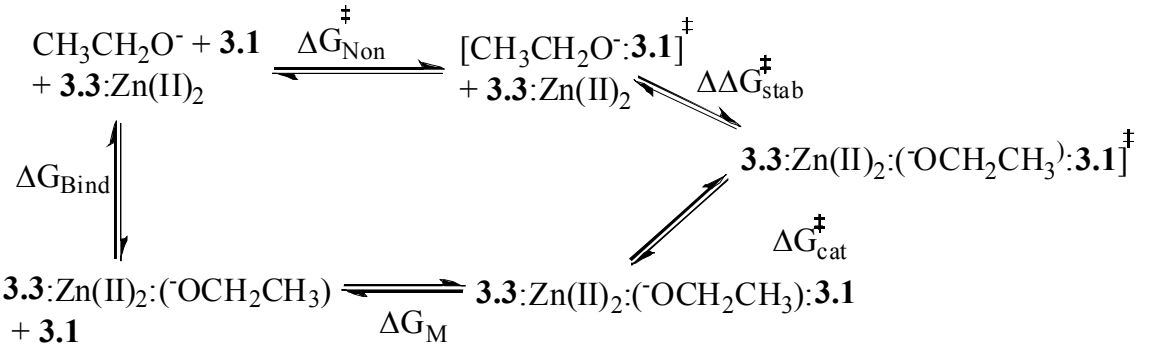

$$\Delta\Delta G^{\neq}_{stab} = (\Delta G_{Bind} - \Delta G_{m} + \Delta G^{\neq}_{cat}) - \Delta G^{\neq}_{Non} = -RT\ln\left[\frac{(k_{cat}/K_{m})({}^{s}_{s}K_{a}/K_{auto})}{k_{2}^{-OEt}}\right] \quad (8)^{37}$$

The $k_{cat}^{max\ corr.}$ and k_2^{-OEt} values are from Table 3-2 with the k_2^{-OEt} values for the less reactive substrates **3.1e-g** being extrapolated from the Brønsted plot in Figure 3-1. The upper limit for the K_m values for all substrates was taken to be $10^{-6.5}$ M and the ${}^{s}_{s}pK_a$ for the formation of **3.3**:Zn(II)$_2$:(-OCH$_2$CH$_3$) from **3.3**:Zn(II)$_2$:(HOCH$_2$CH$_3$) was taken to be 7.2 from the fitting of the data shown in Figure 3-5. While there may be some error in the latter two numbers, this does not affect the general picture greatly except for a small numerical uncertainty of the ΔG terms that depend on those constants. In Table 3-3 are given the $(k_{cat}^{max\ corr.}/K_m)({}^{s}_{s}K_a/K_{auto})$ and the computed $\Delta\Delta G^{\ddagger}_{stab}$ values for the catalyzed reactions of **3.1a-g**.

The data in ethanol invite comparison with those determined earlier for the catalyzed reactions in methanol[4] and shown in Figure 3-7 are the free energy data for the cleavage of **3.1c** in both solvents at a standard state of 1 M and 25 ^{o}C. The most striking

feature is that the $\Delta\Delta G^{\ddagger}_{stab}$ in ethanol (ranging from -33 to -36.5 kcal/mol) is very large in absolute terms and some 11-13 kcal/mol more negative than for the same substrate in methanol. Figure 3-7 visually informs us that the main differences in the ΔG values in the two solvents arise from three terms: a much stronger binding in ethanol of alkoxide to **3.3**:$Zn(II)_2$ and of **3.1c** to **3.3**:Zn(II):($^{-}$OR) as well as the ~65-fold slower reaction of alkoxide in ethanol than in methanol.

Table 3-3. Tabulation of the $(k_{cat}^{max}/K_m)(^{s}_{s}K_a/K_{auto})$ constants and the computed free energies for the formation of catalytic complexes (ΔG_{Bind}-ΔG_M), the free energies of activation for $k_{cat}^{max\ corr.}$ ($\Delta G^{\ddagger}_{cat}$), and the free energies of stabilization of the ethoxide transition state through binding to **3.3**:$Zn(II)_2$ ($\Delta\Delta G^{\ddagger}_{stab}$)[a] for the catalyzed reaction of substrates **3.1a-g** at 25 ^{o}C in ethanol.

3.1	$(k_{cat}^{max\ corr.}/K_m)$ $(^{s}_{s}K_a/K_{auto})$ $(M^{-2}s^{-1})$[b,c]	ΔG_{Bind}-ΔG_M (kcal/mol)[d]	$\Delta G^{\ddagger}_{cat}$ (kcal/mol)[e]	$\Delta G^{\ddagger}_{Non}$ (kcal/mol)[e]	$\Delta\Delta G^{\ddagger}_{stab}$ (kcal/mol)
a	4.2×10^{20}	-25.1	14.4	22.3	-33.0
b	3.3×10^{20}	-25.1	14.5	23.0	-33.6
c	3.5×10^{20}	-25.1	14.5	24.2	-34.8
d	9.0×10^{19}	-25.1	15.3	25.9	-36.5
e	3.6×10^{19}	-25.1	15.8	26.2	-35.5
f	1.1×10^{19}	-25.1	16.5	26.8	-35.4
g	6.7×10^{18}	-25.1	16.8	27.1	-35.4

a. $\Delta\Delta G^{\ddagger}_{stab}$ computed from application of kinetic and equilibrium constants to eq. (8).

b. $(k_{cat}^{max\ corr.}/K_m)/k_2^{-OEt}$ values from Table 3-2 where the K_m values for **3.1a-g** are assumed to have a upper limit of $10^{-6.5}$ M.

c. ${}^{s}_{s}K_a$ of $10^{-7.22}$ determined from the fit of the data in Figure 3-5 corresponding to the first ionization in

d. Scheme **3-3**; $K_{auto} = 10^{-19.1}$; ${}^{s}_{s}K_a/K_{auto} = 7.94 \times 10^{11}$ and corresponds to the binding constant of $^{-}$OEt and **3.3**:Zn(II)$_2$.

e. Computed as $(\Delta G_{Bind}-\Delta G_m) = -RTln((^{s}_{s}K_a/K_{auto})/K_m)$.

f. Computed from $\Delta G^{\ddagger}_{cat} = -RTln(k_{cat}^{max\ corr.}/(kT/h))$ or $\Delta G^{\ddagger}_{Non} = -RTln(k_2^{-OEt}/(kT/h))$ from the Eyring equation where $(kT/h) = 6x10^{12}\ s^{-1}$ at 298K.

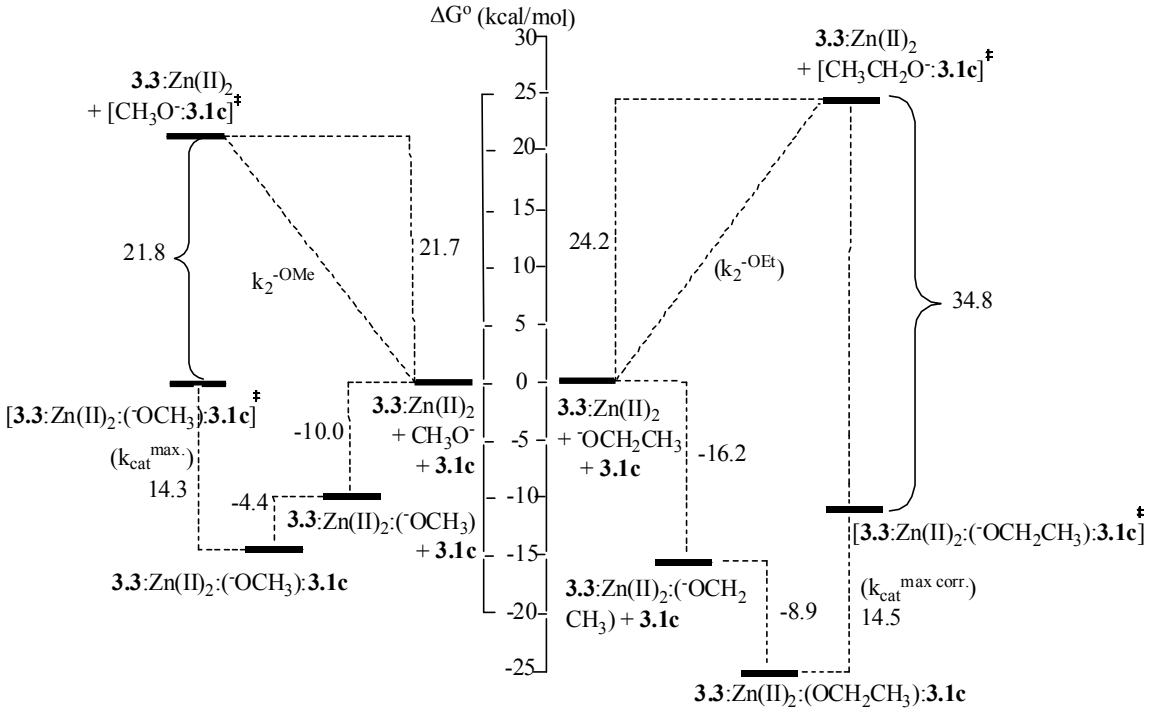

Figure 3-7. A comparison of the activation energy diagram for the **3.3**:Zn(II)$_2$:($^{-}$OR) and RO^{-}-catalyzed cleavages of **3.1c** in ethanol and methanol at standard state of 1 M and 25 ^{o}C showing the calculated energies of binding the alkoxide by **3.3**:Zn(II)$_2$, of binding of **3.1**c to **3.3**:Zn(II)$_2$:($^{-}$OR) and the calculated activation energies associated with k_{cat}^{max} and k_2^{-OR}. Methanolysis data taken from ref [4].

The first two terms place the three reaction components into a 10-11 kcal/mol deeper thermodynamic well when fully bound in ethanol, while the third raises the alkoxide reaction's transition state by about 2.5 kcal/mol. However, the surprising aspect is that the $k_{cat}^{max\ corr.}$ term is about the same in both solvents, the $\Delta G_{cat}^{\ddagger}$ being 14.5 and 14.3 kcal/mol. It is also very interesting that the free energy of the (**3.3**:$Zn(II)_2(^-OEt)$:**3.1**)‡ is lower than the ground state for the uncomplexed reaction partners by 10-11 kcal/mol in ethanol while in methanol the corresponding TS is roughly isoenergetic with the free reaction partners.

It is worthwhile to attempt to compare the accelerations for the reactions achieved by this catalytic system in ethanol with what is achievable by phosphodiesterase enzymes, bearing in mind that the medium, substrates and, in particular, the leaving groups are different. The cleavage of 3′,5′-UpA is reported to have a first order rate constant at pH 6, T = 25 ^{o}C of 5 x 10^{-9} s^{-1} [38] while a rate constant of 2.2 x 10^{-11} s^{-1} was observed for the cleavage of 3′,5′-ApG moiety inside a strand of deoxynucleotides at 23 °C and pH 6[39]. Since it is probable that both these processes are specific base catalyzed throughout the accessible pH regions,[40] respective second order rate constants for the base catalyzed process of 5 x 10^{-1} and 2.2 x 10^{-3} $M^{-1}s^{-1}$ are calculated which can be compared with the reported value of 2 x 10^{-3} $M^{-1}s^{-1}$ cleavage of UpU.[41,42] Since enzymes that promote the cleavage of RNA type phosphodiesters typically have k_{cat}/K_M values of 10^6 to 10^8 $M^{-1}s^{-1}$,[1d] the computed acceleration as measured by $(k_{cat}/K_M)/k_2^{-OH}$ for the enzyme catalyzed cleavage of RNA would be ~ 10^7 to 10^{11}. In this study values of 1-2 x10^{14} acceleration are seen for substrates **3.1d-g** where the $k_{cat}^{max\ corr.}$ term specifically refers to the chemical cleavage step of the bound substrate.

3.6 – Conclusions

The catalytic acceleration for the cleavage of substrates **3.1** by a dinuclear Zn(II) catalyst in methanol and ethanol far exceeds anything so far reported for metal ion containing catalysts in aqueous solution.[2] It is notable that the reaction in question is not a hydrolytic process in any case, but rather an intramolecular cyclization so the importance of the solvent as a nucleophile is not relevant. It has been stated that the effective dielectric constants in enzyme active sites resemble those of organic solvents rather than water.[43,44] In the present case, reductions in dielectric constant such as what happens when one proceeds from water, to methanol and then ethanol, seem to be a particularly effective strategy for accelerating the rate of metal catalyzed acyl and phosphoryl transfer reactions.[45] The dinuclear catalyst (**3.3**:$Zn(II)_2$) in water is reported[6] to be poor, and in fact no more effective in promoting the hydrolysis of bis-*p*-nitrophenyl phosphate than the Zn(II) complex of 1,5,9-triazacyclododecane so the strong activities seen in methanol and ethanol for phosphate diester cleavage[4,5] point to a synergistic interaction between the catalyst and medium. It is an essential, but not exclusive, requirement that the catalyst must readily recruit the reaction partners (**3.3**:$Zn(II)_2$ + **3.1** + ^{-}OR) into a reactive complex and clearly the reduced polarity medium enhances these interactions between oppositely charged components. However, simple binding of the reaction partners cannot lead to rate accelerations unless there is a greater binding of the transition state for the catalyzed reaction. Indeed this binding amounts to 33-36 kcal/mol in ethanol while that in methanol is 21-23 kcal/mol, the difference in the two solvents being largely dependent on the far stronger binding of the anionic reactants by the positively charged dinuclear complex in ethanol. What is interesting is the fact that the k_{cat}^{max} terms are very similar in

ethanol and methanol for the substrates where this term relates to a chemical cleavage step. Perhaps this results from the fact that once bound by the catalyst, the polar groups such as the metal ions and transforming phosphate are at the interior of the catalyst:substrate complex and so not subject to significant solvent effects.

3.7 - References and Notes

[1] (a) Wolfenden, R. *Chem. Rev.* **2006**, *106*, 3379; (b) Wolfenden, R.; Snider, M. J. *Acc. Chem. Res.* **2001**, *34*, 938; (c) Schroeder, G. K.; Lad, C.; Wyman, P.; Williams, N. H.; Wolfenden, R. *Proc. Natl. Acad. Sci. USA* **2006**, *103*, 4052; (d) Raines, R. T. *Chem. Rev.* **1998**, *98*, 1045.

[2] (a) Mancin, F.; Tecillia, P. *New J. Chem*. **2007**, *31*, 800; (b) Mancin, F.; Scrimin, P.; Tecilla, P.; Tonellato, U. *Chem. Commun.* **2006**, 2540; (c) Morrow, J. R.; Iranzo, O. *Curr. Opin. Chem. Biol*. **2004**, *8*, 192; (d) Williams, N. H. *Biochim. Biophys. Acta*, **2004**, *1697*, 279; (e) Livieri, M.; Mancin, F.; Saielli, G.; Chin, J.; Tonellato, U. *Chem. Eur. J.* **2007**, *13*, 2246; (f) Webb, S. J. *Annu. Rep. Prog. Chem., Sect. B,* **2007**, *103*, 392. (g) Parkin, G. *Chem. Rev.* **2004,** *104,* 699.

[3] (a) Yang, M.-Y.; Morrow, J. R.; Richard, J. P. *Bioorg. Chem.* **2007**, *35*, 366; (b) Iranzo, O.; Kovalevsky, A. Y.; Morrow, J. R.; Richard, J. P. *J. Am. Chem. Soc.* **2003**, *125*, 1988.

[4] Bunn, S. E.; Liu, C. T.; Lu, Z.-L.; Neverov, A. A.; Brown, R. S., *J. Am. Chem. Soc.* **2007**, *129*, 16239.

[5] (a) Neverov, A. A.; Liu, C. T.; Bunn, S. E.; Edwards, D.; White, C. J.; Melnychuk, S. A.; Brown, R. S. *J. Am. Chem. Soc*. **2008**, *130*, 6639; (b) Neverov, A. A.; Lu, Z.-L.; Maxwell, C. I.; Mohamed, M. F.; White, C. J.; Tsang, J. S. W.; Brown, R. S., *J. Am. Chem. Soc.*, **2006**, *128*, 16398; (c) Lu, Z.-L.; Liu, C. T.; Neverov, A. A.; Brown, R. S. *J. Am. Chem. Soc*. **2007**, *129*, 11642.

[6] Kim, J.; Lim, H. Bull. *Korean Chem. Soc*. **1999**, *20*, 491

[7] (a) Feng, G.; Natale, D.; Prabaharan, R.; Mareque-Rivas, J. C.; Williams, N. H. *Angew. Chem. Int. Ed.* **2006**, *45*, 7056; (b) Feng, G.; Mareque-Rivas, J. C.; Williams, N. H. *Chem. Commun.* **2006**, 1845.

[8] Sánchez-Lombardo, I.; Yatsimirsky, A. K. *Inorg. Chem.* **2008**, *47*, 2514.

[9] Harned, H. S.; Owen, B. B., *The Physical Chemistry of Electrolytic Solution*; ACS Monograph Series 137, 3rd ed.; Reinhold Publishing: New York, 1957, p 161.

[10] Liu, C. T.; Neverov, A. A.; Brown, R. S. *Inorg. Chem.* **2007**, *46*, 1778.

[11] Gibson, G. T. T.; Mohamed, M. F.; Neverov, A. A.; Brown, R. S. *Inorg. Chem.* **2006,** *45*, 7891.

[12] (a) Guanti, G.; Cevasco, G.; Thea, S.; Dell'Erba, C.; Petrillo, G. *J. Chem. Soc. Perkin II.* **1981**, *2*, 327; (b) England, B. D.; House, D. A. *J. Chem. Soc.* **1962**, 4421.

[13]

$$k_{obs} = k_i + k_a(1 + K_b * [cat] + [^-\mathrm{OTf}] * K_b - X)/[cat]/(2K_b)$$

where:

$$X = \{1 + 2K_b * [cat] + 2 * [^-\mathrm{OTf}] * K_b + K_b^{\,2} * [cat]^2 - 2 * K_b^{\,2} * [^-\mathrm{OTf}][cat] + [^-\mathrm{OTf}]^2 * K_b^{\,2}\}^{0.5}$$

The above expression is a modified version of the universal binding expression eq. (3). Here, k_i is the computed rate constant (k_{obs}) at zero concentration of triflate anion, k_a corresponds to the change in the k_{obs} value from zero triflate to infinite triflate concentration, and K_b (in units of M^{-1}) is defined as the binding constant between triflate anion and the catalyst-substrate complex (**3.3**:Zn(II)$_2$:($^-$OCH$_2$CH$_3$):**3.1**) to form the nonreactive species (**3.3**:Zn(II)$_2$:($^-$OCH$_2$CH$_3$):**3.1**:($^-$OTf)). Therefore, the triflate inhibition constant (K_i; in units of M) for the **3.3**:Zn(II)$_2$-catalyzed reactions is defined as the reciprocal of the K_b presented here. The [cat] and [$^-$OTf] terms correspond to the total concentrations of the catalyst and triflate in a given reaction mixture.

[14] Nelson, D. L.; Cox, M. M., *Lehninger Principles of Biochemistry*, 3rd ed.; Worth Publishers: New York, 2000, p 266-268.

[15] Since the triflate binding is quite strong, the more accurate method for determining the K_i is to use a variant of the universal binding equation (see ref.[13]). However, using this form lowers the values of the $k_{obs}^{corr.}$ by only 4% which is within the experimental uncertainty, so we have opted to use simplified method of eq.s (1, 2).

[16] Eq. (3) was obtained from the equations for equilibrium binding and for conservation of mass by using the commercially available MAPLE software, Maple V Release 5, Waterloo Maple Inc., Waterloo, Ontario, Canada.

[17] The data in the ${}^{s}_{s}\mathrm{pH}$ /log ($k_{obs}^{\text{max corr.}}$) profile for the cleavage of **3.1e** (8 x 10^{-5} M) catalyzed by 0.1 mM of **3.3**:$Zn(II)_2$:($^{-}OCH_2CH_3$) at 25 ^{o}C in de-gassed absolute ethanol (presented as Figure 3-5) are fitted to the expression below, which is derived for a two ${}^{s}_{s}\mathrm{pK_a}$ model shown in Scheme 3-3.

$$\log\ (k_{obs}^{\text{max corr.}}) = \log\ (A) + \log\ (10^{-{}^{s}_{s}pKa^{1}}/(10^{-{}^{s}_{s}pKa^{1}} + 10^{-({}^{s}_{s}pH)})) + \log\ (10^{-({}^{s}_{s}pH)}/(10^{-{}^{s}_{s}pKa^{2}} + 10^{-({}^{s}_{s}pH)}))$$

where A is a constant.

[18] The first ${}^{s}_{s}\mathrm{pK_a}$ is not well-defined by the data of Figure 3-5 due to the presumed decomposition of the catalyst. However, an experimentally similar ${}^{s}_{s}\mathrm{pH}$ vs log k_{obs} profile is seen for the cleavage of a series of aryl methyl phosphate esters in ethanol catalyzed by **3.3**:$Zn(II)_2$:($^{-}$OEt), ${}^{s}_{s}\mathrm{pK_a}^{1} = \sim 7$ and ${}^{s}_{s}\mathrm{pK_a}^{2} = 10.8$.

[19] Williams, N. H.; Takasaki, B.; Wall, M.; Chin, J. *Acc. Chem. Res.* **1999**, *32*, 485.

[20] (a) Bourne, N.; Williams, A. *J. Org. Chem*. **1984**, *49*, 1200; (b) Bourne, N.; Williams, A. *J. Am. Chem. Soc.* **1984**, *106*, 7591.

[21] (a) Williams, A., *Concerted Organic and Bio-Organic Mechanisms*, CRC Press: Boca Raton, USA, 2000, p 161-181; (b) Bourne, N.; Chrystiuk, E. Davis, A. A.; Williams, A. *J. Am. Chem. Soc.* **1988**, *110*, 1890; (c) Ba-Saif, S. A.; Davis, A. M.; Williams, A. *J. Org. Chem.* **1989**, *54*, 5483.

[22] Lönnberg, H.; Strömberg, R.; Williams, A. *Org. Biomol. Chem.* **2004**, *2*, 2165.

[23] Brown, D. M.; Usher, D. A. *J. Chem. Soc.* **1965**, 6558.

[24] Sánchez-Lombardo and Yatsimirsky have estimated[8] the pK_a of the 2-hydroxy group in **3.1a** as 14.9 in water. Based on the relationship of $^{s}_{s}pK_a^{EtOH} = (1.24 \pm 0.01)pK_a^{H2O} + (3.2 \pm 0.1)$ given in the Experimental Section herein, the computed $^{s}_{s}pK_a^{EtOH}$ is 21.7.

[25] The extent of breaking of the P-OAr bond in the TS can be measured by the Leffler parameter, α, which measures the change in the Brønsted β_{lg} for the TS relative to the β_{eq} for equilibrium transfers of the phosphoryl group between oxyanion nucleophiles. In the case of the transfer of the $(RO)P(=O)O^-$ group[20a], the β_{eq} value is -1.74 with the O-Ar oxygen in the starting material having a net effective charge of +0.74. For the cyclization reaction involving attack of the 2-hydroxypropyl oxyanion, the Leffler parameter, α, is given as β_{lg}/β_{eq} = 0.52 suggesting that the P-OAr cleavage is 43% of the way from starting material to product, this assuming that the β_{eq} determined in water can be transposed into ethanol.

[26] Tsang, J. S.; Neverov, A. A.; Brown, R. S. *J. Am. Chem. Soc.* **2003**, *125*, 1559.

[27] O'Donoghue, A. M.; Pyun, S. Y; Yang, M.-Y.; Morrow, J. R.; Richard, J. P. *J. Am. Chem. Soc.* **2006**, *128*, 1615.

[28] Bonfá, L.; Gatos, M.; Mancin, F. Tecilla, P. Tonellato, U. *Inorg. Chem.* **2003**, *42*, 3943.

[29] Neverov, A. A.; Sunderland, N. E.; Brown, R. S. *Org. Biomol. Chem.*, **2005**, *3*, 65.

[30] Levine, I. N. *Physical Chemistry*, Fourth Ed.; McGraw-Hill, Inc.; U.S.A., 1978, p.p. 276-281.

[31] The first formed phosphate product is the cyclic five-membered phosphate and the observed product is the phenol/phenoxide of the parent **3.1**. We have observed that the cyclic phosphate opens up very rapidly ($t_{1/2}$~2 sec) in the presence of **3.3**:$Zn(II)_2$ in methanol to form a kinetic mixture of 2-hydroxypropyl ethyl phosphate and its isomeric (1-(hydroxymethyl)ethyl) ethyl phosphate in a 30:70 mixture. While we have not checked the situation in ethanol, there is no reason to suspect that the cyclic phosphate will not react rapidly with ethanol in the presence of the catalyst. Tsang, W. Y; Edwards, D.; Melnychuk, S. A.; Liu, C. T.; Liu, C.; Neverov, A. A.; Williams, N. H.; Brown, R. S. *J. Am. Chem. Soc*. **2009**, *131*, 4158.

[32] Yang, M.-Y.; Iranzo, O.; Richard, J. P.; Morrow, J. R. *J. Am. Chem. Soc.* **2005,** *127*, 1064.

[33] Schwarz, H.A.; Gill, P.A. *J. Phys. Chem*. **1977**, *81*, 22.

[34] Since we know that the activity of **3.3**:$Zn(II)_2$:($^-$OEt) is maintained down to $^{s}_{s}$pH 7.9, the acceleration relative to the base promoted reaction at that $^{s}_{s}$pH would be over 10^{18}-fold.

[35] Wolfenden, R. *Nature*, **1969**, *223*, 704.

[36] For applications of this to phosphate cleavage and other reactions see Yatsimirsky, A. K. *Coord. Chem. Rev*. **2005**, *249*, 1997 and references therein.

[37] Eq. (8) is a correct form of the equation (5) in the original methanol manuscript[4] where a typographical error appeared in the expression ($\Delta\Delta G^{\neq}_{stab} = (\Delta G_{Bind} + \Delta G_{M} + \Delta G^{\neq}_{cat}) - \Delta G^{\neq}_{Non}$) placing a (+)-sign in front of the ΔG_M term. Since K_M refers to the dissociation constant for the Michaelis complex, and we are interested in the binding energy of catalyst and **3.1**, the correct form of the equation should be $-\Delta G_M$.

[38] Thompson, J. E.; Kutateladze, R. G.; Schuster, M. C.; Venegas, F.D.; Messmore, J. M.; Raines, R. T. *Bioorg. Chem.* **1995**, *23*, 471.

[39] Li, Y.; Breaker, R. *J. Am. Chem. Soc.* **1999**, *121*, 5364.

[40] Oivanen, M.; Kuusela, S.; Lönnberg, H. *Chem. Rev.* **1998**, *98*, 961.

[41] Järvinen, P.; Oivanen, M.; Lönnberg, H. *J. Org. Chem*. **1991**, *56*, 5396.

[42] Substrates **3.1** have better leaving groups than the dinucleotides, but the computed background reactions for these at $^{s}_{s}$pH 9.0 are slower than that of the dinucleotides at pH 6 in water due to three main reasons. First the concentration of base at $^{s}_{s}$pH 9 in ethanol is 8 x 10^{-11} M while in water at pH 6 the [$^{-}$OH] is 10^{-8}M; second, as discussed in Section 3.5.1 due to electrostatic repulsion, the lyoxide reaction in ethanol is about 100 time slower than in water; third, model studies show that the 2-OH group in RNA provides about 10^9 acceleration of the cleavage reaction while the acceleration provided in the 2 hydroxypropyl substrates is only about 10^5. See ref. 19.

[43] Cleland, W. W.; Frey, P. A.; Gerlt, J. A. *J. Biol. Chem*. **1998**, *273*, 25529.

[44] Richard, J. P.; Ames, T. L. *Bioorg. Chem.* **2004**, *32*, 354.

[45] Brown, R.S.; Neverov, A.A. *Adv. Phys. Org. Chem.* Richard, J. P.; Ed. Elsevier: San Diego, Calif. **2007**, *42*, 271.

Chapter 4 – Biomimetic Cleavage of DNA Models Promoted by a Dinuclear Zn(II) in Methanol

4.1 – Model DNase and Leaving Group Assistance

In Chapters 2 and 3, we examinated the mechanistic aspects of a very efficient dinuclear catalytic system that promotes the cyclization of RNA model substrates. However, solvolytic stability[1] of phosphate esters can only be fully appreciated in diesters that do not have an internal nucleophile, such as DNA and DNA analogues. Because of the remarkable rate enhancements of up to 10^{17} for P-O cleavage achieved by the enzymes[2,3], much research has centered on the ability of small metal containing complexes to promote the cleavage of DNA model substrates[4]. Many of the recently reported studies have provided invaluable mechanistic information on the role by which the metal ions in specially tailored dinuclear Zn(II) complexes[4a] promote the cleavage of simple RNA models such as 2-hydroxypropyl *p*-nitrophenyl phosphate[5]. However, due to the lower reactivity of DNA model substrates, which do not contain an intermolecular 2-hydroxy nucleophile**,** the great bulk of the substrates studied are those with good leaving groups such as 4-nitro- and 2,4-dinitrophenoxy.[6]

As a continuation of our effort to probe the catalytic capacity of **4.1**:$Zn(II)_2$:$^-OCH_3$, we have studied its ability to catalyze the methanolyses of fourteen methyl aryl phosphates (**4.2a-n**).[7] Saturation kinetics were observed for all substrates, from which both the dissociation constants (K_M) and the maximum rate constants (k_{cat}^{max}) were determined for the catalyzed methanolysis of **4.2a-n**. The results show that the reactions followed the same three-step mechanism described in the previous chapters, with rate-

limiting P-OAr bond cleavage for all substrates tested. The catalysis for the cleavage of DNA model compounds is equally impressive with rate accelerations for the series ranging from 4 x 10^{11} to 3 x 10^{13} relative to the background methoxide reactions at $^{s}_{s}$pH 9.8 and 25°C in methanol. This can be compared with a recent report of alkaline phosphatase[8] promoted hydrolysis of a series of methyl aryl phosphates (including **4.2f**, **i**, **j**, **m**) that have second order rate constants (k_{cat}/K_M) approximately 230-880 times smaller than what we found for our synthetic systems with **4.1**:$Zn(II)_2$:$^{-}OCH_3$ in methanol. It is important to point out that the natural substrates for alkaline phosphatase are phosphate monoesters.

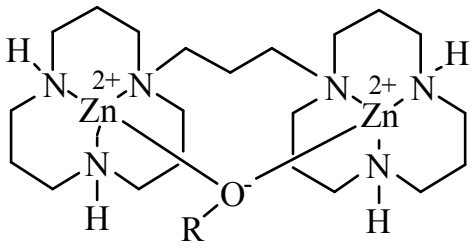

4.1:$Zn(II)_2$:^{-}OR

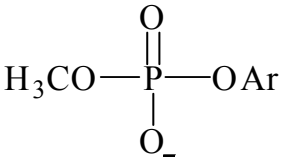

4.2

a. 2, 4-dinitrophenyl
b. 2-chloro-4-nitrophenyl
c. 4-chloro-2-nitrophenyl
d. 2-(methoxycarbonyl)-4-nitrophenyl
e. 2, 4, 5-trichlorophenyl
f. 4-nitrophenyl
g. 2-nitrophenyl
h. 2-nitro-4-methoxyphenyl
i. 3-nitrophenyl
j. 4-chlorophenyl
k. 3-methoxyphenyl
l. 2-(methoxycarbonyl)phenyl
m. phenyl
n. 4-methoxyphenyl

In addition we found an unusual effect where *ortho*-nitro and *ortho*-carbomethoxy functionalized derivatives of **4.2** (**a**,**c**,**d**,**g**,**h**,**l**) react faster than those that do not have this substitution pattern. Spectroscopic data suggest that the enhanced catalysis is due to favorable interaction between the catalyst and the leaving group on the substrates (Scheme 4-1). In contrast, phenols that lack *ortho*-nitro and *ortho*-carbomethoxy substituents do not seem to bind to the catalyst **4.1**:$Zn(II)_2$:$^{-}OCH_3$ in solution.

Scheme 4-1. Possible binding modes between the dinuclear catalyst, **4.1**:$Zn(II)_2$:$^{-}OCH_3$, and phosphate diesters with (A) and without (B) the extra binding *ortho*-substituents X (nitro or carbomethoxy) on the leaving group.

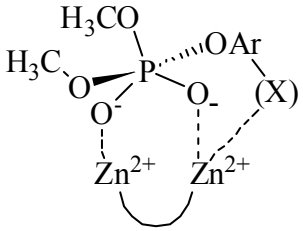

A

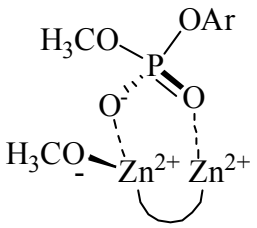

B

Kinetic data show that there is a reduced gradient for the Brønsted plot (Figure 4-1) for these *ortho*-substituted derivatives (β_{lg} = -0.34 ± 0.01), when compared to substrates that do not have these special *ortho*-substituents (β_{lg} = -0.59 ± 0.03), and also when compared to the background methoxide reactions (β_{lg} = -0.57 ± 0.06; Figure 4-2).[7] This is consistent with increased electrostatic interaction between the catalyst and the leaving group to decrease (or stabilize) the developing negative charge on the departing oxygen in the transition state, which should lead to a less negative β_{lg} value. Electrostatic stabilization of the departure of leaving groups via general acid assistance has been

proposed to explain the low β_{lg} value (in terms of absolute magnitude) found for the cleavage of uridine-3'-phosphate aryl esters promoted by bovine pancreatic RNase A.[9] An interesting consequence of the Brønsted relationships in (Figure 4-1 and Figure 4-2) is that with this built-in additional affinity for the catalysts (**4.2a**,**c**,**d**,**g**,**h**,**l**), higher catalytic efficiency will be obtained for substrates with poorer leaving groups (as judged by the ${}^{s}_{s}pK_a$ value for the corresponding phenol), because the methoxide reaction is more sensitive to the ${}^{s}_{s}pK_a$ of the leaving group than the catalyzed process.

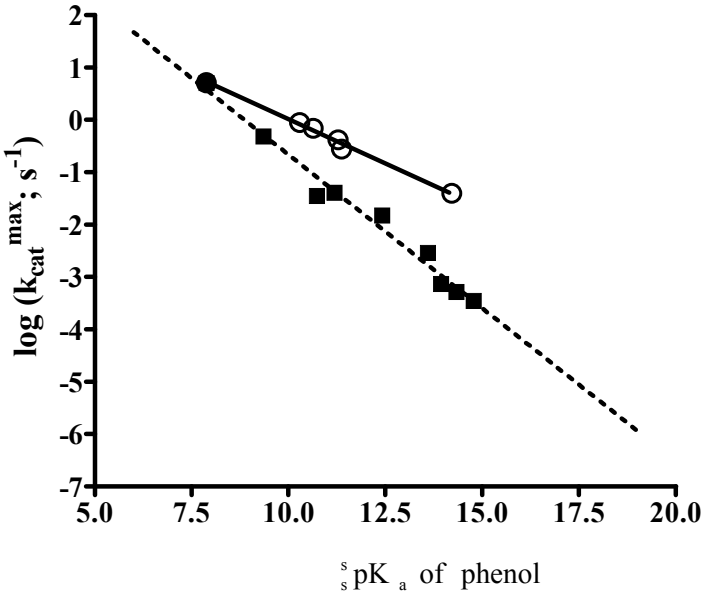

Figure 4-1. Brønsted plots of log (k_{cat}^{max}) vs the ${}^{s}_{s}pK_a$ values for the **4.1**:$Zn(II)_2$:$^{-}OCH_3$-catalyzed methanolysis of phosphates **4.2a**, **c**, **d**, **g**, **h**, and **l** (○) which fits a linear regression of log k_{cat}^{max} = (-0.34 ± 0.01) ${}^{s}_{s}pK_a$ + (3.4 ± 0.2); r^2 = 0.9933 and phosphates **4.2b**, **e**, **f**, **i-k**, **m**, and **n** (■) which fits a linear regression of log k_{cat}^{max} = (-0.59 ± 0.03) ${}^{s}_{s}pK_a$ + (5.2 ± 0.4); r^2 = 0.9816.

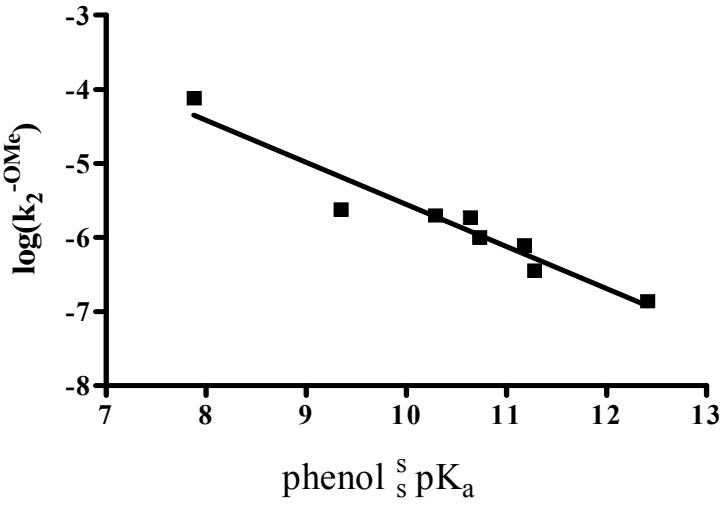

Figure 4-2. A Brønsted plot for the methoxide promoted methanolysis of phosphates (**4.2a-g**, **i**). The eight data points (■) were fit to a standard linear regression of log k_2^{-OMe} = (-0.57 ± 0.06) $^{s}_{s}pK_a$ + (0.14 ± 0.68), r^2 = 0.9279.

Although leaving group assistance has been proposed as a vital component of enzymatic catalysis,[2] it has been difficult to emulate in small molecule model systems. In the presence of special *ortho*-substituents on the substrate, dinuclear complex **4.1**:$Zn(II)_2$:$^{-}OCH_3$ can provide additional catalysis (amounting to ~ 3 kcal/mol of additional energy stabilization of the transition state of the reaction in the series of substrates tested) through metal-faciliated leaving group assistance. The enhanced catalysis raised the question of the effectiveness of leaving group assistance compared to other modes of catalysis (notably nucleophile and substrate activation) employed by the bulk of the synthetic mimics. This prompted our investigation of metal-promoted solvolyses of phosphate mono-, di-, and triesters, where we were able to isolate and

quantify the catalytic efficacy of leaving group assistance in the absence of other modes of catalysis. This is described in the next chapter.

4.2 – Postscript

The detailed account of the study described above can be found in the original publication (Neverov, A. A.; Liu, C. T.; Bunn, S. E.; Edwards, D.; White, C. J.; Melnychuk, S. A.; Brown, R. S. J. Am. Chem. Soc. **2008**, *130*, 6639). It was a collaborative effort between various members of Dr. R. Stan Brown's lab. The majority of the experiments (syntheses, kinetics, and data collection) were performed by C. Tony Liu and Shannon E. Bunn. Figure 4-1 and Figure 4-2 have been slightly modified from those in the published report to accommodate the discussion here. The catalyzed methanolysis of 2-*tert*-butyl-4-nitrophenyl methyl phosphate (k_{cat} = 8.5 x $10^{-4}s^{-1}$; ${}^{s}_{s}pK_a^{lg}$ = 12.03) sits considerably below both Brønsted lines in Figure 4-1, implying that the enhanced catalysis observed for substrates with *ortho*-nitro and *ortho*-carbomethoxyl substituents cannot be rationalized simply on the basis of a steric effect.

4.3 – References and Notes

[1] Schroeder, G. K.; Lad, C.; Wyman, P.; Williams, N. H.; Wolfenden, R. *PNAS USA.* **2006**, *103*, 4052.

[2] (a) Cowan, J. A. *Chem. Rev.* **1998,** *98*, 1067; (b) Wilcox D. E. *Chem. Rev.* **1996**, *96*, 2435; (c) Sträter, N.; Lipscomb, W. N.; Klabunde, T.; Krebs, B. *Angew. Chem. Int. Ed. Engl.* **1996**, *35*, 2024.

[3] Wolfenden, R.; Snider, M. J. *Acc. Chem. Res.* **2001**, *34*, 938.

[4] (a) Mancin, F; Tecillia, P. *New J. Chem.,* **2007**, *31*,800; (b) Weston, J. *Chem. Rev.* **2006***, 105*, 2151; (c) Molenveld, P.; Engbertsen, J. F. J.; Reinhoudt, D. N. *Chem. Soc. Rev.* **2000**, *29*, 75; (d) Williams, N. H.; Takasaki, B.; Wall, M.; Chin, J. *Acc. Chem. Res.* **1999**, *32*, 485; (e) Mancin, F.; Scrimin, P.; Tecilla, P.; Tonellato, U. *Chem. Commun.* **2006**, 2540; (f) Morrow, J. R.; Iranzo, O. *Curr. Opin. Chem. Biol.* **2004**, *8*, 192.

[5] (a) Feng, G.; Mareque-Rivas, J. C.; Williams, N. H. *Chem. Commun.* **2006**, 1845; (b) Mancin, F., Rampazzo, E.; Tecilla, P.; Tonellato, U. *Eur. J. Chem.* **2004,** 281; (c) Yang, M.-Y.; Iranzo, O.; Richard, J. P.; Morrow, J. R. *J. Am. Chem. Soc.* **2006,** *127*, 1064; (d) O'Donoghue, A. M.; Pyun, S. Y; Yang, M.-Y.; Morrow, J. R.; Richard, J. P. *J. Am. Chem. Soc.* **2006**, *128*, 1615; (e) Iranzo, O.; Elmer, T.; Richard, J. P.; Morrow, J. R. *Inorg. Chem.* **2003**, **42**, 7737; (f) Iranzo, O.; Richard, J. P.; Morrow, J. R. *Inorg. Chem.* **2004**, **43,** 1743; (g) Iranzo, O.; Kovalevsky, A. Y.; Morrow, J. R.; Richard, J. P. *J. Am. Chem. Soc.* **2003**, *125*, 1988.

[6] (a) Blasko, A.; Bruice, T.C. *Acc. Chem. Res*. **1999**, *32*, 475 and references therein; (b) Moss, R. A.; Park, B. D.; Scrimin, P.; Ghirlanda, G. *J. Chem. Soc. Chem. Comm*. **1996**, 1627; (c) Moss, R. A.; Zhang, J.; Bracken, K. *J. Chem. Soc. Chem. Comm*. **1997**, 1639; (d) Sumaoka, J.; Miyama, S.; Komiyama, M. *J. Chem. Soc. Chem. Comm*. **1994**, 1755; (e) Morrow, J. R.; Buttrey, L. A.; Shelton, V. M.; Berback, K. A. *J. Am. Chem. Soc.* **1992**, *114*,1903; (f) Breslow, R. Zhang, B. *J. Am. Chem. Soc.* **1994**, *116*, 7893; (g) Takeda, N.; Irisawa, M.; Komiyama, M. *J. Chem. Soc. Chem. Comm*. **1994**, 2773; (h) Hay, R. W.; Govan, N. *J. Chem. Soc. Chem. Commun.* **1990**, 714; (i) Schneider, H.-J.;

Rammo, J.; Hettich, R. *Angew. Chem. Int. Ed. Engl.* **1993**, *32*, 1716; (j) Ragunathan, K. G.; Schneider, H.-J. *Angew. Chem. Int. Ed. Engl.* **1996**, *35*, 1219 ; (k) Gómez-Tagle, P.; Yatsimirsky, A. K. *J. Chem. Soc. Dalton Trans.* **1998**, 2957; (l) Roigk, A.; Hettich, R. Schneider, H.- J. *Inorg. Chem.* **1998**, *37*, 751, and references therein; (m) Gómez-Tagle, P.; Yatsimirski, A. K. *J. Chem. Soc. Dalton Trans.* **2001**, 2663 ;(n) Jurek, P. E.; Jurek, A. M.; Martell, A. E. *Inorg. Chem.* **2000**, *39*, 1016.

[7] Neverov, A. A.; Liu, C. T.; Bunn, S. E.; Edwards, D.; White, C. J.; Melnychuk, S. A.; Brown, R. S. *J. Am. Chem. Soc.* **2008**, *130*, 6639.

[8] Zalatan, J. G.; Herschlag, D. *J. Am. Chem. Soc.* **2006**, *128*, 1293.

[9] Davis, A. M.; Regan, A. C.; Williams, A. *Biochemistry*, **1988**, *27*, 9042.

Chapter 5 – Efficient Catalysis through Cu(II)-Promoted Leaving Group Stabilization of the Transition States for the Cleavage of a Homologous Set of Phosphate Mono-, Di-, and Triesters in Methanol

5.1 – Preface

With minor formatting changes and slight modification of the text for clearification, this chapter is largely as it was published in Journal of American Chemical Society (Liu, C. T.; Neverov, A. A.; Maxwell, C. I.; Brown, R. S. *J. Am. Chem. Soc.* **2010**, *132*, 3561). All experiments (syntheses, kinetics, titrations, and data analysis) were performed by C. Tony Liu. The original kinetic data and the complete characterization of the new compounds synthesized for the study can be found in the Supporting Information section for the original paper. The first draft of the manuscript was composed by me and the final version was prepared in collaboration with Dr. R. Stan. Brown and Dr. Alex A. Neverov. The bulk of the supplementary experimental data that was originally in the Supporting Information section of the published article have been modified and placed in the Postscript section (5.7) at the end of the chapter to avoid obstructing the flow of the main concepts with an excessive volume of technical experimental descriptions.

5.2 – Introduction

Phosphate mono-, di- and triesters have important roles in living systems. Phosphorylation and hydrolysis reactions of phosphate monoesters play vital roles in protein function, energy regulation, metabolism, signal transduction and many other

processes.[1,2,3] Phosphate diesters are extremely resistant to solvolytic cleavage, making them suitable functionalities for the backbones for DNA and RNA which are responsible for storing genetic information.[3] Phosphate triesters are not naturally occurring and have no known natural biological function but they are commercially important as pesticides[4] owing to their toxicity as acetylcholinesterase inhibitors.[5]

Due to the great accelerations required to bring the various phosphate cleavage reactions into a useful timescale for living systems, considerable effort has been expended to understand the mechanistic diversity of phosphoryl transfer reactions mediated by enzymes. In the absence of catalysts, the solvolytic reaction rates of phosphate mono- and diesters with unactivated leaving groups are such that the half-time for hydrolysis of a monoester is ~10^{12} years, and those for hydrolysis of RNA and DNA under physiological conditions are ~110 and ~$10^{8\text{-}10}$ years respectively.[6] However, the rate of phosphoryl transfer reactions in the presence of the most efficient enzymes can be accelerated by 10^{11} to 10^{12} times for phosphate triesters,[7] 10^{15} to 10^{21} for diesters[7], and >10^{17} times for phosphate monoesters[8].

Many enzymes that cleave phosphate esters contain two or more transition metal ions (Zn^{2+}, Ca^{2+}, Mg^{2+}, Fe^{3+}, and Mn^{2+}) in close proximity in their active sites[3] and their catalytic roles have been discussed at length.[2,3,9] Four main catalytic modes that metallo-enzymes are proposed to employ are: 1) Lewis acid activation of the substrate via M^{+x}---O=P binding; 2) delivery of a metal-bound hydroxide or alkoxide that serves as a nucleophile or a base; 3) electrostatic stabilization of the anionic substrate and nucleophile/base through binding to its (+)-charged active site and subsequent lowering of the transition state energy of the reaction[10]; and 4) stabilization of the leaving group

through metal ion coordination. Model catalysts have been designed that employ several, but rarely all, of these modes of catalysis in the hopes of achieving the efficiency of enzymatic catalyses in man-made systems.[11,12] Our recent work demonstrated that a simple dinuclear catalyst (**5.1**) promotes the cleavage of phosphate diesters **5.2** and **5.3** in methanol[13] and ethanol[14] with up to $10^{11\text{-}13}$ and $10^{14\text{-}17}$ rate accelerations over the background methoxide-catalyzed processes. That no such acceleration is seen for the cleavage of a phosphate diester promoted by **5.1** in water[15] indicates that medium effects[16] play a key role in producing large rate enhancements with metal ions, perhaps amplifying weak effects and inducing other modes of catalysis not easily seen in water.

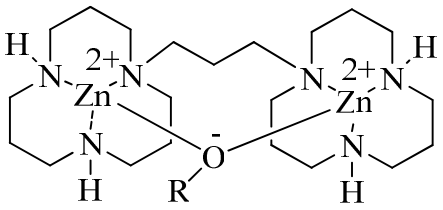

5.1

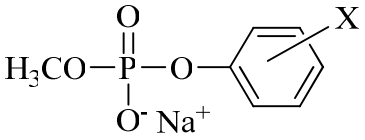

5.2
5.2b. X = *o*-nitro
5.2c. X = *o*-methoxycarbonyl

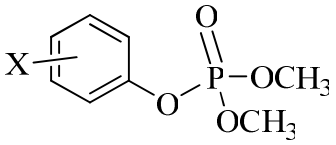

5.3
5.3b. X = *o*-methoxycarbonyl

There are surprisingly few, albeit informative, reports documenting LGA promoted by general acids or metal ions even though this should be a vital component of phosphoryl transfer reactions catalyzed by enzymes where the natural substrates contain non-activated leaving groups. This type of catalysis is expected to be most readily

observed for a reaction considered to proceed via a dissociative TS^2 with extensive leaving group departure and little nucleophile participation. Consistent with this, significant metal ion promoted LGA is seen for the alkaline phosphatase catalyzed cleavage of dianionic phosphate monoesters.[17] Accelerations up to 10^8 have been documented for intramolecular general acid catalysis of the hydrolyses of (8-dimethylammonium)naphthyl-1-phosphate **5.4a**[18] and salicyl phosphate[19] monoesters relative to the uncatalyzed reactions of these dianions. There is also a handful of examples of LGA for cleavage of phosphate monoesters promoted by metal ion, notable examples being the Cu(II)-catalyzed cleavages of 2-(4-(5)-imidazoyl)phenyl phosphate[20], 8-quinolyl phosphate[21], salicyl phosphate[22], and 2-(1,10-phenanthrolyl) phosphate **5.5**[23] where the metal ion promoted LGA increases the reactivities of these by 10^4 to 10^8 over the background reactions.

The hydrolysis of the phosphate diester methyl (8-dimethylammonium)naphthyl-1-phosphate **5.4b**[24] is accelerated by intramolecular general acid catalysis as is the cleavage of bis(8-hydroxyquinoline) phosphate[25]. The cleavage of adenosine 3′-alkyl phosphate diesters in the presence of some transition metals and lanthanides is suggested[26] to involve coordination of the departing group to the metal ions, particularly La^{3+}. Our recent work demonstrated a LGA of 10^{12} for the cleavage of diester **5.2c** promoted by Yb^{3+},[27] as well as an apparent LGA for the dinuclear Zn(II) complex **5.1** in promoting cleavage of diesters having an *ortho*-NO_2 or -CO_2Me substituent on the aryloxide leaving groups (**5.2b,c**).[13c]

For triesters like diethyl (8-dimethylammonium)napthyl-1-phosphate **5.4c**,[28] intramolecular general acid catalysis enhances the attack of water and oxyanion

nucleophiles. However, unambiguous examples of metal ion promoted LGA for triesters are exceedingly rare[29], and the only unambiguous example of which we are aware where metal-assisted LG departure was quantified is that of La^{3+}-promoted methanolyses of triesters **5.3b**, which are cleaved about 60 times faster than triesters without LGA.[30]

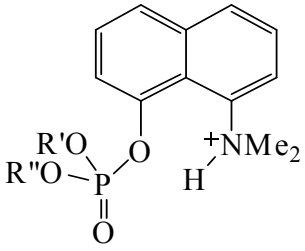

5.4a. OR' = OR" = O^-
5.4b. OR' = OMe; OR" = O^-
5.4c. OR' = OR" = OEt

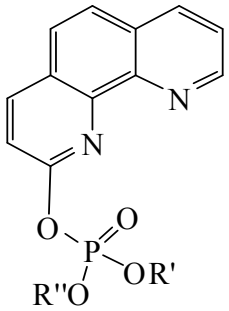

5.5

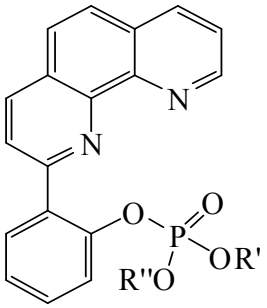

5.6. OR' = OR" = O^-
5.7. OR' = OMe; OR" = O^-
5.8. OR' = OR" = OMe

Scheme 5-1. Cu(II)-assisted cleavages of phosphate esters (**5.6** – **5.8**) in methanol. R′ and R″ = H or CH_3.

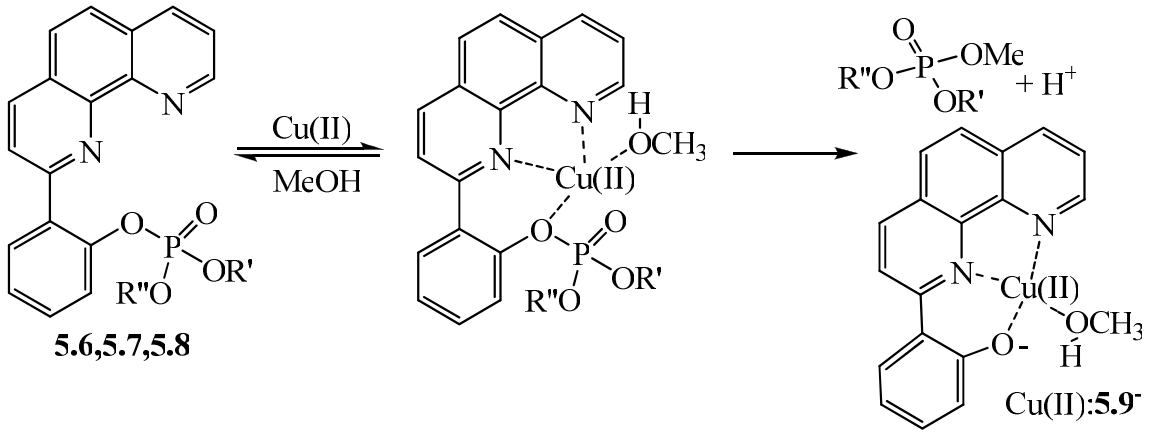

5.6,5.7,5.8

Cu(II):**5.9**$^-$

While phosphoryl mono, di and triester systems with the 8-(dimethylamino)-1-naphthyl leaving group[18,24,28] allow one to compare the effectiveness of general acid

assistance of LG departure on the three ester types, there is no analogous set of esters from which one can draw comparisons of the effectiveness of metal ion LGA. In this study we describe the kinetics Cu(II)-promoted methanolyses of a set of phosphoesters **5.6**, **5.7**, and **5.8** containing the 2-(2-hydroxyphenyl)-1,10-phenanthroline[31] leaving group which is known to bind strongly to M^{x+} ions (Scheme 5-1). The results show that Cu(II)-promoted LGA gives a 10^{13} acceleration or more for the methanolysis of monoester **5.6** and diester **5.7** in the neutral $^{s}_{s}$pH region. By contrast, the methanolysis of triester **5.8** in the presence of Cu(II) shows more a moderate, but still appreciable, 10^5 rate acceleration at neutrality due to metal ion promoted LGA.

5.3 – Experimental

5.3.1 - Materials

Methanol (99.8%, anhydrous), sodium methoxide (0.50 M in methanol, titrated against N/2 certified standard aqueous HCl solution and found to be 0.50 M), $Cu(CF_3SO_3)_2$ (98%), $Zn(CF_3SO_3)_2$, 2-picoline (98%), 2,6-lutidine (99+%), 2,4,6-collidine (99%), triethylamine (99%), 2,2,6,6-tetramethylpiperidine (99+%), Amberlite® IR-120H ion-exchange resin (functionalized as sulfonic acid), sodium carbonate, imidazole (99%), dimethyl chlorophosphate (96%), *p*-nitrophenyl (98%), 1,10-phenanthroline (99+%), 2-bromoanisole (97%), lithium (high sodium granule, 99%), $KMnO_4$ (99+%), pyridine hydrochloride (98%), methanol-*d* (99.5 atom % D), NaOH (reagent grade, 97%), and phosphorus oxychloride (99%) were purchased from Aldrich and used as supplied. $HClO_4$ (70% aqueous solution, titrated to be 12.09 M) was obtained from Acros

Organics. Lithium chloride and $MnSO_4$ monohydrate were purchased from Anachemia Chemical LTD while 1-methylpiperidine (99%) was obtained from Alfa Aesar and used as supplied. $MgSO_4$ anhydrous and 1-ethylpiperidine (99%) were obtained from Fisher Scientific and TCI America Laboratory Chemicals respectively. 2-(2-Hydroxyphenyl)-1,10-phenanthroline was prepared following a published procedure.[31] The disodium salt of phosphate monoester **5.6** was synthesized following a literature method[32] using 2-(2-hydroxyphenyl)-1,10-phenanthroline and $POCl_3$. Both the phosphate diester **5.7** and the triester **5.8** were prepared according to a general method[33] with small modifications.[13c] ^{1}H NMR, ^{31}P NMR, and exact MS spectra of phosphate **5.6**, **5.7**, and **5.8** are consistent with the structure.

Disodium salt of 2-(1,10-phenanthrolin-2-yl)phenyl phosphate (5.6). ^{1}H NMR (400MHz, CD_3OD, 25 ^{o}C) δ 9.05 (1H, dd, *J* = 4.3, 1.5 Hz, H^9), δ 8.47 (1H, dd, *J* = 8.3, 1.8 Hz, H^7), δ 8.37 (1H, d, *J* = 8.3 Hz, H^4 or H^3), δ 8.35 (1H, d, *J* = 8.3 Hz, H^4 or H^3), δ 8.03 (1H, d, *J* = 8.3 Hz, phenyl H^3), δ 7.95 (1H, d, *J* = 8.8 Hz, H^5 or H^6), δ 7.89 (1H, d, *J* = 8.8 Hz, H^5 or H^6), δ 7.81 (1H, d, *J* = 7.6 Hz, H^8), δ 7.75 (1H, dd, *J* = 8.1, 4.6 Hz, phenyl H^5), δ 7.38 (1H, td, J = 8.6, 1.8, phenyl H^6), δ 7.11 (1H, m, phenyl H^4). ^{31}P NMR (162.04 MHz, D_2O, 25 ^{o}C) δ 0.95 referenced to 70% phosphoric acid. HRMS(ESI-TOF): calcd for $C_{18}H_{12}N_2O_4P^-$ [M-2Na^++H^+]: 351.0540 amu, found 351.0540 amu.

Acid form of 2-(1,10-phenanthrolin-2-yl)phenyl methyl phosphate (5.7). ^{1}H NMR (400MHz, CD_3OD, 25 ^{o}C) δ 9.02 (1H, dd, *J* = 4.3, 1.5 Hz, H^9), δ 8.49 (1H, d, *J* = 8.3 Hz, H^4 or H^3), δ 8.48 (1H, dd, *J* = 8.1, 1.8 Hz, H^7), δ 8.31 (1H, d, *J* = 8.3 Hz, H^4 or H^3), δ

8.03 (1H, m, phenyl H^3), δ 7.95 (2H, m, H^5 or H^6), δ 7.77 (1H, dd, *J* = 8.1, 4.3 Hz, H^8), δ 7.65 (1H, td, *J* = 8.6, 1.8 Hz, phenyl H^5), δ 7.45 (1H, dd, *J* = 8.3, 1.8 Hz, phenyl H^6), δ 7.28 (1H, t, *J* = 7.6 Hz, phenyl H^4), δ 3.42 (3H, d, *J* = 11.1 Hz, OCH_3). ^{31}P NMR (162.04 MHz, CD_3OD, 25 ^oC) δ –3.40 referenced to 70% phosphoric acid. HRMS(ESI-TOF): calcd for $C_{19}H_{14}N_2O_4P^-$ [M-H^+]: 365.0696 amu, found 365.0700 amu.

2-(1,10-phenanthrolin-2-yl)phenyl dimethyl phosphate (5.8). ^1H NMR (400MHz, CD_3OD, 25 ^oC) δ 9.05 (1H, dd, *J* = 4.3, 1.5 Hz, H^9), δ 8.50 (1H, d, *J* = 8.6 Hz, H^4 or H^3), δ 8.47 (1H, dd, *J* = 8.1, 1.5 Hz, H^7), δ 8.12 (1H, d, *J* = 8.6 Hz, H^4 or H^3), δ 8.09 (1H, m, phenyl H^3), δ 7.98 (2H, d, *J* = 4.3 Hz, H^5 or H^6), δ 7.76 (1H, dd, *J* = 8.1, 4.3 Hz, H^8), δ 7.55 (1H, td, *J* = 8.6, 1.8 Hz, phenyl H^5), δ 7.50 (1H, m, phenyl H^6), δ 7.44 (1H, m, phenyl H^4), δ 3.61 (6H, d, *J* = 11.4 Hz, OCH_3). ^{31}P NMR (162.04 MHz, CD_3OD, 25 ^oC) δ –4.69 referenced to 70% phosphoric acid. HRMS(ESI-TOF): calcd for $C_{20}H_{18}N_2O_4P$ [M+H^+]: 381.0998 amu, found 381.0997 amu.

5.3.2 -General Methods

^1H NMR and ^{31}P NMR spectra were determined at 400 and 162.04 MHz. $CH_3OH_2^+$ concentrations were determined potentiometrically using a combination glass Fisher Scientific Accumet® electrode model # 13-620-183A calibrated with certified standard aqueous buffers (pH = 4.00 and 10.00) as described in previous papers.[34] The ${}^{s}_{s}pH$ values in methanol were determined by subtracting a correction constant of -2.24[34] from the electrode readings and the autoprotolysis constant for methanol was taken to be $10^{-16.77}$ M^2. The ${}^{s}_{s}pH$ values for the kinetic experiments were measured at the end of the

reactions to avoid the effect of KCl leaching from the electrode. For methanolysis of Cu(II):**5.7** the ${}^{s}_{s}\mathrm{pH}$ measured at the beginning of the reactions were the same as those determined at the end.

5.3.3 - General UV-visible Kinetics

The Cu(II)-catalyzed methanolysis of **5.7** and **5.8** were followed at 414 nm for the appearance of the Cu(II) bound phenoxide **5.9** using a UV-vis spectrophotometer with the cell compartment thermostatted at 25.0±0.1 °C. $Cu(OTf)_2$ was used as the source of Cu ion. The reactions were conducted in the presence of buffers composed of various ratios of $HClO_4$ and amines (2-picoline (${}^{s}_{s}\mathrm{pH}$ = 4.8-6.9), 2,6-lutidine (${}^{s}_{s}\mathrm{pH}$ = 7.0-7.5), 2,4,6-collidine (${}^{s}_{s}\mathrm{pH}$ = 7.8-8.5), *N-iso*-propylmorpholine (${}^{s}_{s}\mathrm{pH}$ = 8.5-9.0), 1-methylpiperidine (${}^{s}_{s}\mathrm{pH}$ = 9.4-9.7), 1-ethylpiperidine (${}^{s}_{s}\mathrm{pH}$ = 9.8-10.5), triethylamine (${}^{s}_{s}\mathrm{pH}$ = 10.9), and 2,2,6,6-tetramethylpiperidine (${}^{s}_{s}\mathrm{pH}$ = 11.0-12.1)) to maintain the ${}^{s}_{s}\mathrm{pH}$ in methanol. For reactions at ${}^{s}_{s}\mathrm{pH}$ 3 or lower, an appropriate amount of $HClO_4$ was added to achieve the targeted initial $[CH_3OH_2^+]$ in solution. A typical kinetic experiment involved preparing a methanol solution of the phosphate substrate (between 0.01 and 0.05 mM) containing excess buffer (0.2 to 1.0 mM) in a 1 cm path length UV cuvette. The rate constants for the methanolysis of **5.6** and **5.7** in the presence of Cu(II) did not exhibit [buffer] effects (from 0.1 mM to 20 mM of 2-picoline or 2,2,6,6-tetramethylpiperidine buffer) nor was the rate sensitive to the presence of 0.01 to 20 mM of tetrabutylammonium chloride, tetrabutylammonium bromide, or free pyridine. Initiation of the reaction involved addition of an aliquot of Cu(II) stock solution in methanol to the substrate solution in the cuvette to achieve the desired concentrations of the reaction components in a final

volume of 2.5 mL. Duplicate kinetics were done and in cases where the reactions are reasonably fast, the abs. vs. time traces for product appearance were fit to a standard first order exponential equation to obtain the observed first order rate constants (k_{obs}). For very slow reactions, such as those of the Cu(II)-promoted methanolysis of **5.8** at higher ${}^{s}_{s}\mathrm{pH}$, initial rates of the reactions were obtained by fitting the first 5-10% of the abs. vs. time traces to a linear regression, followed by dividing the initial rates by the expected absorbance change (ΔAbs) if the reaction were to reach 100% completion to get the k_{obs} constants.

Separate ${}^{s}_{s}\mathrm{pH}$/rate profiles were constructed for the 0.05 mM Cu(II)-catalyzed cleavages of 0.05 mM of **5.7** and 0.05 mM of **5.8** in the presence of 1 mM of buffer in methanol. A concentration dependent study was also conducted with increasing [Cu(II)] and [**5.7**] in 1:1 ratio from 0.05 mM to 0.3 mM in the presence of excess $HClO_4$ such that the ${}^{s}_{s}\mathrm{pH}$ was kept at 3.5 ± 0.2. The solvent kinetic isotope experiment for the Cu(II)-assisted breakdown of **5.7** was carried out as follows. Stock solutions of 5 mM of $Cu(OTf)_2$, 7.0 mM of substrate **5.7**, and 50 mM of picoline (with 1/2 equivalent of added $HClO_4$) buffer in CH_3OD were prepared. Aliquots of these solutions were diluted in UV cells containing either CH_3OH or CH_3OD so that the final concentrations of $Cu(OTf)_2$, **5.7**, and picoline were 0.05, 0.05, and 1 mM. Duplicate kinetic runs were done and the ${}^{s}_{s}\mathrm{pH}$ values measured after the reactions were found to be 6.2 ± 0.2. A similar experiment was also done for substrate **5.8** with final concentrations of $Cu(OTf)_2$, **5.8**, and picoline buffer (${}^{s}_{s}\mathrm{pH}$ 3.5 ± 0.2) were 0.05, 0.05, and 1 mM.

5.3.4 - Stopped-Flow Kinetics

The Cu(II)-promoted cleavage of **5.6** was monitored at 414 nm for the appearance of product using a stopped-flow apparatus thermostatted at 25.0 ± 0.1 ^{o}C. One syringe of the stopped-flow analyzer was loaded with 0.02 mM of **5.6** and 0.4 mM of the desired buffer in methanol. The second syringe was loaded with 0.02 mM of $Cu(OTf)_2$ in methanol. When mixed, the final concentrations of $Cu(OTf)_2$, **5.6**, and buffer were 0.01, 0.01, and 0.2 mM. At least five kinetic runs were recorded at each ${}^{s}_{s}pH$, and the k_{obs} constants are the averages. A concentration dependent experiment was also conducted by following the reactions of 4×10^{-6} M ≤ [Cu(II):**5.6**] ≤ 5×10^{-4} M in the presence of a 40-fold excess 1-methylpiperidine buffer (${}^{s}_{s}pH$ = 10.4 ± 0.2). The effect of increasing [Cu(II)] was investigated by increasing the [$Cu(OTf)_2$] from 1×10^{-5} to 7×10^{-5} M while keeping the [**5.6**] constant at 1×10^{-5} M in the presence of 0.2 mM of 1-methylpiperidine buffer (${}^{s}_{s}pH$ = 10.2 ± 0.2). A solvent kinetic isotope experiment was done in a similar fashion to that described for substrate **5.7**, where stock solutions of $Cu(OTf)_2$, **5.6**, and 1-methylpiperidine buffer were 0.5, 5, and 50 mM in CH_3OD. Aliquots of the solutions were diluted into solutions of CH_3OH or CH_3OD to attain the desired concentrations. In this case, one of the syringes of the stopped-flow analyzer was loaded with 0.02 mM **5.6** and 0.4 mM of buffer, and the other syringe contained 0.02 mM of $Cu(OTf)_2$. Two separate experiments were conducted with 1-methylpiperidine buffer setting the measured but uncorrected ${}^{s}_{s}pD$ values at 9.6 ± 0.2 and 10.4 ± 0.2 in methanol. (These uncorrected values were measured at the end of the reactions simply as the electrode readings + 2.24 and have not been corrected for the effect of the deuterated solvent on the

electrode reading or on the ${}^{s}_{s}pK_a$ of the buffer. As will be discussed, the actual ${}^{s}_{s}pD$ is less important since this is in the plateau region of the ${}^{s}_{s}pH$ /rate profile.) The average of the first order rate constants from seven kinetic runs were used for analysis.

5.3.5 - Methanolysis of 4-Nitrophenyl Phosphate (5.10) at 50 ^{o}C

The progress for the methanolysis of 10 mM of 4-nitrophenyl phosphate at 50 ^{o}C in 20 vol.% of CD_3OD in CH_3OH was followed using ^{31}P NMR. To six separate standard NMR tubes, each containing 10 mM of disodium 4-nitrophenyl phosphate, was added: 100 mM NaOMe, 10 mM NaOMe, 10 mM $HClO_4$, 20 mM $HClO_4$, 30 mM $HClO_4$, and 50 mM $HClO_4$. In another sample, no additional base or acid was added to 10 mM of the phosphate. The seven samples (all with final volume of 1 mL solution) were capped and sealed with Parafilm® before being incubated in a water bath set at 50.0 ± 0.5 ^{o}C. At different times samples were removed from the water bath and ^{31}P NMR spectra were acquired with at least 600 scans on each. ^{31}P NMR spectra of the starting phosphate as well as that for monomethyl phosphate in methanol were used as references. All kinetic reactions were followed to a maximum of 15% completion and for each sample (each concentration of added base or acid) at least triplicate experiments were conducted. The % product conversions vs. time plots were fit to a linear regression to obtain the rates of the reactions. The rates were converted to first order rate constants by dividing the % conversion/time data by 100%.

5.3.6 - Spectrophotometric Titrations of 5.9

A 1 cm UV cell was charged with 0.1 mM of phenol **5.9** in 2.5 mL of anhydrous methanol. Small aliquots of a 1.0 M tetrabutylammonium hydroxide in methanol were

added to vary its concentration from 0 – 1.0 M in small increments and the UV-vis spectrum (250 – 500 nm) of the mixture was collected at 25 ^{o}C after each addition of base. The titration was done in duplicate. The absorbance values at 400 nm (appearance of the phenoxide) were corrected for volume change and the log of the corrected absorbance at 400 nm was plotted against the –log [H^+] in solution. The data were fit to the expression in eq. (1) to yield the acid dissociation constant of the phenolic OH group of compound **5.9**.

$$\log(\text{Abs}) = \log(\text{A} * (\frac{K}{K + [H^+]}) + A_o) \qquad (1)$$

In eq. (1), A is the overall absorbance change expected from converting one species completely into another, A_0 is the initial absorbance when the initial species (phenol **5.9**) exists in 100% and K is the dissociation constant of interest. The average $^{s}_{s}\text{pK}_{a}$ value of phenol **5.9** was determined to be 16.16 from duplicate titrations.[35]

5.3.7 - Binding Constant of Cu(II) to Phenol 5.9

To a 2.5 mL methanol solution containing 0.1 mM of phenol **5.9** and 0.1 mM of $Cu(OTf)_2$ were added small aliquots of 0.6 M triflic acid in methanol and the UV-vis spectrum (220 – 500 nm) was recorded after each addition. The absorbance values at 450 nm corresponding to the decrease in [complex] were corrected for volume changes and the titration data were analyzed using Hyperquad 2000[36] with a model defined by species: **5.9**, **5.9**-H^+, Cu(II):**5.9**, Cu(II):**5.9**$^-$ (see chapter Postscript). The acid dissociation constants of **5.9** and **5.9**-H^+ were fixed to be $10^{-16.16}$ M and $10^{-4.73}$ M as determined independently (see chapter Postscript), while the autoprotolysis constant of methanol was

taken to be $10^{-16.77}$ M^{2}.[34] With these inputs, the dissociation constants of Cu(II):**5.9**$^{-}$ $\rightleftharpoons$ Cu(II) + **5.9**$^{-}$ and Cu(II):**5.9** $\rightleftharpoons$ Cu(II) + **5.9**$^{-}$ + H^{+} were computed as –log (K_d) values of 23.64 ± 0.03 and 24.13 ± 0.01, respectively, from duplicate titrations (see chapter Postscript).

5.3.7 - Binding constant of Cu(II) and Phosphate Triester 5.8

To a UV cell containing 7 x 10^{-5} M of **5.8** and 1 mM of collidine buffer ($^{s}_{s}$pH 7.4) in 2.5 mL of methanol, were added aliquots of 5.6 mM $Cu(OTf)_2$ stock solution in 5 μL increments. The absorbance at 490 nm after each addition was plotted against the [$Cu(OTf)_2$] and the data were fit to a binding equation[37,38] applicable to strong and weak situations.

A more accurate value for the dissociation constant of Cu(II):**5.8** was acquired as follows. To a UV cell containing 0.1 mM of the complex in 2.5 mL of anhydrous methanol was added small aliquots of triflic acid in methanol with subsequent determination of the UV-vis spectrum from 220–500 nm after each addition. The absorbance values at 263 nm for the reduction in [complex] were corrected for volume change and plotted against the –log [H^{+}] of the solution. Data from duplicate titrations were analyzed using Hyperquad 2000 to compute an average dissociation constant (K_d) of 2.8 x 10^{-7} M.

5.3.9 - Activation Parameters

The kinetic runs at different temperatures for substrate **5.6** and **5.7** were done using a thermostatted stopped-flow analyzer and the averaged rate constants determined

at each temperature were used to construct Eyring plots. Kinetic runs for substrate **5.8** at different temperatures were followed by UV-vis spectrophotometry, and the solution temperatures determined with a thermometer inserted into the cell at the end of the reaction. First order rate constants were measured in quadruplicate at six different temperatures ranging from 10 to 35 ^{o}C for the Cu(II)-promoted methanolysis **5.6** (both at 0.01 mM) in the presence of 0.2 mM of 1-methylpiperidine buffer $^{s}_{s}$pH 10.4 ± 0.2. Fitting the natural log of the averaged k_{obs}/T vs. 1/T data to the Eyring equation gives the $\Delta H^{\ddagger}$ and $\Delta S^{\ddagger}$ values. For substrate **5.7**, the activation parameters were determined with 0.05 mM of $Cu(OTf)_2$, 0.05 mM of **5.7**, 0.25 mM of $HClO_4$ ($^{s}_{s}$pH 3.6 ± 0.2) and using seven temperatures ranging from 12.0 to 39.8 ^{o}C. For substrate **5.8**, duplicate experiments were conducted with 0.05 mM of $Cu(OTf)_2$, 0.05 mM of **5.8**, 1.0 mM of 2-picoline buffer ($^{s}_{s}$pH 3.8 ± 0.2) at seven temperatures ranging from 16.0 to 42.5 ^{o}C.

5.4 - Results

5.4.1 - Cu(II) Complexation with 5.8 and 5.9 in Methanol

The X-ray diffraction structure of $[(Cu(II)_2$:**5.9**$^{-}_2$:(μ-$MeCO_2)][PF_6]$ shows the Cu(II) bound to **5.9** in a planar fashion with Cu(II)-N bond distances of ~ 2 Å and the Cu(II)-phenoxide-O bond distance of ~ 1.9 Å.[31] Similar structures are reported with Ni(II),[31] Pd(II),[39a] and Fe(III)[39b] which indicate that once bound, the metal ion directly interacts with the phenoxide oxygen. The binding constant for Cu^{2+} and **5.9** was determined by spectrophotometric titration under acidic conditions (see chapter Postscript) and the data were analyzed using Hyperquad 2000 to give a K_d of 2.3 x 10^{-24}

M. Ancillary information from the Hyperquad fitting points to a significant drop of the $^{s}_{s}pK_a$ of **5.9** from 16.16 to 0.49 when bound to Cu(II) indicative of a large electrostatic interaction of the phenoxide oxygen of **5.9**$^-$ with the Cu ion.

Triester **5.8** reacts slowly in the presence of Cu(II) and allows spectrophotometric titration studies. At $^{s}_{s}pH$ 7.4 (1 mM collidine containing 7 x 10^{-5} M of **5.8** and varying [Cu^{2+}]), the dissociation constant for Cu(II):**5.8** was found to be (5.1 ± 2.4) x 10^{-7} M. A separate study monitoring the [Cu(II):**5.8**] under acidic conditions yield a similar dissociation constant of (2.8 ± 0.4) x 10^{-7} M after analyzing the data with Hyperquad 2000 (see chapter Postscript). The reactivities of the Cu(II) complexes of **5.6** and **5.7** are too great to allow experimental determination of their dissociation constants, although we assume that these are similar to that of Cu(II):**5.8** but may have somewhat stronger binding due to electrostatic attraction between the metal ion and anionic phosphates.

5.4.2 - Background Reaction for Methoxide with 5.8 and 5.7

The second order rate constant of (2.94 ± 0.09) x 10^{-3} M^{-1} s^{-1} for the CH_3O^--promoted cleavage of **5.8** was determined under pseudo first order conditions with [$^-OCH_3$] ranging from 10 - 50 mM in methanol.

The CH_3O^--promoted methanolysis of **5.7** is too slow to follow experimentally so the $^{s}_{s}pK_a$ value for the leaving group phenol **5.9** (16.16), as determined above, was used to estimate the second order rate constant for the methoxide background reaction of **5.7**. The Brønsted plot for the methoxide-promoted cleavages of a series of methyl aryl phosphate diesters in methanol[13c] fits the expression log (k_2^{-OMe}) = (-0.57 ± 0.06) $^{s}_{s}pK_a$ + (0.14 ± 0.68). From this, the k_2^{-OMe} for methoxide attack on **5.7** is 8.5 x 10^{-10} $M^{-1}s^{-1}$

assuming the reactivity of **5.7** adheres to the same relationship as do methyl aryl phosphates.

5.4.3 - Methanolysis of 4-Nitrophenyl Phosphate (5.10)

An estimate for the background reaction of **5.6**, which reacts too slowly to observe, was made from the rate constant for methanolysis of 4-nitrophenyl phosphate (**5.10**) which exhibits a plateau region between ${}^{s}_{s}pH$ ~10 and 14. The cleavage of **5.10** at 50.0 ± 0.5 ^{o}C in methanol was monitored using initial rate techniques at three ${}^{s}_{s}pH$ values greater than 10.6 (the second ${}^{s}_{s}pK_a$ value of **5.10** determined by half neutralization) at various times using ^{31}P NMR, (see chapter Postscript) and the average k_{obs} for the methanolysis of dianionic **5.10** between ${}^{s}_{s}pH$ 11.6 and 14.0 was determined to be 1.4 x 10^{-7} s^{-1}. This value can be compared with the reported value for cleavage of the dianion of **5.10** in water of 1.55 x 10^{-8} s^{-1} at 39 ^{o}C[40], from which a k_{obs} of 8 x 10^{-8} s^{-1} is calculated at 50 ^{o}C based upon the activation parameters in water listed by Guthrie and Jencks.[41] No methanolysis product (methyl phosphate) was observed for the cleavage of 3-nitrophenyl phosphate (${}^{s}_{s}pK_a$ = 12.41 for 3-nitrophenol in methanol)[13c] after incubating at 50 ^{o}C in methanol for 300 hours. Assuming the limit of detectability of product would be 5%, this corresponds to an upper limit for the decomposition rate constant of 1 x 10^{-8} s^{-1}. An upper limit for the Brønsted β value of ~ -1.0 can be computed from these two data, and while there is a large error in the number, it is similar to the values of -1.23 and -1.11 obtained for the cleavage of the dianions of monoesters in water[42] and in *t*-amyl alcohol[43], indicating that sensitivity to substituent is not greatly affected by these sorts of hydroxylic solvents.

Because the Brønsted slopes for the cleavage of the dianions are not very different in water, methanol and *t*-amyl alcohol, one may estimate a rate constant for the spontaneous cleavage of **5.6** in methanol based on the above k_{obs} for **5.10** and the difference in ${}^{s}_{s}pK_a$ values for the two leaving groups (11.18[13] and 16.16). We assume the β_{lg} value in methanol has limits of -1.23, and -1.0. An approximate k_{obs} for the spontaneous methanolysis of the dianion of **5.6** at 50 ^{o}C is computed as $k_{obs}^{\mathbf{5.6}} = 10^{-((\beta)({}^{s}_{s}pK_a \text{ 4-nitrophenol} - {}^{s}_{s}pK_a \mathbf{5.9}) - \log(k_{obs\,4\text{-nitrophenol}}))} = 10^{-((\beta)(11.18-16.16) - (-6.85))}$. The rate constant spans a 13-fold range of 1.1 x 10^{-13} s^{-1} to 1.5 x 10^{-12} s^{-1} if the β = -1.23 or -1.0 respectively, but despite the ambiguity, this is an exceedingly slow reaction and such error will not affect greatly the analysis.

5.4.4 - Cu(II)-Promoted Methanolysis of Phosphate Monoester 5.6

The ${}^{s}_{s}pH$/rate profile given in Figure 5-1 for the Cu(II)-catalyzed cleavage of **5.6** in methanol (● symbols) can be fit to eq. (2) derived for a model given in Scheme 5-2 with two ionizable groups having ${}^{s}_{s}pK_a$ values of 7.8 and 11.8, a maximum rate constant (k_{cat}^{max}) of 14.7 ± 0.4 s^{-1} in the plateau region and a low ${}^{s}_{s}pH$ plateau of (6.3 ± 0.4) x 10^{-3} s^{-1}. The k_{cat}^{max} value in the neutral ${}^{s}_{s}pH$ region corresponds to a $t_{1/2}$ of 50 msec for catalyzed cleavage of **5.6**.

Scheme 5-2. A kinetic scheme for the ${}^{s}_{s}pH$ dependence of the cleavage of Cu(II):**5.6** in methanol having a reactive form with maximum activity in the ${}^{s}_{s}pH$ region between the ${}^{s}_{s}pK_a$ values of the two ionizable groups.

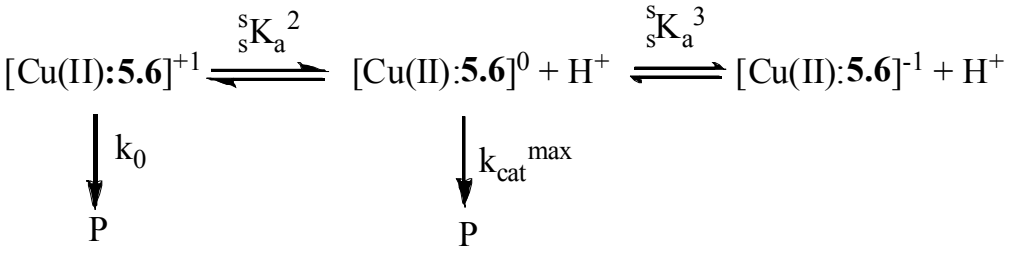

$$k_{obs} = \left(\frac{k_{cat}^{max}\ {}^{s}_{s}K_a^2}{{}^{s}_{s}K_a^2 + [H^+]}\right)\left(\frac{[H^+]}{{}^{s}_{s}K_a^3 + [H^+]}\right) + k_0\left(\frac{[H^+]}{{}^{s}_{s}K_a^2 + [H^+]}\right) \qquad (2)$$

The deuterium kinetic isotope effect was determined at two measured estimated values of "${}^{s}_{s}pD$" 10.4 ± 0.2 and 9.6 ± 0.2 in the plateau region where the rate is independent of ${}^{s}_{s}pH$ (0.2 mM 1-methylpiperidine buffer). The "${}^{s}_{s}pD$" values were simply those from the readings of the electrode made in the deuterated solvent plus the added correction factor of 2.24 for passing from water to methanol. The actual ${}^{s}_{s}pD$ values measured in the plateau region are only approximate but are less important than demonstrating that the rate constant obtained at two different "${}^{s}_{s}pD$" values is invariant. This proves to be the case since the k_{MeOH}/k_{MeOD} value determined at "${}^{s}_{s}pD$" 9.6 is (14.7 ± 0.3 s^{-1})/(14.3 ± 0.4 s^{-1}) = 1.03 ± 0.04 and at "${}^{s}_{s}pD$" 10.4 is (15.9 ± 0.6 s^{-1}/14.7 ± 0.4) = 0.95 ± 0.05.

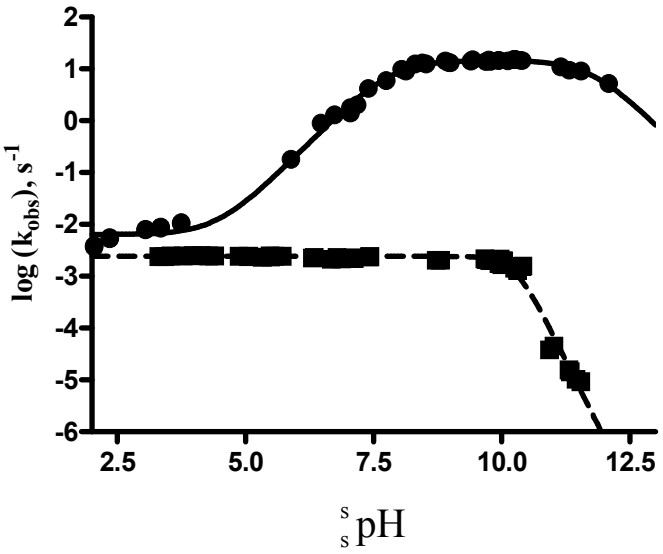

Figure 5-1. A plot of log (k_{obs}) vs. $^{s}_{s}$pH for the Cu(II)-promoted cleavage of **5.6** (●, 0.01 mM of Cu(II) and **5.6**) in methanol with 0.2 mM buffered solutions and **5.7** (■, **5.7** 0.05 mM of Cu(II) and **5.7**) in methanol with 1 mM of amine buffer as described in the Experimental Section or excess added $HClO_4$ in the acidic region, in methanol at 25 ^{o}C. The line through the (●) data is computed by NLLSQ fit to eq. (2) giving two macroscopic $^{s}_{s}pK_a^2$ and $^{s}_{s}pK_a^3$ values of 7.8 ± 0.1 and 11.8 ± 0.2 and a maximum rate constant (k_{cat}^{max}) of 14.7 ± 0.4 s^{-1} and k_0 of (6.3±0.4) x 10^{-3} s^{-1} ; r^2 = 0.9883. The line through the (■) data is computed by NLLSQ fit of the data to eq. (5) derived for the process in Scheme **5-4**, giving log ($^{s}_{s}K_a^2/K_{dim}$) = -20.5 ± 0.2, k_{cat} = 0.0024 ± 0.0001 s^{-1}; r^2 = 0.9798.

In Scheme 5-3 is an expanded version of Figure 5-2 where the species [Cu(II):**5.6a**]$^{+1}$ formed at lower $^{s}_{s}$pH through binding of **5.6**$^{-}$ to Cu^{2+} undergoes two possible microscopic ionizations[44] to yield two formally neutral complexes [Cu(II):**5.6b**]^{0}

and [Cu(II):**5.6c**]^{0}. Chemical intuition suggests that [Cu(II):**5.6b**]^{0}, drawn as having a P-O^{-}·····Cu(II) coordination, should be the more active of the two since both non-bridging oxyanions on P can assist departure of the leaving group with assistance of an electropositive Cu(II). A second set of microscopic ionizations converts the neutral complex into an inactive anionic complex, [Cu(II):**5.6d**]$^{-1}$. It is known that the simple phenanthroline:Cu(II):$^{-}$OCH$_3$ complex dimerizes to produce (phenanthroline:Cu(II):$^{-}$OMe)$_2$ at low concentrations in methanol,[45] so rate vs [complex] experiments were conducted in the plateau region of Figure 5-1 at $^{s}_{s}$pH 10.5 where the dominant species are the two [Cu(II):**5.6**]^{0} forms given in Scheme 5-3.

Scheme 5-3. Possible microscopic ionizations for Cu(II):**5.6** species (counterions omitted for simplicity).

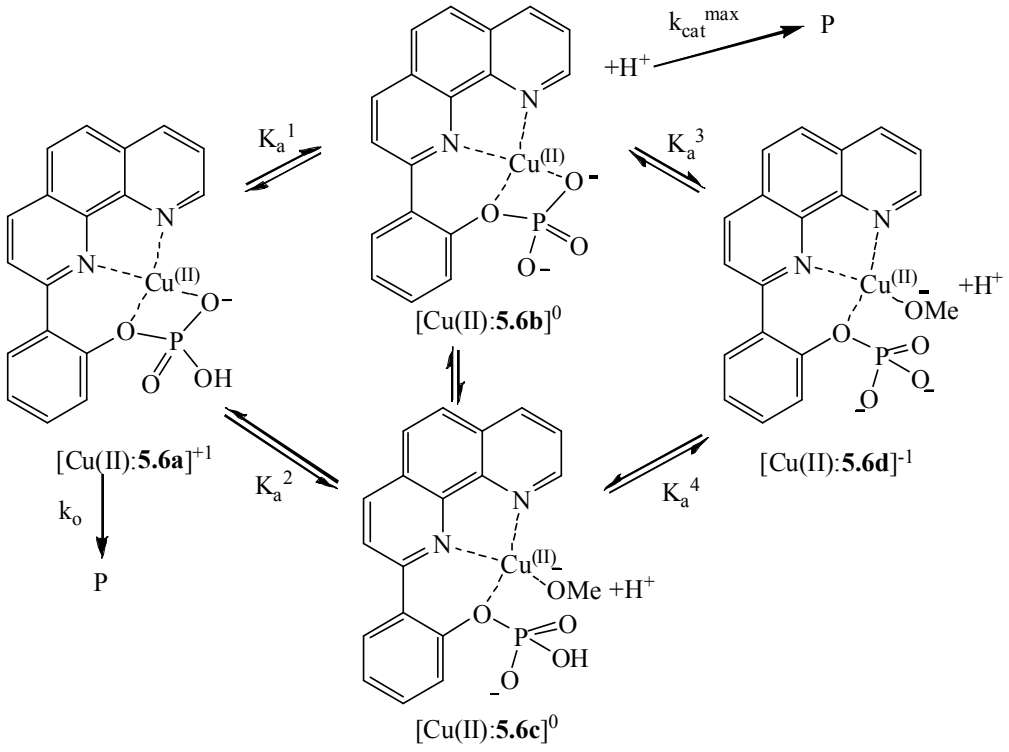

The data in Figure 5-2 follow a square root dependence on the [Cu(II):**5.6**]^0 which stems from the equilibrium formation of an inactive dimer as in eq. (2). Such monomer/dimer equilibrium behavior is treated by NLLSQ fitting of the rate vs concentration data to eq. (4)[45] derived for the process in eq. (3) where the complex is completely formed at all concentrations used, and the active monomer [Cu(II):**5.6**]^0 which decomposes with a rate constant, k_{cat}, is in equilibrium (with dissociation constant K_{dis}) with an inactive dimer [Cu(II):**5.6**]$^0{}_2$. Because it is the rate, not the rate constant, used for the y-axis in Figure 5-2, k_{cat} has the units (Abs/s)/M. A k_{cat} value of ~ 1.3 x 10^5 (Abs/s)/M is estimated from the rate constants and the changes in absorbance obtained at low [Cu(II):**5.6**] where the majority specie in solution is the monomer. Fixing this k_{cat}, the Figure 5-2 data were fit to eq. (3) to give K_{dis} = (1.12 ± 0.03) x 10^{-5} M.

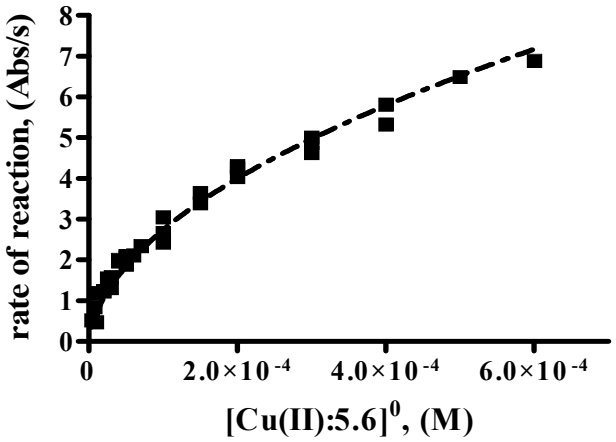

Figure 5-2. A plot of the rate of the reaction (Abs/s) vs. [Cu(II):**5.6**]^0 for the cleavage of **5.6** monitored at 414 nm in the presence of 8 mM of 1-methylpiperidine buffer (^s_spH = 10.4 ± 0.2) at T = 25 ^{o}C. The dotted line through the data is computed from a fit of the data to eqn. (3) having a fixed k_{cat} of 1.3 x 10^5 (Abs/s)/M as described in the text. The computed K_{dis} is (1.12 ± 0.03) x 10^{-5} M with r^2 = 0.9784.

$$P \xleftarrow{k_{cat}} 2[Cu(II):\mathbf{5.6}]^0 \rightleftharpoons[K_{dis}] [Cu(II):\mathbf{5.6}]^0_2 \quad (3)$$

$$rate = \{k_{cat} K_{dis} (\sqrt{1 + 8[Cu(II):\mathbf{5.6}]^0 / K_{dis}} - 1)/4\} \quad (4)$$

5.4.5 - Cu(II)-Catalyzed Methanolysis of Phosphate Diester 5.7

Also shown in Figure 5-1 is the ${}^{s}_{s}pH$/rate profile for the Cu(II)-promoted cleavage of **5.7** under buffered conditions in methanol which exhibits a broad ${}^{s}_{s}pH$ insensitive region from ${}^{s}_{s}pH$ 3.3 to 10. At higher ${}^{s}_{s}pH$ the plot has a gradient of -2, suggesting that two methoxides are responsible for forming an inactive dimeric entity. In the proposed mechanism the most reactive species is [Cu(II):**5.7b**]$^{+1}$ shown in Scheme **5-4** with the monoanionic phosphate bound to the metal ion, or its kinetic equivalent where the phosphate is not bound (not shown). A fit of the kinetic data to the expression in eq. (5), gives the line through the (■) data in Figure 5-1 and log (${}^{s}_{s}K_a^2/K_{dim}$) = -20.5 ± 0.2 and a k_{cat} of 0.0024 ± 0.0001 s^{-1}.

Scheme 5-4. Proposed scheme for the reaction of different ${}^{s}_{s}pH$ dependent [Cu(II):**5.7**] species (counterions omitted for simplicity).

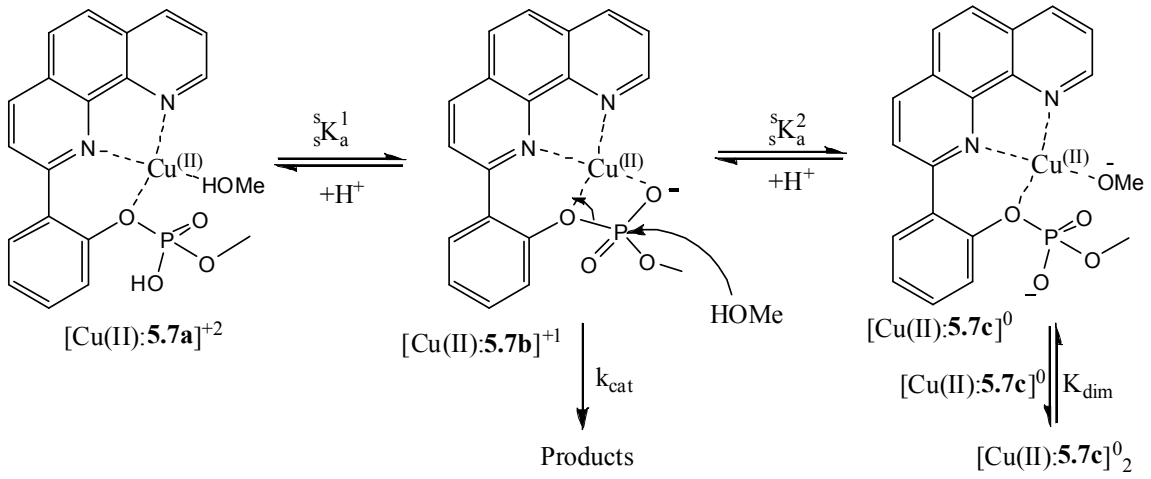

$$\log(k_{obs}) = \log(k_{cat}) + \log(\frac{[H^+]^2}{{}^{s}_{s}K^2_a / K_{dim} + [H^+]^2}) \qquad (5)$$

A solvent kinetic isotope study at a measured "${}^{s}_{s}pD$" of 6.2 ± 0.2 at the midpoint of the plateau in the ${}^{s}_{s}pH$/rate profile (Figure 5-1) gives k_{MeOH}/k_{MeOD} of 1.01 ± 0.04 (k_{MeOH} = 2.37 ± 0.03) x 10^{-3} s^{-1}; k_{MeOD} = (2.35 ± 0.05) x 10^{-3} s^{-1}.

Finally, a concentration dependence experiment was conducted by monitoring the rate constant for the solvolytic cleavage of **5.7** as a function of increasing [Cu(II):**5.7**] in the plateau region of the ${}^{s}_{s}pH$/rate profile in Figure 5-1 by adding excess $HClO_4$ to keep the ${}^{s}_{s}pH$ at 3.5 ± 0.2. Unlike the case for Cu(II):**5.6**, increasing the [Cu(II):**5.7**] from 0.05 to 0.3 mM does not affect the rate constant of the reaction. This is in agreement with the

monomeric [Cu(II):**5.7b**]$^{+1}$ being the only significant species in solution from $^{s}_{s}$pH 3.3 to 10.

5.4.6 - Cu(II)-Catalyzed Methanolysis of Phosphate Triester 5.8

Inspection of the $^{s}_{s}$pH/rate profile for the Cu(II)-catalyzed methanolysis of **5.8** given in Figure 5-3 reveals two reactive species connected by a single ionization. The data in Figure 5-3 are fit to eq. (6) derived for the process in Scheme 5-5 with two different complexes, each cleaving with a different rate constant (k_1 or k_2), interconnected by an acid dissociation $^{s}_{s}pK_a$ of 6.03. These reactive species are designated as [Cu(II):**5.8a**]$^{+2}$ at $^{s}_{s}$pH < 5.5 with $k_1 = (2.0 \pm 0.2) \times 10^{-5}$ s^{-1}, and [Cu(II):**5.8b**]$^{+1}$ at $^{s}_{s}$pH > 7.5 with $k_2 = (1.2 \pm 0.2) \times 10^{-6}$ s^{-1}. A solvent kinetic isotope study at $^{s}_{s}$pH = 3.5 ± 0.2 in the plateau region of Figure 5-3, where the majority of the species in solution is [Cu(II):**5.8a**]$^{+2}$, gives $k_1^{MeOH} = (2.03 \pm 0.04) \times 10^{-5}$ s^{-1} and $k_1^{MeOD} = (9.3 \pm 0.2) \times 10^{-6}$ s^{-1}, and $k_1^{MeOH}/k_1^{MeOD} = 2.2 \pm 0.1$ for the phosphoryl transfer reaction to solvent.

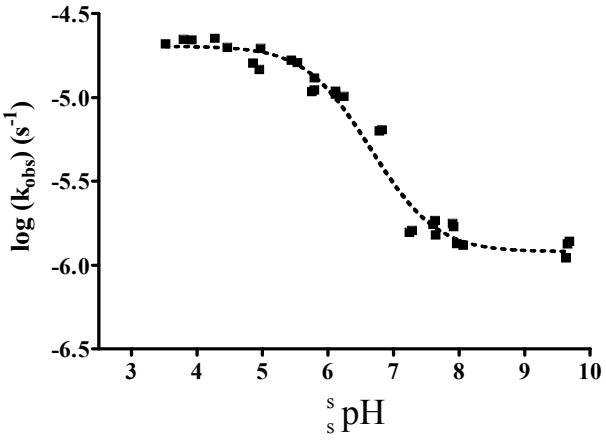

Figure 5-3. A plot of log(k_{obs}) vs. $^{s}_{s}$pH for the Cu(II)-promoted cleavage of **5.8** (0.05 mM of Cu(II) and **5.8**) with 1 mM of amine buffer or excess added $HClO_4$ in the acidic region, T = 25 ^{o}C. The dotted line is obtained from the fit of the data to eqn. (6) derived for the process of Scheme 5-5, giving computed $k_1 = (2.0 \pm 0.2) \times 10^{-5}$ s^{-1}, $k_2 = (1.2 \pm 0.2) \times 10^{-6}$ s^{-1}, $K_a = (9.4 \pm 2.0) \times 10^{-7}$ ($^{s}_{s}pK_a = 6.03$), $r^2 = 0.9643$.

Scheme 5-5. Proposed mechanistic scheme for the formation of different Cu(II):**5.8** species (counterions omitted for simplicity).

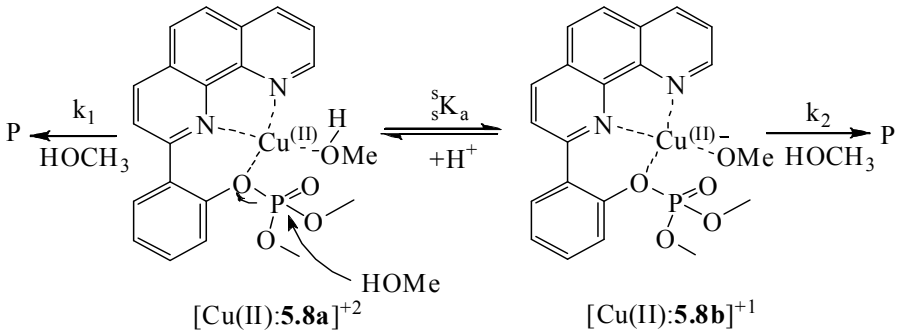

$$\log(k_{obs}) = \log\left(k_1 \frac{[H^+]}{{}^{s}_{s}K_a + [H^+]} + k_2 \frac{{}^{s}_{s}K_a}{{}^{s}_{s}K_a + [H^+]} \right) \qquad (6)$$

5.4.7 - Activation Parameters

To probe further the nature of the Cu(II)-catalyzed reactions of these phosphate esters, the activation parameters were determined in the plateau regions of the plots given in Figure 5-1 and Figure 5-3. The activation data are given in Table 5-1 and the Eyring plots are presented in Figure 5-4. The lines in Figure 5-4 are essentially parallel, indicative of very similar $\Delta H^{\ddagger}$ values for cleavage of each complex, while the $\Delta S^{\ddagger}$ values differ by about 26 cal/mol•K, passing from negative for the triester to positive for the monoester. The values from the solvent kinetic isotope experiments are also included in Table 5-1 for comparison.

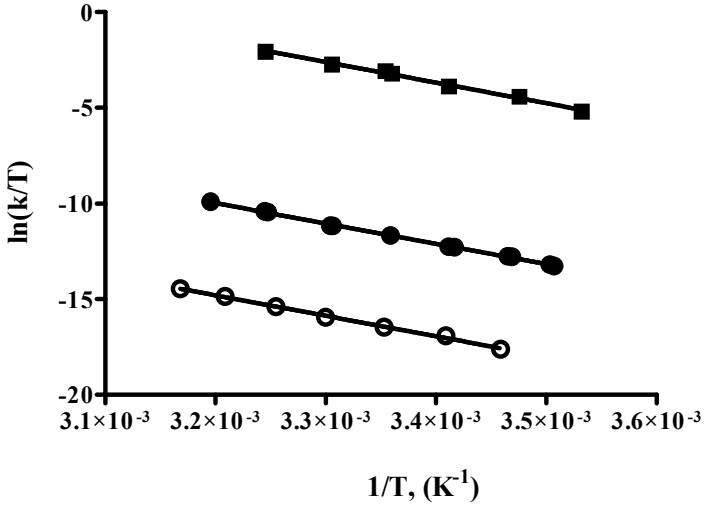

Figure 5-4. Eyring plots of ln(k/T) vs. 1/T for the methanolysis of phosphate esters: (■) 0.01 mM of [Cu(II):**5.6**], 0.2 mM of 1-methylpiperidine buffer, $^{s}_{s}$pH =10.4 ± 0.2; (●) 0.05 mM of [Cu(II):**5.7**], 0.25 mM of $HClO_4$, $^{s}_{s}$pH =3.6 ± 0.2; (○) 0.05 mM of [Cu(II):**5.8**], 1.0 mM of 2-picoline buffer, $^{s}_{s}$pH =3.8 ± 0.2. Fits of the data to the Eyring equation give the activation parameters presented in Table 5-1.

5.5 – Discussion

The concept of, and requirement for, LGA of the cleavage of phosphate esters mediated by enzymes is widely acknowledged,[10b,46] particularly where the leaving group is poor. However, LGA is difficult to demonstrate in small molecule chemistry[13,20-23,26,27,29,30,47] due to the limitations imposed by size and the synthetic difficulties in precisely positioning the metal ions for assisting LG departure. Demonstration of metal ion promoted LGA in small molecule turnover catalysts is a challenge yet to be met in any substantial way unless the substrates contain specially positioned auxiliary groups that transiently coordinate to the metal center during cleavage.[48]

Table 5-1. Activation parameters ($\Delta H^{\ddagger}$, $\Delta S^{\ddagger}$, and $\Delta G^{\ddagger}$ at 25 ^{o}C) and the k^{MeOH}/k^{MeOD} values for the Cu(II)-assisted cleavages of phosphates **5.6**, **5.7**, **5.8** in the plateau region of the respective $^{s}_{s}$pH / rate profiles.

Phosphate complex [a]	$\Delta H^{\ddagger}$ (kcal/mol)	$\Delta S^{\ddagger}$ (cal/mol/K)	$\Delta G^{\ddagger}$ (25 ^{o}C) (kcal/mol)	k_{MeOH}/k_{MeOD}
[Cu(II):**5.6**]^{0} [b]	21.4 ± 0.7	18 ± 2	16.0	0.95 ± 0.05
[Cu(II):**5.7**]$^{+1}$ [c]	21.6 ± 0.4	2.3 ± 1.1	20.9	1.01 ± 0.04
[Cu(II):**5.8**]$^{+2}$ [d]	21.6 ± 0.5	-7.4 ± 1.7	23.8	2.2 ± 0.1

a. The activation parameters for substrate **5.8** are computed at standard state condition with 1 M of nucleophile. This allows for comparison with the values obtained for substrates **5.6** and **5.7**.

b. Activation parameters determined at $^{s}_{s}$pH 10.4 ± 0.2.

c. Activation parameters determined at $^{s}_{s}$pH 3.6 ± 0.2.

d. Activation parameters determined at $^{s}_{s}$pH 3.8 ± 0.2.

In this proof-of-concept study we have employed a strategy where a departing phenoxy group is connected to an *ortho*-phenanthroline ligand that firmly positions a Cu(II) ion within ~1.9Å of the departing oxygen in a series of mono-, di- and triesters, [Cu(II):**5.6**], [Cu(II):**5.7**] and [Cu(II):**5.8**]. We note that the ${}^{s}_{s}pK_a$ of 16.16 for phenol **5.9** suggests this is not a particularly activated leaving group, lying between CF_3CH_2OH (${}^{s}_{s}pK_a$=15.8) and CFH_2CH_2OH (${}^{s}_{s}pK_a$ 17.2)[49]. The unusually high ${}^{s}_{s}pK_a$ value (relative to normal phenols (${}^{s}_{s}pK_a$ of phenol is 14.3)) possibly results from some steric hindrance to solvation of the phenoxy O^- imposed by the bulky 2-phenanthrolyl group, but this same feature ideally sets up the tight coordination environment for Cu(II). Each of **5.6**, **5.7** and **5.8** binds a Cu(II) ion sufficiently strongly that the complexes are fully formed at all concentrations and ${}^{s}_{s}pH$ values by *in situ* addition of one equivalent each of the metal ion and ligand. Once bound, these are not turnover catalysts, but rather molecular complexes that cleave quickly by a unimolecular reaction, but the principle of LGA is amply demonstrated and can be quantified because the ${}^{s}_{s}pH$/rate profiles in Figure 5-1 and Figure 5-3 show plateau regions that correspond to a solvent mediated decomposition of fairly well well-defined species. The ground-state forms of [Cu(II):**5.6b**]^0 and [Cu(II):**5.7b**]$^{-1}$ in Scheme 5-3 and Scheme 5-4 are depicted having a non-bridging oxyanion of the mono and diester coordinated to the Cu(II). This is based on a marked difference in the UV/vis spectrum of Cu(II):**5.7** where the P-O^- can coordinate, relative to that of Cu(II):**5.8** where such coordination is unlikely. In any event, we have no information which of these two kinetically equivalent forms of the mono and diesters are

the preferred reactive species. Such a distinction, while of fundamental interest, does not alter the conclusions of the study.

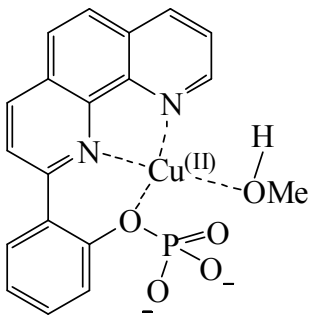

[Cu(II):**5.6b'**]^{0}

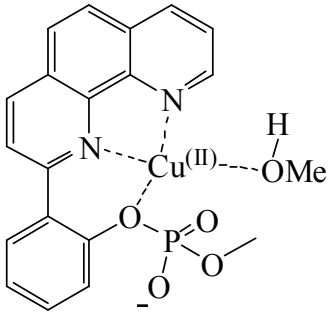

[Cu(II):**5.7b'**]$^{+1}$

Of relevance to the question of LGA is how much acceleration one can expect from positioning the Cu(II) metal ion close to the departing phenoxy oxygen of the leaving group in the three complexes investigated here. In principle, the catalysis is evaluated in terms of energy of binding the Cu(II) of the TS for each of the cleavage reactions relative to the TS for the uncatalyzed reaction. Hyperquad 2000 analysis of the titration data (Results Section 5.4.1) indicates that the dissociation constants of Cu(II):(**5.9**) and Cu(II):**5.9**$^{-}$ are 1.1 x 10^{-8} M and 2.3 x 10^{-24} M which translate into free energies of binding of 10.8 and 32.2 kcal/mol at 25 ^{o}C (see calculation based on the Hyperquad determined β_3 and β_4 equilibrium values in chapter Postscript). The 21.4 kcal/mol difference in these values can be taken as the additional energy attributable to a fully bound phenoxide O^{-}, a portion of which is realized in the TS for cleavage of the P—OLg bond. Not all of this need be realized in a given case, but the magnitude of the stabilization should be directly proportional to the extent of bond ArO--P bond cleavage as measured by the Leffler index α, which is given as the ratio of the Brønsted β_{lg} for the

P--OAr cleavage reaction relative to the β_{eq} for equilibrium transfer phosphoryl groups between oxyanion nucleophiles.[50]

A compendium of the various kinetic rate constants for cleavage of the three complexes is presented in Table 5-2 to allow easy comparison. Below we deal with Cu(II) promoted cleavage of esters **5.6**, **5.7**, and **5.8** in the context of extant relevant data for the background solvolytic cleavages of mono-, di- and triesters, particularly the solvent mediated cleavages, when such data are available.

Table 5-2. Rate constants for the cleavage of phosphates **5.6-5.8** and their Cu(II) complexes.

reactant	k_{obs} (s^{-1})[a]	k_2^{-OMe} ($M^{-1}s^{-1}$)[b]	k_s (s^{-1})[c]	Acceleration ($k_{obs}/k_{background}$)
[Cu(II):**5.6b**]^{0}	14.7±0.4[b] (200)[c]			(1-14)x10^{13} [d,g]
[Cu(II):**5.6a**]$^{+1}$	(6.3±0.4)x10^{-3} [d]			
[Cu(II):**5.7b**]$^{+1}$	(2.5±0.1)x10^{-3} [b]			7.1x10^{14} [b,h]
[Cu(II):**5.8a**]$^{+2}$	(2.0±0.2)x10^{-5} [b]			4.0x10^{9} [b,i]
[Cu(II):**5.8b**]$^{+1}$	(1.2±0.2)x10^{-6} [b]			1.0x10^{5} [b,j]
5.6			(1.1-15)x10^{-13}	
5.7		8.5x10^{-10} [e]		
5.8		(2.9±0.1)x10^{-3} [f]		

a k_{obs} indicates the spontaneous rate constant for decomposition of the Cu(II) complexes at the indicated $^{s}_{s}$pH values in footnotes g,h,i.

b. T = 25 ^{o}C

c. T = 50 ^{o}C

d. ${}^{s}_{s}pH < 2.5$

e. Determined from application of the ${}^{s}_{s}pK_a$ of 16.16 for the 2-(2'-phenanthrolyl)phenol leaving group **5.9** to log (k_2^{-OMe}) = (-0.57 ± 0.06) ${}^{s}_{s}pK_a$ + (0.14 ± 0.68).[13c]

f. Experimentally determined as described in Section 5.4.2.

g. Determined by comparing the spontaneous rate of decomposition of the complex at ${}^{s}_{s}pH$ 10.4 with the projected rate of cleavage of the dianion of **5.6** as computed in Section 5.4.3.

h. Determined by comparing the k_{obs} for cleavage of [Cu(II):**5.7b**]$^{+1}$ at neutral ${}^{s}_{s}pH$ 8.38 with that calculated for the methoxide promoted reaction of **5.7** from k_2^{-OMe}.

i. Determined by comparing the k_{obs} for cleavage of [Cu(II):**5.8a**]$^{+2}$ at neutral ${}^{s}_{s}pH$ 5.0 with that calculated for the methoxide promoted reaction of **5.8** from the observed rate constant of k_2^{-OMe} = (2.94 ± 0.09) x 10^{-3} M^{-1} s^{-1}.

j. Determined by comparing the k_{obs} for cleavage of [Cu(II):**5.8b**]$^{+1}$ at neutral ${}^{s}_{s}pH$ 8.38 with that calculated for the methoxide promoted reaction of **5.8** from the observed rate constant of k_2^{-OMe} = (2.94 ± 0.09) x 10^{-3} M^{-1} s^{-1}.

5.5.1 – Phosphate Monoester

Kirby and Varvoglis[25] showed that phosphate monoesters with good LG's (e.g. 2,4-dinitrophenol; pK_a= 4.07) react faster through the dianionic form than the monoanion via a "dissociative-like" transition state with P-OLg bond being almost completely broken (β_{lg} = -1.23).[25] However, as the Lg becomes poorer, the monoanion reacts faster due to a rate enhancing protonation of the departing oxygen, either through the formation of a zwitterionic ($^{-}O)_2P$-$O(H^{+})$-Lg species prior to the rate-limiting chemical step or through an intramolecular proton transfer process with an intervening water molecule. Because of the reduced charge on the now-protonated phenoxy oxygen in the TS, the latter reaction is less sensitive to the nature of the leaving group (β_{lg} = -0.27).[25]

Subsequently, Hengge and Hoff determined that that the solvolytic cleavage of 4-nitrophenyl phosphate dianion in *tert*-butanol is about 2000-times faster than the monoanion in *tert*-butyl alcohol.[43] They attributed the increased difficulty in the proton transfer process for the monoanion to a higher pK_a value of the phosphate group in *tert*-butanol coupled with a less favorable four-membered transition state for the intramolecular proton transfer process in alcohol, contrasting the more favorable six-membered arrangement in water.

In the present work in methanol we find that **5.6**, when coordinated to Cu(II) as [Cu(II):**5.6**]^0, reacts rapidly (~15 s^{-1}) in the plateau region of the ^s_spH /rate profile given in Figure 5-1. The plateau stems from spontaneous, solvent mediated decomposition of dianionic phosphate complexed to Cu^{2+} as [Cu(II):**5.6**]^0 where the non-bridging phosphoryl oxygens (one perhaps coordinated to the Cu(II)) partake in pushing the Cu(II)-complexed 2'-(2-phenoxy)-1,10-phenanthroline Lg away from an emerging metaphosphate-like unit with little nucleophilic assistance from solvent methanol. This is consistent with the $\Delta S^{\ddagger}$ of (18 ± 2) cal/mol•K and a solvent kinetic isotope effect of unity indicating little change in the participating solvent CH_3O-L force constant during the solvent capture of the emerging PO_3^-- unit. On the other hand, the Figure 5-1 data show a plateau at ^s_spH < 2.5 where the monoprotonated complex of the monoester [Cu(II):**5.6a**]$^{+1}$ reacts with a ^s_spH independent rate constant similar to that of the diester [Cu(II):**5.7b**]$^{+1}$. The data show that the extra phosphoryl oxyanion created by via deprotonation enhances the spontaneous decomposition [Cu(II):**5.6**]^0 of by ~2500-fold.

In methanol, which is structurally more similar to water than *tert*-butyl alcohol and has an intermediate dielectric constant (ε_r = 80.2, 32.7, 12.5 for water, methanol, and

tert-butyl alcohol respectively)[51], we find that the decompositions of 4-nitrophenyl phosphate mono and dianions at 50 ^{o}C have approximately equal rate constants of 1.4 x 10^{-7} s^{-1}.[52] From this rate constant and the $^{s}_{s}pK_{a}$ of 16.16 for the 2'-(2-phenoxy)-1,10-phenanthroline leaving group we estimate (as in the Results section) that the spontaneous decomposition of the dianion of **5.6** should have a rate constant between 1.1 x 10^{-13} s^{-1} and 1.5 x 10^{-12} s^{-1} at 50 ^{o}C. Comparison of this rate constant with the 200 s^{-1} for the decomposition of Cu(II):**5.6** computed at 50 ^{o}C indicates that the Cu(II) induced LGA is worth about 1.3 x 10^{14} to 1.8 x 10^{15} times or ~19.3 to 20.8 kcal/mol in free energy terms.[53] Although we do not have reliable activation parameters for the cleavage of **5.6** in methanol, this LGA should be somewhat higher if the comparison were made at 25 ^{o}C. All these numbers must be regarded as estimates given the uncertainties in the rates of the background reactions due to the long extrapolations required, but this will not change the following analysis substantially. Using the above free energy data as limits for the rate acceleration for the Cu(II)-catalyzed vs uncatalyzed reactions, and the 21.3 kcal/mol for the differential binding of the phenolate leaving group to Cu(II) relative to its binding to the 2'-(2-phenoxy)-1,10-phenanthroline unit in the starting material, one can compute a Leffler index of greater than 90% P--OAr cleavage in the TS. Interestingly, the Leffler index for uncatalyzed cleavage of phosphate monoesters in water is reported to be[25] -1.23/-1.37 = 90%, suggesting that the strong leaving group catalysis we see here does not alter the amount of cleavage of the departing group to any great extent.

5.5.2 – Phosphate Diester

Kirby and Younas[54] showed that the aqueous cleavage of phosphate diesters at 100 ^{o}C is an exceedingly slow process that is highly dependent on the LG basicity. The

reaction with a reasonably good leaving group, 4-nitrophenoxy, involves hydroxide attack on the monoanion down to pH ~5 with a short, but discernable, plateau region indicative of a water reaction, flanked by a hydronium ion catalyzed process. The water reaction was observable with leaving groups as good as, or better than, 4-nitrophenoxy but not with poorer ones like phenoxy or 4-methoxyphenoxy. The methanolytic cleavage of aryl methyl phosphate diesters at 25°C has been reported[13c], but the only observed reaction was methoxide attack on the monoanion under the reported conditions. Based on the ${}^{s}_{s}pK_a$ of 16.16 for 2-(2'-phenanthrolyl)phenol **5.9**, the predicted k_2^{-OMe} for methoxide attack on diester **5.7** is 8.5 x 10^{-10} $M^{-1}s^{-1}$ assuming that this leaving group falls on the Brønsted relationship described for methoxide attack on methyl aryl phosphate diesters[13c,55].

The long plateau between ${}^{s}_{s}pH$ 3 and 10 given in Figure 5-1 is attributable to the spontaneous cleavage of [Cu(II):**5.7b**]$^{+1}$ (see Scheme **5-4**) having a single non-bridging phosphate oxyanion. The data given in Table 5-1 for this process indicate a lower $\Delta S^{\ddagger}$ (2.3 ± 1.1) than is the case for decomposition [Cu(II):**5.6b**]^{0} as well as a solvent kinetic isotope effect of 1.0 indicating little nucleophilic participation of the solvent in the rate-limiting step. The rate constant for this process is (2.5 ± 0.1) x 10^{-3} s^{-1}, ($t_{1/2}$ = 4.6 min) and at the neutral ${}^{s}_{s}pH$ of 8.38 is about 7 x 10^{14} faster than the estimated methoxide reaction for cleavage of **5.7**. Evaluation of the energetics of the Cu(II) induced LGA is complicated by the fact that the catalyzed reaction appears to proceed by a solvent mediated mechanism while such a process is probably not present for cleavage of uncomplexed **5.7** given the high ${}^{s}_{s}pK_a$ for the leaving group.

5.5.3 - Phosphate Triester

Kirby and Khan[56] have reported that the cleavage of dialkyl aryl phosphate triesters (actually 2-aryloxy-2-oxo-1,3,2-dioxaphosphorinans) having good leaving groups in water at 39 ^{o}C is subject to HO^{-}, H_3O^{+} and solvent promoted reactions. For the least reactive esters (such as the 4-nitrophenyl derivative) the base and acid wings account for the hydrolysis over almost all the pH range except for a small deviation at ~pH 4 that may result from a water reaction. We reported that the methoxide promoted reactions of a series of dimethyl aryl phosphates at 25 ^{o}C exhibit a Brønsted β_{lg} value of (-0.51 ± 0.04)[30a] and have no evidence for spontaneous reactions of triesters in methanol. The k_2^{-OMe} for the cleavage of **5.8** determined here ((2.94 ± 0.09) x 10^{-3} M^{-1} s^{-1}) gives a computed pseudo-first order rate constant for the background reaction of 1.2 x 10^{-11} s^{-1} at neutral $^{s}_{s}$pH of 8.38, and 5 x 10^{-15} s^{-1} at $^{s}_{s}$pH 5 assuming the methoxide reaction dominates at both $^{s}_{s}$pH values. Comparing these with the rate constants obtained from the Figure 5-3 data for the decomposition of [Cu(II):**5.8a**]$^{+2}$ and [Cu(II):**5.8a**]$^{+1}$ in the two plateau regions indicates that Cu(II) complexation gives accelerations of 1 x 10^{5} at $^{s}_{s}$pH 8.38 and 4 x 10^{9} at $^{s}_{s}$pH 5. The calculated acceleration at lower $^{s}_{s}$pH is larger than at neutrality mainly because the background base-promoted reaction decreases linearly with [$^{-}OCH_3$]. The data rule out an active role for the Cu(II)-coordinated methoxide as a nucleophile or general base since this would imply that the methoxide form should react faster than the one without, contrary to what is observed. The favored reaction at $^{s}_{s}$pH <5 involves spontaneous decomposition of [Cu(II):**5.8a**]$^{+2}$ which reacts about 20 times faster than [Cu(II):**5.8b**]$^{+1}$ due to the greater Lewis acidity of the Cu(II) in the former. The

decomposition of [Cu(II):**5.8b**]$^{+1}$ must involve a larger participation of methanol as a nucleophile than with the diester and monoester, possibly with the assistance of a second methanol to aid in displacing the Cu(II) coordinated LG as judged by the solvent kinetic isotope effect of 2.2, and the negative $\Delta S^{\ddagger}$ of -7.4 ± 1.7 consistent with some restriction of the degrees of freedom of the reacting species.

5.5.4 - Activation Parameters and Solvent Kinetic Isotope Effects

The data in Table 5-1 suggest that the major differences in the activation free energies of the decomposition of [Cu(II):**5.6**]^{0}, [Cu(II):**5.7**]$^{+1}$ and [Cu(II):**5.8**]$^{+2}$ stem not from enthalpy differences, but from entropy differences which can be analyzed in terms of the tightness or looseness of the transition states for the cleavage processes. In Figure 5-5 is a More O'Ferrall Jencks diagram for the solvolytic cleavage of the mono- di- and triesters. For simple, non-catalyzed solvolysis reactions, the reaction coordinate profiles for the three sets of esters follow the lower curve (monoester), central diagonal (diester), and upper curve (triester) with the transition states (TS) being marked with (‡).[2] Binding of Cu(II) to the OLg component of the lower left and upper left corners should stabilize these corners by similar amounts, assumed for all esters to be on the order of 8.9 kcal/mol from the dissociation constant of Cu(II):**5.8** of 3 x 10^{-7} M. However, Cu(II) binding to the $^{-}$OLg (**5.9**$^{-}$) is determined by potentiometric titration to be very much stronger as indicated by $K_d = 10^{-23.64}$ M. Thus, the entire right hand side of the diagram is pulled down by ~ 32.2 kcal/mol. The net effect of Cu(II) binding to all the corner species is to shift the TS positions (arrows on Figure 5-5) toward the starting material along the reaction coordinate in the Hammond sense, and in the anti-Hammond sense toward the

dissociative metaphosphate-like corner. Thus the predicted three new transition states (shown as $\ddagger_{new}$ on Figure 5-5) have little perturbation of the extent of P-OLg cleavage, but have significantly less nucleophilic $CH_3(H)O$------P bond development.

5.5.4.1 – Monoester

Activation entropies of 3.5 cal/mol•K[26] and 24.5 cal/mol•K[43] are reported for the solvolysis of 4-nitrophenyl phosphate dianion in water and *tert*-butanol. Considerable evidence[2] indicates that PO_3^- transfer from phosphate monoesters involves concerted processes in water with a small nucleophilic participation of solvent through a loose TS situated in the lower right corner of the diagram in Figure 5-5. In the weaker nucleophilic solvent, *tert*-butanol, the $\Delta S^{\ddagger}$ and observed production of racemic *tert*-butyl phosphate from chiral [^{16}O,^{17}O,^{18}O]-*p*-nitrophenyl phosphate supports a two-step mechanism with a rate limiting dissociation to form a freely diffusing metaphosphate intermediate which is subsequently captured by solvent. The large positive $\Delta S^{\ddagger}$ of 18 cal/mol•K for [Cu(II):**5.6**]^0 obtained at $^{s}_{s}$pH 3.8 is consistent with a considerably looser TS than is generally the case for decomposition of phosphate monoester dianions in water and can be compared with the 14.1 cal/ mol•K that is seen for cleavage of (8-dimethylammonium)naphthyl-1-phosphate which involves strong intramolecular H-bonding in the starting material followed by general acid assistance to the leaving group departure.[18] The Cu(II)-mediated LGA moves the TS for decomposition of the coordinated dianion further toward the bottom side of the diagram with less participation of the nucleophilic solvent and perhaps closer to the point where the process becomes a stepwise one.

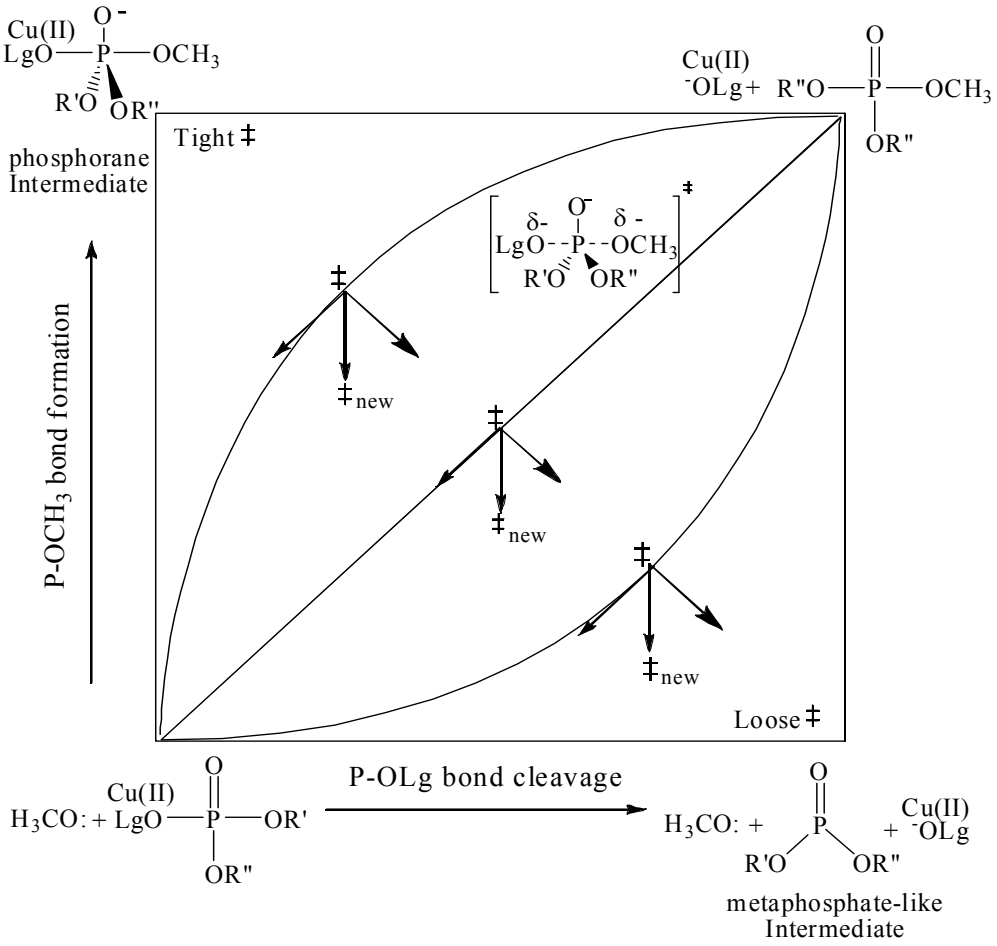

Figure 5-5. A simplified More O'Ferrall Jencks diagram illustrating the energy surface for three general phosphoryl transfer reactions where the decomposition of a phosphate monoester is believed to have a loose transition state which becomes increasingly "tighter" TS for phosphate diesters and triesters.[2] The three TS for the uncatalyzed reactions of tri- di and mono-esters are shown as the ‡ symbols. Binding of the Cu(II) to substrates **5.6**, **5.7** and **5.8** moves each TS toward the starting material in the Hammond sense, and toward the metaphosphate-like corner in the anti-Hammond sense, leading to a new TS ($‡_{new}$) for each of the catalyzed reactions with a similar amount of P—OLg cleavage as in the uncatalyzed reaction, but significantly less CH_3O—P bond development.

5.5.4.2 - Diester

The neutral hydrolysis of *bis*-2,4-dinitrophenyl phosphate monoanion in water has a $\Delta H^{\ddagger}$ = 19 kcal/mol and $\Delta S^{\ddagger}$ of -25.5 cal/mol•K[54] which is some 30 entropy units lower than that for decomposition of the corresponding monoester dianion. This, coupled with the fact that there is a significant solvent deuterium isotope effect of k_H/k_D = 1.55 at 39 ^{o}C and 1.45 at 100 ^{o}C, whereas k_H/k_D is unity for the monoester dianion[26], is consistent with the notion that the diester reacts by a bimolecular mechanism with some involvement of a molecule of water (assisted by a second) in the TS.[54] The decomposition of a phosphate diester subject to intramolecular H-bonding LGA still has a negative $\Delta S^{\ddagger}$ of -12.0 cal/mol•K in the neutral pH region.[24] The solvent promoted methanolysis of the Yb^{3+}:phosphate diester complex **5.11** exhibits a 10^{12} acceleration relative to the uncatalyzed reaction as well as a k_H/k_D of 1.10 ± 0.15 and a $\Delta H^{\ddagger}$ of 16.1 kcal/mol and $\Delta S^{\ddagger}$ value of -15.0 cal/mol•K. These data support a reaction (eq. (7)) proceeding via a looser TS (**5.12**) having less involvement of a nucleophilic $CH_3O(H)$ relative to the solvent reaction alone.[27] The spontaneous decomposition of [Cu(II):**5.7**]$^{+1}$ has a $\Delta S^{\ddagger}$ of 2.3 cal/mol•K, which is more positive than what has been observed to date for the purely solvolytic and LG assisted cleavages of phosphate diesters and closer to what was observed for the hydrolysis of phosphate monoester monoanions[26,25] (typically -0.6 to -6.0 entropy units for the monoanions of methyl, phenyl, 4-nitrophenyl and 2,4-dinitrophenyl phosphate) which are considered to proceed through loose "dissociative-like" transition states subject to LGA by protonation of the departing group. Thus, whereas the solvolytic reactions of phosphate diesters are generally considered[2] to be concerted ones having a reaction coordinate close to the diagonal of the diagram shown

in Figure 5-5, the LGA brought about by the Cu(II) coordination to **5.7** shifts the new, looser TS closer toward the bottom side of the Figure with little change in the extent of cleavage of the P-OLg bond, and less development of the CH_3O--P bond.

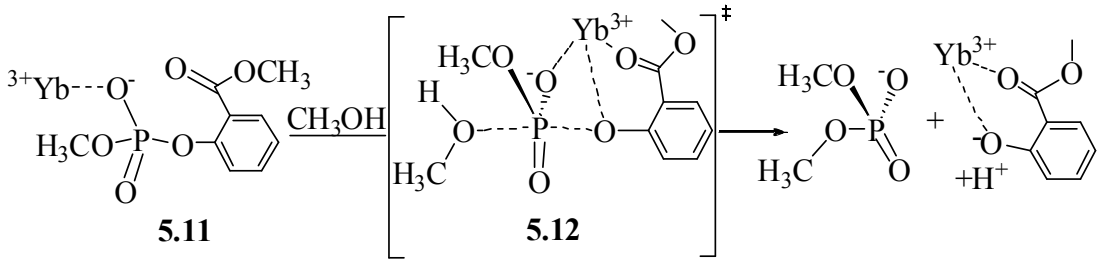

(7)

5.5.4.3 - Triester

Khan and Kirby[56] studied the hydrolysis of dialkyl aryl phosphate triesters (2-aryloxy-2-oxo-1,3,2-dioxaphosphorinans) in water at 39 ^oC and found that those with leaving groups better than 4-nitrophenoxy have pH/rate profiles comprising hydroxide and hydronium ion wings with a plateau region below pH 7, the breadth of which increases with decreasing pK_a of the leaving phenoxy group. In the case of the 2,4-dinitrophenoxy leaving group, the spontaneous hydrolysis is characterized by a very low entropy of -35.6 cal/mol•K and a significant solvent deuterium kinetic isotope effect of k_H/k_D = 2.0, both data being consistent with a process where an attacking water on P is assisted by a second water acting as a general base. Depending on the leaving group and the nature of the attacking oxynucleophile, there appears to be a continuum of mechanisms from concerted displacement of the leaving group to a stepwise reaction for cyclic 6-membered phosphate triesters.[56,57] However, the bulk of the linear free energy[58]

and heavy atom kinetic isotope[59] evidence concerning phosphoryl transfer from acyclic triesters to oxygen acceptors indicates that the reactions are concerted.

As far as we are aware there are no solvolytic data pertaining to acyclic phosphate triesters (or even cyclic ones with poorer leaving groups than 4-nitrophenoxy) that support a water or solvent mediated reaction, and it is likely that the high ${}^{s}_{s}pK_a$ of **5.9** precludes triester **5.8** from reacting with the poorly nucleophilic methanol solvent. Hence a comparison between the $\Delta S^{\ddagger}$ and solvent kinetic isotope data for those reactions with good leaving groups in water and what we observe here for the decomposition of [Cu(II):**5.8**]$^{+2}$ in methanol cannot be made unless we are allowed to use Khan and Kirby's data[56] for the 2-aryloxy-2-oxo-1,3,2-dioxaphosphorinans. The reaction of [Cu(II):**5.8**]$^{+2}$ at ${}^{s}_{s}pH$ 3.8 gives a $\Delta S^{\ddagger}$ of -7.4 entropy units and a solvent kinetic isotope effect of k_H/k_D = 2.2. The latter effect supports a direct nucleophilic attack by methanol possibly with general base assistance by a second alcohol and the entropy term, being at least 20 units higher than the value for the 2,4-dinitrophenyl derivative above suggests that there is a considerably looser TS for the Cu(II) assisted process probably due to decreased formation of the developing P-OCH_3 bond.

5.6 – Conclusions

As part of a continuing effort[13,27,30] to investigate the magnitudes and mechanisms of catalysis resulting from metal ion promoted LGA, the reactions of the Cu(II) complexes of substrates **5.6**, **5.7** and **5.8** were investigated. In this system, the coordinated Cu(II) is bound tightly by the phenanthroline moiety[60] and positioned very close to (possibly touching) the bridging phenoxy oxygen as in Scheme 5-1. Each

complex decomposes by one or more solvent mediated pathways through relatively well-defined species. The most active form of the monoester is [Cu(II):**5.6b**]^{0} where both of the nonbridging phosphoryl oxygens are deprotonated, generating a species that is about 2500 times more reactive than [Cu(II):**5.6a**]$^{+1}$ where one of the non-bridging oxygens is protonated. The active forms for the diester and triester in the neutral $^{s}_{s}$pH plateau region are [Cu(II):**5.7b**]$^{+1}$, [Cu(II):**5.8a**]$^{+2}$ and [Cu(II):**5.8b**]$^{+1}$ where the diester has a negatively charged phosphoryl oxygen and the triester has, respectively, Cu(II):methanol coordination ($^{s}_{s}$pH < 5.5) or a Cu(II) bound methoxide ($^{s}_{s}$pH > 7). The process of transforming Cu(II):**5.6**,**5.7**,**5.8** into Cu(II):**5.9**$^{-}$ releases ~23.3 kcal/mol (8.9 - 32.2 kcal/mol based on the experimental binding constants for the triester and phenoxide) and the endothermicity of progressively greater P--OLg bond cleavage will be offset by a larger transition state binding attributable to the emerging Cu(II):$^{-}$OLg interaction. It is interesting that the $\Delta H^{\ddagger}$ values for the reactions of all three coordinated esters are essentially the same and the differences in the reaction free energies are dictated solely by the $\Delta S^{\ddagger}$ values which span 25 entropy units, passing from 18 to 2.4 to -7.4 cal/mol•K for mono-, di- and triester. The data support the interpretation that Cu(II)-promoted LGA loosens the transition states for the cleavage reactions by reducing both the extent of solvent involvement in forming the CH_3O-P bond and restriction of degrees of methanols of solvation, with little change in the extent of cleavage of the P-OLg bond.

There has been much interest in whether enzyme and man-made catalysts of phosphoryl transfer employ the same or altered transition states as the solution based reactions[61] and evidence consistent with the same transition states[61a,b] or different transition states[61,c,d,e,f] in the catalyzed and uncatalyzed reactions exists. In the present

study, the available data indicate that for the triester 5.8, and diester 5.7, the Cu(II) promoted LGA brings on a solvent mediated reaction that replaces the lyoxide reaction: now a weakly nucleophilic solvent (methanol) is sufficient to displace the coordinated leaving group. This is to be expected from extant data provided by Kirby *et al* demonstrating that the β_{nuc} for attack of oxynucleophiles on phosphate triesters drops as the leaving group becomes better[56], and the rate constants for water attack on phosphate diesters[54] and the dianions of monoesters[25] increase as the phenoxide leaving groups get better. In the present case the ${}^{s}_{s}pK_a$ of **5.9** drops from 16.16 to 0.49 when fully coordinated to Cu(II), which now provides a very good leaving group capable of being displaced by the weakly nucleophilic solvent. This is reminiscent of the discussion and predictions put forth by Jencks and Kirby about the nucleophilic cleavage of 4-nitrophenyl phosphate dianion by nitrogen-containing nucleophiles where the β_{nuc} was 0.13.[26] They suggested that increasing the reactivity of nucleophilic groups in the active site of an enzyme that cleaves phosphate monoester dianions "will not, in itself, make a large contribution to the rate enhancement brought about by enzymatic catalysis of reactions of phosphate dianions. More effective catalysis might be brought about by the enzyme by enhancing the leaving ability of the leaving group, by reduction of the activation energy through distortion or compression of the substrate(s), or by bringing about a change in the mechanism of the reaction, perhaps by metal ion catalysis."

Chin and co-workers have presented an insightful account[62] detailing the magnitudes of the accelerating effects brought on by metal ions for each mode of catalysis in order to reach the rates of the enzymatic cleavages of phosphate esters, and have concluded that LG assistance giving a 10^6 acceleration would be required to cleave

natural substrates with poor leaving groups. Previously we have demonstrated that simple systems comprising a metal containing catalyst and a medium effect brought on by the light alcohols can provide rate accelerations of up to 10^{17} for the cleavage of phosphate tri-[30b,10a] and diesters[10a] by capitalizing on the first three of the four main effects by which metal ions can accelerate the cleavage of phosphate esters. What we have shown here is that a simple man-made system taking advantage of a close positioning of a metal ion and the bridging phenoxy oxygen departing from phosphate mono-, di- and triesters as well as a medium effect provided by methanol solvent is easily capable of providing 10^{12} to 10^{14} acceleration of the cleavage reactions for the mono- and diesters, and 10^{5} to 10^{9} for the triester (depending on the comparison pH) relative to a background reaction at the same ${}^{s}_{s}\mathrm{pH}$.

5.7 – Postscript

The majority of the materials in the Supporting Information component of the original publication (Liu, C. T.; Neverov, A. A.; Maxwell, C. I.; Brown, R. S. *J. Am. Chem. Soc.* **2010**, *132*, 3561) are included here. They are placed here to maintain a smooth and progressive flow of the main concepts without being obstructed by the overwhelmingly large volume of important, but technically and conceptually demanding, analyses described here.

5.7.1 - Universal Binding Expression

Eq. (P1) is a universal binding expression that is applicable to both strong and weak binding cases. Here B represents the plateau value when [X] is either infinitely large or infinitely small, A is the change in absorbance, [S] is the concentration of $Cu(OTf)_2$, and

K_B is the inverse of the metal-complex dissociation constant, K_d. It was derived from the equations for equilibrium binding and for conservation of mass by using the commercially available MAPLE software, Maple V Release 5, Waterloo Maple Inc., Waterloo, Ontario, Canada.

$$Y = B + A(1 - ((1 + K_B * [S] + [X] * K_B - C))/(2K_B)/[S]) \qquad \text{(P1)}$$

where:

$$C = \{1 + 2K_B * [S] + 2 * [X] * K_B + K_B{}^2 * [S]^2 - 2 * K_B{}^2 * [X][S] + [X]^2 * K_B{}^2\}^{0.5}$$

5.7.2 - Potentiometric Titrations

5.9-H^+. The potentiometric titrations in methanol were performed using a Metrohm model 798 Titrino automatic titrator equipped with an Accumet glass double-junction electrode (Cat. # 13-620-183A) under N_2 at 25.0 ± 0.1 ^oC. The electrode was calibrated with Fisher pH 4.0 and 10.0 buffer solutions and the titrant (NaOMe or tetrabutylammonium hydroxide in methanol) was standardized with Fisher certified standard HCl (N/50) in water prior to experiments. After each titration the electrode was immersed in pH 4.00 aqueous buffer for several minutes. In one titration, the mixing cell containing 20 mL of methanol solution (initial ionic strength = 43 mM) containing 1 mM of phenol **5.9**, 2 mM of triflic acid, and 40 mM of tetrabutylammonium triflate was titrated with 28.2 ± 0.6 mM of tetrabutylammonium hydroxide (prepared by diluting a 1.0 M tetrabutylammonium hydroxide stock solution with methanol) in anhydrous methanol at 25.0 ± 0.1 ^oC (Figure 5-6). The same titration was done two more times and the data

were imported into Hyperquad 2000 (version 2.1 NT; footnotes [1],[2],[3]) to determine the acid dissociation constant of the most basic proton on the nitrogens of the phenanthroline component of phenol **5.9** (eqn. (P2)). From three reproducible titrations, the average ${}^{s}_{s}pK_a$ (**5.9**-H^+) value was found to be 4.73 ± 0.03 (footnote [4]).

$$\textbf{5.9}\text{-}H^+ \overset{K_a^{(\textbf{5.9}\text{-}H+)}}{\rightleftharpoons} \textbf{5.9} + H^+ \qquad \text{(P2)}$$

4-Nitrophenyl Phosphate (5.10). In a separate experiment, the mixing cell containing 1 mM 4-nitrophenyl phosphate disodium salt, 2.5 mM triflate acid, and 40 mM of tetrabutylammonium triflate in 20 mL of anhydrous methanol (initial ionic strength = 42.5 mM) was titrated with 28.2 ± 0.6 mM of tetrabutylammonium hydroxide (prepared from diluting 1.0 M tetrabutylammonium hydroxide stock solution with methanol). The average ${}^{s}_{s}pK_a$ values for the two OH groups of 4-nitrophenyl phosphate are calculated to be 4.32 ± 0.03 and 10.28 ± 0.05 from triplicate titrations (Figure 5-7) using Hyperquad 2000. In a similar experiment the mixing cell containing 1.25 mM of 4-nitrophenyl phosphate disodium salt and 3.75 mM of triflic acid in 20 mL anhydrous methanol (initial ionic strength = 3.75 mM) was titrated with 23.1 ± 0.4 mM of sodium methoxide

[1] Hyperquad 2000 is a computer program that fits titration data into nonlinear expressions containing a series of formation constants (log β) for species input to a model, published in: Gans, P.; Sabatini, A.; Vacca, A. *Talanta*, **1996**, *43*, 1739.

[2] The autoprotolysis constant of pure methanol was taken to be $10^{-16.77}$ (3) at 25 ^{o}C.

[3] Gibson, G. T. T.; Neverov, A. A.; Teng, A. C-T.; Brown, R. S. *Can. J. Chem*. **2005**, *83*, 1268.

[4] Unless specified, the errors for the titration results are calculated from the standard deviation of the means of repeated titrations.

(prepared from diluting 0.5 M NaOMe stock solution into methanol). The average $^{s}_{s}pK_a$ values for the two OH groups of 4-nitrophenyl phosphate are calculated to be 4.78 ± 0.11 and 10.74 ± 0.10 from triplicate titrations (Figure 5-8) using Hyperquad 2000.

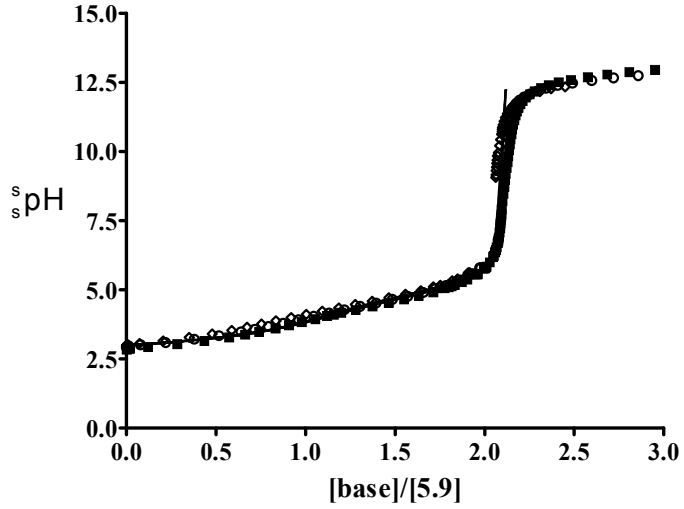

Figure 5-6. Plot of $^{s}_{s}pH$ vs. the [base]/[**5.9**] for the potentionmetric titrations (triplicate experiments) of a solution containing 1 mM **5.9**, 2 mM triflic acid, and 40 mM tetrabutylammonium triflate in 20 mL of anhydrous methanol using 28.2 mM tetrabutylammonium hydroxide as titrant at 25.0 ± 0.1 ^{o}C. The lines through the points are from nonlinear fit of the data into Hyperquad 2000 and the analysis results are given in Table 5-3.

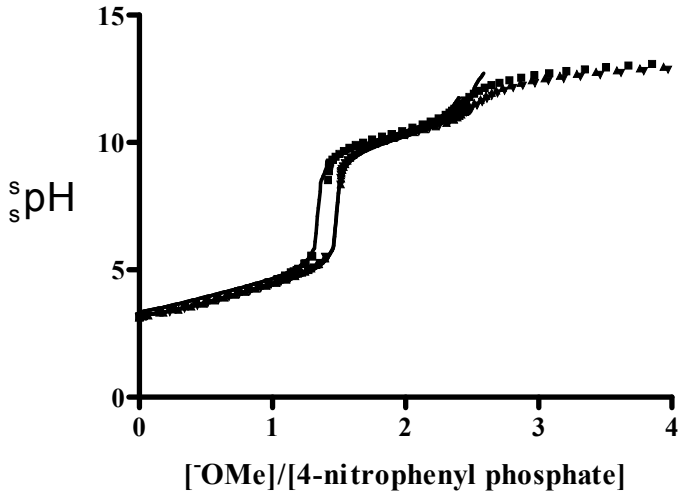

Figure 5-7. Plot of $^{s}_{s}$pH vs. the [$^{-}$OMe]/[4-nitrophenyl phosphate] for the potentionmetric titrations (triplicate experiments) of a solution containing 1.0 mM disodium 4-nitrophenyl phosphate, 2.5 mM triflate acid, and 40 mM tetrabutylammonium triflate in 20 mL anhydrous methanol using 28.2 mM tetrabutylammonium hydroxide in methanol as titrant at 25.0 ± 0.1 ^{o}C. The lines through the points are from nonlinear fit of the data into Hyperquad 2000 and the analysis results are given in Table 5-3.

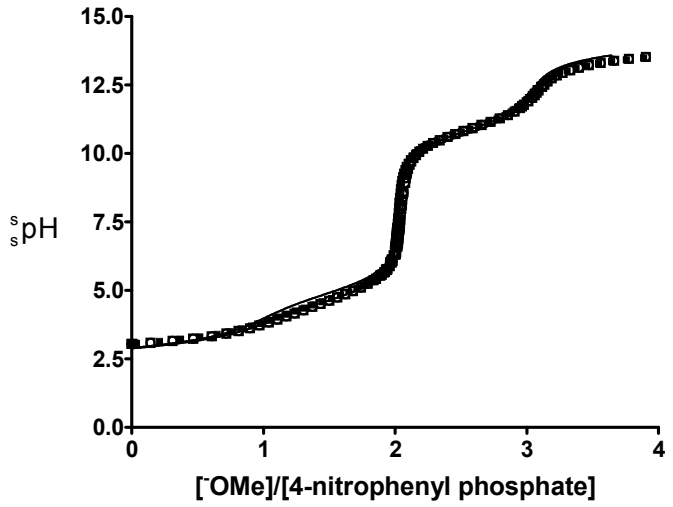

Figure 5-8. Plot of $^{s}_{s}pH$ vs. the [$^{-}$OMe]/[4-nitrophenyl phosphate] for the potentionmetric titrations (triplicate experiments) of a solution containing 1.25 mM disodium 4-nitrophenyl phosphate and 3.75 mM triflate acid in 20 mL anhydrous methanol using 23.1 mM sodium methoxide as titrant at 25.0 ± 0.1 ^{o}C. The lines through the points are from nonlinear fit of the data into Hyperquad 2000 and the analysis results are given in Table 5-3.

5.7.3 - Spectrophotometric Titrations

(**5.9←→5.9^{-}**) A 1 cm path length UV cell was charged with 0.1 mM of phenol **5.9** in 2.5 mL of anhydrous methanol. Small aliquots of a 1.0 M tetrabutylammonium hydroxide in methanol was added to slowly increase its concentration from 0 – 0.36 M in small increments and the UV-vis spectrum (250 – 500 nm) of the mixture was collected using a Cary 100 UV-vis spectrophotometer thermostatted at 25.0 ± 0.1 ^{o}C after each addition of base. The titration was done in duplicate. The absorbance values at 400 nm (appearance of the phenoxide) were corrected for volume change and the log of the corrected absorbance at 400 nm was plotted against the –log [H^{+}] in solution (Figure 5-9). The [H^{+}]

was calculated from the autoprotolysis constant[2] of methanol/[$^-$OMe] = $10^{-16.77}$ $M^2/[^-$OMe]. Fitting the data to a nonlinear expression in eqn. (P3) yields the dissociation constant of the phenolic OH group of compound **5.9** (eqn. (P4)).

$$\log(abs) = \log\left(A \bullet \left(\frac{K_a}{K_a + [H^+]} \right) + A_0 \right) \qquad \text{(P3)}$$

$$\mathbf{5.9} \overset{K_a^{\mathbf{5.9}}}{\rightleftharpoons} \mathbf{5.9}^- + H^+ \qquad \text{(P4)}$$

For eqn. (P3), A is the overall absorbance change one would expect from converting one species completely into another, and A_0 is the initial absorbance when the initial species (in this case phenol **5.9**) exists in 100%. X is the –log[H^+] or the ${}^{s}_{s}pH$ in methanol and K is the dissociation constant of interest. The fitting of the data in Figure 5-9 to eqn. (P3) yields the computed A values of 0.89 ± 0.03 and 0.91 ± 0.03 abs, and A_0 = 0.126 ± 0.02 and 0.115 ± 0.02 absorbance units (Abs) for two duplicate runs. The computed average ${}^{s}_{s}pK_a$ (**5.9**) is calculated to be 16.16 ± 0.01 at 25 ^oC (see Table 5-3) from the fit. Based on the average A values (expected absorbance change) of 0.90 ± 0.01 units, one can estimate the extinction coefficient of phenoxide of **5.9** to be 9000 $M^{-1}cm^{-1}$ at 400 nm. Figure 5-10 shows the UV/vis spectra of a solution containing 0.1 mM **5.9** in 1.0 M tetrabutylammonium hydroxide in methanol and one having 0.1 mM **5.9** in anhydrous methanol in the absence of added base at 25 ^oC. Based on the extinction coefficient value of 9000 $M^{-1}cm^{-1}$ at 400 nm for phenoxide **5.9** and the UV/vis spectra shown in Figure 5-10, one can estimate the ratio of phenol and phenoxide of **5.9** in 1.0 M tetrabutylammonium hydroxide in methanol to be about 23:77.

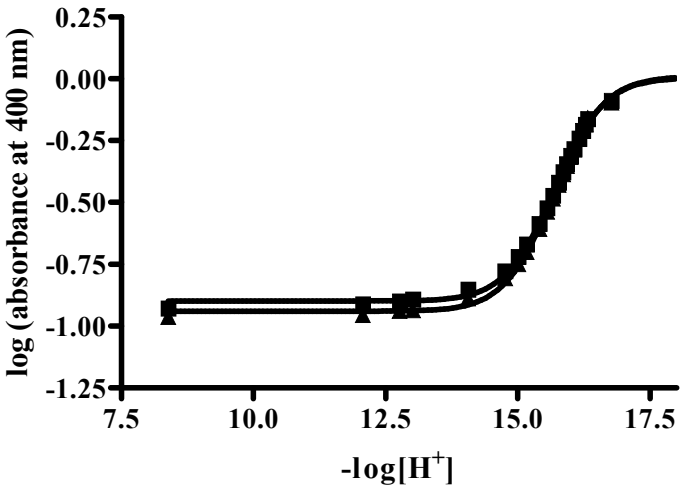

Figure 5-9. Plot of log (absorbance at 400 nm) vs. the $-\log[H^+]$ in anhydrous methanol for duplicate spectrophotometric titrations of 0.1 mM phenol **5.9** using 1.0 M tetrabutylammonium hydroxide in methanol as titrant at 25.0 ± 0.1 ^{o}C. The data are fitted to eqn. (P3) and the computed A values = 0.89 ± 0.03 and 0.91 ± 0.03 abs, A_0 = 0.126 ± 0.02 and 0.115 ± 0.02 abs, and the computed average $^{s}_{s}pK_a$ (**5.9**) is calculated to be 16.16 ± 0.01 at 25 ^{o}C (see Table 5-3). From the computed average expected absorbance change of 0.90 ± 0.01 units, one can estimate the extinction coefficient of phenoxide of **5.9** to be 9000 $M^{-1}cm^{-1}$ at 400 nm.

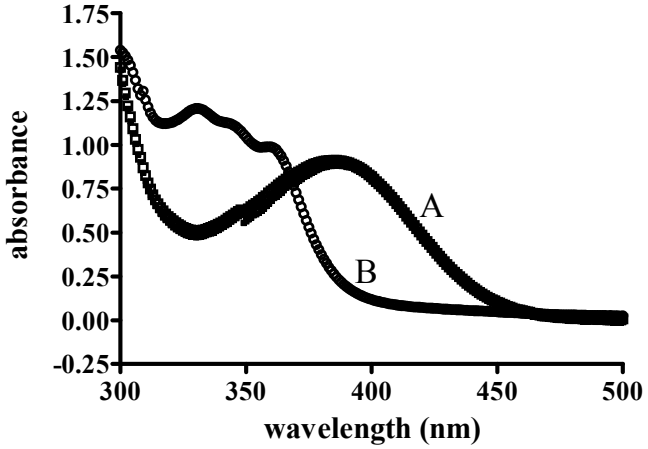

Figure 5-10. Plot of UV/vis absorbance vs. wavelength for A) duplicate samples of 0.1 mM phenol **5.9** in 1.0 M tetrabutylammonium hydroxide in methanol, and B) 0.1 mM of phenol **5.9** in anhydrous methanol in side a 1 cm path length UV cell at 25.0 ^{o}C. Based on an extinction coefficient of 9000 Abs/M/cm for phenoxide **5.9** at 400 nm, spectrum A represents a distribution of approximately 77 % phenoxide and 23% phenol.

Acid Dissociation Constant for Phenol Determined by Addition of Tetrabutylammonium Methoxide as Described Above.

In order to demonstrate the legitimacy of such methodology for the determination of the ${}^{s}_{s}pK_a$ value in methanol, 1.0 mM of phenol in 2.5 mL anhydrous methanol was titrated with 0.01 M tetrabutylammonium hydroxide in methanol. The absorbance values at 295 nm (appearance of phenoxide) were recorded after each addition of base and corrected to account for volume change. The experiment was done in duplicate (Figure 5-11). The titration data were analyzed with eqn. (P3) and the average ${}^{s}_{s}pK_a$ value of phenol was determined to be 14.33 ± 0.02 at 25 ^{o}C (reported as 14.33 at 25 ^{o}C in methanol in Rived, F.; Rosés, M.; Bosch, E. *Analytica Chim Acta* **1998**, *374*, 309).

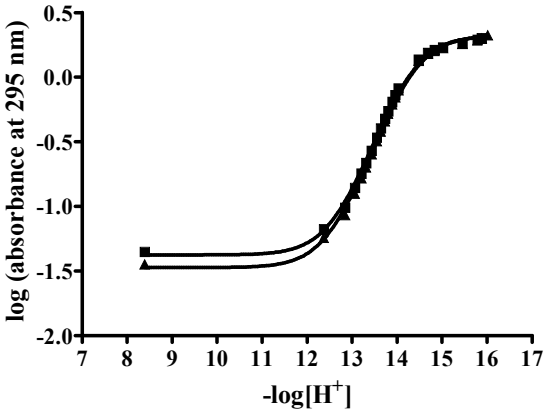

Figure 5-11. Plot of log (absorbance at 295 nm) vs. the –log[H^+] in anhydrous methanol for duplicate spectrophotometric titrations of 1.0 mM of phenol using 10 mM tetrabutylammonium hydroxide in methanol as titrant at 25.0 ± 0.1 ^oC. The data are fitted to eqn. (P3) and the average ${}^{s}_{s}pK_a$ of phenol is calculated to be 14.33 ± 0.02 at 25 ^oC (see Table 5-3).

Second Method for Determining the Formation Constant of Cu(II):5.8

An alternative determination of the Cu(II):**5.8** complex formation constant (β_2) was performed by formulating a 0.1 mM of the complex in 2.5 mL anhydrous methanol inside a UV cell. Small aliquots of a 0.6 M triflate acid solution in methanol were added and the UV-vis spectrum was recorded from 220 – 500 nm after each addition of acid. The absorbance values at 263 nm (for the destruction of the metal complex) were corrected for volume change. The log of the absorbance at 263 nm was plotted against the –log [H^+] in solution (Figure 5-12) and the data were fitted to eqn. (P3) to determine the β_1 value as defined in eqn. (P5), which has an average log (β_1) value of 2.32 ± 0.03 from duplicate titrations. Assuming the acid dissociation constants for the more basic proton on the nitrogens of the phenanthroline component of **5.8** and **5.9** (eqn. P2) are the similar,

the ${}^{s}_{s}pK_a$ (**5.8**H^+) as defined in eqn. (P6) is estimated to be 4.73. Since the complexation of Cu(II) and **5.8** in methanol (eqn. P8) can be derived from eqn. (P5) minus eqn. (P6), the formation constant (β_2) in eqn. (P7) can be calculated as β_1/K_a (**5.8**H^+). Therefore, the log(β_2) can be estimated as log (β_1) + ${}^{s}_{s}pK_a$ (**5.8**-H^+) = 2.32 + 4.73 = 7.05.

$$\text{Cu(II)} + \textbf{5.8}\text{-}H^+ \overset{\beta_1}{\rightleftharpoons} \text{Cu(II):}\textbf{5.8} + H^+ \qquad \text{(P5)}$$

$$\textbf{5.8}\text{-}H^+ \overset{K_a^{(\textbf{5.8}\text{-}H+)}}{\rightleftharpoons} \textbf{5.8} + H^+ \qquad \text{(P6)}$$

$$\text{Cu(II)} + \textbf{5.8} \overset{\beta_2}{\rightleftharpoons} \text{Cu(II):}\textbf{5.8} \qquad \text{(P7)}$$

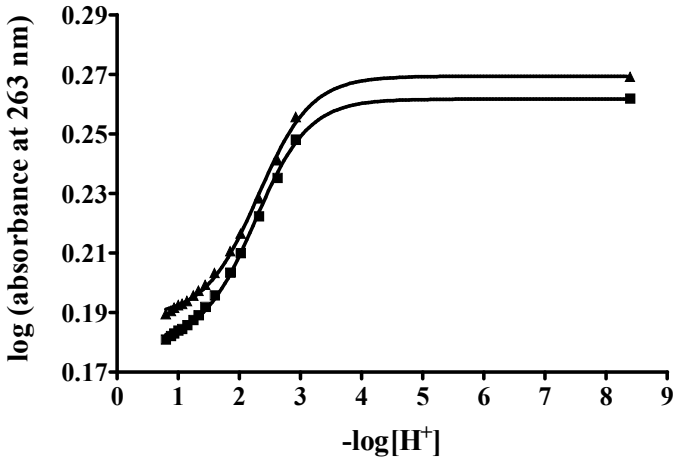

Figure 5-12. Plot of log (absorbance at 263 nm) vs. the –log[H^+] in anhydrous methanol for duplicate spectrophotometric titrations of 0.1 mM of complex Cu(II):**5.8** through sequential addition of 0.6 M triflic acid in methanol at 25.0 ± 0.1 ^{o}C. The data are fitted to eqn. (P3) and the average log (β_1) as defined in eqn. (P5) is computed to be 2.32 ± 0.03 at 25 ^{o}C (Table 5-3).

Binding Constant of Cu(II):5.9$^-$. To a 2.5 mL methanol solution charged with 0.1 mM of phenol **5.9** and 0.1 mM of $Cu(OTf)_2$ small aliquots of 0.6 mM triflic acid in methanol was added in sequential steps and the UV-vis spectrum (220 – 500 nm) was recorded after each addition of acid. The absorbance values at 450 nm (destruction of the metal complex) were corrected for volume change and the titration data (Figure 5-13) were analyzed by Hyperquad 2000 with a model defined by the processes illustrated in eqn. (P2, P4, P8, P9).

$$\text{Cu(II)} + \mathbf{5.9^-} \overset{\beta_3}{\rightleftharpoons} \text{Cu(II):}\mathbf{5.9^-} \qquad \text{(P8)}$$

$$\text{Cu(II)} + \mathbf{5.9^-} + H^+ \overset{\beta_4}{\rightleftharpoons} \text{Cu(II):}\mathbf{5.9} \qquad \text{(P9)}$$

The ${}^{s}_{s}pK_a$ (**5.9**-H^+) and ${}^{s}_{s}pK_a$ (**5.9**) values are known from the titrations described above, and their values were fixed to be 4.73 and 16.16 for the Hyperquad 2000 analysis in order to determine the β_3 and β_4 values. Also, the autoprotolysis constant of methanol was taken to be $10^{-16.77}$ M^{2}.[3] The average values for log (β_3) and log (β_4) computed from duplicate titrations were 23.34 ± 0.03 and 23.83 ± 0.02 respectively. The β_3 value is the formation constant between Cu(II) and **5.9**$^-$ in methanol, which has an average value of $10^{23.34}$ M^{-1} as computed from Hyperquad 2000. Furthermore, eqn. (P10) can be derived from subtracting eqn. (P9) from eqn. (P8).

$$\text{Cu(II):}\mathbf{5.9} \overset{K_a\,(\text{Cu(II):}\mathbf{5.9})}{\rightleftharpoons} \text{Cu(II):}\mathbf{5.9^-} + H^+ \qquad \text{(P10)}$$

Eqn. (P10) is for the acid dissociation constant of the phenolic proton of **5.9** in the complex Cu(II):**5.9**. The K_a (Cu(II):**5.9**) value can be computed as β_3/β_4 from eqn. (P8) and eqn. (P9). Thus, the log K_a (Cu(II):**5.9**) equals log (β_3) – log (β_4) = 23.34 – 23.83 = -0.49, which can be converted to a ${}^{s}_{s}pK_a$ (Cu(II):**5.9**) value of 0.49 in methanol at 25 ^{o}C. The various equilibrium constants are summarized in Table 5-3.

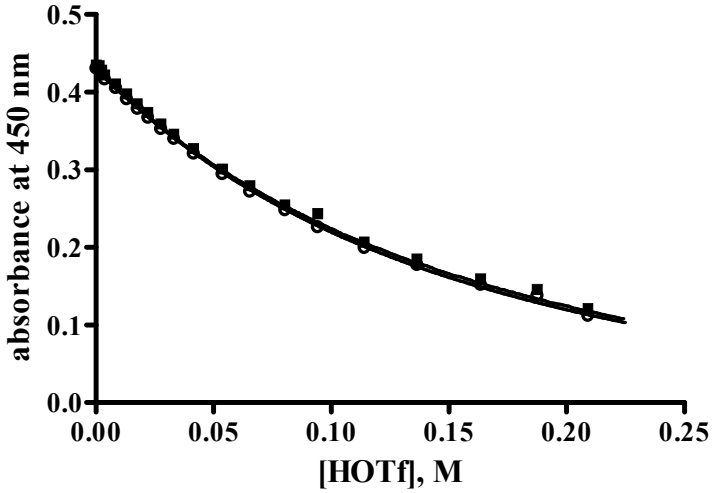

Figure 5-13. Plot of absorbance at 450 nm vs. the [triflic acid] in anhydrous methanol for duplicate spectrophotometric titrations of 0.1 mM complex Cu(II):**5.9** through sequential addition of 0.6 M triflic acid in methanol at 25.0 ± 0.1 ^{o}C. The lines through the points are from a nonlinear fit of the data with Hyperquad 2000 using a muti-speciation model as described in the supporting text, and the analysis results are given in Table 5-3.

Table 5-3. Summary of the various ${}^{s}_{s}pK_a$ (acid dissociation constant) and β (formation constant) values in anhydrous methanol from spectrophotometric and potentiometric titrations at 25.0 ± 0.1 °C.

Species	Individual ${}^{s}_{s}pK_a$ or log (β) at 25 °C [b]	Average ${}^{s}_{s}pK_a$ or log (β) at 25 °C [c]
4-nitrophenyl phosphate (initial Ionic strength = 42.5 mM)	${}^{s}_{s}pK_{a\,1}$:4.30±0.03, 4.35±0.03, 4.32±0.04 ${}^{s}_{s}pK_{a\,2}$:10.25±0.03, 10.33±0.03, 10.25±0.04	${}^{s}_{s}pK_{a\,1}$ = 4.32±0.03 ${}^{s}_{s}pK_{a\,2}$ = 10.28±0.05
4-nitrophenyl phosphate (initial Ionic strength = 3.75 mM)	${}^{s}_{s}pK_{a\,1}$:4.88±0.05, 4.66±0.04, 4.79±0.03 ${}^{s}_{s}pK_{a\,2}$:10.68±0.03, 10.86±0.03, 10.69±0.02	${}^{s}_{s}pK_{a\,1}$ = 4.78±0.11 ${}^{s}_{s}pK_{a\,2}$ = 10.74±0.10
Phenol	${}^{s}_{s}pK_a$:14.31±0.04, 14.34±0.03	${}^{s}_{s}pK_a$ = 14.33±0.02
5.9 eqn. (P4)	${}^{s}_{s}pK_a$ (**5.9**):16.16±0.12, 16.16±0.11	${}^{s}_{s}pK_a$ (**5.9**) = 16.16±0.00
5.9:H^{+} [a] eqn. (P2)	${}^{s}_{s}pK_a$ (**5.9**H^{+}):4.76±0.03, 4.72±0.03, 4.71±0.03	${}^{s}_{s}pK_a$ (**5.9**H^{+}) = 4.73±0.03
Cu(II):**5.8** + H^{+} eqn. (P5)	log(β_1):2.30±0.02, 2.35±0.02	log (β_1) = 2.32±0.03
Cu(II):**5.8** eqn. (P7)		log (β_2) = 7.05±0.04 [d]
Cu(II):**5.9**$^{-}$ eqn. (P8)	log(β_3):23.32±0.05, 23.36±0.04	log (β_3) = 23.34±0.03 [e]
Cu(II):**5.9**$^{-}$:H^{+} eqn. (P9)	log(β_4):23.81±0.10, 23.84±0.11	log (β_4) = 23.83±0.02 [e]

a. The acid dissociation constant of the more basic proton on the phenanthroline nitrogens.

b. Errors computed from the fits to eqn. (P3) or from Hyperquad 2000 analyses.

c. Errors determined as the standard deviation of the mean.

d. Determined from log (β_2) = (2.32 ± 0.03) + (4.73 ± 0.03) = 7.05 ± 0.04.

e. Analyzed using Hyperquad 2000 (footnote [1]) with a complex speciation model consisted of the processes in eqn. (P2, P4, P8, P9). The autoprotolysis constant of methanol was taken to be $10^{-16.77}$ M^2 (footnote [3]). The log (β_3) and log (β_4) were optimized while fixing the values for ${}^{s}_{s}pK_a$ (**5.9**H^+) and ${}^{s}_{s}pK_a$ (**5.9**) values to 4.73 and 16.16 respectively.

5.7.4 - Additional Supporting Figures

The various supporting Figures showing the experimental data of the many results discussed in the main text of this chapter are shown here. The plot of absorbance (490 nm) vs. added [Cu(II)] in a solution containing 8.3 x 10^{-5} M **5.8** in methanol is displayed in Figure 5-14. This was used to estimate the affinity of Cu(II) ion for phosphate **5.8**. The ${}^{s}_{s}pH$ /rate profile for the spontaneous methanolysis of 10 mM 4-nitrophenyl phosphate in anhydrous methanol containing 20% CD_3OD at 50 ± 1 ^oC is shown in Figure 5-15. The initial rates of the methanolysis reactions were determined from fitting the % formation of product (methyl phosphate; from ^{31}P NMR as described in Section 5.3.5) vs. time plots to a standard linear regression forced through the origin. The pseudo-first order rate constants (k_{obs}) can then be computed from the initial rates obtained at each ${}^{s}_{s}pH$ and the expected complete conversion of 4-nitrophenyl phosphate into methyl phosphate when the reaction goes to completion (k_{obs} = ([product]/([product] + [substrate]))/[substrate]).

A plot of k_{obs} vs. [Cu(II):**5.6**] for the catalyzed methanolysis of **5.6** can be found in Figure 5-16, showing the propensity of dimerization at high [Cu(II):**5.6**] to generate (Cu(II):**5.6**)$_2$ as described in Section 5.4.4. A similar phenomenon was not observed for diester **5.7** under acidic condition (Figure 5-17).

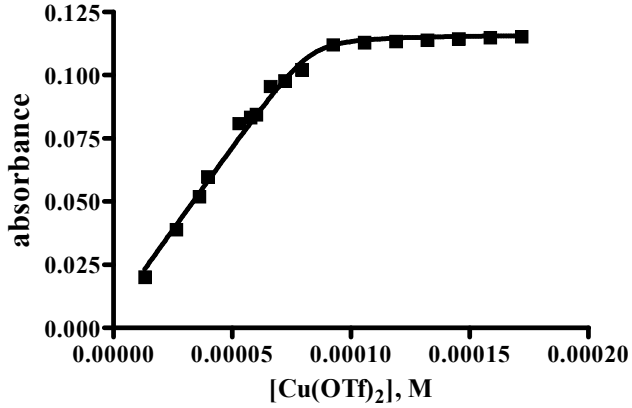

Figure 5-14. A plot of absorbance at 490 nm vs. [$Cu(OTf)_2$] in the presence of 8.3 x 10^{-5} M of **5.8** in anhydrous methanol at 25 ^{o}C. Fitting the data to eqn. (P1) yields B = 0.116 ± 0.002, A = -0.110 ± 0.003, K_d = (5.1 ± 2.4) x 10^{-7} M, r^2 = 0.9935.

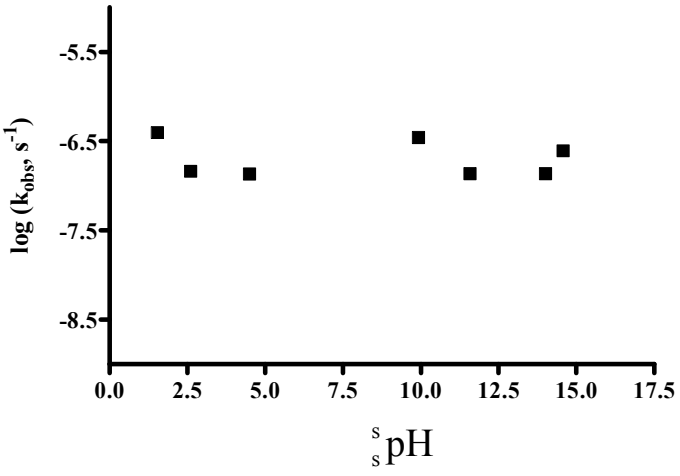

Figure 5-15. $^{s}_{s}$pH /rate profile for the spontaneous solvolysis of 4-nitrophenyl phosphate (10 mM) in anhydrous methanol containing 20% CD_3OD at 50 ± 1 ^{o}C.

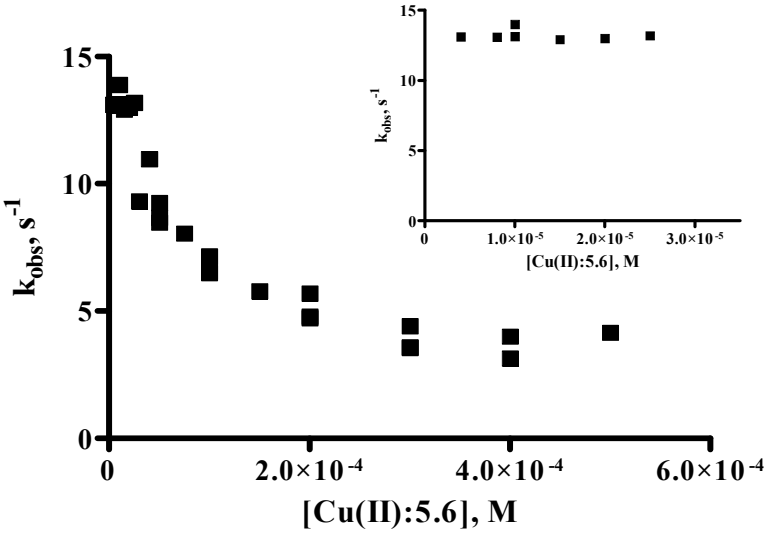

Figure 5-16. A plot of pseudo first order rate constants (k_{obs}) vs. the concentrations of **5.6** and Cu(II) 1:1 ratio for the cleavage of **5.6** in anhydrous methanol containing 8 mM of 1-methylpiperidine buffer, ${}^{s}_{s}$pH = 10.5 ± 0.1, and 25 ^{o}C. The inserted diagram focuses on the rate constants at low [Cu(II):**5.6**].

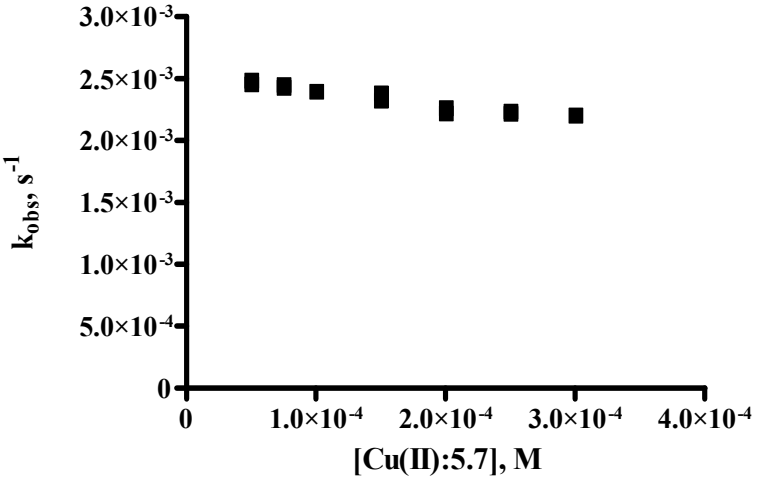

Figure 5-17. A plot of pseudo first order rate constants (k_{obs}) vs. the concentrations of **5.7** and Cu(II) 1:1 ratio for the cleavage of **5.7** in anhydrous methanol containing excess $HClO_4$, ${}^{s}_{s}$pH = 3.5 ± 0.1, and 25 ^{o}C.

5.8 - References and notes

[1] Westheimer, F. H. *Chem. Rev.* **1981**, *64*, 317.

[2] (a) Hengge, A.C. *Adv. Phys. Org. Chem.* **2005**, *40*, 49 and references therein; (b) Hengge, A. C.; Onyido, I. *Curr. Org. Chem.* **2005**, *9*, 61.

[3] (a) Cowan, J. A. *Chem. Rev.* **1998**, *98*, 1067; (b) Weston, J. *Chem. Rev.* **2005**, *105*, 2151; (c) Wilcox D. E. *Chem. Rev.* **1996,** *96*, 2435; (d) Sträter, N.; Lipscomb, W. N.; Klabunde, T.; Krebs, B. *Angew. Chem. Int. Ed. Engl.* **1996**, *35*, 2024; (e) Lipscomb, W. N.; Sträter, N. Chem. Rev. 1996, 96, 2375.

[4] (a) Toy, A.; Walsh, E. N. In Phosphorus Chemistry in Everyday Living. 2nd ed.; American Chemical Society: Washington, DC. 1987: Chapters 18-20. (b) Quin, L. D. In A Guide to Organophosphorus Chemistry. Wiley: New York, 2000. (c) Gallo, M. A.; Lawryk, N. J. In Organic Phosphorus Pesticides. The Handbook of Pesticide Toxicology. Academic Press: San Diego, CA. 1991.

[5] (a) Main, R. A.; Iverson, F. *Biochem. J.* **1966**, *100*, 525; (b) Emsley, J.; Hall, D. In The Chemistry of Phosphorus. Wiley, New York. 1976, p 494.

[6] (a) Wolfenden, R. *Chem. Rev.* **2006**, *106*, 3379; (b) Wolfenden, R.; Snider, M. J. *Acc. Chem. Res.* **2001**, *34*, 938; (c) Schroeder, G. K.; Lad, C.; Wyman, P.; Williams, N. H.; Wolfenden, R. *Proc. Natl. Acad. Sci. USA* **2006**, *103*, 4052; (d) Wolfenden, R.; Ridgeway, C.; Young, G. *J. Am. Chem. Soc.* **1998**, *120*, 833; (e) Warshel, A.; Sharma, P. K.; Kato, M.; Xiang, Y.; Liu, H.; Olsson, M. H. *Chem. Rev.* **2006**, *106*, 3210.

[7] Donarski, W. J.; Dumas, D. P.; Heitmeyer, D. P.; Lewis, V. E.; Raushel, F. M. *Biochemistry*, **1989**, *28*, 4650.

[8] Zalatan, J. G.; Herschlag, D. *J. Am. Chem. Soc.* **2006**, *128*, 1293.

[9] (a) Brown, R. S.; Lu, Z.-L.; Liu, C. T.; Tsang, W. Y.; Edwards, D. R.; Neverov, A. A. *J. Phys. Org. Chem.* **2009**, *22*, 1; (b) Williams, N. H.; Takasaki, B.; Wall, M.; Chin, J. *Accts. Chem. Res.* **1999**, *32*, 485; (c) Morrow, J. *Comments on Inorganic Chemistry.* **2008**, *29*, 169;

[10] Fothergill, M.; Goodman, M. F.; Petruska, J.; Warshel, A. *J. Am. Chem. Soc.* **1995**, *117*, 11619

[11] (a) Mancin, F.; Tecillia, P. *New J. Chem.* **2007**, *31*, 800; (b) Morrow, J. R.; Iranzo, O. *Curr. Opin. Chem. Biol.* **2004**, *8*, 192; (c) Livieri, M.; Manci, F.; Saielli, G.; Chin, J.; Tonellato, U. *Chem. Eur. J.* **2007**, *13*, 2246.

[12] (a) Feng, G.; Natale, D.; Prabaharan, R.; Mareque-Rivas, J. C.; Williams, N. H. *Angew. Chem. Int. Ed.* **2006**, *45*, 7056; (b) Iranzo, O.; Kovalevsky, A. Y.; Morrow, J. R.; Richard, J. P. *J. Am. Chem. Soc*. **2003**, *125*, 1988; (c) O'Donoghue, A.; Pyun, S. Y.; Yang. M.-Y.; Morrow, J. R.; Richard, J. P. *J. Am. Chem. Soc.* **2006**, *128*, 1615; (d) Williams, N. H.; Cheung, W.; Chin, J. *J. Am. Chem. Soc.* **1998**, *120*, 8079.

[13] (a) Neverov, A. A.; Lu, Z.-L.; Maxwell, C. I.; Mohamed, M. F.; White, C. J.; Tsang, J. S. W.; Brown, R. S. *J. Am. Chem. Soc.* **2006**, *128*, 16398; (b) Bunn, S. E.; Liu, C. T.; Lu, Z.-L.; Neverov, A. A.; Brown, R. S. *J. Am. Chem. Soc.* **2007**, *129*, 16238; (c)

Neverov, A. A.; Liu, C. T.; Bunn, S. E.; Edwards, D. R.; White, C. J.; Melnychuk, S. A.; Brown, R. S. *J. Am. Chem. Soc*. **2008**, *130*, 16711.

[14] Liu, C. T.; Neverov, A. A.; Brown, R. S. *J. Am. Chem. Soc*. **2008**, *130*, 16711.

[15] Kim, J.; Lim, H. *Bull. Korean Chem. Soc.* **1999**, *20*, 491.

[16] Sánchez-Lombardo, I.; A. K Yatsimirsky, *Inorg. Chem.* **2008**, *47*, 2514.

[17] Zalatan, J. G.; Catrina, I.; Mitchell, R.; Grzyska, P. K.; O'Brien, P. J.; Herschlag, D.; Hengge, A. C. *J. Am. Chem. Soc.* **2007**, *129*, 9789.

[18] Kirby, A. J.; Dutta-Roy, N.; da Silva, D.; Goodman, J. M.; Lima, M. F.; Roussev, C. D.; Nome, F. *J. Am. Chem. Soc*. **2005**, *127*, 7033.

[19] Bromilow, R. H.; Kirby, A. J. *J. Chem. Soc. B* **1972**, 149.

[20] Benkovic, S. J.; Dunikoski, L. K., Jr. *J. Am. Chem. Soc*. **1971**, *93*, 1526.

[21] Hay, R. W.; Basak, A. K.; Pujari, M. P. *J. Coord. Chem*. **1991**, *23*, 43.

[22] Hay, R. W.; Basak, A. K.; Pujari, M. P.; Perotti, A. *J. Chem. Soc. Dalton Trans.* **1986**, 2029.

[23] Fife, T. H.; Pujari, M. P.; *J. Am. Chem. Soc*. **1988**, *110*, 7790.

[24] Kirby, A. J.; Lima, M. F.; da Silva, D.; Roussev, C. D.; Nome, F. *J. Am. Chem. Soc.* **2006**, *128*, 16944.

[25] Browne, K. A.; Bruice, T. C. *J. Am. Chem. Soc*. **1992**, *114*, 4951.

[26] Bruice, T. C.; Tsubouchi, A.; Dempcy, R. O.; Olson, L. P. *J. Am. Chem. Soc*. **1996**, *118*, 9867.

[27] Edwards, D. R.; Neverov, A. A. Brown, R. S. *J. Am. Chem. Soc*. **2009**, *121*, 368.

[28] (a) Kirby, A. J.; Tondo, D. W.; Medeiros, M.; Souza, B. S.; Priebe, J. P.; Lima, M. F.; Nome, F. *J. Am. Chem. Soc.* **2009**, *131*, 2023; (b) Asaad, N.; Kirby, A. J. *J. Chem. Soc. Perkin Trans. 2.* **2002**, 1708.

[29] (a) Trogler, W. C.; Morrow, J. R. *Inorg. Chem.* **1989**, *28*, 2330; (b) Kühn, U.; Warzeska, S.; Pritzkow, H.; Krämer, R. *J. Am. Chem. Soc.* **2001**, *123*, 8125.

[30] (a) Edwards, D. R.; Liu, C. T.; Garrett, G.; Neverov, A. A.; Brown, R. S. *J. Am. Chem. Soc.* **2009** *131*, 13738; (b) Liu, T.; Neverov, A. A.; Tsang, J. S. W.; Brown, R. S. *Org. Biomol. Chem.* **2005**, *3*, 1525.

[31] Holligan, B. M.; Jeffery, J. C.; Ward, M. D. *J. Chem. Soc. Dalton Trans*. **1992**, 3337.

[32] Williams, A.; Naylor, R. A. *J. Chem. Soc. B*, **1971**, *10*, 1973.

[33] Padovani, M.; Williams, N. H.; Wyman, P. *J. Phys. Org. Chem.* **2004**, *17*, 472.

[34] (a) Gibson, G.; Neverov, A. A.; Brown, R. S. *Can. J. Chem.* **2003**, *81*, 495; (b) For the designation of pH in non-aqueous solvents we use the nomenclature recommended by the IUPAC, *Compendium of Analytical Nomenclature. Definitive Rules 1997* 3rd ed., Blackwell, Oxford, U. K. 1998. The pH meter reading for an aqueous solution determined with an electrode calibrated with aqueous buffers is designated as ${}^{w}_{w}\mathrm{pH}$; if the electrode is calibrated in water and the 'pH' of the neat buffered methanol solution

then measured, the term ${}^{s}_{w}pH$ is used; and if the electrode is calibrated in the same solvent in which the 'pH' reading is made, then the term ${}^{s}_{s}pH$ is used. In methanol ${}^{s}_{w}pH$ - (-2.24) = ${}^{s}_{s}pH$, and since the autoprotolysis constant of methanol is $10^{-16.77}$, neutral ${}^{s}_{s}pH$ is 8.4.

[35] The total ΔA for conversion of a 0.1 M solution of phenol **5.9** to phenoxide **5.9**$^{-}$ was determined to be 0.9 units at 400 mm from fits of the Absorbance vs. [$^{+}NBu_4{}^{-}OCH_3$] to a standard single ionization model (See Supporting Information).

[36] Hyperquad 2000 is a computer program that fits titration data into nonlinear expressions containing a series of formation constants (log β) for species input to a model, published in: Gans, P.; Sabatini, A.; Vacca, A. *Talanta*, **1996**, *43*, 1739.

[37] $k_{obs} = k_{cat}(1 + K_B*[S] + [Cat]*K_B - X)/(2K_B)/[S]$

where:

$$X = (1 + 2K_B*[S] + 2*[Cat]*K_B + K_B{}^2*[S]^2 - 2*K_B{}^2*[Cat][S] + [Cat]^2*K_B{}^2)^{0.5}$$

[38] Detailed description and examples where the equation has been applied can be found in ref.13.

[39] (a) Bardwell, D.; Black, D.; Jeffery, J. C.; Ward, M. D. *Inorg. Chem.* **1993**, *12*, 1577; (b) Jeffery, J. C.; Moore, C. S. G.; Psillakis, E.; Ward, M. D.; Thornton, P. *Polyhedron*, **1995**, *14*, 599.

[40] Kirby, A. J.; Jencks, W. P. *J. Am. Chem. Soc*. **1965**, *87*, 3209.

[41] Guthrie, R. D.; Jencks, W. P. *Acc. Chem. Res.* **1989**, *22*, 343.

[42] Kirby, A. J.; Varvoglis, A. G. *J. Am. Chem. Soc.* **1967**, *89*, 415.

[43] Hoff, R. H.; Hengge, A. C. *J. Org. Chem.* **1998**, *63*, 6680.

[44] For the ionization process of the dibasic acid shown in Scheme 5-3, the macroscopic ionization constants K_a^1 and K_a^2 are given in terms of the microscopic ionization constants as: $K_a^1 = k_a^1 + k_a^2$; $1/K_a^2 = 1/k_a^3 + 1/k_a^4$; $K_a^1K_a^2 = k_a^1k_a^3 = k_a^2k_a^4$. See Cookson, R. F. *Chem. Rev.* **1974**, *74*, 5.

[45] Neverov, A. A.; Brown, R. S. *Org. Biomol. Chem.* **2004**, *2*, 2245.

[46] (a) Morrow, J. *Comments on Inorganic Chemistry.* **2008**, *29*, 169; (b) Catrina, I.; O'Brien, P. J.; Purcell, J.; Nikolic-Hughes, I.; Zalatan,J. G.; Hengge, A. C.; Herschlag, D. *J. Am. Chem. Soc*. **2007**, *129*, 5760. (c) Admiraal, S. J.; Herschlag, D. *Chem. Biol.* **1995**, *2*, 729; (c) Cleland, W. W.; Hengge, A. C. *Chem. Rev.* **2006**, *106*, 3252.

[47] (a) Bone, R.; Frank, L.; Springer, J. P.;Atack, J. R. *Biochemistry* **1994**, *33***,** 9468; (b) Tsubouchi, A.; Bruice, T. C. *J. Am. Chem. Soc*. **1994**, *116*, 11614; (c) Tsubouchi, A.; Bruice, T. C. *J. Am. Chem. Soc.* **1995**, *117,* 7399; (d) Tibbits, T. T.; Xu, X.; Kantrowitz, E. R. *Protein Science* **1994**, *3,* 2005; (e) Rishavy, M. A.: Hengge, A. C.; Cleland, W. W. *Bioorg. Chem.* **2000**, *28,* 283. (f) Dempcy, R. O.; Bruice, T. C. *J. Am. Chem. Soc.* **1994**, *116*, 4511. (g) Bruice, T. C.; Tsubouchi, A.; Dempcy, R. O.; Olson, L. P. *J. Am. Chem. Soc.* **1996**, *118*, 9867; (h) Souza, B. S.; Brandão, T. A. S.; Orth, E. S.; Roma, A. C.; Longo, R. L.; Bunton, C. A.; Nome, F. *J. Org. Chem.* **2009**, *74*, 1042.

[48] While the Yb^{3+}- and **5.1**-promoted cleavage of methyl *ortho*-carbomethoxyaryl phosphate diesters[27,13c] **5.2b,c** and La^{3+}-promoted cleavage of triesters[30] **5.3b** can exhibit turnover, binding of the lanthanide metal ions to the departing phenoxy group is very strong so that product inhibition occurs.

[49] Tsang,, W.-Y.; Edwards, D. R.; Melnychuk, S. A.; Liu, C. T.; Neverov, A. A.; Williams, N. H.; Brown, R. S. *J. Am. Chem. Soc.* **2009**, *131,* 4158.

[50] (a) Thea S.; Williams, A. *Chem. Soc. Rev.* **1986**, *15*, 125; (b) Williams, A. *Acc. Chem. Res.* **1984**, *17*, 425; (c) Williams, A. *Concerted Organic and Bio-organic Mechanisms,* CRC Press, Boca Raton, 2000, pp 161-181.

[51] Furniss, B. S.; Hannaford, A. J.; Smith, P. W. G.; Tatchell, A. R. *Vogel's Textbook of Practical Organic Chemistry.* 5th ed.; Longman Scientific & Technical: Harlow with John Wiley & Sons, Inc.: New York, 1989; p 1442-1443.

[52] While 4-nitrophenyl phosphate monoanion and dianion react at 39 ^{o}C with rate constants of 1.07 x 10^{-6} and 1.55 x 10^{-8} s^{-1} respectively, the reported rate constants for 2-chloro-4-nitrophenyl phosphate at 39^{o}C are 2.43 x 10^{-7} and 2.26 x 10^{-7} s^{-1} respectively (ref. 25).

[53] Computed as $\Delta G^{\ddagger}_{cat} = -RTln(k_{cat}/k_{bacground})$ from the Eyring equation at 298K, k_{cat} = 15 s^{-1} and $k_{background}$ = 1.1 x 10^{-13} to 1.5 x 10^{-12} s^{-1}.

[54] Kirby, A. J.; Younas, M. *J. Chem. Soc. B.* **1970**, 510.

[55] Given that the reactions of phosphate diesters are exceedingly slow, the only estimate that we have for the reaction of **5.7** at neutral pH is that obtained by the presumed fit to the Brønsted relationship, but this is probably too low an estimate based on the data we have with methoxide attack on dimethyl aryl triesters at 25 ^{o}C where the Brønsted relationship is log $k_2^{-OMe} = (-0.51\pm0.04)\,{}^{s}_{s}pK_a^{LG} + (4.68\pm0.56)$[30a]. The predicted rate constant for methoxide attack of **5.8** is 2.7 x 10^{-4} $M^{-1}s^{-1}$ which is 10 times less than that experimental rate constant of 2.94 x 10^{-3} $M^{-1}s^{-1}$ determined here.

[56] Khan, S. A.; Kirby, A. J. *J. Chem. Soc. B.* **1970**, 1172.

[57] Rowell, R.; Gorenstein, D. G. *J. Am. Chem. Soc.* **1981**, *103*, 5894.

[58] (a) Bourne, N.; Williams, A. *J. Am. Chem. Soc.* **1984**, *106*, 7591; (b) Bourne, N.; Chrystiuk, E. Davis, A. M.; Williams, A. *J. Am. Chem. Soc.* **1988**, *110*, 1890; (c) Ba-Saif, S. A.; Davis, A. M.; Williams, A. *J. Org. Chem.* **1989**, *54*, 5483.

[59] Cassano, A. G.; Anderson, V. E.; Harris, M. E. *J. Am. Chem. Soc.* **2002**, *124*, 10964; (b) Hengge, A. C.; Tobin, A. E.; Cleland, W. W. *J. Am. Chem. Soc.* **1996**, *117*, 5919.

[60] The stability constant reported for Cu(II) + phenanthroline $\rightleftharpoons$ Cu(II):phenanthroline is log K = 9.20 in water; Sillén, L. G.; Martell, A. E. in *Stability Constants*; Spec. Publ.-Chem. Soc. **1964**, 664-665; Supp. No. 1 **1971**, 676.

[61] (a) O'Brien, P. J.; Herschlag, D. *Biochemistry* **2002,** *41,* 3207; (b) Zalatan, J. G.; Herschlag, D. *J. Am. Chem. Soc.* **2006**, 128, 1293; (c) McWhirter, C.; Lund, E. A.; Tanifum, E.; Feng, G.; Sheikh, Q. I.; Hengge, A. C.; Williams, N. H. *J. Am. Chem. Soc.* **2008**, *130*, 13673; (d) Humphry, T.; Forconi, M.; Williams, N. H.; Hengge, A. C. *J. Am.*

Chem. Soc. **2004**, *126*, 11864; (e) Humphry, T.; Iyer, S.; Iranzo, O.; Morrow, J. R.; Richard, J.; P.; Paneth, P.; Hengge, A. C. *J. Am. Chem. Soc.* **2008**, *130*, 17858; (f) Feng, G.; Tanifum, E. A.; Adams, H.; Hengge, A. C.; Williams, N. H. *J. Am. Chem. Soc.* **2009**, 131, 12771.

[62] Williams, N. H.; Takasaki, B.; Wall, M.; Chin, J. *Acc. Chem. Res.* **1999**, *32*, 485.

Chapter 6 – Enzyme-like Acceleration for the Hydrolysis of a DNA Model in Dilute Aqueous Ethanol

6.1 – Preface

This chapter presents a slightly modified version of the article published in Journal of American Chemical Society (Liu, C. T.; Neverov, A. A.; Brown, R. S. *J. Am. Chem. Soc.* **2008**, *130*, 13870). All experiments (syntheses, kinetics, titrations, and data analysis) were performed by C. Tony Liu. The original kinetic data and the complete characterization of the new compounds synthesized for the study can be found in the Supporting Information section for the original paper. The first draft of the manuscript was composed by me and the final version was prepared in collaboration with Dr. R. Stan. Brown and Dr. Alex A. Neverov. The bulk of the materials in the Supporting Information section of the published article has been modified and placed in the Experimental section (6.3) of the chapter. The references have also been altered from the original publication to accommodate the changes made.

6.2 - Introduction

The previous chapters demonstrate the importance of an appropriate low polarity alcohol reaction medium for enhancing the catalytic efficiency of metal-promoted phosphoryl transfer reactions. Phosphate diesters' inherent stability toward hydrolytic and nucleophilic cleavage reactions is readily apparent in reactions that involve DNA-like substrates, which do not have an internal nucleophile. Despite considerable research being directed at understanding the mechanisms of hydrolysis and alcoholysis of RNA,

DNA and their model systems, [1,2,3] as well as toward designing M^{2+}-containing catalysts for facilitating their cleavage,[4] enzyme efficiency still far exceeds that displayed by the most potent synthetic catalysts reported in the literature.

In Chapters 2-4, we show that the cleavages of the RNA and DNA models **6.1** and **6.2** promoted by the $Zn(II)_2$ complex **6.3**[5,6] in methanol and ethanol are greatly accelerated by 10^{12} times or more relative to the background methanolysis reactions. In water, complex **6.3b** is no more active than the mono Zn(II) complex of 1,5,9-triazacyclododecane toward the cleavage of phosphate diesters[7] and we surmised that the acceleration of catalysis in methanol is attributable to a medium effect of reduced dielectric constant and polarity.[5,6] The catalyzed cleavages in methanol and ethanol, although fast, are transesterifications and not hydrolytic reactions. In the case of the RNA models, the first formed product arises from intramolecular ring closure as it does in water, but in the DNA model cases the OAr leaving group is replaced by OR. Thus, depending on the solvent, either alcoholysis or hydrolysis would take place. To come full circle back to our ultimate goal of designing a highly effective enzyme hydrolytic model, in this chaper we demonstrate that in ethanol, containing trace amount of water, di-Zn(II) catalyst **6.3** can selectively promote the hydrolysis of a DNA model (**6.2a**) with enzyme-like efficiency (10^{17}-fold relative to background base reaction).

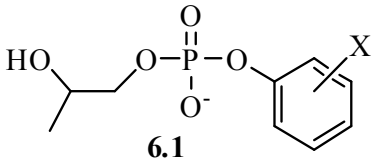

6.1

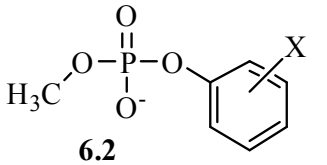

6.2

6.2a X=2-Cl,4-NO_2

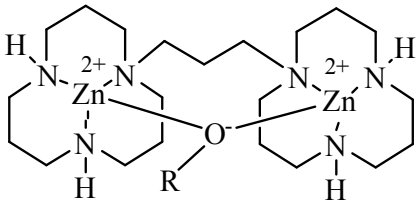

6.3a R=CH_3
6.3b R=H
6.3c R=CH_2CH_3

6.3 – Experimental

6.3.1 - Materials and Methods

$Zn(CF_3SO_3)_2$, monomethyl phosphate bis(cyclohexylammonium) salt, Amberlite® IR-120H ion-exchange resin (functionalized as sulfonic acid), tetrabutylammonium ethoxide in ethanol (~40% M; titrated against 1N Fisher Certified standard aqueous HCl solution and found to be 1.08 ± 0.01M), and sodium ethoxide (21 wt. % solution in denatured ethanol; titrated against N/50 Fisher Certified standard aqueous HCl solution and found to be 2.68M) were obtained from Aldrich/Fluka and used without further purification. *p*-Nitrophenyl benzoate (97%) was purchase from Alfa Aesar and used as supplied. $HClO_4$ (70% aqueous solution, titrated to be 11.40 M) was purchased from Acros Organics and used as supplied. Absolute ethanol was purchased from Commercial Alcohols Inc. and was de-gassed by bubbling Argon through it for 1h and then stored under Ar. Freshly dispensed ethanol was used prior to every kinetic experiment and kept (for a maximum duration of 1h) in a capped oven dried Erlenmeyer flask. The [water] in

the freshly dispensed de-gassed ethanol was found to be around 0.028 ± 0.007 M based on 5 titrations using a Mettler Toledo DL32 Karl Fischer Coulometer. The [water] of the ethanol kept in an Erlenmeyer flask that has been exposed to the atmosphere during use for 1h after dispensing was determined to be 0.029 ± 0.007 M. The acid form of methyl 2-chloro-4-nitrophenyl phosphate (**6.2a**)[5e] and 1,3-bis-*N*,*N*′-(1,5,9-triazacyclododecyl)propane[5b] were prepared for prior studies. The dinuclear complex of **6.3** was constituted as 2.5 mM stock solution in de-gassed absolute ethanol by sequential addition of aliquots of stock solutions of sodium ethoxide, 1,3-bis-*N*,*N*′-(1,5,9-triazacyclododecyl)propane, and $Zn(CF_3SO_3)_2$ in a 1:1:2 ratio. The complete formation of the catalyst complex requires 50 min in ethanol (as monitored by the change in catalytic activity over time).

6.3.2 – Kinetics

Kinetic experiments were done in duplicate using a Cary 100 Bio UV/vis spectrophotometer thermostatted at 25.0 ± 0.1 ^{o}C. The progress of the **6.3**-catalyzed (0.03 mM ≤ [**3**] ≤ 0.12 mM) cleavage of **6.2a** (0.05 mM, introduced as the acid) in ethanol was followed by monitoring the rate of appearance of the phenol product at 323 nm. Figure 6-1 shows that the binding of **6.3** to **6.2a** is very strong such that the concentration range of **6.3** varied from less than the [substrate] to more than the [substrate]. It is important to note that in all the cases investigated, the absorbance vs time traces followed good first order behaviour for at least three half times, thus indicating product inhibition was not an important factor at these concentrations and at $^{s}_{s}$pH 7.9. Also, even when [**6.3**] is less than [**6.2a**], full release of the phenol product was found, indicating efficient catalyst

turnover. The kinetic data were fitted to a non-linear least squares binding expression given in eq. (1), which can be applied to both weak and strong binding situations.

$$k_{obs} = k_{cat}(1 + K_B * [sub] + [\text{cat}] * K_B - X)/[sub]/(2K_B) \quad (1)$$

where:

$$X = \{(1 + 2K_B * [sub] + 2 * [\text{cat}] * K_B + K_B{}^2 * [sub]^2 - 2 * K_B{}^2 * [\text{cat}][sub] + [\text{cat}]^2 * K_B{}^2\}^{0.5}$$

Here, K_B is the binding constant (units of M^{-1}) for the formation of complex **6.3**:**6.2a**, and the reciprocal of K_B is the dissociation constant, K_M, (units of M) of **6.3**:**6.2a**. The [cat] in eq. (1) refers to the concentration of "viable" catalyst, which is derived from the expression [**6.3**] = $[\mathbf{6.3}]_{total}$ – A, where A is an independently fitted parameter corresponding to the observed x-intercept (Figure 6-1). The origin of the slight x-axis intercept for the plot in Figure 6-1, and thus the necessary correction factor A, is attributed to a dissociation of one or both of the Zn(II) ions from the complex at low concentrations.

The fit gives a complex dissociation constant (K_d) and maximum catalytic rate constant ($k_{cat}{}^{max}$) of 3.2 x 10^{-8} M and 1.47 x 10^{-3} s^{-1}. The complex dissociation constant was varied, but held as a constant once the goodness of the fit was optimized. The so-obtained value must be regarded as an estimate. A base-dependent kinetic study was conducted with 0.1 mM of **6.3**, 0.08 mM of **6.2a** added as the phosphoric acid, and varying amounts of additional NaOEt or $HClO_4$ stock solutions (0.01 M) in ethanol. The stock solution of **6.3** was prepared as described above at least 50 min prior to the onset of the experiment. An appropriate amount of the NaOEt or $HClO_4$ was added to the UV-

cells containing substrate **6.2a**. The reactions were then initiated by introduction of the catalyst **6.3**. The data indicate a bell-shaped rate constant vs. added [ethoxide] plot with maximum activity for the system consisting of **6.3c** (one ligand, two Zn(II) and one lyoxide) plus the anionic form of **6.2a**.

The base-promoted cleavage of **6.2a** (0.1 mM) was carried out at 25 ^{o}C with 0.1 - 0.14 M of tetrabutylammonium ethoxide added, and the reaction was followed at 408 nm for the appearance of the phenoxide product. Fitting the first order rate constants (k_{obs}) vs. [ethoxide] to a standard linear regression while forcing the line through the origin gives a second order rate constant of k_2^{EtO} = (5.5 ± 0.3) x 10^{-7} M^{-1} s^{-1}. A series of kinetic experiments was also conducted by keeping the [tetrabutylammonium ethoxide] (0.04 or 0.1 M) and [**6.2a**] (0.1 mM) constant while varying the concentration of added water in ethanol from 0 to 1 M. For the base-catalyzed cleavage of *p*-nitrophenyl benzoate (0.04 mM) in ethanol, three separate kinetic experiments with different amounts of added water (0, 0.5, and 2.0 M added water) were conducted with 0.5 to 2.0 mM of tetrabutylammonium ethoxide.

6.3.3 – Product Analyses

Product analyses for the **6.3**-promoted cleavage of **6.2a** in ethanol were done in three ways to ensure the validity and the consistency of the results. The first method involved isolating the phosphate products at the end of the reaction. Catalyst **6.3** and substrate **6.2a** (2.5 mM of each) were combined into an oven-dried 50 mL round bottom flask with a final volume of 25 mL in ethanol. Two samples were prepared with one sample having a final [water] = 0.007 M in ethanol (dried over molecular sieves and

[water] determined from Karl-Fischer titration) and the other sample possessing a final [water] of 0.528 M in ethanol. The appropriate amount of water was added to the solution containing the catalyst **6.3** (constituted as described above and allowed to sit for 50 min for complete complex formation) and the mixture was allowed to sit at room temperature for an additional 10 min prior to the introduction of the substrate **6.2a** (added as the sodium salt by pre-mixing with one equiv. of sodium ethoxide). The samples were allowed to sit at room temperature in round bottom flasks that were sealed with rubber septa and Parafilm® for 24h to ensure the completion of the reactions. After the 24h period, three equiv. of NaOEt were added to quench the reaction before the solvents were removed with a vacuum pump. The dried residues were dissolved in 20 mL of water and washed with three 20 mL portions of methylene chloride. The aqueous mixture was then passed through ~ 30 g of Amberlite® IR-120H ion-exchange resin with water as the eluent. The aqueous eluent containing all the acidic species was collected, and the combined aqueous mixture was washed with three 30 mL portions of methlyene chloride and dried under vacuum. The dried residues were then re-dissolved in 800μL of D_2O for NMR analyses. The % of the hydrolytic product generated was determined by comparing the relative integrations of the ^{1}H and ^{31}P spectra determined at 400 and 162.04 MHz for the peaks attributable the hydrolysis and the ethanolysis products. Authentic monomethyl phosphate was used to spike the NMR sample in order to determine the position and the identity of the hydrolysis product. Part of the dried residues (before dissolving into D_2O) was submitted for ESI-MS analysis, which confirmed the presence of both the hydrolysis and the ethanolysis products.

The second method for product analysis involved combining 2.5 mM of both catalyst **6.3** and substrate **6.2a** along with 2.5 mM sodium ethoxide and diluting to a final volume of 1.6 mL with ethanol in capped vials sealed with Parafilm®. Different amounts of water were added to the vials with catalyst **6.3** (constituted as described above and allowed to sit for 50 min for complete complex formation) and allowed to sit at room temperature for an additional 10 min before the introduction of **6.2a** (added as the sodium salt by pre-mixing with one equiv. of NaOEt). The reaction mixtures were allowed sit overnight at room temperature and then quenched by adding ~4 equiv. of $HClO_4$ before the solvents were carefully removed with a vacuum pump. The residues were re-dissolved in 800µl of CD_3OD for NMR analyses. The % of the hydrolytic product generated was determined by comparing the relative integrations of the ethyl ^1H peaks to the 2-chloro-4-nitrophenol ^1H peaks and the methyl ^1H peaks. For the experiment with 7.6 mM of [water] in the system, approximately 200 mL of de-gassed ethanol was dispensed into an oven-dried and sealed Erlenmeyer flask containing a thin layer of dry molecular sieves under N_2. This further-dried ethanol was used to prepare the stock solutions, and eventually the reaction system (7.6 mM of total water in the system as determined from Karl-Fischer titration) under N_2.

The third analytical method involved running ESI+ mass spectroscopy. Five samples were prepared with final [water] = 0.01, 0.0286, 0.0592, 0.1286, and 0.5286 M in ethanol. Each sample contained 0.4 mM of **6.2a** and 0.6 mM of **6.3** in a final volume of 1 mL in ethanol. After allowing the reaction to proceed overnight at room temperature the samples were analyzed by ESI mass spectroscopy using a QSTAR XL MS/MS system with the following conditions: ESI+ mode, declustering potential = 80.0 V, N_2

carrier gas, ion spray voltage = 5500 V, resolution = 10,000, and direct syringe injection. While the MS experiments cannot be analyzed to give quantitative ratios of the hydrolysis and ethanolysis products, they can be used to verify that each product (associated with the complexes) is present. A typical MS spectrum shows peaks for the hydrolysis product and the ethanolysis product as complexes with the dinuclear **6.3**.

6.3.4 - Product Analysis for Reaction of *p*-Nitrophenyl Benzoate in Basic Ethanol Containing Water in the Absence of Catalyst

The product analysis for the base-catalyzed cleavage of *p*-nitrophenyl benzoate was conducted by mixing the appropriate amounts of water and sodium ethoxide first in ethanol before the addition of *p*-nitrophenyl benzoate in such a way that the final volume of the solution was 2 mL in ethanol and the final concentrations of *p*-nitrophenyl benzoate and sodium ethoxide were 3.5 mM and 20 mM respectively. Four samples were prepared with 0, 0.5, 1.0, and 5.0 M added water. The reactions were done at room temperature. Two minutes after initiating the reactions, 0.9 equiv. (relative to the amount of base) of HCl (as 0.1 M stock solution in ethanol) was added to the reaction mixtures to stop the reactions and neutralize the systems. The reaction mixtures were then carefully dried under vacuum before re-dissolving in 800μL of CD_3OD for NMR analyses. The % of the hydrolysis product generated was determined by comparing the integration of the aromatic ^1H peaks for the sodium benzoate to the *p*-nitrophenoxide peaks. Authentic sodium benzoate was used to spike a NMR sample in order to determine the position of the hydrolytic product.

6.3.5 – Ethoxide-Promoted Cleavage of 6.2a

Due to the slowness of the base-promoted cleavage of **6.2a** in the absence of **6.3**, analysis for the products of the base reaction was not possible. However, addition of water to the system appears to lead to a decrease in the overall rate of the reaction as determined from initial rate experiments by fitting the first 2% of the reaction to a linear regression model. Because the values determined from the initial rate methods are associated with appreciable errors due to the small change in absorbance, it was not possible to obtain precise comparison of the rates of the reactions for systems containing different [water] within the experimental limitations. For this experiment, a sample containing 0.1 M tetrabutylammonium ethoxide and 0.1mM of **6.2a** was formulated in commercial ethanol (28mM H_2O) and divided into four smaller samples. To two of these was added additional H_2O to bring the amount to 0.50 M. All four samples were placed in a thermostatted spectrophotometer cell holder at 25 ^{0}C, and the rate of appearance of phenolate product was monitored at 408 nm. Within the limitations discussed above, the rate constant for the base-promoted cleavage of **6.2a** in ethanol with 0.5 M added water was $k_{obs} = (3.5 \pm 0.4) \times 10^{-8}$ s^{-1} which is considered to be is less than or equal to the rate constant determined in ethanol without added water (average $k_{obs} = 4.6 \pm 0.3) \times 10^{-8}$ s^{-1}.

6.4 – Results and Discussion

The X-ray structure of **6.3b** with a bridging HO^- was determined[5c] as grown from methanol solution at ambient conditions. The X-ray structure of the di-Cu(II) complex of the same ligand also grown at ambient temperature shows both a bridging hydroxide and a bridging water, the latter being replaced by a bridging phosphate when the crystal is

grown in the presence of dibenzyl phosphate.[5d] This suggests that the catalyst might have a special affinity for a bridging HO^- ion, so under appropriate conditions the medium effect might be harnessed to accelerate the **6.3**-promoted hydrolytic reactions of phosphate diesters.[8] We report here a realization of this goal obtained through a study of the cleavage of the DNA model **6.2a** promoted by **6.3** in ethanol which reveals not only a large rate acceleration but an interesting phenomenon where as little as 3.8 vol% (2.1 M) of water in ethanol leads to 93:7 ratio of the hydrolysis product (**6.4**) to ethanolysis product (**6.5**).

$$\underset{\textbf{6.4}}{(CH_3O)PO_3^{2-}} + \underset{\textbf{6.5}}{(CH_3O)(CH_3CH_2O)PO_2^-}$$

There are two main points of note. First, the plot in Figure 6-1 of the observed rate constant for cleavage of **6.2a** (5×10^{-5} M added as the acid) promoted by varying [**6.3**] with added equimolar NaOEt in anhydrous ethanol (used as supplied, but contains 28 mM H_2O by Karl-Fischer titration) shows very strong **6.3** + **6.2a** saturation binding, followed by decomposition of the complex. Non-linear least squares fitting of the data to a universal binding equation (eqn. (1)) gives the computed line through the data an upper limit (determined iteratively by varying the K_d until the goodness of fit did not change) for the complex dissociation constant (K_d) of 3.2×10^{-8} M and maximum catalytic rate constant for release of the 2-Cl-4-NO_2-phenol (k_{cat}^{max}) of 1.47×10^{-3} s^{-1}. The apparent second order rate constant for the catalyzed reaction (k_2^{cat}), given as k_{cat}^{max}/K_d, is 4.6×10^4 $M^{-1}s^{-1}$ which is a factor of 8.4×10^{10} larger than the second order rate constant for the ethoxide-promoted reaction of **6.2a** in ethanol ($k_2^{EtO} = (5.5 \pm 0.3) \times 10^{-7}$ M^{-1} s^{-1}).

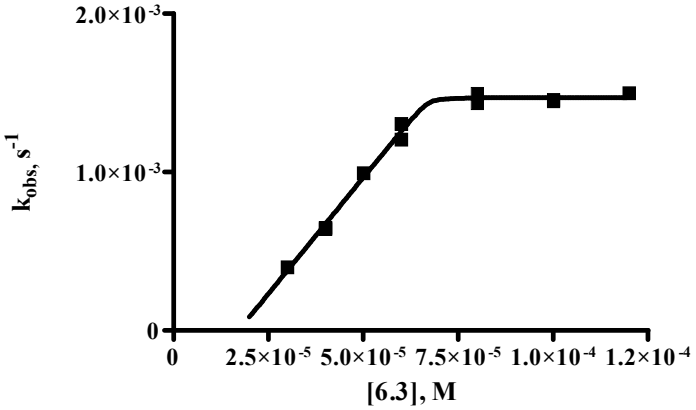

Figure 6-1. A plot of the observed first order rate constant for cleavage of **6.2a** (5 x 10^{-5} M) in ethanol with 28 mM H_2O vs varying [**6.3**], T = 25°C, $^{s}_{s}$pH = 7.90.[9,10] The small apparent x-intercept of ~ 1.7 x 10^{-5} M is attributed to a dissociation of Zn^{2+} from **6.3** at very low concentrations.[5,6]

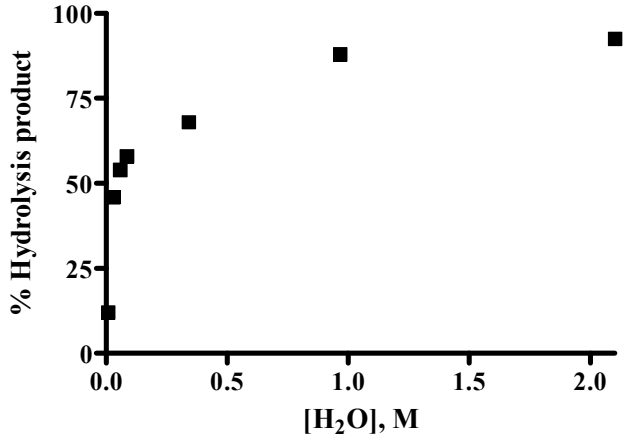

Figure 6-2. A plot of the percentage of analyzed hydrolysis product ($CH_3OPO_3^{2-}$) produced from the reaction of 2.5 mM **6.2a** promoted by 2.5 mM **6.3** in ethanol with varying amounts of water at room temperature.

Second, the products of cleavage of **6.2a** mediated by **6.3** in ethanol containing varying, but small, amounts of water (8 mM ≤ [H_2O] ≤ 2.1 M) were quantitatively determined by ^{1}H NMR analysis of the ethoxy, methoxy and phenol peaks of the products isolated after reaction and confirmed by MS and ^{31}P NMR. In Figure 6-2 is a plot of the % hydrolytic product (**6.4**) as a function of added H_2O. To complement the above product determinations, the kinetics of the cleavage of 2.5 mM **6.2a** promoted by 2.5 mM **6.3** in ethanol containing one equivalent of NaOEt were investigated at a few [H_2O]. The results, shown in Figure 6-3, indicate a drop in rate of slightly more than a factor of two in passing from 16 mM to 1 M water, probably due to a change in the medium. One also sees that the rate constant for the catalyzed reaction at the much higher concentration of catalyst is ~ three times lower than under the conditions of Figure 6-1, probably due to the inhibitory effect of triflate anion.[5,6]

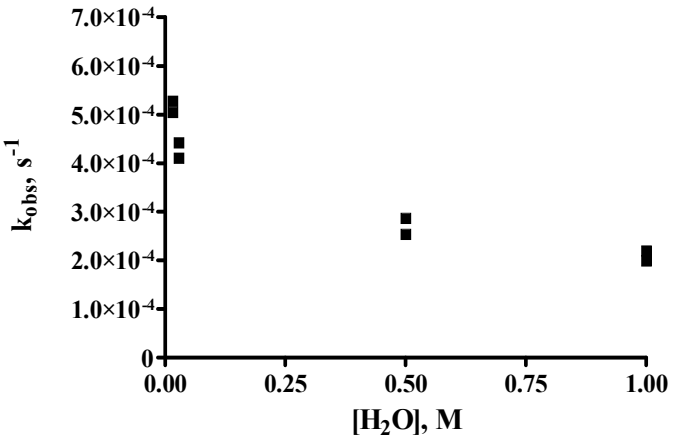

Figure 6-3. A plot of the observed first order rate constant for cleavage of **6.2a** (2.5mM) in ethanol with 2.5 mM of **6.3** in ethanol vs. varying [H_2O] in ethanol at T = 25 ^oC. The rate constants were determined from initial rate methods where the first 5 – 10% of the Abs vs. time trace for the appearance of the phenolic product at 323 nm are fitted to a standard linear regression model.

The unusual points brought to light in this study are the large amount of hydrolysis and increase in rate of the hydrolytic rates brought about by the combination of a dinuclear Zn(II) catalyst and a medium effect in ethanol. That as little as 28 mM of water (0.05 vol%), in the presence of an overwhelming excess of ethanol gives 46 % of hydrolysis product from a relatively inert phosphodiester suggests a process that selects for H_2O or ^-OH (either external or di-Zn(II) complex-coordinated) relative to ethanol or ethoxide as the active nucleophile attacking the **6.3**:**6.2a** complex. Solvolytic reactions in mixed ethanol/water media are known to be complex[11] but the available evidence allows us to rule out external H_2O and ^-OH as being responsible for the hydrolysis, leaving complex **6.3b** with an intramolecularly coordinated HO^- as the most likely catalyst.

Our earlier study of the **6.3**-catalyzed methanolysis[5b] of methyl *p*-nitrophenyl phosphate indicated that the rate maximized at a 1:2:1 ratio of ligand:Zn^{2+}:$^-OCH_3$, suggesting that the optimally effective catalyst is **6.3a**. The same is seen for the **6.3**-catalyzed reaction of **6.2a** in ethanol[5e] indicating that the transition state contains a 1:2:1:1 ratio of ligand, Zn(II), anionic substrate and lyoxide (EtO^- and/or HO^-) or its chemical equivalent. This assertion requires that the species leading to the hydrolysis product is a complex-coordinated HO^-, so we must rule out reasonable alternatives such as attack of hydroxide on the **6.3**:**6.2a** complex. On first inspection, one might expect, on the basis of autoprotolysis constants, that water ($K_W = 10^{-14}$) is more acidic than ethanol ($K_E = 10^{-19.1}$)[10] and thus preferentially ionized to HO^- in ethanol. However, in mixed solvents, this ignores the effect of transferring the dissociating water into a less polar medium so the situation is complicated by a several altered equilibrium constants and

activity coefficients of various species that are unknown because they depend heavily on the composition of the medium: these preclude exact calculation at the present time.[12]

Fortunately, we can experimentally estimate the ionization constant of water in ethanol. In a little known, but important paper, Caldin and Long[13] presented evidence that in ethanol, or ethanol containing "not more than a few percent water", the acid dissociation constants of ethanol and water are similar with water being slightly weaker. We confirmed this by determining the rate constants and cleavage products of cleavage of *p*-nitrophenyl benzoate under basic conditions in ethanol containing 0.53 and 1.03 M water where the amounts of hydrolysis products are 1.0 and 2.3%. Using a computational approach based on that provided[13] we find that the ratio between the acid dissociation constant of water and ethanol ($_s^sK_a^w/{}_s^sK_a^E$) in ethanol at these two water concentrations is 0.83 and 0.91. Assuming a linear correlation of the ratio with [water], $_s^sK_a^w/{}_s^sK_a^E$ = 0.75 was computed for ethanol containing 28 mM water, showing water to be slightly less acidic than ethanol at the concentrations employed, in agreement with what Caldin and Long determined.[13] The acid dissociation constant of ethanol containing 28 mM H_2O is assumed to be reliably computed from the autoprotolysis constant of pure ethanol as $_s^spK_a^E = -\log(10^{-19.1}/[EtOH]) = 20.33$ while that of water ($_s^spK_a^w$) in the same medium is 20.45.

The so-determined acidities of water and ethanol indicate that free $^-$OH cannot be the active nucleophile in hydrolyzing **6.3**:**6.2a** in ethanol under the kinetic conditions of Figure 6-1. This is because under experimental $_s^spH$ of 7.9 and $[H_2O]$ = 0.028 M, $[OH^-] = {}_s^sK_a^w([H_2O]/[H^+]) = 7.9 \times 10^{-15}$ M. To account for the fact that 46% of the reaction at this water content gives hydrolysis product, the rate constant for external $^-$OH attack

would be (0.46 x k_{cat}^{max})/[HO^-] = 8.6 x 10^{10} $M^{-1}s^{-1}$ which exceeds the diffusion limit in ethanol by a factor of 8.6.[14] By exclusion, the active species is most simply formulated as **6.3b**, or some closely related complex having an asymmetrical, doubly coordinated or singly coordinated HO^-.

Scheme 6-1. Catalyzed ethanolysis and hydrolysis of phosphate dister in ethanol with trace amount of water (Zn(II) charges omitted for clarity).

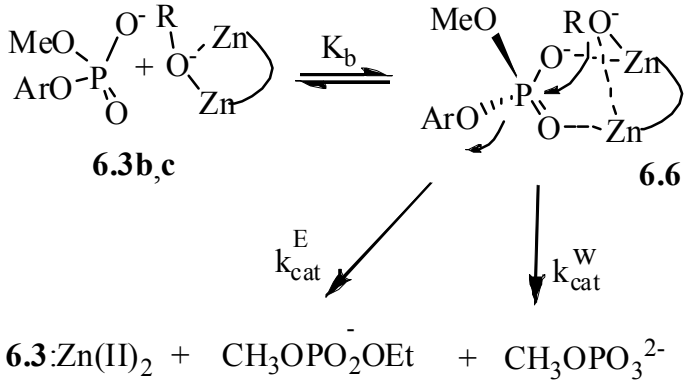

Given in Scheme 6-1 is a proposed pathway which is common to **6.3b** and **6.3c** catalyzed cleavage of **6.2a**. The scheme builds on our previous interpretation that the substrates become doubly activated through binding to both Zn(II) ions followed by an intramolecular delivery of the coordinated nucleophile (ethoxide or hydroxide). Structure **6.6** in the Scheme is proposed by analogy to the X-ray structure of the di-Cu(II) complex where a bridging dibenzyl phosphate and a bridging hydroxide are observed to complete the five-coordinate metal ion ligation.[5d] Whether the actual attack is stepwise, through a phosphorane intermediate, or concerted cannot be established with the information at hand.[3, 6]

It has been stated that "the active sites of enzymes are non-aqueous, and the effective dielectric constants resemble those in organic solvents rather than that in water".[15] The low dielectric interior of enzymes also means that ion-dipole and ion-ion interactions will be larger than in water[16] and thus might provide a very effective way to lower the transition state energies for metal promoted reactions of anionic substrates, but it is difficult to quantify the effect given the complexity of the enzyme catalyzed processes. The present data indicate that the reduced dielectric constant of ethanol relative to water (24.3 vs. 78) plays an important role in achieving the acceleration for the hydrolytic process observed here with a rather simple dinuclear Zn(II) complex. Just how great is the acceleration can be quantified in two simple ways, comparing the second order rate constants (k_{cat}^{max}/K_d) for the catalytic reaction and those for the lyoxide reactions or by comparing the k_{cat}^{max} value for cleavage of the **6.3**:**6.2a** complex to the background lyoxide reactions at ${}^{s}_{s}pH = 7.90$. For the first method, the 54:46 ratio of the products **6.5**:**6.4** at 28 mM H_2O, requires k_2^{cat} (ethanolysis) = 0.54 x (k_{cat}^{max}/K_d) = 2.48 x 10^4 $M^{-1}s^{-1}$ and k_2^{cat} (hydrolysis) = 2.11 x 10^4 $M^{-1}s^{-1}$. Initial rate experiments indicate that the rate constant for the lyoxide reaction does not increase with increasing [H_2O], so that an upper limit for the k_2 value for the hydroxide reaction is approximately that of the ethoxide reaction in the absence of catalyst. Thus, the accelerations are $k_2^{cat}(\text{ethanolysis})/k_{EtO^-} = 4.5 \times 10^{10}$, and $k_2^{cat}(\text{hydrolysis})/k_{HO^-} \geq 3.8 \times 10^{10}$.

When comparing the catalytic rate accelerations relative to the assumed base-promoted background reactions at ${}^{s}_{s}pH = 7.90$ in ethanol with 28 mM water, the ${}^{s}_{s}K_a^{w}$ and ${}^{s}_{s}K_a^{E}$ values indicate that [OH^-] = 7.9 x 10^{-15} M and [EtO^-] = 6.3x10^{-12} M.[17] Thus k_{obs}^{EtO} = 3.5 x 10^{-18} s^{-1} while the upper limit for k_{obs}^{HO} = 4.4 x 10^{-21} s^{-1}.[18] Since 54% of the k_{cat}^{max}

term of 1.47 x 10^{-3} s^{-1} leads to ethanolysis product, the acceleration for this process is (0.54 x k_{cat}^{max})/[EtO^-] $\leq$ 2.3 x 10^{14} and the hydrolysis is accelerated by $\geq$ 1.6 x 10^{17}, suggesting that complex **6.3** promotes the hydrolytic reaction at least 1000 times more efficiently than ethanolysis.

Phosphodiesterases are among the most efficient enzymes in promoting hydrolytic reactions relative to their background reactions, with accelerations of ~10^{17} being reported.[19] Despite active investigation of numerous simple metal ion containing catalytic systems for cleaving phosphodiesters, none of those reported to date demonstrate a catalytic acceleration for hydrolysis approaching that of the enzymes. In this study, a model system comprising a dinuclear Zn(II) complex and a synergistic medium effect provided by ethanol containing small amounts of H_2O gives an impressive acceleration (a factor of 1.6x10^{17} relative to the background HO^- promoted reaction) for the hydrolysis of a phosphodiester. Catalyst **6.3** shows a very large selectivity for activating water as a nucleophile in the presence of an overwhelming concentration of ethanol. These results demonstrate in a convincing way an underappreciated mode by which very large rate accelerations for hydrolytic reactions might be achieved by coupling of a catalytically important functional groups and medium effects.

6.5 - References and Notes

[1] Weston, J. *Chem. Rev*. **2005**, *105*, 2151.

[2] Sträter, N.; Lipscomb, W.N.; Klabunde, T.; Krebs, B. *Angew. Chem. Int. Ed. Engl.* **1996**, *35*, 2024; Wilcox, D. E. *Chem. Rev.* **1996,** *96*, 2435.

[3] Perrault, D.M.; Anslyn, E.V. *Angew. Chem. Int. Ed. Eng.* **1997**, *36*, 432.

[4] (a) Mancin F.; Tecillia, P. *New J. Chem.* **2007**, *31*, 800; (b) Molenveld, P.; Engbertsen, J.F.J.; Reinhoudt, D.N., *Chem. Soc. Rev.* **2000**, *29*, 75; (c) Williams, N.H.; Takasaki, B.; Wall, M.; Chin, J. *Acc. Chem. Res.* **1999**, *32*, 485; (d) Morrow, J.R.; Iranzo, O. *Curr. Opin. Chem. Biol.* **2004,** *8*, 192.

[5] (a) Brown, R.S.; Neverov, A.A. *Adv. Phys. Org. Chem.* J. P. Richard, Ed. Elsevier: San Diego, Calif. **2007**, *42*, 271; (b) Neverov, A. A.; Lu, Z.-L.; Maxwell, C.I.; Mohamed, M.F.; White, C.J.; Tsang, J.S.W.; Brown, R.S.; *J. Am. Chem. Soc.* **2006**, *128*, 16398; (c) Bunn, S.E.; Liu, C.T.; Lu, Z.-L.; Neverov, A.A.; Brown, R.S. *J. Am. Chem. Soc.* **2007**, *129*, 16238; (d) Lu, Z.-L.; Liu, C. T.; Neverov, A. A.; Brown, R. S. *J. Am. Chem. Soc*., **2007**, *129*, 11642; (e) Liu, C. T.; Neverov, A. A.; Brown, R. S. *J. Am. Chem. Soc*. **2008**, *130*, 16711.

[6] Neverov, A.A.; Liu, C.T.; Bunn, S.E.; Edwards, D.; White, C.J.; Melnychuk, S.A.; Brown, R.S. *J. Am. Chem. Soc.* **2008**, *130*, 6639.

[7] Kim, J., Lim, H. *Bull. Korean Chem. Soc.* **1999**, *20*, 491.

[8] There is a report that some Cu(II) complexes with functionalized bipyridyl ligands give hydrolysis products in 95% ethanol/water but medium effects were specifically excluded as being operative. Kövári, E.; Krämer, R. *J. Am. Chem. Soc.* **1996**, *118*, 12704.

[9] The symbol ${}^{s}_{s}\mathrm{pH}$ is used for designation of pH in non-aqueous solvents; the autoprotolysis constant of ethanol is $10^{-19.1}$ so neutral ${}^{s}_{s}\mathrm{pH}$ is 9.55.[10]

[10] Gibson, G.T.T.; Mohamed, M.F.; Neverov, A.A.; Brown, R.S. *Inorg. Chem*. **2006**, *45*, 7891.

[11] Ta-Shma, R.; Rappoport, Z. *Adv. Phys. Org. Chem.* **1992**, *27*, 239; Minegishi, S.; Kobayashi, S.; Mayr, H. *J. Am. Chem. Soc.* **2004**, 126, 5174.

[12] Fonrodona, G.; Ràfols, C.; Bosch, E.; Rosés M., *Anal. Chim. Acta* **1996**, *335*, 291.

[13] Caldin, E. F.; Long, G. *Nature* **1954**, 3757.

[14] Schwarz, H.A.; Gill, P.A. *J. Phys. Chem*. **1977**, *81*, 22.

[15] Cleland, W.W.; Frey, P.A.; Gerlt, J.A *J. Biol. Chem.* **1998**, *273*, 25529.

[16] Richard, J. P.; Ames, T. L. *Bioorg. Chem.* **2004**, *32*, 354.

[17] Using autoprotolysis constant of $10^{-19.1}$ M^2 for pure ethanol and the computed ${}^{s}_{s}\mathrm{pK}^{E}_{a} = 20.33$ for ethanol and ${}^{s}_{s}\mathrm{pK}^{w}_{a} = 20.45$ for water in ethanol containing 28 mM of water, one can determined the concentrations of hydroxide and ethoxide at ${}^{s}_{s}\mathrm{pH} = 7.9$ as: $[OH^-] = (10^{-20.45})*(0.028M)/(10^{-7.9}) = 7.9\text{x}10^{-15}$ M and $[EtO^-] = 10^{-19.1-7.9} = 6.31\text{x}10^{-12}$ M.

[18] $k_{obs}^{EtO} = (5.5 \pm 0.3)\text{x}10^{-7}\ M^{-1}s^{-1}$ x 6.31×10^{-12} M = $3.47 \times 10^{-18}\ s^{-1}$

The hydroxide reaction in ethanol with **6.2a** cannot be faster than the ethoxide reaction, otherwise the observed rate constant for the base promoted cleavage would have to increase with water content. For the purposes of computation, we assume that the second

order rate constant for the "cleavage" reaction of **6.2a** represents an upper limit for the hydroxide reaction. Thus, the observed pseudo-first order rate constant for the hydrolysis at ${}^{s}_{s}pH = 7.9$ would be: $k_{obs}^{HO} = (5.5 \pm 0.3)x10^{-7}\ M^{-1}s^{-1}$ x $7.9x10^{-15}\ M = 4.35x10^{-21}\ s^{-1}$.

[19] Schroeder, G.K.; Lad, C.; Wyman P.; Williams, N.H.; Wolfenden, R. *Proc. Nat. Acad. Sci. USA.,* **2006**, *103*, 4052.

Chapter 7 – Conclusions and Summary

The driving force for undertaking this body of work is based on a fundamental inquiry: to gain better overall understanding of biological processes and the mechanisms behind the various efficient chemical operations that sustain life. Our interest focuses on phosphoryl transfer reactions, which are perhaps the most prevalent chemical transformations in living systems. These are involved in a diverse profile of biological functions, and enzymes that are responsible for catalyzing phosphoryl transfer reactions have been shown to be among the most efficient catalysts known. We followed the common approach of studying small molecule enzyme mimics in order to give general information regarding catalyzed phosphoryl transfer reactions. In the best examples, this allows one to avoid the complexity and uncertainity that is often associated with enzymatic reactions. For example, enzymatic reactions often exhibit product inhibition, and the release of the product from the reactive site, rather than the chemical transformation, can be rate limiting. Furthermore, it is difficult to dissect the individual effect of various catalytically significant interactions (such as hydrophobic effect, dipole-dipole and hydrogen bond interactions) in the enzyme active site. It can also be tricky to assess how the various catalytically significant factors might be affected by different experimental conditions.

Biomimetic studies such as this aim to simplify the experimental parameters and offer an opportunity to probe the individual components that contribute to the overall catalysis. We expand upon the conventional approach of modeling the dinuclear core inside the active site of metallo-phosphoesterases by choosing a reaction medium that better represents the effective polarity believed to be inside the active site. The

compilation of data presented here demonstrates the importance of the reaction medium, and offers solid evidence for the large catalytic improvement that can be realized by conducting metal-catalyzed processes in alcohols. Perhaps the most profound manifestation can be seen by comparing our catalytic systems in alcohols with those containing the same metal complexes in water, which have been shown to be no more effective than hydroxide at promoting the hydrolysis of phosphate diesters. This will hopefully provide new strategies and approaches for future studies in similar fields.

We found a simple dinuclear complex that can greatly accelerate the cleavage of phosphate diesters in alcohols. This yielded an opportunity to probe some interesting mechanistic details that are not accessible in less activated systems, which encompass the majority of metal catalysts in water. In selected cases, our catalytic systems in alcohols are sufficiently efficient that the chemical phosphoryl transfer reaction progresses more readily than bimolecular binding, and positioning catalyst and substrate into a reactive complex. In Chapter 2, we described a detailed mechanistic study showing that the dinuclear **2.2**:$Cu(II)_2$ complex catalyzed the cleavage of DNA and RNA model substrates through a three-step process that involves the bimolecular binding of the catalyst to the substrate, followed by a unimolecular rearrangement step and subsequent bond fission to release the products. This presents a rare case in the literature, where all three steps of the catalytic process can be visualized and quantified through determination of the rate constants for each event. While the catalytic activity exhibited by the di-Cu(II) complex is lower than that for the di-Zn(II) counterpart, **2:2**:$Cu(II)_2$ still offered a respectable 10^{12}-fold rate acceleration for the cleavage of an RNA model (**2.1**; HPNPP) and a DNA model (**2.3**; MNPP) over the background methoxide reactions at $^{s}_{s}$pH 7.2 and 25 ^{o}C in

anhydrous methanol. The results from this study also provided visual evidence for the three-step catalytic mechanism proposed for catalysis in the presence of the corresponding di-Zn(II) complex, which should behave in a similar fashion. Energetics evaluation shows that binding of catalyst **2.2**:$Zn(II)_2$ to the transition state of the methoxide and substrate reference process stabilizes it by 22 – 24 kcal/mol in terms of ΔG^o.

While the di-Cu(II) complex offered useful mechanistic insights regarding the different events in the catalytic process, we wanted to understand better the more efficient di-Zn(II) system, especially since many metallo-phosphoesterases employ a di-Zn(II) catalytic core in their active sites. In Chapter 3, we described the catalyzed transesterification of a series of 2-hydroxypropyl aryl phosphates (**3.1**; RNA models) by the dinuclear **3.3**:$Zn(II)_2$ catalyst in ethanol. This served as a model for RNase, and the data can be compared with our reported results with the same metal complex in methanol. A main curiosity is the effect of further decreasing the dielectric constant of the reaction medium by using ethanol. The most noticeable difference in the two solvents is the extremely high affinity between the cationic catalyst and the anionic substrate (dissociation constant $\leq 3 \times 10^{-7}$ M in ethanol). This is not surprising since the overall polarity of the medium drops as one goes from methanol to ethanol leading to a greater interaction between oppositely charged species. In ethanol, the rate-limiting step of the transesterification of the series of RNA models studied shifted from catalyst-substrate complex rearrangement to chemical bond fission as the leaving group on the substrates became poorer as measured by the higher pK_a of the departing phenols. This is different from the results in methanol, where the rate-limiting step changed from the binding

between catalyst and substrate to the chemical bond fission moving through the same series of 2-hydroxypropyl aryl phosphates. Catalyst **3.3**:$Zn(II)_2$ affords an impressive $10^{12\text{-}14}$-fold rate enhancement (when comparing the second order rate constants for the catalyzed process vs. the ethoxide reactions) for the transesterfication of phosphate diesters **3.1** in ethanol. Energetic evaluation shows that catalyst **3.3**:$Zn(II)_2$ is able to stabilize the transition state of the reference process (ethoxide and substrate) by 33 – 36 kcal/mol. The large energy of stabilization is due to stronger binding between the catalyst, ethoxide, and substrate in ethanol, as well as the higher energy barrier for the uncatalyzed ethoxide reactions relative to the methoxide-promoted reactions.

The same dinuclear complex, **4.1**:$Zn(II)_2$ (**2.2** = **3.3** = **4.1**), is also capable of providing efficient catalysis for the methanolysis of a series of DNA model substrates (methyl aryl phosphates), which are even more resistant to solvolytic cleavage reactions than the RNA models (2-hydroxypropyl aryl phosphates). Because of the intrinsic stability of DNA model substrates, there are very few catalytic systems in the literature that have been shown to cleave phosphate diesters less activated than methyl *p*–nitrophenyl phosphate or bis-*p*-nitrophenyl phosphate. In Chapter 4, we described the catalyzed solvolysis of a large series of methyl aryl phosphates (from very activated methyl 2,4-dinitrophenyl phosphate to the less reactive methyl *p*-methoxyphenyl phosphate) by **4.1**:$Zn(II)_2$ in methanol. This was feasible due to the catalyst's ability to bring extremely slow reactions into a manageable experimental timescale. We have also shown that complex **4.1**:$Zn(II)_2$ is capable of promoting the cleavage of dimethyl phosphate in methanol with similar catalytic efficiency (Neverov, A. A.; Liu, C. T.; Bunn, S. E.; Edwards, D.; White, C. J.; Melnychuk, S. A.; Brown, R. S. J. Am. Chem.

Soc. **2008**, *130*, 6639). For all the substrates studied in Chapter 4, saturation kinetics were observed, indicating binding of the catalyst and the phosphates. When comparing the second order rate constants, the catalyzed reaction (k_{cat}/K_m) is about 10^{8-9} times larger than the corresponding methoxide reactions (k_2^{-OMe}). A series of Brønsted relationships was presented for the catalyzed and uncatalyzed processes. The most interesting phenomenon is the evidence of leaving group assistance for substrates that contain *ortho*-nitro and *ortho*-carbomethoxy substituents on the leaving groups. This presents a rare example where three main modes of enzyme catalysis (nucleophile activation, substrate activation, and leaving group assistance) are recruited in a simple enzyme mimic. Conceptually, this is what one would want in an ideal enzyme mimic, to be able to utilize all three modes in one catalytic system. Although a shortcoming of this system resides in the fact that leaving group assistance is only available to a small set of special substrates, this study does present itself as a proof-of-principle case and offers a glimpse of the potential that a system that can utilize all three catalytic modes on any phosphate diesters might possess.

Since metal-promoted leaving group assistance in phosphoryl transfer reactions has rarely been demonstrated in the literature, our observations presented in Chapter 4 prompted further investigation. In Chapter 5, we showed that Cu(II) can greatly enhance the solvolysis of a homologous set of phosphate mono-, di-, and triesters that have a common leaving group (OLg = 2'-(2-phenoxy)-1,10-phenanthroline), which can position a Cu(II) ion to directly stabilize the developing negative charge on a phenoxy Lg in the transition state. Detailed kinetics investigations revealed that efficient leaving group assistance results in 'looser' transition states for the phosphoryl transfer reactions. This is

especially true for the solvolysis of the Cu(II) complex of monoester **5.6**, where the experimental data suggest that it proceeds rapidly via a dissociative pathway with weak solvent assistance , possibily with a metaphosphate, or a metaphosphate-like intermediate being generated, which is quickly captured by a solvent molecule. It has been reported that uncatalyzed hydrolysis and enzymatic cleavage of phosphate monoesters involves a substantial degree of P-OLg bond scission in the transition state. This means that leaving group stabilization in the transition state should have a significant influence on the rate of the reaction. Metalloenzymes, such as alkaline phosphatase, that cleave phosphate mono- and diesters have been suggested to employ metal-assisted leaving group stabilization as one of the main forms of catalysis. In this study, kinetic data allow for relevant speciation of the metal complexes of Cu(II) and the phosphate substrates to be identified, and we showed that metal-promoted leaving group assistance is indeed a highly effective catalytic mode affording ~$10^{12\text{-}15}$-fold rate acceleration for the solvolysis of the phosphate mono- and diesters, and $10^{5\text{-}9}$-fold for solvolysis of the triester relative to the background reactions in the absence of Cu(II) at the same ${}^{s}_{s}\mathrm{pH}$ in methanol.

Small biomimetic enzyme models provide a convenient means by which to study and understand effects that may be important for enzyme catalysis, and constructing a simple artificial enzyme with catalytic efficacy that rivals natural enzymes has always been an ambitious target. Academically, it demonstrates a solid understanding of the factors that affect catalysis. Practically, a simple and easily accessible artificial enzyme could have useful applications in the biotechnology and pharmaceutical sectors. In Chapter 4, we described very efficient catalysis for the methanolysis of DNA model substrates. However, in biological systems, enzymes perform hydrolysis of phosphate

diesters. In Chapter 6 we present a case where a di-Zn(II) complex (**6.3**) preferentially promotes the hydrolysis of a DNA model substrate (**6.2a**) with enzyme-like efficiency ($>10^{17}$-fold over the background hydrolysis process under the same experimental conditions) in ethanol containing small amounts of water. The kinetic and product analysis data indicate that, subsequent to binding of the phosphate substrate to the dinuclear catalyst, a metal-bound hydroxide attacks the bound substrate. This is notable considering our previous attempts to grow crystals of dinuclear complexes of **6.3** (Chapter 2 and 3) in methanol resulted in species having a hydroxide (not alkoxide) bound to the metal ions. Overall, we demonstrated that a highly efficient enzyme mimic of phosphoesterases can be derived from combining the solvent effect (using alcohols to model the non-aqueous medium in enzyme active sites) and a simple di-Zn(II) complex (emulating the catalytically vital dinuclear core in the active sites).

Through the series of studies described here, we have gained valuable knowledge regarding the factors that may contribute to the impressive enzyme catalysis for phosphoryl transfer reactions. While the synthetic catalytic systems presented here exhibit enzyme-like efficiency that far exceeds any other reported examples, there is still plenty of room for improvement. The next generation of catalysts should focus on incorporating all three major modes of enzyme catalysis (nucleophile activation, substrate activation, and leaving group assistance) and have them all be accessible to carry out any phosphoryl transfer reactions. Also it is still a huge challenge to construct a simple artificial enzyme that is capable of catalyzing the cleavage of actual DNA and RNA with high proficiency and specificity. Specificity is especially important so that a given

substrate can be selectively cleaved at desirable sites. Realization of such a goal will have incredible practical implications.